

BIOZENTRUM

Universität Basel
The Center for
Molecular Life Sciences



Regulation of poly-GlcNAc expression and fimbriation in uropathogenic *E. coli*

Inauguraldissertation

zur

Erlangung der Würde eines Doktors der Philosophie

vorgelegt der

Philosophisch-Naturwissenschaftlichen Fakultät

der Universität Basel

von

Lucie Hosch

aus Celerina, Schweiz

Basel, März 2013

Originaldokument gespeichert auf dem Dokumentenserver der Universität Basel
edoc.unibas.ch



Dieses Werk ist unter dem Vertrag „Creative Commons Namensnennung-Keine kommerzielle Nutzung-Keine Bearbeitung 2.5 Schweiz“ lizenziert. Die vollständige Lizenz kann unter <http://creativecommons.org/licenses/by-nc-nd/2.5/ch/> eingesehen werden.

Genehmigt von der Philosophisch-Naturwissenschaftlichen Fakultät

Auf Antrag von

- Prof. Dr. Urs Jenal
- Prof. Dr. rer. nat. Ulrich Dobrindt

Basel, den 27. März 2012

Prof. Dr. Martin Spiess



Namensnennung-Keine kommerzielle Nutzung-Keine Bearbeitung 2.5 Schweiz

Sie dürfen:



das Werk vervielfältigen, verbreiten und öffentlich zugänglich machen

Zu den folgenden Bedingungen:



Namensnennung. Sie müssen den Namen des Autors/Rechteinhabers in der von ihm festgelegten Weise nennen (wodurch aber nicht der Eindruck entstehen darf, Sie oder die Nutzung des Werkes durch Sie würden entlohnt).



Keine kommerzielle Nutzung. Dieses Werk darf nicht für kommerzielle Zwecke verwendet werden.



Keine Bearbeitung. Dieses Werk darf nicht bearbeitet oder in anderer Weise verändert werden.

- Im Falle einer Verbreitung müssen Sie anderen die Lizenzbedingungen, unter welche dieses Werk fällt, mitteilen. Am Einfachsten ist es, einen Link auf diese Seite einzubinden.
- Jede der vorgenannten Bedingungen kann aufgehoben werden, sofern Sie die Einwilligung des Rechteinhabers dazu erhalten.
- Diese Lizenz lässt die Urheberpersönlichkeitsrechte unberührt.

Die gesetzlichen Schranken des Urheberrechts bleiben hiervon unberührt.

Die Commons Deed ist eine Zusammenfassung des Lizenzvertrags in allgemeinverständlicher Sprache: <http://creativecommons.org/licenses/by-nc-nd/2.5/ch/legalcode.de>

Haftungsausschluss:

Die Commons Deed ist kein Lizenzvertrag. Sie ist lediglich ein Referenztext, der den zugrundeliegenden Lizenzvertrag übersichtlich und in allgemeinverständlicher Sprache wiedergibt. Die Deed selbst entfaltet keine juristische Wirkung und erscheint im eigentlichen Lizenzvertrag nicht. Creative Commons ist keine Rechtsanwalts-gesellschaft und leistet keine Rechtsberatung. Die Weitergabe und Verlinkung des Commons Deeds führt zu keinem Mandatsverhältnis.

Dedicated to

My supervisor and mentor Dr. Alex Böhm,

My parents Jeannette and Hansjörg and my sister Barbara

1 Summary

Uropathogenic *E. coli* (UPEC) are the number one cause of urinary tract infections (UTIs) and are responsible for a remarkable pathogenesis. Once in the bladder motile pathogens adhere to the epithelial cells lining the bladder lumen, internalise into superficial cells where they shift into a sessile biofilm-like state capable of persisting for a long time. Functioning as a protected reservoir of bacteria these intracellular biofilm like structures are believed to be the source for recurring UTIs. This transition of motile and virulent uropathogens into sessile and quiescent intracellular bacterial communities (IBCs) requires the presence of a developmental program that coordinates the presence or absence of virulence traits at the right time and place. This work investigates several characteristics of the developmental program governing the lifestyle-switch in UPECs. Two representative output systems are used to investigate the importance of the bacterial second messenger c-di-GMP and the carbon storage regulator (Csr) system during the transition of motile to sessile bacteria. These output systems are type I fimbriae, associated with acute infections, and the biofilm matrix component poly- β -1,6-N-acetyl-glucosamine (PGA).

The first manuscript included in this thesis (chapter 5) shows that biofilm formation of UPECs and their responsiveness to c-di-GMP levels is comparable to what was established for the non-pathogenic *E. coli* strain MG1655. It is shown that derepression of the carbon storage regulator (Csr) system is a prerequisite for *in vitro* biofilm formation of cystitis and pyelonephritis isolates and that this biofilm formation solemnly depends on the exopolysaccharide PGA. Furthermore, this PGA dependent biofilm formation is shown to respond to the second messenger c-di-GMP, which in the model cystitis isolate UT189 predominantly gets synthesised by the dedicated cyclase YdeH. Similar to MG1655, translation inhibitors are shown to mediate a reduction of the bacterial alarmone ppGpp, which then results in enhanced PGA dependent attachment. This project is rounded up by a murine cystitis model, which addresses the *in vivo* involvement of PGA dependent biofilm formation over the period of three weeks.

The second manuscript of this thesis (chapter 6) shows that type I fimbriae have a negative effect on PGA dependent attachment. Furthermore, it reveals a regulatory cross talk between type I fimbriae and the exopolysaccharide PGA. Genetic approaches are used to show that this regulatory cross talk is mediated by the Csr system: it allows the expression of type I fimbriae if repressed and stimulates PGA dependent biofilm formation upon derepression. Moreover, this work introduces a model in which a derepressed Csr system negatively affects the phase variable expression of type I fimbriae by interfering with the activity of the FimE, but not the FimB recombinase. Furthermore, it is shown that CsrD of the

Summary

Csr system fine-tunes the expression of type I fimbriae during growth of a population over time.

Chapter 7 was published in 2010 and introduces a standardised assay used to quantify type I fimbriae mediated aggregation of cells via their mannosylated surface-exposed receptors. The measured aggregation depends on FimH, which is found as tip adhesin on type I fimbriae and is proven essential in mediating mannose binding and initial establishment of cystitis. This method is then used to investigate the therapeutic potential of substances that interfere with FimH mediated adhesion of UPECs to highly mannosylated protein-receptors on eukaryotic cells. Tested substances are classified as α -D-Mannopyranosides and are shown to be potent FimH antagonists as determined by measuring their effect on the disaggregation of UPECs from mannose moieties on *Candida albicans* cells and guinea pig erythrocytes (GPE).

Finally the appendix in chapter 8 contains supplemental figures and additional data used to refine the model established in chapter 6. These results show that not only the Csr system has inversed effects on type I fimbriae and PGA expression but that ppGpp and presumably c-di-GMP also inversely affect the two output systems. In the end it is concluded that a regulatory network ensures expression of type I fimbriae during the planktonic lifestyle and switches to PGA expression upon i) derepression of the Csr system, ii) elevation of c-di-GMP levels and iii) reduction of ppGpp levels. Last but not least the impact of this model with respect to the disease progression during UTI is briefly addressed.

2 Index

1	Summary	i
2	Index	1
3	General Introduction	5
3.1	Two distinct bacterial lifestyles.....	5
3.2	Escherichia coli: A model organism with commensal or pathogenic traits	5
3.3	Urinary tract infections	6
3.3.1	The pathogenesis of acute cystitis.....	7
3.3.2	The formation of intracellular bacterial reservoirs during UTIs	8
3.4	Temporal processes involved in the formation of biofilms	10
3.4.1	The exopolysaccharide β -1,6-N-acetylglucosamine is synthesised by PgaABCD	13
3.4.2	The regulation of PGA synthesis	14
3.5	The Carbon Storage Regulator (Csr) system	14
3.5.1	The carbon storage regulator system and its central role in bacterial physiology	14
3.5.2	Post-translational regulation of CsrA levels	16
3.6	Bacterial second messengers modulate <i>E. coli</i> lifestyles	18
3.6.1	The bacterial second messenger c-di-GMP.....	19
3.6.2	C-di-GMP input systems and c-di-GMP receptor proteins.....	19
3.6.3	Regulation of c-di-GMP metabolism	21
3.6.4	The bacterial alarmone ppGpp	23
3.7	Fimbriae and Pili in bacteria.....	23
3.7.1	Type I fimbriae of UPECs.....	24
3.7.2	The chaperone/usher dependent assembly of type I fimbriae.....	25
3.7.3	Regulation of type I fimbriae and the phase variation of <i>fimS</i>	27
4	Aims of this Thesis	32
5	The role of Poly-GlcNAc in biofilm formation of uropathogenic <i>E. coli</i>	33
5.1	Statement of work	33
5.2	Abstract	34
5.3	Introduction.....	35

Index

5.4	Material and Methods.....	37
5.4.1	Bacterial strains and plasmids	37
5.4.2	Standard growth conditions.....	37
5.4.3	Selection of UPEC isolates inducible by sub-MICs of tetracycline	37
5.4.4	Congo red binding assay	37
5.4.5	Motility assay.....	38
5.4.6	Construction of isogenic deletion mutants	38
5.4.7	Attachment assay.....	40
5.4.8	Electron microscopy.....	40
5.4.9	Allelic exchange	41
5.4.10	Preparation of P1 phage lysates.....	41
5.4.11	P1 Transduction	41
5.4.12	Preparation of bacterial inoculum for murine cystitis model	42
5.4.13	Infection of mice	42
5.5	Results	43
5.5.1	General characterization of motility and Congo red binding of different UPEC strains	43
5.5.2	Biofilm formation in UPECs is regulated by the Csr cascade and by c-di-GMP.....	43
5.5.3	Sub-MIC of translation inhibitors differentially stimulate attachment in UPECS.....	45
5.5.4	UTI89 attachment can be modulated by several unrelated genes	46
5.5.5	UPEC <i>ydeH</i> alleles do not complement the function of MG1655 <i>ydeH</i>	47
5.5.6	Murine cystitis models over 3 weeks are not sufficient to determine a role for PGA <i>in vivo</i>	48
5.6	Discussion	50
5.6.1	UPECs form PGA dependent biofilms upon derepression of the Csr system	50
5.6.2	Sub-MICs of translation inhibitors affect attachment of most UPECs	51
5.6.3	c-di-GMP increases attachment of UPECs.....	52
5.6.4	Biofilm formation in clin591 is different than in UTI89.....	53
5.6.5	YdeH _{UTI89} and YdeH ₈₃₉₇₂ alleles do not complement YdeH _{MG1655}	54
5.7	Figure Legend	55
5.8	Figures	60
5.9	Tables.....	74
5.10	Acknowledgements	79
5.11	References	80

Index

6	Inverse regulation of poly-GlcNAc and fimbriae adhesins in uropathogenic <i>E. coli</i>.....	84
6.1	Statement of Work	84
6.2	Abstract	85
6.3	Introduction.....	86
6.4	Material and Methods.....	89
6.4.1	Strains and plasmids used in this study.....	89
6.4.2	Construction of isogenic deletion mutants	89
6.4.3	Construction of p_{fimA-H} Locked strains (p_{fimA-H}^{ON} and p_{fimA-H}^{OFF})	90
6.4.4	Construction of <i>fimA::gfp</i> and <i>fimH-gfp</i> reporter constructs.....	91
6.4.5	Construction of deletion mutants in UTI89 <i>fimH-gfp</i>	92
6.4.6	Preparation of guinea pig erythrocytes for aggregometry.....	93
6.4.7	Aggregometry.....	93
6.4.8	Biofilm assay	93
6.4.9	Scanning electron microscopy	94
6.4.10	Phase variation PCR.....	94
6.4.11	Analysis of <i>fimA::gfp</i> and <i>fimH-gfp</i> by flow cytometry.....	95
6.4.12	Fluorescent staining of surface-exposed type I fimbriae via indirect immunofluorescence.....	96
6.5	Results	97
6.5.1	Type I fimbriae interfere with PGA-mediated attachment	97
6.5.2	Type I fimbriae functionally interfere with PGA dependent attachment.....	97
6.5.3	<i>csrB</i> overexpression has no effects on fimbriation if <i>fimS</i> switching is impaired.....	99
6.5.4	Deletion of FimE and CsrD influences the <i>csrB</i> - effects on the <i>fimS</i> orientation.....	102
6.5.5	PGA and type I fimbriae mediated bacterial self-aggregation can be distinguished by flow cytometry.....	103
6.6	Discussion	105
6.6.1	The inverse effect of the Csr system on type I fimbriae and PGA involves <i>csrB</i> , CsrD, FimE and the phase variation of <i>fimS</i>	107
6.6.2	During biofilm formation type I fimbriae and PGA expression are separated.....	109
6.6.3	Disruption of the <i>fimAICDFGH</i> operon reduces the signal reporting fimbrial expression.....	111
6.7	Figure Legend	113
6.8	Figures	120
6.9	Tables.....	134

Index

6.10	Acknowledgements	139
6.11	References	140
7	Development of an aggregation assay to screen FimH antagonists.....	146
7.1	Statement of work	146
8	Appendix	154
8.1	Supplemental Results and Discussion.....	154
8.1.1	Raw data for flow cytometric analysis of fimH-gfp construct	154
8.1.2	C-di-GMP and ppGpp affect the phase variation in <i>fimH-gfp</i>	154
8.2	Supplemental Figure Legends	158
8.3	Supplemental Figures	163
9	Outlook.....	172
10	Acknowledgements	175
11	References	177
12	Curriculum Vitae	191

3 General Introduction

3.1 Two distinct bacterial lifestyles

Evolution over several billion years allowed bacteria to adapt and colonise almost every habitat on this planet. For a long time bacteria were believed to live as primitive loners or planktonic cells deprived of any interaction with their relatives. Advances in microbiological techniques over the past 60 years led scientists realize that bacterial lifestyles are far more complex than initially described, as extensive microbial density on surfaces was revealed. By now it is well established that surface associated bacteria are generally enclosed in a protective, self-produced matrix composed of hydrated polymers that encase and immobilize the microbial aggregates, allowing growth as three-dimensional structures, generally referred to as biofilms. The oldest biofilms identified so far were found in fossils and date back to over 3.2 billion years (1). Intriguingly, the discovery of bacteria by Antonie van Leeuwenhoek in 1676 was made from a sample most likely consisting of biofilm-derived bacteria, as the sample was scraped from dental plaques, a typical dental biofilm structure. Research over the last decade suggests that the prevalence of sessile lifestyles dominates over the planktonic lifestyle initially described for bacteria. By now biofilms have been identified in the entire bacterial kingdom and in virtually all niches: from space stations to deep-sea vents, from hot springs to arctic cold springs, from fossils to modern industrial plants but also in form of benign or pathogenic biofilms within hosts or on foreign body implants. A model organism often used to study biofilms is *Escherichia coli* (*E. coli*).

3.2 Escherichia coli: A model organism with commensal or pathogenic traits

E. coli are facultative anaerobic bacteria, which occur in the environment as commensals in the gastrointestinal tract or as pathogens that cause many different types of infections. They are generally classified into three different groups, commensal *E. coli*, intestinal pathogenic *E. coli* and extraintestinal pathogenic *E. coli* (ExPEC), which can all prevail in sessile lifestyles (2, 3). While commensal *E. coli* are generally benign, intestinal pathogenic *E. coli* (classified into EPEC, EHEC, ETEC, EAEC, EIEC and DAEC) might cause different enteric / diarrhoeal diseases within the lower digestive tract (2). Other than their intestinal relatives, ExPECs are capable to disseminate and colonize niches outside the gut. However, they retain their ability to survive within the gut (3). ExPEC strains, which colonize and infect the urinary tract, have further been classified as uropathogenic *E. coli*

(UPEC). This class of pathogens has been difficult to profile as it is not associated with the expression of specific traits or virulence factors (3-5). Based on the anatomical location of the niche colonised within the urinary tract, UPECs can further be subdivided into a variety of pathotypes including colonisation of the bladder (cystitis), colonisation of kidneys (pyelonephritis), asymptomatic bacteriuria (ABU; bacteriuria = bacteria in the urine) or catheter associated infections. Pyelonephritis pathotypes are often very similar to the pathotype of cystitis (see chapter 3.3). The majority of these strains initiate colonisation of the upper urinary tract and kidneys through the bladder, just like the cystitis isolates, which do not ascent into the kidneys. The most common model isolate for cystitis is UT189 (6, 7). Isolates 536 and CFT073 are well-studied pyelonephritis isolates (8, 9). These three strains have all been sequenced and are used as laboratory strains since several years. The strain clin591 was isolated from a cystitis patient with a urethral stent and is used for comparison with the other cystitis isolates. In this work, clin591 represents the catheter-associated isolates, since no other catheter-associated isolate has yet been sequenced. Another class of *E. coli* strain has been shown to cause asymptomatic bacteriuria (ABU). ABU strains are closely related to pathogenic / symptomatic isolates but they prevail asymptotically in the bladder for a long time and do not cause symptoms in carriers. The prototypic ABU isolate (83972) does not adhere to any cell types and it does not disseminate to kidneys or blood stream but can still persist in the bladder (10, 11). Furthermore, ABU strains do not trigger any host response while the causative agents of symptomatic urinary tract infections (UTIs) do so (12). The absence of immune response might be related to impaired bacterial motility and deprivation of extracellular structures including flagella, capsule and the O- respectively, K-surface antigens (12-14). 83972 is well adapted for growth in the urinary (10, 15) and has been used *in extenso* to deliberately establish protective ABU in patients suffering from severe chronic UTIs. Interestingly, investigations of 83972 re-isolates, show that the selective pressure within the patients bladder results in rapid and divergent evolution, as visualised for one of the 83972 re-isolate named PIII-4 (16, 17).

3.3 Urinary tract infections

The urinary tract offers several distinct niches, which are used by pathogens for colonisation and long-term persistence. UPECs are by far the most prevailing agents of UTIs accounting for up to 90 % of the cases (18). Different Gram-positive and Gram-negative bacteria, as well as different fungi cause the remaining 10 % (19, 20). The majority of microorganisms colonising the urinary tract originate from the rectal flora. After temporarily residing in the periurethra and vagina (21, 22) the pathogens ascend through the urethra into

the bladder lumen where they might colonise the urinary tract and cause UTIs. In the year 2000, 14 million medical visits were associated with uncomplicated UTIs resulting in financial burden of over 4 billion dollars (23). These uncomplicated cases of UTIs usually affect healthy female outpatients. However, sexual activity has been shown to be a predisposition for uncomplicated UTIs and might be responsible for some of these cases (24, 25). Other known predispositions for UTI besides structural and urodynamical abnormalities include pregnancy (26), diabetes (27), bladder catheterisation (28) and urethral stents (DJ catheter) (29), prostate enlargement (23) or HIV infections (30). Currently it is estimated that 50 % of all women will suffer from a UTI at some point during their life and 25 % will suffer from a second UTI. Importantly, 3 % of all women are reported to suffer a third recurring UTI within six months following treatment of the preceding UTI (18). It was shown that the majority of recurring UTI cases arise from the same clonal strain as the initial UTI (18, 31, 32) and do not require re-migration of the clonal pathogen from the anus through the urethra into the bladder (33). Though generally caused by the same group of pathogenic *E. coli* the pathologies of UTIs might vary greatly i) in their precise location within the urinary tract, ii) the severity of the infection, iii) the treatment efficacy, iv) the bacterial burden or v) the arsenal of virulence factors used by the pathogens to cause disease. Uncomplicated cystitis can be treated effectively by antibiotic therapy in most of the cases, especially at the early onset of symptoms. Treatment becomes less effective or impossible once UPECs have effectively colonised the bladder, as this step involves intracellular bacteria, which might already be in a latent irresponsive state until the onset of recurring UTI (see chapter 3.3.2). In other cases, acute UTI turn into severe infections upon bacterial infiltration of the kidneys (pyelonephritis) through the ureter and possible dissemination of the pathogen into the bloodstream causing severe bacteraemia or sepsis.

3.3.1 The pathogenesis of acute cystitis

The ability of uropathogens to progress through the urethra into the bladder lumen is a prerequisite for successful colonisation of a healthy urinary tract, a process which is not fully understood. However, flagellar motility has been reported to facilitate ascension into the bladder and progression throughout the urinary tract (34, 35). Once in the bladder, it is important for the pathogen to circumvent washout upon bladder voidance. This is generally achieved through rapid adherence of the pathogen to the epithelial cells lining the bladder lumen (urothelium). At this stage of the infection, the titres of bacteria and leukocytes in the urine (pyuria) begin to be elevated, which is generally associated with an elevated urgency and frequency of painful urination (dysuria). During adhesion, the bladder epithelium

recognizes microbial structures like LPS, which trigger TLR4 signalling (36, 37) and production of IL-8 (38-40). The release of IL-8 induces the infiltration of neutrophils and dendritic cells to the site of infection. Neutrophils begin to phagocytose and kill UPECs by reactive oxygen species (ROS), nitric oxide NO or antimicrobial peptides, while dendritic cells phagocytose bacteria and present antigens to activate adaptive immune cells. Furthermore, the cell mediated host defence is supported by changes in urine composition (pH, osmolarity) and its increased flow (41). To prevent washing out, UPEC strains adhere through type I fimbriae, one of the best-characterised virulence factors in UPECs (see chapter 3.7) (42-44).

3.3.2 The formation of intracellular bacterial reservoirs during UTIs

Type I fimbriae are proteinacious adhesins that bind to mannosylated receptor proteins such as uroplakin 1a and the integrins $\beta 1$ and $\alpha 3$ (45, 46), which are expressed on the apical surface of epithelial cells. This initial contact induces engulfment of UPECs into urothelial cells where they are protected from host response. In the cytoplasm of superficial cells lining the urothelium the pathogen can rapidly multiply and accumulate. Shifting into a sessile biofilm-like state, it can reside silently for a long time and serve as a reservoir for recurrent UTIs (47, 48).

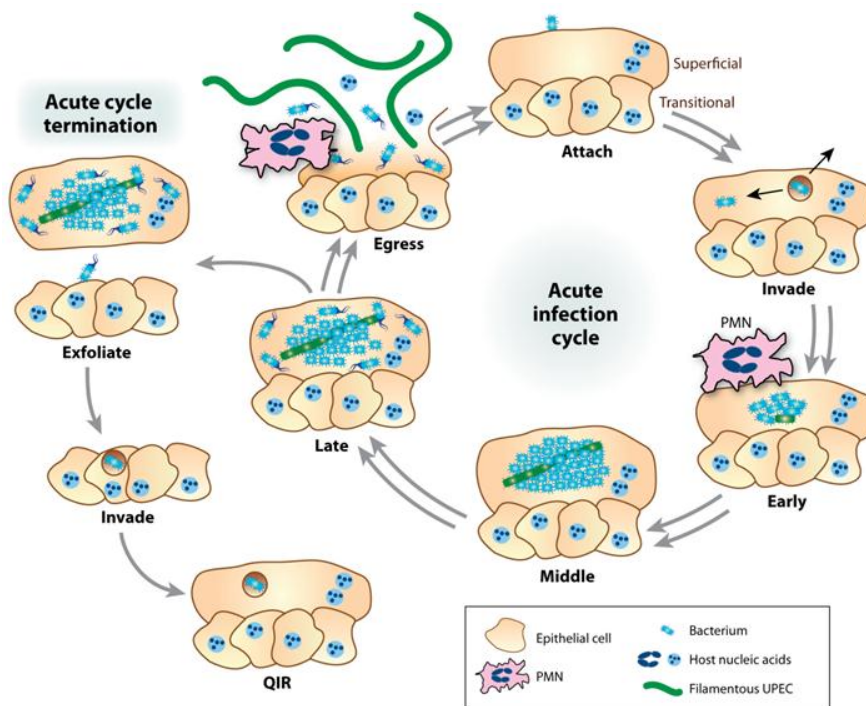


Figure 1: Schematic representation of the intracellular cycle of UPECs

The first round of UPEC infection occurs in superficial bladder epithelial cells once bacteria attached to the intact epithelium. Upon invasion, a few UPECs gain access to the cytoplasm and its nutrients, the majority of bacteria get expelled again via vesicles (indicated by black arrows). Once in the cytoplasm, the acute phase of infection is initiated by fast growth (early). Latter is followed by the formation of

Intracellular Bacterial Communities (IBC) (middle) and a subsequent aging process (late), in which some bacteria dissociate from the IBC regain motility and in the end result in the exfoliation of single cells, bacterial filaments or entire IBCs from the superficial bladder cells. Exfoliation damages the intact urothelium and gives access to underlying urothelial cell layers, which can again be infected for bacterial reservoir formation. This image was taken from Hunstad DA and Justice SS 2010 (49).

* * *

The formation of intracellular bacterial reservoirs occurs stepwise (Figure 1) (49). The internalisation of UPECs into urothelial cells is a passive process that is not triggered by the adhered bacterium but rather a consequence of vesicle transport to and from the membrane. However, bacterial binding to integrins (45, 46) results in localised actin rearrangements and membrane extensions around the bacterium, which finally leads to engulfment of the bacterium by the membrane and internalisation (50, 51). However, only a small number of bacteria is capable of persisting intracellularly, as the majority of the bacteria get expelled again via exocytosis. Those bacteria that persist within epithelial cells gain access to the nutrient rich cytoplasm where they can grow exponentially and form amorphous, loose and unorganised bacterial clusters. The cytoplasmic environment causes reduced growth rates, a morphological shift toward coccoid structures and a reorganisation of the bacterial clusters into a tight highly organised bacterial clump. This new state of bacteria features several properties associated with classical biofilms (48) and is usually referred to as intracellular bacterial community (IBC). Among others, the autotransporter adhesive antigen 43 as well as type I fimbriae were shown to be expressed at this stage of pathogenesis (52). Upon slow growth of IBCs, the bacterial mass reaches the cell membrane of the epithelial cell and causes a pod like protrusion into the bladder lumen (52). The next maturation step of IBCs leads to the disassociation and regain of motility of some UPECs located at the edge of the IBC, a typical characteristic of mature biofilms. The trigger for this maturation step is believed to involve nutrient limitation, stress due to heavy bacterial burden and bacterial fluxing, or cell lysis. As a consequence, bacteria exit infected cells individually or by forming bacterial filaments, which consist of replicated bacteria that have not completed septation. Interestingly these filaments can also flux out of infected cells and it was shown that they cannot be attacked by polymorphonuclear leucocytes (PMNs) (48, 53). Loss of membrane integrity upon bacterial fluxing and bursting of cells thereafter is believed to release chunks or entire IBCs into the bladder lumen. Consequently these bacteria might disseminate through the urine to find a new niche or might re-initiate another round of intracellular IBCs (49). Interestingly, the second round of internalisation by UPECs appears to be slightly different from the first round described above. First of all, the second cycle appears to be slower and result in the infection of differentiated and undifferentiated urothelial cells, which have been exposed due to disruption of the superficial cell layer. Furthermore, instead of progressing through the IBC cycle described above, bacteria infecting these cells grow very slowly, localize to the late endosomal vesicles instead of the cytoplasm where they remain as quiescent intracellular reservoir (QIR) (6, 48, 54-56). The quiescent state of these bacteria does not interfere with the differentiation process of the epithelial cells and thus QIRs are maintained within infected cells until they have fully differentiated into superficial facet cells

(54). Localised in the superficial cell layer, the QIRs of UPECs are capable of re-emerging into the bladder and cause a recurrent UTI even after a long period without symptoms and the absence of bacteria in the urine. The pathogenesis described above indicates that acute episodes of cystitis might be associated to IBC formation while bacteria that asymptotically dwell within epithelial cell layers reside QIRs. However, it was not yet possible to fully proof such a hypothesis, and elucidate the processes and conditions, which result in IBC and QIR formation, respectively (6, 47-49, 54-57). Indeed, the establishment of IBCs and even QIR has been reported for several UPECs isolates as well as *K. pneumonia* (58, 59), which indicates that this pathogenesis is not strain specific but rather a common process used by uropathogens. Although the pathogenesis behind IBC and QIR formation have only been studied in murine infection models, IBCs and filamentous UPECs have also been detected in exfoliated cells from the urine of human cystitis patients (60). Thus it is likely that IBCs and the underlying pathogenesis remains conserved among different UTO susceptible hosts.

3.4 Temporal processes involved in the formation of biofilms

Initiation and development of biofilms are conserved among most bacteria that form biofilms and apply to pathogenic as well as non-pathogenic bacteria. It involves transition through distinct stages of multicellular organisation accompanied by the expression of a coordinated set of genes (Figure 2). The initial stage is represented by planktonic bacteria, which are capable to move within their surrounding environment. This movement can be active e.g. through flagella or type IV pili, passive through Brownian motion or gravitational forces. Under certain circumstances and environmental signals such as nutrient availability, pH, temperature, ionic force of the medium surrounding the planktonic bacteria, or the nature of the surface, bacteria reversibly attach and induce gene expression of factors that stimulate biofilms formation (61-63). On abiotic surfaces such as polyvinylchloride (PVC) this weak initial interaction is non-specific and often involves a motility apparatus such as flagella or type IV pili (64). Non-motile bacteria lacking flagella or type IV pili might use other factors for initial contact with a surface, for example curli fimbriae (65) or conjugative plasmids (66), which can replace the force generating movements of flagella (67). The switch between reversible and irreversible surface attachment of bacteria occurs through the expression of adhesive proteinaceous organelles of the fimbrial family, which strengthen the bacteria-to-surface interactions. Examples include curli fimbriae, conjugative pili or type I fimbriae, structures that have all been determined as virulence factors in different pathogenic *E. coli* strains but also aid in bacterial attachment to surfaces or host cells. (42, 64, 66-72). (Type I

fimbriae and their relevance as a virulence factors will be explained in detail in chapter 3.7). Upon cell division of irreversibly attached bacteria or translocation of cells across surfaces, inter-bacterial adhesions and three-dimensional growth of the microcolony into a mature biofilm occurs (67, 73).

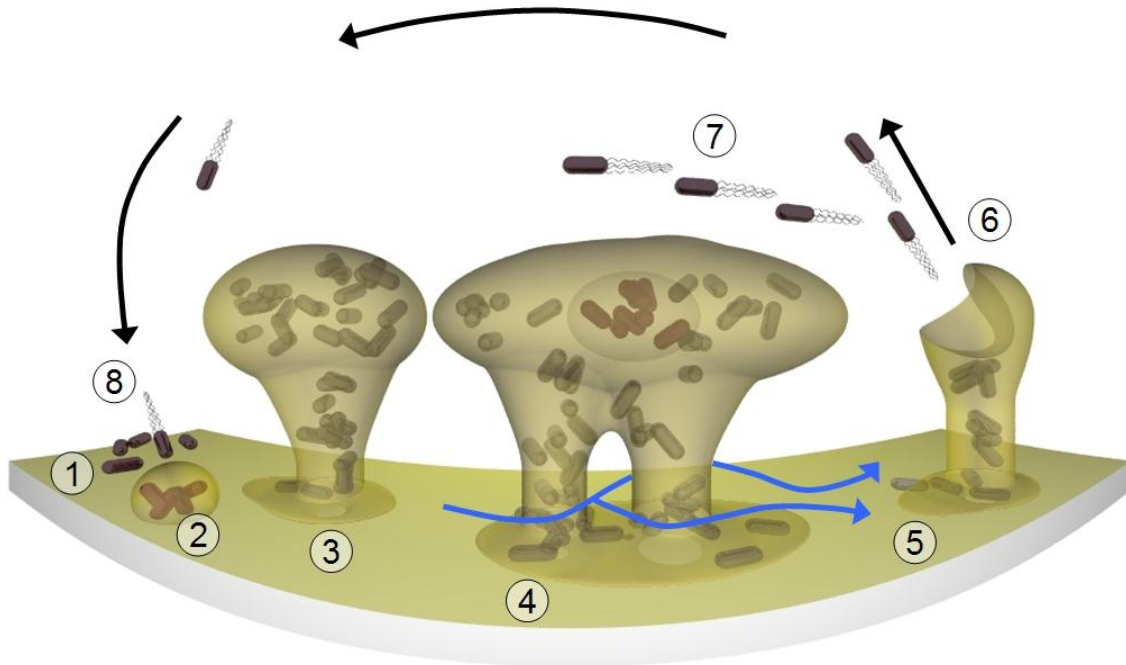


Figure 2: The formation of Biofilms

The formation of biofilms is a temporal process, which can be subdivided into eight steps. The first step involves initial contact and interaction of bacteria with a surface (1). Growth of bacteria on the surface results in the formation of microcolonies (2), which are characterised by bacteria-surface interactions (e.g. via type I fimbriae). The production of EPS including PGA results in bacterium-bacterium interactions and the formation of three-dimensional structures (3). Maturation of this structure guarantees among others a hydrated environment with channels responsible for fluid and nutrient influx and waste product disposal (4). Finally, the biofilm and its bacterial community start to age (5) and bacteria at the periphery regain their motility and dissociate from the biofilm (6) re-entering their planktonic lifestyle (7). The cycle of biofilm formation is terminated once planktonic bacteria start to interact with surfaces again (8). Image was taken from cronodon.com/BioTech/Bacterial_Society.html

* * *

This three-dimensional structure is supported, and strengthened through the production of a matrix that embeds the bacteria and functions as protective scaffold between the cells. The “**extracellular polymeric substances**” (EPS) make up for 50 % to 90 % of the organic carbon within a biofilm (63). The nature of the polymers composing the EPS exhibit great variability, with a multitude of different chemical and physical properties (74), they are composed of different biopolymers, adhesive proteins, lipids, phospholipids, dead cells, or extracellular DNA, and can be quite heterogeneous, featuring adjustable physiochemical environments for bacteria (75). A biofilm’s EPS is highly hydrated, prevents desiccation and retains nutrients or metabolites (67, 75). Nutrient uptake and waste disposal is usually reassured in a mature biofilm matrix through the presence of channels, which infuse fluid

from the surrounding through the biofilm (76). Moreover, the EPS scaffold protects bacteria from the host defence by preventing the recognition of biofilm-enclosed bacteria and impeding bacterial accessibility (9, 77). In the scaffold of the biofilm matrix, bacteria have intense inter-bacterial interactions, cell-to-cell communication, facilitated horizontal gene transfer, protection against toxins, biocides and antimicrobial chemicals and long term persistence of a bacterial population. Numerous reports also document the importance of the bacterial second messenger c-di-GMP during the formation of biofilms (see chapter 3.6) (78-84). In many species including *E. coli*, and *Pseudomonas* (85-90) elevated levels of c-di-GMP result in an increased synthesis of EPS components, primarily proteinacious adhesins and exopolysaccharides (63, 67, 73, 75, 91, 92). Proteinacious adhesins are often involved in the irreversible attachment of bacteria to surfaces and host cells, and are expressed earlier than exopolysaccharides. In *E. coli*, the very heterogeneous family of proteinacious adhesins comprises several surface associated autotransporters like antigen 43, proteases, and a plethora of different fimbriae (67, 93-99). *E. coli* biofilms usually start to mature upon synthesis and secretion of several exopolysaccharides, including colanic acid (100, 101), cellulose (102), and poly β -1,6-N-acetyl-D-glucosamine polymers (poly-GlcNAc or PGA) (103, 104), the latter of which is extensively explained in chapter 3.4.1. Importantly, this large arsenal of proteinacious adhesins and exopolysaccharides in pathogenic and non-pathogenic bacteria offers the possibility to adapt the matrix of a biofilm according to its environmental conditions. Furthermore, lack of one specific factor can be compensated by other factors, at least *in vitro*. Such different matrix compositions under altered conditions however, require a tight and interlinked regulatory network whose investigations have only started recently (9, 105-109).

Finally, the last maturation steps of the biofilm life-cycle coincide with an aging phenomenon, in which some bacteria undergo age related cell death and lysis (110). Also, this late stage is usually associated with bacterial dissociation from the biofilm matrix. Passive dispersal results from sloughing of cells and erosion from the biofilm. Active dispersal occurs through the highly regulated process within a few differentiated bacteria of the biofilm that regain their motility and disseminate into the environment. These planktonic cells finally finish the life-cycle of a biofilm. One feature of these so called dispersal cells is to recolonize a new surface or a new host and re-initiate the life-cycle of biofilms (110-113).

3.4.1 The exopolysaccharide β -1,6-N-acetylglucosamine is synthesised by PgaABCD

Some environmental conditions, including carbon limitation might push bacteria to adapt their metabolism into glycogen synthesis. Glycogen synthesis and turnover was shown to be needed for optimal biofilm formation upon transition into stationary phase (114, 115). In *E. coli*, the biofilm induced mainly upon carbon limitation depends on β -1,6-N-acetylglucosamine (PGA). PGA promotes intracellular adhesion as well as attachment to surfaces in mature biofilms (116). It is synthesised by the PgaABCD machinery and consists of β -1,6 linked GlcNAc aminosugars (Figure 3) (103, 117). The PGA machinery of *E. coli* consists of four proteins encoded by *pgaA-D*, which are transcribed as a poly-cystronic *pgaABCD* mRNA. The heterotetrameric machinery resides in the cell envelope where it uses UDP-GlcNAc as a precursor for the coordinated biosynthesis, partial deacetylation and export of PGA-polymers through the cell wall (Figure 3). Synthesis of PGA fully depends on PgaC and PgaD where PgaC functions as a glycosyltransferase in the inner membrane and executes the catalysis of PGA polymerisation from the UDP-GlcNAc precursor. The small inner membrane bound PgaD was shown to be essential for PGA biosynthesis although its precise role was not yet determined (103, 118, 119). PgaB is involved in partial *N*-deacetylation of PGA and is required for proper export of the polymer through the PgaA porin, which spans the periplasm and the outer membrane of *E. coli* (119).

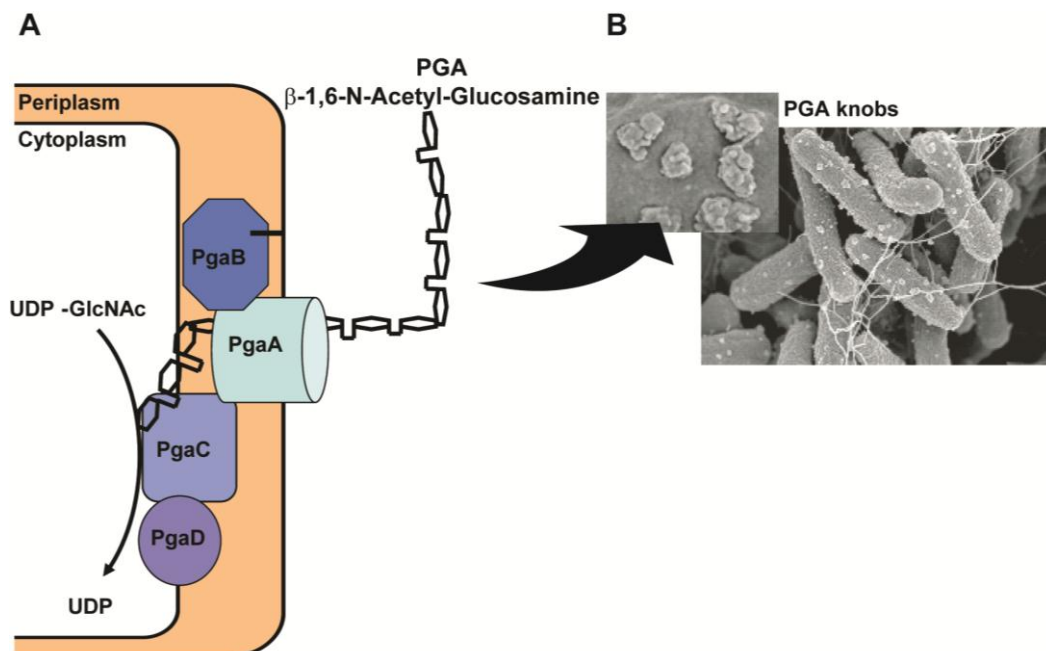


Figure 3: Synthesis of poly β -1,6-N-acetylglucosamine in *E. coli*

Poly β -1,6-N-acetylglucosamine (PGA) is a sugar polymer of *E. coli*. **A**) PGA synthesised by a membrane spanning machinery encoded by *pgaABCD*. The large PgaA protein forms a pore, which is essential for the

synthesis and spans the periplasm and the outer membrane. The lipoprotein PgaB is required for partial *N*-deacetylation of PGA and is also essential for export of the polymer through the PgaA porin. Together with the unknown function of PgaD, the glycosyltransferase (PgaC) executes the catalysis of PGA polymerisation from the UDP-GlcNAc precursor in the inner membrane. **B)** Electron microscopy pictures of PGA knobs found on the bacterial surface. Adapted from T. Romeo

Once synthesised and exported, PGA serves as an adhesin that stabilizes biofilms (103, 120) and forms knobs on the surface of bacteria (Figure 3B). Similar to its role as an adhesin in pathogenic Gram positive bacteria (104, 121-123), PGA was recently shown to be encoded and expressed in pathogenic *E. coli* strains isolated from the blood or the urinary tract (124). After *intra-peritoneal* injection of lethal doses of pathogenic *E. coli* strains, mice were protected by administration of antibodies raised against staphylococcal PGA (124). Thus, it appears that PGA is expressed by different pathogenic *E. coli* strains during infection and might serve as an important pathogenic trait during *E. coli* pathogenesis.

3.4.2 The regulation of PGA synthesis

The expression of *E. coli pgaA-D* is mainly controlled on transcriptional and translational level. Transcription of *pgaA-D* depends on its sole transcriptional regulator NhaR, which recognizes and binds to the single promoter of *pgaA-D*. NhaR is a DNA binding protein that belongs to the family of LysR type transcriptional regulators (LTTRs). LTTRs respond to elevated concentrations of sodium (125) and alkaline pH (126) by changing the conformation of the LTTR-DNA complex. NhaR was shown to be a virulence factor during UTIs caused by *Proteus mirabilis* (127) and has been suggested to promote survival of *E. coli* (126). On translational level, the expression of *pgaA-D* is controlled by CsrA, which binds the 5' leader sequence of *pgaA-D* and *nhaR* mRNA and inhibits the initiation of translation (117, 128).

3.5 The Carbon Storage Regulator (Csr) system

3.5.1 The carbon storage regulator system and its central role in bacterial physiology

The existence of global regulators, which function as a switch between different lifestyles greatly facilitate bacterial adaptation to altered conditions, especially since global regulators often inversely regulate antagonistic pathways. One of these global regulators is the **Carbon Storage Regulator A** (CsrA), the central component of the Csr system. This 61 amino acid homodimeric protein was first identified in 1993 in a transposon mutagenesis

screen where the hit in *csrA* resulted in glycogen accumulation compared to the *E. coli* wild type (129). Further analysis showed that CsrA has an important regulatory role during carbon metabolism in general. It inhibits the storage of energy through gluconeogenesis and glycogenesis while stimulating glycolysis (130-132). Almost ten years after its initial discovery CsrA has been shown to regulate many other unrelated processes including biofilm formation (117, 133, 134), motility (135, 136), secondary metabolite production (136), environmental stress resistance (135, 137), cytotoxic factor production (134, 137), interaction with animal and plant hosts (134, 137, 138), quorum sensing (139), or oxidative stress (140). The regulatory influence by the Csr system is enabled by a unique mechanism, in which the RNA binding protein (CsrA) modifies the stability and/or translation of mRNAs and hence imposes a post-transcriptional level of control (115, 132, 141). In many cases CsrA prevents translation of mRNAs by binding to the 5' leader of the transcript near the Shine-Dalgarno sequence and thus disables ribosomes from initiating translation. Lack of translation upon binding of CsrA often activates transcript degradation by endonuclease attack. The best characterised mRNA targets of CsrA are: i) the *glgCAP* encoding glycogen biosynthetic proteins (132), ii) the transcriptional regulator *nhaR* (128), or iii) *pgaA-D* (117) (see chapter 3.4.1 and 3.4.2). The mRNA of *pgaA-D* contains six distinct CsrA binding sites, one of which overlaps with the start codon of *pgaA*. Four of the remaining CsrA binding sites lie in the untranslated leader sequence of the mRNA and the last one overlaps the Shine-Dalgarno sequence, thus competing with the 30S subunit of the ribosome (117). Bound CsrA destabilizes the transcript of *pgaA-D* mRNA, and enhances its decay, which impedes PGA dependent biofilm formation. Besides inhibition of mRNAs, CsrA stabilizes some mRNAs and activates their gene expression by protecting the transcript's degradation. A prominent examples of mRNA stabilisation by CsrA is the master transcriptional regulator of flagellum biosynthesis *flhDC* (142).

The translation of many transcripts depends on the cellular concentrations of CsrA, which requires a tight and reactive regulation thereof, especially since modulation of CsrA levels often result in physiological adaptations. An example would be the transition from planktonic to sessile bacteria, in which CsrA can be seen as a checkpoint affecting signalling cascades that contribute to biofilm formation (Figure 4). Optimal biofilm formation requires glycogen synthesis and glycogen turnover but also synthesis of PGA, all of which are repressed by CsrA (103, 114, 143). Furthermore, CsrA inhibits *glgCAP* expression, which is necessary for carbon flux into glycogen and subsequent conversion of glycogen into glucose-1-phosphate (a possible precursor of PGA), hence indirectly repressing PGA synthesis. With respect to such dramatic and often irreversible effects, the input(s), which govern the active levels of CsrA, have to be tightly controlled and contain several feedback loops that stabilize the system.

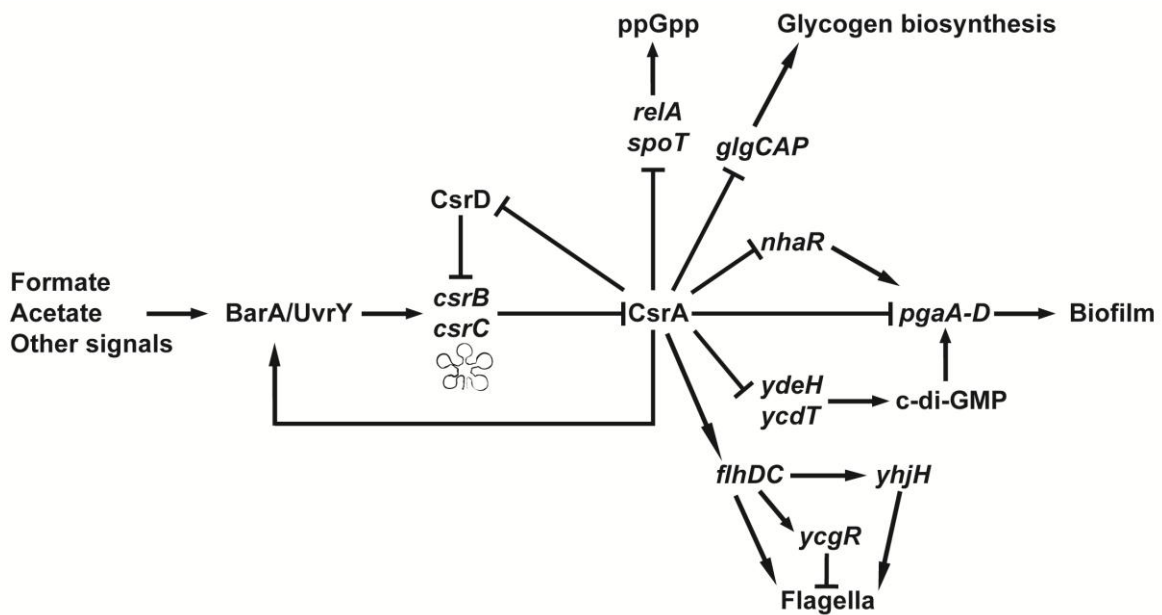


Figure 4: Schematic representation of the Csr System

Regulation by Csr is limited to genes, which are involved in the transition of from planktonic to sessile bacteria. Positive effects are indicated with regular arrows, negative effects are indicated as (τ). The BarA/UvrY two component system (TCS) gets activated by different signals including formate, acetate, weak acids or Krebs cycle intermediates and upon activation positively regulates the small noncoding RNAs *csrB* and *csrC*. The RNAs *csrB* and *csrC* negatively control the activity of CsrA through sequestering the protein. Feedback control of the Csr system is ensured by CsrD, which targets *csrB* and *csrC* for RNase E mediated degradation and by a positive effect of CsrA on the BarA/UvrY TCS. CsrA binds to the 5' untranslated region of mRNAs, which can either result in mRNA stabilisation (e.g. *flhDC*) or interfere with translation initiation and enhanced destabilisation (e.g. *pgaA-D*; *ydeH*; *ycdT*; *nhaR*; *glgCAP*; *csrD*; *relA* and *spot*). Several c-di-GMP metabolising enzymes are tightly linked to the status of the Csr system (e.g. YdeH and YcdT). A repressed Csr system results in high CsrA levels, which is associated with planktonic bacteria and favours the expression of the PDEs YhjH and the c-di-GMP receptor protein YcgR. YhjH and YcgR together regulate flagellation of bacteria. De-repression of Csr system, e.g. upon entry into stationary phase results in low activity of CsrA, which again results in the expression of the DGCs YcdT and YdeH and thus elevated level of c-di-GMP. Elevated levels of c-di-GMP are associated with sessile bacteria and the formation of bacteria.

* * *

3.5.2 Post-translational regulation of CsrA levels

The level of active CsrA is controlled post-translationally by two small non-coding RNAs (snRNA) called *csrB* and *csrC* (Figure 4). These two snRNA sequester CsrA through their multiple CsrA binding sites (139, 144-146) with the consensus sequence 5'-RUACARGGAUGU-3' (R = purin). The GGA motif of this sequence mostly localises in the loops of predicted hairpins in *csrB* and *csrC* where it increases the affinity of the cooperative CsrA-RNA interaction (139, 147). Interestingly the snRNAs known to sequester CsrA vary greatly in sequence and also in their number of CsrA binding sites. The 366 nucleotide long

csrB comprises 22 potential CsrA binding sites and was shown to sequester up to 9 CsrA dimers (145). The shorter *csrC* (245-nucleotides) only has 13 potential CsrA binding sites (144). Up to this point, the importance of the redundancy of *csrB* and *csrC* in *E. coli* remains unclear although it is believed that these two snRNAs might partially respond to different inputs. Similar to the distribution of CsrA in the bacterial kingdom, functional homologs of *csrB* and *csrC* can be found in many different species.

It has been shown that *csrB* and *csrC* have a short half-life of ~ 1.5 – 4 minutes, thus enhanced turnover of *csrB* and *csrC* further contributes to the effectiveness and responsiveness of the Csr system. The turnover is mediated through degradation by RNase E and is enhanced by CsrD in an unknown mechanism (148). CsrD is a membrane bound protein with two domains usually associated to the synthesis (GGDEF-motif) and degradation (EAL-motif) of the bacterial second messenger c-di-GMP (see chapter 3.6). While both motifs have degenerate key residues in their GGDEF and EAL motifs and therefore do not influence the levels of the second messenger, the EAL motif was shown to be necessary for degradation of *csrB* and *csrC* by RNase E (148).

Several direct or indirect negative feedback loops within the Csr system exist, which promote homeostasis of CsrA levels under constant environmental conditions and allow quick adaptation of CsrA levels upon environmental alterations (Figure 4). One of these feedback loops affects *csrD* expression of *E. coli* (*yhdA*) and *S. typhimurium* (STM3375), and is imposed by the negative effects of CsrA on *csrD* translation (149, 150). The second known feedback loop is more indirect and involves the two-component system (TCS) BarA/UvrY, which is wide spread in the bacterial kingdom (151). In *E. coli* BarA is the sensor kinase of the TCS while UvrY is its cognate response regulator (146). Activation of this TCS was shown to cause elevated levels of the snRNAs *csrB* and *csrC* during the transition into stationary phase (144, 152) and hence results in an increased sequestration of CsrA. One of the components capable of activating the BarA/UvrY phosphorylation relay is CsrA itself. Until this TCS gets activated by an alternative signal, CsrA indirectly controls its own activity by stimulating *csrB* and *csrC* expression. Besides CsrA, the BarA/UvrY TCS has been shown to be triggered in a pH dependent manner (153), an imbalance in Krebs cycle intermediates (154), or weak acids including formate or acetate (155). Interestingly, asymptomatic *E. coli* strains used for treatment of severe UTIs were shown to have elevated levels of *csrB* and *csrC*, if grown in urine or re-isolated from patients (156, 157). However, it is not known whether the elevated levels of the small RNAs is due to intrinsically activated BarA/UvrY TCS in asymptomatic UPECs once in the urinary tract. Recently it was shown that two components of the stringent response (DksA and ppGpp; see chapter 3.6.4) interacted with the Csr system on various levels. They activated the transcription of *csrB* and *csrC*

suggesting that the CsrA mediated regulation is relieved during the stringent response (158). However, CsrA also represses the translation of the ppGpp synthase gene *relA*, indicating that the Csr system might fine-tune the stringent response according to the environment (158).

3.6 Bacterial second messengers modulate *E. coli* lifestyles

Bacteria assess and register environmental signals and translate them into appropriate output system. Depending on environmental conditions, bacteria have to decide whether the conditions are favourable enough to persist within the colonised niche or whether movement into a new environment might enhance their fitness and survival. This vital switch between sessility and motility is often irrevocable and thus requires tight and robust control mechanisms (159). An important part in the molecular control mechanisms residing over sessility and motility can be assigned to the bacterial second messenger bis-(3'-5')-cyclic dimeric GMP, which is present in the vast majority of eubacteria (160). C-di-GMP translates environmental signals into appropriate output systems, e.g. motility via flagellar rotation or EPS production for bacterial adhesion (67, 161-165).

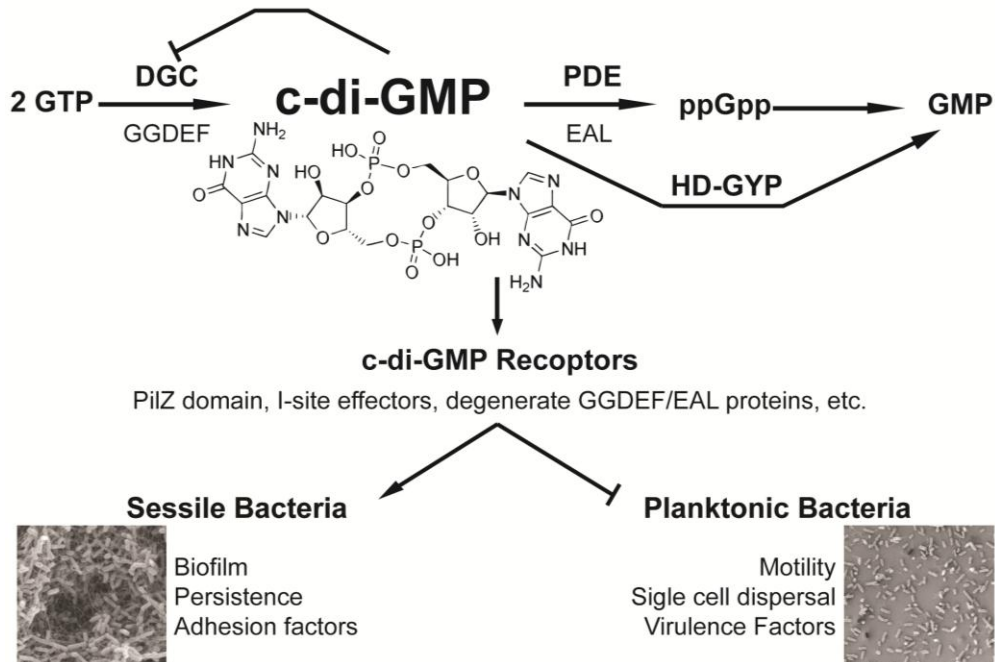


Figure 5: The principles of c-di-GMP signalling

C-di-GMP is synthesised from two molecules GTP in the active site of GGDEF domains, which are part of diguanylate cyclases (DGC). Elevated levels of c-di-GMP result in a non-competitive inhibition of DGC, as indicated by with the (τ) symbol. Degradation of c-di-GMP requires the activity of specific phosphodiesterases (PDE). Two types of PDEs exist, which contain unrelated domains: EAL containing proteins degrade c-di-GMP

into a linear intermediate (pGpG) that is then further processed non-specifically into two molecules of GMP. Alternatively, HD-GYP domains degrade c-di-GMP into two GMP molecules in one step. The intracellular concentration of c-di-GMP is detected by c-di-GMP receptors, which then signal to different output systems. High concentrations of c-di-GMP are generally associated with sessile bacteria while low levels of c-di-GMP are associated with planktonic bacteria. Illustration was adapted from Tamayo *et al.*, 2007 (164).

3.6.1 The bacterial second messenger c-di-GMP

C-di-GMP was first discovered in 1987 by Benziman and his co-workers in *Gluconacetobacter xylinus* where it allosterically activated the synthesis of cellulose (166). Biochemical analysis and reverse genetics identified two classes of multi-domain enzymes involved in synthesis and degradation of c-di-GMP (167). **diguanylate cyclases (DGCs)** contain the GGDEF domain while **phosphodiesterases (PDEs)** contain EAL domains (Figure 5). The enzymatic activity of DGCs requires the GG(D/E)EF motif, which defines the active site of the protein (A-site) (98, 168-180). Only upon dimerization of two DGCs the A-site, which is located at the dimer interface, becomes complete and active and synthesizes c-di-GMP. In the process of synthesising c-di-GMP each GG(D/E)EF motif binds and contributes one GTP and any alterations of the A-site abrogates c-di-GMP synthesis (170-173, 181). Most DGCs are subject to an allosteric product inhibition, imposed through binding of c-di-GMP with high affinity to the proteins inhibitory site (I-site). This I-site consists of the RxxD motif, which is located in the GGDEF domain but separated from the A-site through five amino acids and positioned distant from the dimer interface. Binding of c-di-GMP to the I-site avoids excessive consumption of GTP, buffers against stochastic variations in intracellular c-di-GMP concentration and most importantly sets an upper limit for the accumulation the second messenger (175). PDEs with EAL domains linearize c-di-GMP into 5'-phosphoguanylyl-(3'-5')-guanosine (pGpG), which is further transformed into two GMP molecules by nonspecific yet unidentified PDEs. The specific action of the first step requires the presence of an active monomeric EAL domain, which is named after the amino acids in the active site, and requires the presence of either Mg^{2+} or Mn^{2+} as co-factor (98, 174, 176-178). Recently, another family of proteins with specific phosphodiesterase activity was shown to degrade c-di-GMP. Their potential to degrade c-di-GMP was associated to the HD-GYP domain, which is completely unrelated to the EAL domain (182). HD-GYP domain proteins are members of the metal-dependent phosphohydrolase superfamily and were shown to degrade c-di-GMP into GMP in one step (179).

3.6.2 C-di-GMP input systems and c-di-GMP receptor proteins

The era of whole genome sequencing has shed some light on the vast abundance and distribution of GGDEF, EAL and HD-GYP containing proteins and has provided substantial

evidence that these families of signalling proteins together with c-di-GMP are near-ubiquitous in eubacteria (183). Sequence analysis of GGDEF and EAL domains has further shown that most of these domains are linked directly or indirectly via a two-component phosphorylation cascade to a signal input domain (184). These signal input domains (including PAS, blue light sensing (BLUF), haemerythrin, GAF, CHASE and MASE domains) link numerous environmental and intracellular signals to the production of c-di-GMP and create a diverse set of modules, each of which translates into a defined physiological output system. In these modules c-di-GMP acts as a second messenger that positively or negatively affects specific and often important cellular functions. Some of the best characterised functions are the formation of biofilm through biosynthesis of adhesins and exopolysaccharide matrix components (e.g. PGA; see chapter 3.4.1 and 3.4.2) (133, 168, 185-192), regulated proteolysis or cell cycle progression (180) and bacterial virulence (165, 177, 193-197).

In order to fulfil these diverse functions, c-di-GMP must be sensed or bound by an effector molecule, which then transmits the signal to a specific output system (Figure 5). So far, several different types of c-di-GMP sensing and signal transfer system have been found. Many of the identified effectors belong to the PilZ family of proteins, which are activated upon binding of c-di-GMP. PilZ proteins translate the signal through protein-protein interactions into several different cellular outputs (189, 198-202). The first identified protein of this family was PilZ of *Pseudomonas aeruginosa* where it has a negative effect on twitching motility (198). In some cases, PilZ domains remained attached to the C-terminus of the GGDEF, EAL or HD-GYP domains. In other cases a PilZ domain is linked to a protein directly involved in generating an output, for example cellulose or alginate synthases (189, 203, 204). Other recently identified c-di-GMP effector proteins show no homology to PilZ proteins. One of these proteins is FleQ (205), which is a master regulator of flagellar gene expression in *P. aeruginosa* and functions as a c-di-GMP effector protein. Upon binding of c-di-GMP, the association of FleQ with the *pel* promoter is released and the *pel* operon gets derepressed, which results in the production of the Pel exopolysaccharide. Another class of effector proteins bind c-di-GMP at a site, which resemble an I-site (191). An example from this class is PleD of *P. aeruginosa*. The fourth known type of effectors is often represented by PopA of *Caulobacter crescentus*. PopA has a GGDEF domain with a degenerate and thus inactive A-site, but contains a canonical I-site that can still bind c-di-GMP. It was shown that its action requires an intact I-site but not its A-site for correct functioning. Upon binding of c-di-GMP to the I-site PopA migrates to the cell pole of *C. crescentus* where it exerts its crucial function in cell cycle control (180). The example of PopA shows that evolution of GGDEF (and/or EAL) domains can result in molecules that have lost their metabolising activity but gained a function, which transduces a signal upon binding to c-di-GMP (161). An example of a protein with a degenerate and enzymatically inactive EAL domain with retained c-di-GMP binding is

LapD of *P. fluorescence*. It controls biofilm formation by communicating the intracellular c-di-GMP concentration to a membrane associated attachment machinery (206). Several other degenerate GGDEF and/or EAL proteins have been identified and linked to a cellular output recently. However, it still needs to be proven that the novel function of these proteins still involves binding of c-di-GMP. An example would be CsrD of *E. coli*, which harbours a degenerate GGDEF and a degenerate EAL domain. Both domains are catalytically inactive but necessary for its function in mediating the RNase E dependent degradation of the small RNAs *csrB* and *csrC* (see chapter 3.5) (148). Aside from this diverse group of c-di-GMP binding proteins, it was recently described that conserved RNA domains known as riboswitches and present in the 5' untranslated region of different mRNAs are also capable of specifically binding c-di-GMP (207, 208) adding a new class of effector molecules to the rapidly growing list.

3.6.3 Regulation of c-di-GMP metabolism

The number of DGCs, PDEs and c-di-GMP effectors or receptors varies greatly within different bacteria. Besides the few species with no reported c-di-GMP metabolism e.g. *Haemophilus influenzae* and some bacteria with as much as 98 (*Shewanella oneidensis*) GGDEF, EAL or HD-GYP domain proteins, the majority of eubacteria encode for an intermediate number thereof. In *E. coli*, the number of GGDEF, EAL or HD-GYP domain proteins even varies between different strains. The non-pathogenic *E. coli* MG1655 strain harbours 9 EAL, 12 GGDEF and 7 GGDEF/EAL composite proteins. Pathogenic *E. coli* have lost one GGDEF domain protein (YddV) but have gained either one or two EAL domain proteins (homologs of Q0TL46 and Q0TDN1), which are associated with different pathogenicity islands. The abundance of GGDEF and EAL domain proteins generates a flexibility of signalling but raises the question of system redundancy and signal specificity. The question arises how the c-di-GMP network system can get buffered against signalling noise and unspecific signal transduction upon variations in c-di-GMP. The specificity of signal transduction can be controlled through protein expression levels, protein stability, specific activity of DGCs or PDEs, as well as through different affinities of binding sites for c-di-GMP. However, these levels of control might circumvent unwanted crosstalk between different c-di-GMP dependent regulatory pathways. This emphasises on the question whether all proteins involved regulate one global c-di-GMP pool or whether defined c-di-GMP modules act on separate local pools. Global and/or local pools call for some sort of distribution, in which not all proteins are present and active at the same time and location within the cell. Temporal distribution of c-di-GMP would limit the type and number of GGDEF and EAL domain

proteins expressed under specific conditions and allow switching to another set upon alterations in the environment (190, 192). An example of such a temporal distribution is the regulation of the switch between flagellar motility and adhesion at the transition from late exponential to stationary phase in *E. coli*. In this example, YcgR interacts with MotA upon binding of c-di-GMP and reduces the rotational speed of flagella and thus overall motility, which in turn favours bacterial adhesion at the transition into stationary phase (81). The PDE YhjH enhances motility upon degradation of c-di-GMP. Both YhjH and YcgR are under the control of the flagellar master regulator FlhDC and are thus co-regulated with flagella. FlhDC regulated genes are expressed in early stages of growth but are downregulated at the transition into stationary phase (142, 190, 209-212). The conditions, which disfavour flagellar expression favour the expression of the DGCs YdeH and YcdT in a CsrA dependent manner (Figure 4). In stationary phase intracellular c-di-GMP levels increase and allow PGA dependent adherence. In this example, the activities of YhjH and YcgR are separated in time from the activities of YcdT and YdeH. As indicated in chapter 3.5, the basis of this temporal distribution of c-di-GMP metabolising enzymes partially depends on the levels of the carbon storage regulator CsrA (117, 133, 139, 213).

Temporal distribution however, is not conceivable with a situation where several independent but parallel pathways are required. The presence of several parallel c-di-GMP signalling pathways would rather support the model of spatial and functional distribution of DGCs, PDEs and effector proteins into “micro compartments” with local c-di-GMP pools (179, 210, 214, 215). The likelihood of such micro-domains is supported by the domain architecture of proteins where GGDEF, EAL or HD-GYP domains are covalently linked to putative output domains and possibly sequester c-di-GMP to the protein’s close surrounding (204). In *E. coli*, the DGC YegE and the PDE YhjH control flagellar motility and modulate the transcription of *csgD*, the activator gene of curli. However, the DGC YdaM and the PDE YciR, which get expressed under the same conditions as YegE and YhjH affect the expression of *csgD* but not flagellar motility (190, 210) and hence some of the output systems require to be uncoupled from parallel pathways in order to fulfil their highly specific and locally confined functions. Similar examples can be found in several articles and reviews (161, 168, 192, 212, 214, 216). The water bacterium *C. crescentus* is an excellent model organism for spatial distribution of GGDEF, EAL and effector proteins as its asymmetric cell-division requires localisation of c-di-GMP dependent proteins at the cell poles during cell-cycle progression (170, 180, 217, 218).

In the end, bacterial cells have evolved a wide range of diverse regulatory mechanisms to monitor the activity of DGCs and PDEs including control of protein levels, protein activity and stability, allosteric binding, phosphorylation of covalently bound domains in the protein,

or localisation of c-di-GMP modules to micro-domains within the cell. Despite the scarcely identified target molecules and effector mechanisms involved in c-di-GMP signalling, c-di-GMP was revealed to control cellular functions at transcriptional, translational and even posttranslational levels (79, 80, 210, 219, 220).

3.6.4 The bacterial alarmone ppGpp

Independent of the environment in which bacteria reside, nutrients will become limiting at some point. Upon starvation bacteria produce the stress alarmone ppGpp (Guanosin-3',5'-bispyrophospha). RelA, which synthesises ppGpp and SpoT, which synthesises and degrades ppGpp, control the cellular levels of ppGpp. PpGpp is synthesised via RelA upon amino acid starvation but it is also synthesised in response to deprivation of carbon sources, fatty acids, iron or phosphorous. However, under these conditions SpoT catalyses the synthesis of ppGpp (221). The ppGpp response to starvation is generally referred to as stringent response and affects transcription, translation or replication of many genes and many cellular processes, including PGA dependent biofilm formation in *E. coli* (133, 222). When ppGpp levels are low in *E. coli*, PGA dependent biofilm formation is maximal. Thus, ppGpp links PGA dependent biofilm formation to ribosomal stress (133, 222). Recently, ppGpp has also been linked to the Csr system (see chapter 3.5) shown to be under the control of CsrA (133, 158). This clearly indicates the regulatory complexity behind the induction of biofilms at the transition into stationary phase. Furthermore, ppGpp has also been reported to modulate the expression of type I fimbria, which play a role in attachment of bacteria to a surface or host cells and promote virulence during UTIs (223, 224).

3.7 Fimbriae and Pili in bacteria

Long bacterial protrusions named pili or fimbriae serve bacteria to overcome net repulsive forces derived from the negatively charged bacterial and host-cell membrane. They also serve as mediators for host-pathogen interactions through their action as adhesins. Surface-exposed adhesins improve binding of UPECs or other pathogens to host tissue, interactions required for successful colonisation. In the host-pathogen interaction the fimbrial adhesin functions as lectin, which recognizes oligosaccharide residues of glycoprotein. or glycolipid-receptors exposed on the host cell surface. The combination of the expressed bacterial adhesion factor and the expressed host receptor determine the tropism of the pathogen toward a specific tissue, for example UPECs towards the urothelium lining the bladder lumen.

According to their assembly pathways, fimbriae can be subdivided into four distinct groups including i) type I fimbriae and P pili, which are assembled by the chaperone-usher pathway, ii) type IV pili, iii) pili assembled by the extracellular nucleation / precipitation pathway, (e.g. curli pili), and iv) pili assembled by the alternative chaperone-usher pathway, e.g. the CS1 pilus family (96). Despite the different assembly pathways, the pilus shaft or fimbrial rod of Gram-negative bacteria is generated by non-covalent homopolymerisation of the major pilus subunit protein called pilin. Rods can contain several hundreds if not thousands of the major pilin subunit. The addition of minor pilins to the shaft of the pilin fiber render fimbriae useful for functions aside from host cell adhesion, including biofilm formation, phage transduction, DNA uptake or twitching motility. With respect to the content of this dissertation, this introduction of fimbriae will focus on type I fimbriae and their role in host cell adhesion. Other types of fimbriae and their functions are detailed in several reviews (44, 96, 225).

3.7.1 Type I fimbriae of UPECs

Type I fimbriae can be found throughout the family of *Enterobacteriaceae* including UPECs. These type I fimbriae represent one of the most important and best-characterised virulence factor required for successful establishment of UTIs. Using electron microscopy the composite structure of the pilus rod was determined. It comprises a 6.9 nm thick and 1-2 mm long rod with 300-1000 major pilins (FimA) arranged in a right-handed helix. The end of the fimbrial rod is built by FimF, which connects the rod to the short 3 nm wide linear tip fibrillum (FimF, FimG, FimH) (Figure 6).

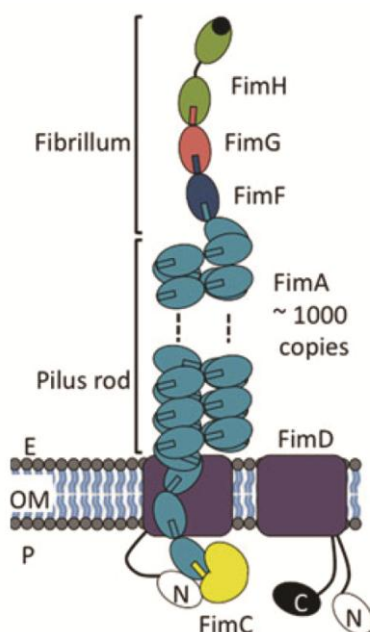


Figure 6: Type I Fimbriae of Gram-negative *E. coli*

Type I fimbriae are composed of four different pilin subunits. The helical pilus rod (turquoise) consists of up to several thousand FimA subunits and is connected to the fibrillum through the pilin FimF. Aside FimF the linear fibrillum consists of FimG and the adhesin FimH, which has an acidic pocket that can bind mannose and mediated adhesion to mannose receptor proteins on eukaryotic cells. The structure of all pilins consists of one (FimA, FimG or FimF) or two (FimH) incomplete Ig-like folds. The incomplete Ig-like fold gets transiently completed through the chaperone protein FimC or upon polymerisation of pilin subunits. Polymerisation of pilin subunits requires the periplasmic chaperone protein FimC and the membrane bound usher FimD. Translocation of pilin subunits into the periplasm occurs via the SecYEG pathway. (E: extracellular milieu; OM: outer membrane; P: periplasm) This figure was adapted from Geibel S. and Waksman G. 2010 (9).

* * *

While the fimbrial rod remains rigid, the tip fibrillum with the monomeric FimH at its tip remains flexible (225-227). *FimH* encodes the type I fimbrial specific adhesin (228, 229), which contains an acidic pocket at the distal tip that accommodates mono-mannose oligosaccharides and is responsible for the adhesive properties of type I fimbriae. Consequently, the adhesin binds to surface exposed glycosylated receptors, which contain accessible mannose moieties (230-233). Prominent receptors for FimH are the uroplakins UP1a, which line the luminal surface of the urothelium as a protective coat (45, 234) or β 1 and α 3 integrins (46). The uroplaking UP1a presents high amounts of terminally exposed mannose residues, which are specifically bound by FimH. The structure of FimH revealed a two-domain fold, which separates the C-terminal pilin domain from the N-terminal receptor-binding domain comprising the mannose binding pocket. Both C- and N- terminal domains have an immunoglobulin (Ig) –like fold (230). Importantly, the Ig-like fold of pilin domain remains incomplete, as it misses the seventh strand. This strand is usually provided by either the chaperone FimC or by another pilin subunit, as explained in chapter 3.7.2 that follows.

3.7.2 The chaperone/usher dependent assembly of type I fimbriae

Upon expression of the *fimAICDFGH* genes, they are secreted into the periplasm via the SecYEG translocon of the type II secretion system. In the periplasm the pilins FimA, FimF, FimG, FimH form a stable complex with FimC, a chaperone protein with boomerang-like shape and composed of two ig-like domains. The interactions of the chaperone-pilin subunit were revealed for the FimC-FimH complex by X-ray (230, 235). In this structure it became visible that the pilin subunits have an Ig-like fold composed of six β -strands that harbour a hydrophobic groove, which needs to be filled with a seventh β -strand for stabilisation. This seventh β -strand is provided either by other pilin monomers or transiently by the chaperon FimC. The interactions between FimC and the pilins in the hydrophobic groove are based on alternating hydrophobic chaperone residues of the G1 donor strand, which interact with hydrophobic residues of the F β -strand of the pilin. This protein-protein interaction is denoted “donor strand complementation” (236). During donor strand complementation, the donor β -strand G1 of the chaperon runs parallel to the pilin’s F β -strand (Figure 7).

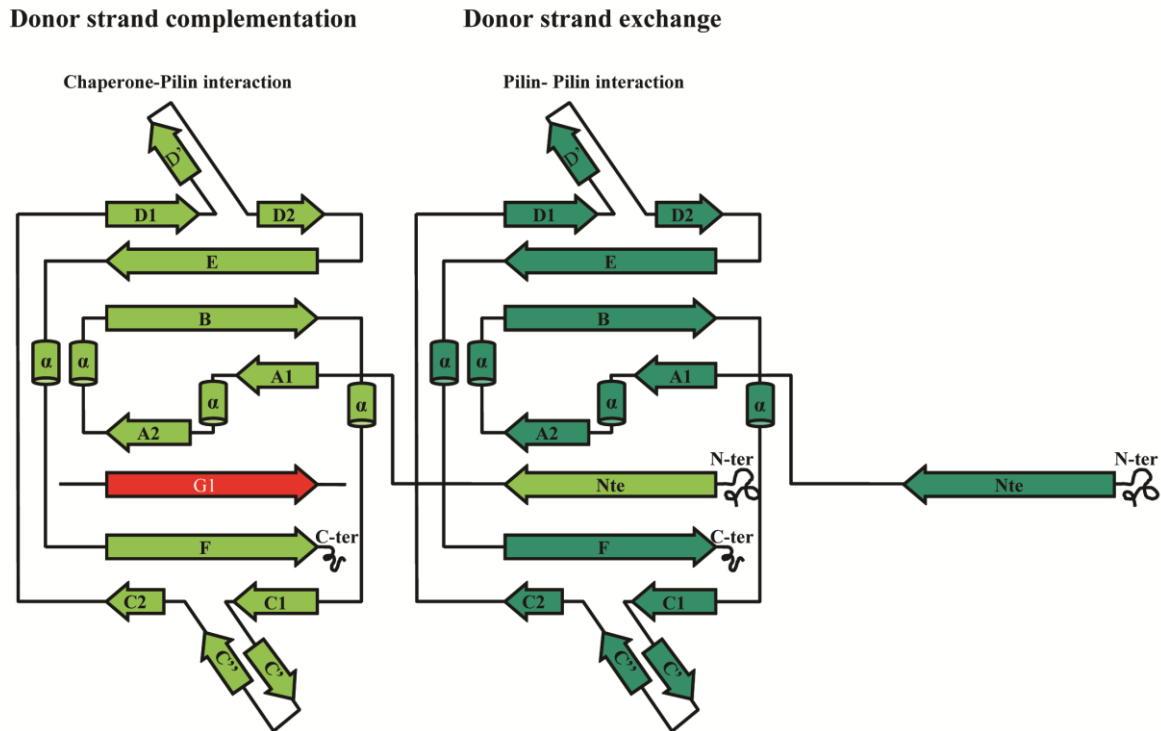


Figure 7: Ribbon model of Ig-like folds during donor strand complementation and donor strand exchange

Biosynthesis of type I fimbriae occurs in the periplasmic space via the chaperone usher pathway. Once pilins (light and dark green) have reached the periplasmic space, they bind to a specific chaperone (FimC; red), which prevents premature assembly of the subunits and aids in proper protein folding via donor strand complementation. The pilin/chaperone (light green/red) complex is then transported to the usher protein (FimD) localised in the outer membrane where donor strand exchange occurs. The interactions in the ternary FimC-pilin-FimD complex result in a stepwise replacement of the chaperone's β G1 strand (red) with the Nte of the pilin subunit. Other than in FimC-pilin interaction the Nte gets inserted into the preceding pilin groove (dark green) in an antiparallel fashion and thus complements the Ig-like fold. The interaction of the Nte of the newly incorporated pilin (light green) with the F strand of the preceding pilin (dark green) are known as donor strand exchange. For more details see text. The ribbon models illustrated here were derived from the Pap-pilins, which are homologous to the Fim-pilins. Image was adapted from Geibel S. and Waksman G. 2010 (9).

* * *

Once the FimC-FimH complex is formed, the transient chaperone-pilin complex is guided to the FimD usher. The usher, a homodimeric channel spanning the outer membrane, catalyses the polymerisation of the pilus subunits and can be subdivided into four functional domains: i) an N-terminal periplasmic domain required for chaperone-pilin recognition and pilus assembly, ii) a domain encoding the central translocation pore, which is located in the outer membrane and mostly consists of antiparallel β -sheets, iii) a plug domain, which

resides within the translocation pore and is required for pilus assembly, and iv) a C-terminal periplasmic domain, which is also required for proper binding of the chaperone-pilin complex (225). The usher catalyses the ordered assembly of pilin subunits while releasing the chaperon and simultaneously translocating the growing pilus to the outer surface (237). This process is called “donor strand exchange” and results in a growing pilus that protrudes through the outer membrane. Donor strand exchange by the usher is similar to the donor strand complementation but with some important differences: Besides their incomplete Ig-like fold, each pilin subunit comprises a 10-20 amino acid long N-terminal extension peptide (Nte) with 4 alternating hydrophobic residues, essential for polymerisation. During polymerisation of pilus rod, the Nte of an incoming pilin takes over the position of the chaperone’s G1 β -strand of the previously incorporated pilin (Figure 7) (238). This replacement occurs progressively by exchanging one hydrophobic residue after another, resulting in a ternary chaperone-pilin-Nte complex. Other than the chaperone’s G1 β -strand, the Nte interacts with the pilin’s F β -strand in an antiparallel fashion and thus completes the canonical Ig-fold (237, 239). Based on the mechanism of donor strand exchange and the fact that the tip of the pilus is composed of FimH, FimH does not require an Nte, and serves as first pilin integrated into the “empty” usher FimD (238). The ordered assembly of the pilus relies on the higher affinity of the usher for the chaperone-adhesin complex, rather than the adhesin or chaperone alone. It also depends on the specific recognition of the FimH lectin domain by FimD (240). Once FimH is bound to FimD, the catalytic activity of the usher gets enhanced through an increased donor strand exchange rate between FimC-FimA complexes. Furthermore, bound FimC-FimH results in a conformational change in FimD, which moves the plug domain located inside the translocation pore aside, and thus allows pilus growth. Once FimD incorporates FimH, correct assembly of the tip fibrillum and the whole pilus is reassured by the different affinities of the Nte for their cognate pilin. Presumably, also the N-terminus of FimD is capable of discriminating between different pilin subunits, as it was shown to specifically interact with them (237, 241). Importantly, the energy, which drives pilus assembly, is stored in the fold of the chaperone-pilin intermediates and gets released upon donor strand exchange (238).

3.7.3 Regulation of type I fimbriae and the phase variation of *fimS*

The promoter for the expression of type I fimbriae is located on a 314 bp long invertible DNA element termed *fimS*, which precedes the structural *fimAICDFGH* genes (Figure 8). This *fimS* is essential for the typical phase variable expression known for type I fimbriae, in which the structural genes of type I fimbriae are only expressed if the promoter on *fimS* is

oriented towards the *fim* structural genes (ON phase). In the OFF phase, the promoter is directed away from the structural genes and hence bacteria remain non-fimbriated (242-244). The inversion of *fimS* involves two inverted repeats (IRs) encoded by the 5' TTGGGGCCA 3' sequence flanked on both sides by *Fim* recombinase binding sites, termed half sites. Thus, *fimS* comprises four binding sites with different sequences and affinities for the *Fim* recombinases.

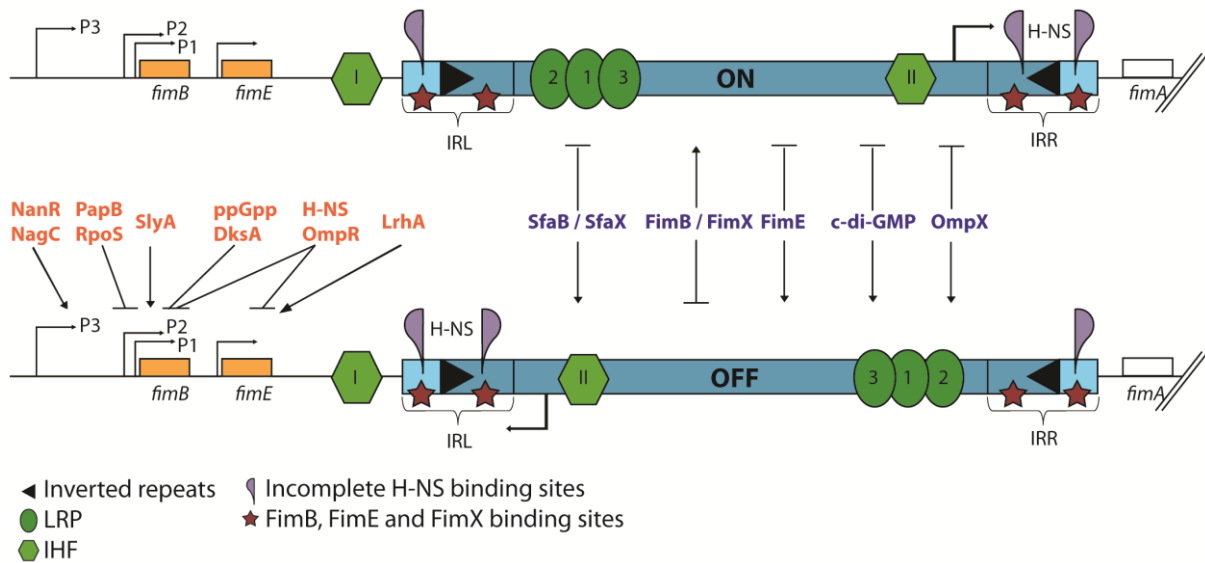


Figure 8: The architecture of the invertible element *fimS*

Expression of type I fimbriae depends on the orientation of an invertible element termed *fimS* (blue box). This invertible *fimS* element precedes the structural genes of type I fimbriae (white box) and harbours the promoter for *fimAICDFGH*. The inversion of *fimS* depends on the action of the recombinases *FimB* and *FimE* (orange boxes), which act on two Inverted Repeats (IR; black triangles). IRs are part of the IRL (left) and IRR (right). Besides the IR itself IRL and IRR are composed of an invariable region (light blue) named IRL-outside and IRR-outside and a region, which is part of the inverted DNA (dark blue) and whose DNA sequence changes upon inversion of *fimS*. These variable regions are called IRL-inside and IRR-inside. IRL and IRR together comprise four binding sites (red stars) for the *Fim* recombinases (red stars). Expression of the recombinases is controlled by three (*FimB*) and a single (*FimE*) promoter(s), which are positively (black arrow) or negatively (τ) regulated by different regulatory proteins of multiple pathways (orange lettering). In addition, the region between *fimE* and *fimA* comprises binding sites for IHF (light green hexagons), LRP (dark green ellipse) and H-NS (violet drops), which contribute to the orientational bias of *fimS* and assist during the inversion process. The complete H-NS binding site (entire drop) is subdivided in three half-sites (half drops) and depending on the orientation of *fimS* a complete binding site is formed on either the IRL or IRR. Other components which affect the switch of *fimS* indirectly or in an unknown mechanism are written in dark blue. (Positive effect (black arrows), negative effect (τ)).

* * *

The IR on the 3' end of *fimS* is termed IRL (left hand inverted repeat), the IR on the 5' end is termed IRR (right hand inverted repeat) (Figure 8). Both IRL and IRR are subdivided into an IR-insight and an IR-outside. During the recombination process, the sequence of IRL-

outside and IRR-outside remain constant while the IRL-inside, the IRR-inside and the sequence containing the *fimAICDFGH* promoter get inverted by the Fim recombinases. This variable composition of *fimS* upon inversion is important for the directional preferences of the Fim recombinases mediating the DNA inversion (243). In *E. coli*, the predominant Fim recombinases residing over the directionality or phase of *fimS* are located upstream of it and are encoded by *fimB* and *fimE* (Figure 8). They bind to four overlapping half sites on IRL and IRR and following occupancy of these sites they recombine the switch within the IR sequence. Both recombinases belong to the λ integrase family of tyrosine site specific recombinases and share 48% amino acid homology with each other (242, 244, 245). The action of Fim integrases or recombinases is unusual as they promote a DNA inversion rather than promoting a DNA-integration or -excision process reported for classical integrases. In addition, both recombinases have been shown to act independent of each other, however they have different directional preferences for the inversion of *fimS* (242, 246-248). Co-expression experiments of FimB and FimE indicate that the activity of FimE dominates over the activity of FimB *in vitro* (245, 247, 249-251). FimE has been shown to predominantly catalyse the inversion from the ON phase into the OFF phase. Expression of *fimE* is under the control of a single promoter upstream of *fimE* (252). The stability of the *fimE* transcript depends on the orientation of *fimS*, as it determines the length and 3' sequence (253, 254). Consequently, *fimE* mRNA is likely to be degraded faster when the switch is in the OFF orientation as when it is in the ON orientation. Furthermore, FimE was shown to preferentially bind *fimS* in its ON conformation, adding to the directional bias (255). FimB on the other hand has bidirectional activity and is capable of inverting *fimS* in both directions, with a slight bias for the OFF to ON inversion (247, 255). Its expression was reported to depend on either two or three promoters, depending on the study (256, 257). The third promoter (P3) of *fimB* is predicted to be very distant from the transcriptional start site and respond to sialic acid and GlcNAc. Besides the differential control of expression of *fimB* and *fimE*, both proteins also exert different inversion frequencies, with the FimB frequencies being markedly lower (10^{-3} to 10^{-4} per cell per generation) compared to FimE (0.3 per cell per generation) (258, 259). FimB was also shown to be susceptible to the level of DNA supercoiling (242). FimB switches *fimS* into the ON state as soon as DNA relaxes, e.g. at the onset of stationary phase (260, 261). Several clinical *E. coli* strains have recently been reported to encode additional recombinases acting on the inversion of *fimS*. These pathogen associated recombinases include proteins like IpuA, IpuB and IpbA of CFT073 (262), HbiF of the meningitis isolate RS218 (263) and FimX of the uropathogenic isolate UTI89 (264). The recently identified FimX recombinase of UTI89 is a homolog of FimB, which is bidirectional and also shows a slight bias for the OFF to ON inversion of *fimS*. The inversion frequencies as well as the

promoters of this recombinase have not yet been described. However, FimX is reported to be slow *in vitro* but highly active *in vivo* (264).

Besides the direct effect of the recombinases FimB, FimE and FimX in UTI89, a plethora of other proteins were shown to contribute to the overall architecture of the *fimS* switch, summarised in Figure 8. H-NS (histone-like structuring protein) is a global regulator responsible for histone-like functions and was shown to contribute to the phase of *fimS* in different ways (265). It binds to sequences at the edges of the *fimS* switch (266-268) and so far, three incomplete H-NS binding sites have been identified. These incomplete binding sites are located on *fimS* adjacent to the fimbrial promoter, the IRL-outside and IRR- outside regions respectively. A complete H-NS binding site is formed at the IRR when *fimS* is in the ON orientation while the complete H-NS binding site localises to the IRL when *fimS* is in the OFF orientation (Figure 8). However, the effects of H-NS binding to IRL or IRR and the inversion process are not yet clear (268). Furthermore, H-NS was also shown to repress the transcription of both recombinases (252, 269, 270) and to affect fimbriation by repressing the transcription of *lrp* gene (271). The leucine-responsive regulatory protein (Lrp), which mostly regulates genes involved in metabolic functions (272) binds to three different sites within *fimS*, which are all in proximity to the IRL site (Figure 8). Binding of Lrp increases the switching frequency of *fimS* (251, 268, 273-276), and it was shown that Lrp interaction with *fimS* might change upon alterations in the intracellular alanine and leucine concentrations (276). Another co-factor for *fimS* switching is the integration host factor (IHF) (249, 250). Mutations in IHF were shown to lock *fimS* in either the ON or the OFF orientation and affect the orientational bias of FimB recombination (248, 251, 267, 277, 278). The intergenic region between *fimE* and *fimA* comprises two binding sites for IHF (249-251), as illustrated in Figure 8 (273). Binding of Lrp and IHF results in bending of the *fimS* DNA region, leading to the formation of a hairpin loop that juxtaposes IRL and IRR and thus facilitates the recombinase mediated inversion of *fimS* (268, 273). If neither Lrp nor IHF are bound to *fimS*, H-NS will bind and maintain the OFF phase of *fimS* (279). While H-NS, Lrp and IHF are crucial for phase switching, several other genes have been shown to affect the expression of type I fimbriae. LrhA (LysT-type regulator), OmpX (outer membrane protein X), OmpR (outer membrane protein R), or the gene products of *ibeA* and *ibeT* act more indirectly by influencing the expression of the recombinases Figure 8. LrhA was found to repress type I fimbriae expression by activating *fimE* through binding to its promoter region (280). Deletion of OmpX was shown to increase FimA production and result in a modification of the cell surface composition (281). Deletion of *ibeA* resulted in diminished fimbriation and a lowered transcription of *fimB* and *fimE*, while *ibeT* deletions resulted in a state where *fimS* was preferentially in the OFF phase (282). Furthermore, another study indicates that the alternative stationary sigma factor RpoS represses *fimB* transcription (283). Deletion of

OmpR of the EnvZ/OmpR two component regulatory system (284) led to derepression of *fimB* and *fimE* transcription compared to wild-type cells (269). Beside the mentioned proteins, c-di-GMP and ppGpp have also been implicated to affect the phase variable expression of type I fimbriae (Figure 8). C-di-GMP (see chapter 3.6) has recently been linked to fimbriation in a study, which showed that increased expression of the phosphodiesterases YhjH or YahA resulted in an increased expression of I type I fimbriae (285). The involvement of ppGpp in fimbrial regulation is not fully understood yet. It is currently believed that ppGpp promotes fimbrial biofilm formation through increased type I fimbrial expression by affecting the P2 promoter of *fimB*. (223). Furthermore, DskA, a co-factor required for ppGpp mediated positive regulation of several promoters of amino acid biosynthesis was shown to activate transcription of the *fimB* P2 promoter (224, 286). Even genes involved in metabolism have directly been linked to phase variation, like the N-acetylglucosamine-6-P responsive protein NagC and the sialic acid-responsive protein NanR. NagC and NanR bind to two deoxyadenosine methylation sites within the intergenic region that contains the P3 promoter of *fimB* (259, 287-290) and stimulate the expression of *fimB* (Figure 8). It is believed that UTIs initiated by type I fimbriae of UPECs elicit an inflammatory response that leads to increased levels of both sialic acid and N-acetylglucosamine, which in turn will abolish transcription of *fimB* (291). Several studies linked the expression of type I fimbriae to the expression of other surface exposed structures. Examples are the pyelonephritis associated pili (Pap) regulator PapB (292-294), which represses *fimB* expression, or the two proteins SfaB and SfaX, which are associated with S fimbriae and negatively affect the expression of type I fimbriae (295). These cross-talks suggest the presence of a competition between different fimbria and indicate that the expression of different types of fimbriae is preferentially avoided by bacteria.

4 Aims of this Thesis

The transition of planktonic to sessile lifestyles in bacteria rests upon a tightly controlled program that gets triggered by the environmental composition and whose implementation requires multiple feedback controls. Uropathogenic *E. coli* (UPEC), the predominant agents of urinary tract infections, use this lifestyle switch to shift from acute to chronic, biofilm associated infections. While the acute phase of infection is dominated by the expression of virulence factors such as type I fimbriae, biofilm matrix components including PGA prevail during biofilm associated infections. In this work, factors reported to induce a lifestyle switch will be used in UPECs to investigate their effects on the expression patterns of two output-systems (type I fimbriae and PGA) during lifestyles transition. To achieve this, it will be assessed if PGA dependent biofilm formation in UPECs requires derepression of the carbon storage regulator (Csr) system. Furthermore, it will be investigated if PGA dependent biofilms respond to the bacterial second messenger c-di-GMP or the alarmone ppGpp of the stringent response and if PGA contributes to UTI pathogenesis. Finally, this work aims at clarifying the role of type I fimbriae in PGA dependent attachment and investigates if the expression patterns of the two surface-exposed structures are subject to a regulatory cross-talk.

5 **The role of Poly-GlcNAc in biofilm formation of uropathogenic *E. coli***

(Manuscript in preparation)

Lucie Hosch¹, Alexander Harms¹, Roswitha Schiller², Alexander Boehm^{1,2}, Ulrich
Dobrindt^{2,3}, Urs Jenal^{1*}

Focal Area of Infection Biology, Biozentrum, University of Basel, Switzerland ¹
Institut für Molekulare Infektionsbiologie, Julius-Maximilians-Universität Würzburg,
Germany ²

Institut für Hygiene Universitätsklinikum Münster, Germany ³

Keywords: Uropathogenic *E. coli*, poly-GlcNAc, PGA, biofilm, *csrB*, c-di-GMP, ppGpp, translation inhibitors, murine cystitis model

* Correspondance: Urs.Jenal@unibas.ch

5.1 **Statement of work**

In this study, I have constructed all UTI89 strains except $\Delta csrB$, $\Delta csrC$, $\Delta csrD$, and $\Delta csrBC$, which were constructed by Alexander Harms, a rotation student I supervised. Roswitha Schiller has introduced me to the murine cystitis model and assisted me during the murine *in vivo* assays, which were performed in the animal facility of the Institut für Molekulare Infektionsbiologie at the Julius-Maximilians-Universität Würzburg in Germany.

5.2 Abstract

Recent reports have shown that recurring infections of the urinary tract are associated with the formation of intracellular biofilm-like structures of uropathogenic *Escherichia coli* (UPECs). While the molecular components and regulation of biofilm formation are well established in non-pathogenic *E. coli* strains, these processes are still poorly defined in pathogenic *E. coli* strains. One of the principle structural components of *E. coli* biofilm formation *in vitro* is the exopolysaccharide poly-GlcNAc (PGA). The PGA machinery is regulated by the global carbon storage (Csr) control module on the translational level and by the second messenger c-di-GMP on the allosteric level. Here we analysed the role of the Csr system, c-di-GMP and PGA in biofilm formation on selected clinical UPEC isolates. In UPECs, derepression of the translational control by the Csr system induced attachment in a PGA dependent manner. The levels of PGA production depended on c-di-GMP and the ribosomal stress alarmone ppGpp. We show that enhanced production of c-di-GMP induces PGA dependent attachment and that YdeH is the main contributor to this induction. Attachment in the presence of translation inhibitors derepressed PGA dependent attachment via SpoT-mediated reduction of ppGpp levels. Initial *in vivo* data derived from murine cystitis infections indicate however that PGA does not play a crucial role during acute cystitis. Further studies will have to analyse the role of PGA in chronic and recurring urinary tract infections.

5.3 Introduction

Pathogenic *Escherichia coli* (*E. coli*) cause a number of severe acute infections, including gastroenteritis (1), neonatal meningitis (2) or urinary tract infections (UTI) (3). Infections caused by *E. coli* or other pathogens can switch from an acute stage to a latent stage where bacteria chronically persist within their hosts. Patients suffering from initially acute UTI by uropathogenic *E. coli* (UPEC) often suffer from recurrence of symptoms after termination of antibiotic treatment (4). While acute and uncomplicated UTIs can often be treated effectively, recurrent infections are associated with episodes of little or no symptoms of inflammation and are thus difficult to eradicate. They often require patients to undergo repeated cycles of antimicrobial therapy. Thus, recurrent infections are associated with considerable morbidity and health care costs (5). The pathogenesis underlying persistent UTIs is not well understood and only very few of the bacterial factors involved in persistence have been identified so far (2, 3). Recurring UTIs are usually associated with the formation of intracellular biofilm-like structures called 'intracellular bacterial communities' (IBC) (6, 7). These structures might explain how the UPEC clone responsible for the initial infection can persist chemotherapy and cause recurrent UTIs after prolonged periods without symptoms (8).

Biofilms are tissue or surface attached aggregates of bacterial cells, which are encased in a self-produced matrix of proteinaceous adhesive organelles, such as different fimbriae and varying exopolysaccharides (9). Together these factors form a viscous matrix, which protects bacteria within biofilms from the host immune system and presents a diffusion barrier for most antibiotics. In addition, biofilms harbour subpopulations of bacteria with little metabolic activity. These dormant 'persister' cells are insensitive to the action of most antibiotics and may serve as a reservoir for recurring infections (6, 10). Other than in UPECs, the molecular basis underlying biofilm formation of non-pathogenic *E. coli* strains including MG1655 has already intensively been studied. Biofilm formation is tightly controlled by the components of the **C**arbon **S**torage **R**egulator (Csr) system. The CsrA protein binds to the 5' UTR of the *pgaACBD* operon, which encodes the biosynthetic machinery of the biofilm matrix component poly- β -1,6-N-acetyl-glucosamine (PGA or poly-GlcNac) (11). Two small non-coding regulatory RNAs, *csrB* and *csrC*, can sequester CsrA and thereby regulate CsrA targeted genes. The expression of *csrB* and *csrC* is itself regulated by the BarA/UvrY two component system (TCS), which responds to the metabolic status of *E. coli* (12, 13). Also, CsrA indirectly activates the transcription of *csrB* and *csrC* via its inducing effects on BarA/UvrY TCS (14). This positive autoregulatory loop imposes rapid upregulation of Csr

target genes upon environmental alterations. CsrA further represses NhaR, the transcriptional regulator of the *pgaA-D* operon, adding an additional level of complexity to the regulation of PGA (15). PgaA, B, C, and D localise to the cell envelope where they catalyse the synthesis and export of the PGA polymer. PgaA forms the export pore in the outer membrane while PgaB deacetylates the PGA polymer in the periplasm (16). The glycosyltransferase PgaC resides in the inner membrane where it catalyses the formation of PGA from its precursors UDP-GlcNAc. Although the inner membrane protein PgaD is essential for the synthesis of PGA (16, 17), its precise function remains unclear (18).

To experimentally derepress PGA biogenesis and biofilm formation in the absence of physiological signals a *csrA::Tn5* allele which encodes a partially inactivated CsrA protein is generally used (designated as *csrA⁻* throughout this work) (11, 19). When challenged with subminimal inhibitory concentrations (sub-MICs) of translation inhibitors, *E. coli* MG1655 *csrA⁻* responds with a strong increase in PGA dependent biofilm production (20). Stimulation of the PGA machinery under these conditions involves an increase of the second messenger c-di-GMP (20) and a SpoT-mediated reduction of the alarmone ppGpp. The second messenger c-di-GMP is a small intracellular signalling molecule that governs the transition from a motile planktonic to a sessile surface attached lifestyle (21-23). The synthesis of c-di-GMP requires two GTP molecules and is performed by diguanylate cyclases (DGC) through their conserved catalytic GGDEF domain. Degradation of c-di-GMP to the linear product pGpG is mediated by the catalytic EAL phosphodiesterases (PDE) domain (24). Several DGCs are controlled by the Csr system (20, 25). This includes YdeH, which was further shown to be important for PGA biogenesis. CsrD, a catalytically inert member of the GGDEF-EAL domain protein family targets *csrB* and *csrC* for degradation by RNase E (26).

In this study, we analyse the role of the Csr system, c-di-GMP and PGA, for biofilm formation of several clinical UPEC isolates. These including UTI89, a UPEC isolate from a patient with an acute bladder infection (27, 28) and two pyelonephritis isolates, CFT073 (29) and 536 (30). We also analyse the prototypic asymptomatic bacteriuria (ABU) isolate 83972, a strain that is well adapted for growth in the urinary tract and establishes long-term bacteriuria (31-33). 83972 has been used to deliberately establish protective ABU in patients. PIII-4 is a re-isolate from a patient who received 83972 as therapeutic treatment (34). Our studies show that most UPECs have a functional Csr system and are able to form PGA dependent biofilms. In UTI89, elevated levels of c-di-GMP strongly boost biofilm formation with YdeH being the primary DGC contributing to biofilm increase. Translation inhibitors stimulate PGA dependent biofilm formation in UPECs in a ppGpp dependent manner. Preliminary *in vivo* data indicate that PGA does not contribute to acute cystitis in a mouse model.

5.4 Material and Methods

5.4.1 Bacterial strains and plasmids

UPEC wild type strains and isogenic deletion mutants used in this study are listed in Table 1. Plasmids used are listed in Table 2. Table 3 lists all sequenced UPEC strains as well as the clinical isolates screened for biofilm induction upon addition of translation inhibitors.

5.4.2 Standard growth conditions

Unless mentioned otherwise, *E. coli* strains were grown in Luria-Bertani (LB) broth at 37 °C while aerated through rotation of cultures by 170 rpm. When required, media were supplemented with antibiotics. The optical density (OD) of bacterial cultures were determined at 600 nm using a photo spectrometer (Genesys6, Thermo Spectronic, WI, USA)

5.4.3 Selection of UPEC isolates inducible by sub-MICs of tetracycline

All clinical isolates listed in Table 3 were isolated at the University hospital of Basel from the urine of hospitalised patients. UTI89 and 536 have been included in the screening as well characterised and sequenced wild type (wt) strains. For the screening, bacteria were grown overnight cultures in tryptic soy broth (TSB). Bacteria were than subdiluted 1:40 in fresh TSB and exposed to serial dilutions of sub-MIC tetracycline in a 96-well plates, grown statically for 24 h at 37° C and then processed as described for attachment assays in chapter 5.4.7. Strains with interesting screening behaviour were selected and their susceptibility to sub-MICs of different translation inhibitors (tetracycline, chloramphenicol, and streptomycin) was confirmed in attachment assays.

5.4.4 Congo red binding assay

Single colonies of each strain were picked from a fresh LB agar plate and restreaked onto a fresh LB plate containing either 0.1% congo red or 0.04 % congo red and 20 µg / ml Coomassi brilliant blue (35). After overnight incubation, plates were kept at 4° C for 2 days for more intense congo red binding of colonies. Images of clones with representative congo

red binding were taken with a Nikon Coolpix through a binocular (Wild; Heerbrugg M3Z) at a magnification of 24x and processed with Photoshop CS5. Plates containing 0.1% congo red were illuminated with the light source from above while 0.04 % congo red and 20 µg / ml Coomassie brilliant blue plates were translucent enough to be imaged with a light source shining through the plate. This ladder illumination method allowed for more subtle differences in congo red binding.

5.4.5 Motility assay

Strains subjected to motility assays were freshly streaked onto LB plates from the UPEC strain collection, than single colonies were picked with toothpicks and transferred onto TB swarmer plates (0.3 % agar). Motility was quantified by scanning the plates on a ScanMaker i800 (Microtek) after 6.5 h of incubation at 37°C. If needed, TB swarmer plates were supplemented with 100 µg/ml ampicillin or 12.5 µg/ml tetracycline for plasmid selection and 100 µM IPTG or 0.2 % arabinose for plasmid induction. Images were processed with Photoshop CS5 (Adobe).

5.4.6 Construction of isogenic deletion mutants

The parent strains used in this study are the sequenced clinical UPEC isolates UTI89 (27, 28), CFT073 (29), 536 (30) 83972 (34, 36) and a re-isolate of 83972, named PIII-4 (34). In addition we used two novel clinical isolate, termed clin571 and clin591. Clin 591 was isolated at the University of Basel from a 76 year old female patient carrying a urethral stent and clin571 was isolated from an 82 year old female patient with a UTI.

The construction of isogenic deletion mutants was performed as previously published (37). In brief, the corresponding UPEC wild type strains were transformed with the temperature sensitive plasmid pKM208 (Addgene plasmid 13077) containing the red recombination genes (38). Once transformed, the parent strain with pKM208 was stocked and used for subsequent gene deletions and modifications. To generate isogenic mutants, the UPEC strain with pKM208 was cultured at 30° C in LB without NaCl and supplemented with ampicillin (100 µg/ml) until the culture reached the end of the logarithmic phase (OD₆₀₀ of 0.9). At this state, cultures were shifted to 37° C and the λRED genes were induced for 30 min with 1 mM IPTG. Cultures were then subjected to a 15 min heat shock at 42 °C and rapidly cooled in ice slurry before washing once with 10 % glycerol and concentrating 100-fold in cold 10 % glycerol.

The kanamycin and chloramphenicol resistance cassettes were PCR amplified from pKD4 or pKD3 (39) with primers designed specifically to delete the desired region in the genome of UTI89. Each λ RED primer contains a constant 3' sequence that binds to the resistance cassette (chloramphenicol or kanamycin) from pKD3 or pKD4, respectively. In the forward primer (P1) this constant region is TGTAGGCTGGAGCTGCTTCG and in the reverse primer (P2) it is CATATGAATATCCTCCTTAG. Furthermore, the 5' end of each λ RED primer contains a homology region (HR) of roughly 50 nt that binds to the flanking regions of the gene to be deleted. λ RED primers used in this study to make isogenic deletion mutants are listed in Table 4. The following genes were deleted by λ RED-mediated recombination: For *pgaA-D* primers 1545-ycdP_KO_P2 and 1546-ycdS-KO-P1 were used, for *ydeH* primers 2400-ydeH_KO_P1 and 2401-ydeH_KO_P2 while *csrB* was deleted via primers 1143_csrB_KO_P1 and 1144_csrB_KO_P2. Primers 1145_csrC_KO_P1 and 1146_csrC_KO_P2 were used for *csrC*, 3880_CsrD_KO_P1, and 3881_CsrD_KO_P2 for *csrD*. The UPEC specific genes *c1116* and *c1117* were deleted via 2878_c1116_KO_P1 and 2879_c1116_KO_P2 or 3547_c1117_KO_P1 and 3548_c1117_KO_P2, respectively. Finally, primers 2125-spoT_KO_P1 and 2126-spoT_KO_P2 were used to delete *spoT* in a UTI89 Δ *relA* background. Other than the mutants listed above where DNA was amplified from pKD3 or pKD4, some DNA fragments used for λ RED mediated gene deletion were amplified from the comprehensive 'Keio collection' published in 2006 (40). Amplification of the locus containing the deleted gene in the collection was performed with normal test primers (~20 nt) and the PCR product was then used to delete the gene in UPECs via λ RED mediated recombination. For *ycdT* the primers used were 2402_ycdT_seq_fwd1 and 2762_ycdT_KO_P2. Analogously we used primers 3927_relA_test_rev and 3928_relA_test_fwd for the deletion of *relA*. After amplification, PCR fragments were gel purified (MN Nucleospin Extract II, Machery Nagel, Oensingen, Switzerland). 10 to 100 ng purified DNA were added to 65 μ l of cold recombination competent bacterial cells and subjected to electroporation in 1 mm Gene Pulser cuvettes using a Gene Pulser (BioRad, Reinach, Switzerland) set to 1.75 V, 25 μ F and 400 Ω . Electro-shocked cells were mixed with cold (4 °C) salt optimised broth (2 % (w/v) bacto trypton; 0.5 % (w/v) yeast extract; 10 mMNaCl and 2.5 mMKCl), incubated for 1.5 h at 37 °C and plated on LB agar plates containing 50 μ g/ml kanamycin or 20 μ g/ml chloramphenicol. After growth, resistant clones were colony purified on LB agar plates containing kanamycin or chloramphenicol and tested by PCR for correct insertion of the resistance cassette. Thereafter, the strain was transformed with pCP20 to remove the resistance cassettes by Flp recombinase-mediated site-specific recombination (39). Loss of the resistance cassette was again checked by PCR.

5.4.7 Attachment assay

Freshly grown LB overnight cultures were diluted 1:40 into 200 μ l LB medium. When appropriate bacteria were grown with the following concentrations of antibiotics to select for plasmids: 12.5 μ g/ml tetracycline (pME6032 plasmids) or 100 μ g/ml ampicillin (pcj30) and were induced with 100 μ M IPTG unless mentioned otherwise. The 96-well plates (Falcon, ordering number 353072) were incubated without shaking for 24 h at 37 °C unless mentioned otherwise after which cell density was recorded on a plate reader at 600 nm. Subsequently, the medium with the non-attached cells was discarded by thorough rinsing of the microtiter plates with deionised water from a hose. Once dried, wells were filled with 200 μ l crystal violet staining solution [0.1 % (W/V) crystal violet (Sigma Aldrich, Article No. C-3886), 1.7 % (W/V) 1-propanol, 1.67 % (W/V) methanol (96.7:1.66:1.66)] and stained on a platform shaker for 15 min at room temperature (RT). The staining solution was discarded and wells were washed and dried as before. Retained crystal violet was dissolved in 200 μ l of 20% acetic acid and quantified at 600 nm in a plate reader. If measurements were outside the dynamic range of the plate reader, crystal violet solutions were further diluted in 20% acetic acid. As previously published (20, 41), bacterial biofilms were quantified as the amount of biomass attached to the polystyrene surface (as absolute attachment). Relative attachment values are ratios of the optical density of dissolved crystal violet (corresponding to the attached biomass) divided by the total cell density (corresponding to bacterial growth). If attachment is indicated as percentage, the relative attachment value is normalised to the corresponding wild type strain carrying the *csrB* overexpressing plasmid, which was determined as 100 %. Error bars were calculated as the standard errors of the mean.

5.4.8 Electron microscopy

For the acquisition of electron microscopy micrographs, bacteria were prepared essentially as described in chapter 5.4.7 but attachment assays were performed in 24-well plates instead of 96-well plates (20). Each well contained 2 ml of LB supplemented with 100 μ g/ml ampicillin and 100 μ M IPTG and a sterile glass slide. After biofilm formation for 24 h, the glass slides were removed, rinsed gently with 1 \times PBS and fixed in 1 \times PBS containing 2.5 % glutaraldehyde for 1 h at room temperature. Then, the glutaraldehyde was washed out with 1 \times PBS and the samples were gradually dehydrated for 10 min per step in acetone step gradient (30%, 50%, 70%, 90%, 100%). Finally, samples were critical point-dried and sputter-coated with a 3–5 nm Pt layer. Micrographs were recorded on a Hitachi S-4800 field emission scanning electron microscope with an acceleration voltage between 1.5 and 5 kV.

5.4.9 Allelic exchange

To obtain MG1655 clones with foreign *ydeH* alleles, *ydeH* of MG1655 was first replaced by the λ RED technology with a counter-selectable marker (the toxin *ccdB* under control of the L-rhamnose promoter plus a linked kanamycin resistance cassette) (39). In a second λ RED recombineering step the *ccdB*-kanamycin marker was replaced with foreign *ydeH* alleles, which were amplified by PCR from UTI89 and 83972 with primers 1651-*ydeH*_test_fwd and 1652-*ydeH*_test_rev. After electroporation and phenotypic expression bacteria were plated on minimal medium containing 0.2 % L-rhamnose as sole carbon source and thus selected for rhamnose resistant clones containing foreign *ydeH* alleles. Rhamnose resistant clones were colony purified, checked for loss of kanamycin resistance and the *ydeH* locus was sequenced to exclude point mutants. After successful allelic exchange of *ydeH*, the *csrA*⁻ allele was introduced by P1 transduction (see chapter 5.4.11) and the resistance cassettes of *csrA*⁻::*kan* was removed by Flp recombinase-mediated site-specific recombination (39).

5.4.10 Preparation of P1 phage lysates

The preparation of P1 lysates was performed essentially as described by Miller in 1992 (42). Briefly, bacteria were grown in 5 ml LB medium until they reached an OD₆₀₀ of roughly 0.3. Then CaCl₂ was added to a final concentration of 10 mM and 10 μ l of the pure MG1655 P1 lysate were added. Next, bacteria were re-cultivated at 37° C for 3-4 hours until the culture became clear and displayed cellular debris. At this point 250 μ l chloroform was added, the tube was centrifuged at 5000 rpm for 10 min in an SS34 rotor for removal of cellular debris. The supernatant containing the phages was transferred into sterile glass screw cap. Finally 50 μ l chloramphenicol were added to kill residual bacteria. Lysates were stored at 4° C until further use.

5.4.11 P1 Transduction

The protocol used for P1 transduction was essentially performed as previously described (42). Briefly, the recipient strain was grown in LB medium to an OD₆₀₀ between 0.5 and 0.8 after which CaCl₂ was added to a final concentration of 10mM. To 1 ml of bacterial culture 100 μ l of P1 phage lysate (chapter 5.4.10) was added and the mixture was incubated at room temperature for 15 min. Thereafter Na-Citrate was added to a final

concentration of 100mM and the bacterial suspension was phenotypically expressed for at least one hour. Then the suspension was plated on selective medium containing 20 mM citrate. Before use, single colonies were colony purified twice on selective plates containing 20mM citrate to remove residual phages.

5.4.12 Preparation of bacterial inoculum for murine cystitis model

Bacteria were grown under aerated conditions at 37° C overnight after which they were rediluted to an OD₆₀₀ of 0.05 and regrown at 37° C until an OD₆₀₀ of 1.2 was reached. Bacteria were collected by centrifugation, washed twice with cold sterile 0.9 % saline solution and concentrated to a final OD₆₀₀ of 80. The CFU of the inoculum was tested on LB plates by serial dilutions.

5.4.13 Infection of mice

For our animal models 6 to 8 week old C57BL/6 female mice were infected with ~ 1,5x10⁹ bacteria concentrated in 30 – 45 µl 0.9 % saline solution. The transurethral infection was performed essentially as described by Garofalo *et al*, (43) on anaesthetised animals (isofluran and oxygen Mixture). Weight of each mouse was measured prior infection, the first three days after infection and regularly thereafter or until mice were sacrificed. Weight loss was used as a parameter for the wellbeing of infected mice. At the endpoint of infection, mice were euthanised by CO₂ and death was confirmed by tweaking the animals between their toes. Once sacrificed, both kidneys as well as the bladder were collected as sterile as possible in 1 ml sterile 0.9% saline solution. Bladders were cut open to remove residual urine from the bladder lumen and dissected into small pieces, which were then again collected in 1 ml sterile 0.9 % saline solution. Kidneys were left intact but rinsed before collecting the organs again in 1ml 1×PBS. All organs were weighted prior homogenisation in 1ml 1×PBS. Organ homogenates were serially diluted and plated out for colony forming unit (CFU) determination on EMB agar plates (BD Diagnostic Systems Switzerland).

5.5 Results

5.5.1 General characterization of motility and Congo red binding of different UPEC strains

The Csr cascade inversely regulates motility and PGA biogenesis (16, 44). As a general characterization of this pathway, we first assessed motility behaviour and congo red binding of different UPEC isolates and compared it to different MG1655 strains. As shown in Figures 1 and 2, MG1655 *csrA*⁻ has reduced motility and an enhanced propensity to form biofilms. Consistent with earlier reports on MG1655 (20, 25) this behaviour is dependent on the DGC YdeH. In comparison, the previously described UPEC strains (UTI89, 536, CFT073, 83972, and PIII-4) showed only weak binding of congo red (Figure 1). Contrary, the newly isolated and uncharacterised clin571 showed increased congo red binding. Motility of the UPEC strains was variable but generally reduced as compared to MG1655 wild type, especially in the two newly isolated strains clin571 and clin591. Interesting motility behaviour was observed for the ABU strains 83972 and its patient re-isolate PIII-4. While 83972 cells formed poorly motile, biofilm-like microcolonies on motility plates, this behaviour reversed in strain PIII-4, as it had regained the ability to swim homogeneously (Figure 2).

5.5.2 Biofilm formation in UPECs is regulated by the Csr cascade and by c-di-GMP

To test if PGA expression and biofilm formation in the UPEC isolates requires activation of the Csr cascade we assayed their behaviour in the absence of the CsrA protein. Several attempts were performed to insert the *csrA*⁻ allele into UTI89 via λ RED, which were unsuccessful due to reactivation of the Tn5 transposon of the *csrA*::Tn5 allele. As an alternative way to derepress Csr target genes, we made use of a plasmid, which overexpresses *csrB* (pCsrB). As shown in Figure 3A, overexpression of *csrB* lead to a stimulation of biofilm formation in MG1655, comparable in extent to the behaviour observed for the *csrA*::Tn5 strain. Stimulation of biofilm formation is slightly stronger upon overexpression of *csrB* as compared to partial inactivation of CsrA. Importantly, *csrB* overexpression also strongly stimulated biofilm formation of strains UTI89, 89372, and PIII-4 (Figure 3B). In contrast, attachment of clin591 was already strongly increased without overexpression of *csrB* and could not be further induced by *csrB* overexpression. This indicates that the catheter-derived strain carries genetic modifications that constitutively

Results

upregulate biofilm formation. Together these data indicate that in most UPEC isolates the Csr cascade is functional and required for the derepression of the PGA pathway.

To test if c-di-GMP is involved in the stimulation of PGA-dependent biofilm formation in UPECs we analysed the behaviour of strains expressing a heterologous DGC (DgcA from *Caulobacter crescentus*). In agreement with Csr playing a key role in PGA control, plasmid driven *dgcA* expression stimulated biofilm formation in all strains but only when *csrB* was overexpressed at the same time (Figure 3C). The attachment of clin591 showed a modest increase upon overexpression of *csrB* and/or *dgcA*, reinforcing the constitutive nature of biofilm formation in this strain. These data suggest that in most UPECs PGA biogenesis and biofilm formation follows similar regulatory principles as in non-pathogenic *E. coli* strains.

To further investigate the role of c-di-GMP and the Csr system in UPEC motility control, we have chosen UTI89 as a representative UPEC strain. As shown in Figure 4, the overexpression of *csrB* completely abolished UTI89 motility. Likewise, overexpression of the DGC WspR (pME6010 WspR) or DgcA (pAB551) had the same effect. A catalytic mutant of DgcA (D164N) did not affect motility, arguing that the observed interference with cell motility is caused by elevated levels of c-di-GMP. These data argue that the Csr system together with c-di-GMP co-ordinately control the motile-sessile switch in clinical UPEC isolates.

To demonstrate that Csr controlled biofilm formation in UTI89 depends on PGA, we overexpressed *csrB* in a mutant lacking the entire *pga* operon (*pgaA-D*). As shown in Figure 5A a *pga* mutant completely failed to induce biofilm formation, even when *csrB* was overexpressed from plasmid. This argues that PGA is the primary EPS responsible for biofilm formation in UPECs under conditions that derepress the Csr system. In the non-pathogenic *E. coli* strain MG1655, activation of the Csr system also leads to enhanced expression of two DGCs YcdT and YdeH (16, 25, 45), both of which are required to fully stimulate the production of PGA (20) (Master Thesis, A. Casanova). As shown in Figure 5A, both YdeH and (to a lesser extent) YcdT were required for full induction of PGA-mediated biofilm formation once the Csr system is derepressed in UTI89. To strengthen these results scanning electron micrographs were taken from wild type and mutant UTI89 biofilms overexpressing *csrB*. While wild type and the $\Delta ycdT$ mutant formed a homogeneous, dense biofilm with few cavities (Figure 5B and 5C), the biofilm of $\Delta ydeH$ appeared less homogeneous and contained larger voids reducing the total biofilm biomass of this strain (Figure 5D). The image of UTI89 $\Delta pgaA-D$ confirmed that PGA is absolutely essential for biofilm formation in UTI89 as only a few dispersed cells were visible on the glass slide (Figure 5E). Finally, the biofilm of the UTI89 $\Delta ydeH \Delta ycdT$ double mutant was also strongly reduced (Figure 5F), confirming the critical role of c-di-GMP and suggesting that the two Csr-

regulated DGCs YdeH and YcdT act synergistically to stimulate PGA-mediated biofilm formation in UPECs.

We also analysed the requirement for biofilm formation of the UPEC isolate clin591 that showed Csr-independent biofilm formation. For this, *pgaA-D*, *ycdT* and *ydeH* were deleted in clin591 and the resulting mutants analysed with respect to surface attachment and biofilm formation. As shown in Figure 6 none of these deletions had a negative effect on clin591 surface colonization, arguing that in this strain constitutive biofilm formation relies on different adhesins and/or matrix components than in other UPEC strains.

5.5.3 Sub-MIC of translation inhibitors differentially stimulate attachment in UPECS

When challenged with sub-minimal inhibitory concentrations (sub-MIC) of translation inhibitors, the non-pathogenic *E. coli* strain MG1655 CsrA⁻ responds with increased PGA dependent surface attachment and biofilm formation (20). This finding is potentially highly relevant, as pathogens can be exposed to sub-MICs of drugs for several hours in patients undergoing antimicrobial chemotherapy (46). We therefore performed a screen to see if UPECs respond to sub-lethal doses of these drugs in a similar way as non-pathogenic *E. coli*. The strains used in this screen are characterised in Table 3 and were isolated from urine of hospitalised patients at the University hospital of Basel. Isolates derived from catheterised patients are mentioned in the table, together with the patient's age and gender. UTI89 and the pyelonephritis isolate 536 were added to the screen as two well characterised isolates. As indicated above, the catheter derived isolate clin591 showed constitutive biofilm formation even in the absence of *csrB* overexpression and was not significantly induced by tetracycline, chloramphenicol or streptomycin (Figure 7). In contrast, clin571 showed no measurable attachment without translation inhibitors but showed strong induction upon addition of tetracycline (Figure 8), chloramphenicol or streptomycin (data not shown). In contrast, UTI89, 536 and the remaining 52 isolates tested were unable to respond to antibiotics without overexpression of *csrB*. However, upon derepression of the Csr system UTI89 responded strongly to tetracycline, chloramphenicol or streptomycin (Figure 9). Importantly, antibiotic-mediated biofilm induction was lost completely in a UTI89 Δ *pga* mutant (Figure 10).

5.5.4 UTI89 attachment can be modulated by several unrelated genes

So far, it has been shown that the mechanisms of biofilm formation are equal in MG1655 and in UPECs like UTI89. However, other factors are linked to this model and have thus been investigated in attachment assays. The first components investigated are genes involved in the Csr system. Though partially complemented through the overexpression of *csrB*, UTI89 $\Delta csrB$ and $\Delta csrC$ attachment decreased in both strains compared to UTI89 wt (Figure 11A). As *csrB* and *csrC* act synergistically in binding CsrA, a $\Delta csrBC$ double mutant was investigated. Surprisingly, the UTI89 $\Delta csrBC$ double mutant attached similar than UTI89 $\Delta csrC$, suggesting that the attachment observed in any of these three mutants is predominantly caused by the overexpression of *csrB* in trans. In line with its reported function, UTI89 $\Delta csrD$ showed a slightly increased attachment, which must be due to prolonged stability and activity of *csrB* and *csrC*.

C1116 was recently identified as a UPEC specific phosphodiesterase, which clusters in the Sfa fimbrial operon on a pathogenicity island (47, 48). Being absent in non-pathogenic *E. coli* strains, we were interested to see if the presumed activity of *c1116* affects PGA dependent attachment through degradation of c-di-GMP. As seen in Figure 11B, deletion of *c1116* caused a small but reproducible increase in attachment, suggesting that C1116 is active as PDE and contributes to the c-di-GMP pools. Interestingly deletion of *c1116* together with the gene adjacent to it (*c1117*) reduced attachment, just like the single deletion of *c1117*. Though the exact function of *c1117* within the Sfa fimbriae has not yet been identified, it appears to affect PGA dependent attachment together with *c1116* over which it dominates.

Boehm et al., have recently shown that the biofilm induction by translation inhibitors depends on the ribosome itself (20). They have identified the alarmone ppGpp as signalling molecule that transfers the ribosomal stress state from the ribosome to the PGA machinery. To test if ppGpp affects PGA dependent biofilm formation in UPECs as well, a ppGpp zero strain (ppGpp⁰) was constructed. This required the deletion of the ppGpp synthases (*RelA* and *SpoT*) and its hydrolase (*SpoT*). As seen in Figure 11C, attachment of a UTI89 ppGpp⁰ strain (UTI89 $\Delta relA\Delta spoT$) was massively induced upon overexpression of *csrB* compared to the wild type UTI89. This corresponds to the phenotype seen in MG1655 *csrA*⁻ ppGpp⁰. Thus, ppGpp is required in UTI89 as well to signal between the ribosome and the PGA machinery and as a consequence influences biofilm formation.

From these attachment assays, we can conclude that the components of the Csr system execute the same functions reported for MG1655: *csrB* and *csrC* boost PGA dependent biofilm formation by titrating away CsrA while CsrD controls the levels of *csrB* and

csrC by targeting them for degradation. Deletion of phosphodiesterases like *c1116* affect PGA dependent biofilm formation by decreasing the pool of c-di-GMP which post-translationally affects PgaA-D. Finally, the signalling cascade required to induce PGA dependent biofilm formation upon ribosomal stress depends on ppGpp and is retained in UPECs, arguing that this signalling cascade is conserved among all *E. coli* strains.

5.5.5 UPEC *ydeH* alleles do not complement the function of MG1655 *ydeH*

This study showed that YdeH is a crucial c-di-GMP synthesising enzyme, which stimulates PGA dependent biofilm production in UTI89. Besides this common function, it became clear that a $\Delta ydeH$ deletion in UTI89 and MG1655 did not equally affect attachment and resulted in a more severe phenotype in MG1655 (see Figure 5A and Boehm *et al.*, 2009 (20)). It is thus plausible that the activities of the different *E. coli* YdeH alleles are not the same. Sequence analysis of *ydeH* revealed a total of 21 SNPs between UTI89 and MG1655, 3 of which were non-silent. The first identified SNP (H31R) was located to the signal input domain, the second SNP (N130S) was within the linker connecting the signal input domain with the domain harbouring the DGC activity. The third SNP (A217T) was in a loop in proximity of the protein's I-site and thus in the DGC domain of the protein. All SNPs are illustrated in Figure 12. Interestingly the *ydeH* ORF of 83972 harbours a deletion of 70 bp. This causes a frame shift and introduces an early stop codon. Interestingly, the deletion also results in a secondary start site, which is in frame with the first ORF of *ydeH*₈₃₉₇₂. Consequently, YdeH₈₃₉₇₂ is cut into two ORFs, one of which contains the signal input domain and the other the DGC domain. If both *ydeH*₈₃₉₇₂ are expressed it would result a DGC domain which is uncoupled from the signal input and thus might be constitutively active or inactive.

Based on the differences between the *ydeH*_{MG1655}, *ydeH*_{UTI89}, and *ydeH*₈₃₉₇₂, a comparison of the different *ydeH* alleles in the genetic context of MG1655 seemed important. The respective *ydeH* alleles of UTI89 and 83972 were therefore introduced by allelic exchange into the native MG1655 *ydeH* locus and CsrA was inactivated to allow attachment. The attachment of these strains at 37° C is shown in Figure 13A where it is compared to MG1655, AB958, and AB959. UTI89 wild type pCsrB was included in both assays as the natural context of the *ydeH*_{UTI89} allele. Surprisingly, attachment of both MG1655 *ydeH*_{UTI89} and MG1655 *ydeH*₈₃₉₇₂ was more comparable to MG1655 *csrA*⁻ $\Delta ydeH$ (AB959) than to MG1655 *csrA*⁻ (AB958), indicating that both foreign *ydeH* are not capable of replacing the *ydeH*_{MG1655} allele at 37° C.

Experiments have shown that UTI89 adheres better at 37° C while MG1655 adheres better at 30° C. Therefore, the assay was repeated at 30° C. The *ydeH*_{UTI89} and *ydeH*₈₃₉₇₂

Results

alleles behaved similarly at 30° and 37° C and did not complement the function of the natural MG1655 *ydeH* allele (Figure 13B). Attachment of UTI89 pCsrB is greatly reduced compared to AB958 at 30 °C while it attaches equally well at 37°C. Furthermore, the attachment of UTI89 pCsrB was in the same range as the attachment of AB959 at 30 °C, indicating that in its natural genetic context either the YdeH of UTI89 or MG1655 is not equally active at 30° C and 37° C.

If the two transferred alleles were inactive in MG1655 (as indicated by the attachment data), the intracellular c-di-GMP concentrations of MG1655 *ydeH*_{UTI89} *csrA*⁻ and MG1655 *ydeH*₈₃₉₇₂ *csrA*⁻ would have to be in the same range as the concentrations measured for a $\Delta ydeH$ strain. To investigate this, intracellular c-di-GMP concentrations were measured in cell lysates of MG1655 *ydeH*_{UTI89} *csrA*⁻ and MG1655 *ydeH*₈₃₉₇₂ *csrA*⁻. The c-di-GMP concentrations of the control strains are shown in Figure 13C and were determined as followed: $5.35 \pm 1.24 \mu\text{M}$ in AB958, $0.31 \pm 0.07 \mu\text{M}$ in MG1655 wild type and below detection limit in AB959. The intracellular c-di-GMP concentration measured for MG1655 *ydeH*₈₃₉₇₂ *csrA*⁻ was only $0.32 \pm 0.09 \mu\text{M}$ and thus even lower than MG1655. Interestingly, the measured intracellular c-di-GMP concentrations for MG1655 *ydeH*_{UTI89} *csrA*⁻ was at $16.27 \pm 3.75 \mu\text{M}$ and thus significantly higher than the concentrations measured in AB958, indicating hyperactivity of this allele in MG1655.

5.5.6 Murine cystitis models over 3 weeks are not sufficient to determine a role for PGA *in vivo*

Considering the ability of UPECs to form intracellular biofilm like communities, and the established model of PGA dependent biofilm formation, it was reasoned that PGA could be relevant during UTIs. We therefore investigated the relevance of PGA in a murine cystitis model where mice were infected transurethrally (43) with UTI89 wild type (positive control), UTI89 $\Delta fimA-H$ as negative control and UTI89 $\Delta pgaA-D$ (Figure 14A). For UTI89 the infection proceeded as following: After one day $1.56 \times 10^{06} \pm 5.51 \times 10^{05}$ CFU / g of bladder were detected. Within 2 days after infection, the CFU count dropped two log scales and stagnated thereafter. The kinetics of UTI89 $\Delta pgaA-D$ were very similar to the one of UTI89 wild type, starting at $8.60 \times 10^{06} \pm 5.41 \times 10^{06}$ CFU / g of bladder after 1 day and decreasing by almost two log scales until day 2. Than the bacterial titres only marginally decreased and stagnated at the same level of the titres in UTI89 wild type. UTI89 $\Delta fimA-H$ is known to have a reduced fitness in the host (7). Therefore, it was expected that the bacterial titres of UTI89 $\Delta fimA-H$ were strongly reduced compared to UTI89 wild type. However, we found that the bacterial titres of UTI89 $\Delta fimA-H$ remained constant over the whole experiment of three

Results

weeks. This finding indicates that UTI89 $\Delta fimA-H$ is capable of persisting in the bladder at very low but detectable titres over 3 weeks, arguing that type I fimbriae are not the sole virulence factor required for *in vivo* survival.

Considering the low bacterial titres after 1 day post infection it was crucial to investigate, if the established animal model allowed differentiating between a strain capable of residing in the bladder and cause cystitis (UTI89), a strain with reduced virulence (UTI89 $\Delta fimA-H$), a non-pathogenic strain (MG1655) and a sterility control. Six mice per strain were therefore infected with UTI89 wild type, UTI89 $\Delta fimA-H$, or the non-pathogenic MG1655 and two mice were infected with sterile PBS to see if a distinction between these four different strains is possible (Figure 14B). While we detected $1.56 \times 10^6 \pm 5.51 \times 10^5$ CFU / g of bladder for UTI89 wild type the titres of UTI89 $\Delta fimA-H$ were at $1.70 \times 10^4 \pm 1.24 \times 10^4$ CFU / g of and very similar to the titres of MG1655 were ($1.87 \times 10^3 \pm 9.78 \times 10^2$ CFU / g of bladder). Thus, the CFU / g of bladder counts of MG1655 were more than 800 times lower than those of UTI89 and only 9 times lower than the CFU / g of bladder counts of UTI89 $\Delta fimA-H$. Similarly, the infection of UTI89 $\Delta fimA-H$ was 92 times lower than the one caused by UTI89 wild type.

5.6 Discussion

Pathogenic bacteria often survive and persist in the host by forming biofilms, in which they are protected from antimicrobial therapies and the host immune system. Treatment with antimicrobial chemotherapies are inefficient in killing biofilm associated pathogens (20, 49-51) but expose them to sub-MICs for several hours (46). Importantly, sub-MIC of translation inhibitors were shown to induce PGA dependent biofilms in non-pathogenic *E. coli* (20) and recent reports suggest that UPECs form biofilms and express PGA during infections (52, 53), arguing that PGA should be relevant during the pathogenesis caused by UPECs. Similar to non-pathogenic *E. coli* MG1655 (20), it is shown here that different UPECs form PGA dependent biofilms upon derepression of the Csr system as well. C-di-GMP synthesised by the DGC YdeH induced PGA synthesis. Furthermore, the PGA dependent biofilms increased upon addition of translation inhibitors, which induced SpoT-mediated hydrolysis of ppGpp. However, deletion of the functional PGA machinery did not affect survival of UPECs during acute cystitis infections in mice. However, this finding might not exclude the importance of PGA expression during chronic infections. Long term effects of PGA genes on chronic infections could not yet be determined.

5.6.1 UPECs form PGA dependent biofilms upon derepression of the Csr system

To investigate the regulation of biofilms by the Csr system, different strategies were compared in the non-pathogenic MG1655. CsrB overexpression induced more attachment than partial CsrA inactivation. Inactivation of CsrA was not successful in the UPEC strain UTI89, probably due to reactivation of the Tn5 transposon in the UPEC strain UTI89. The overexpression of CsrB induced biofilm formation in UTI89, 83972 and PIII-V and hence circumvented the need to inactivate CsrA. Indeed, CsrB-mediated derepression in UPEC strains was comparable to CsrA-mediated derepression of the biofilm in MG1655 (20). Elevated levels of *csrB* and *csrC* were reported upon colonisation or growth of 83972 in human urine (54, 55) arguing that the Csr system is derepressed *in vivo* and could thus favour biofilm formation of UPECs during infection. In the pyelonephritis isolate CFT073 and the *E. coli* isolate DS17, which are able to infect the urothelium, inactivation of BarA/UvrY TCS reduces virulence during cystitis (56, 57), indicating that the Csr system is an important component for UTIs. Since UTI89 forms biofilm like structures upon internalisation into urothelial cells (2, 3, 58, 59), further experiments will show whether derepression of Csr system is relevant for IBCs. Different environmental signals might have an important impact with respect to localisation/colonisation of ABU and cystitis strains.

In our study, we found evidence that the Csr system functions as reported for non-pathogenic *E. coli* and other bacteria (12, 17, 60, 61). It is likely to speculate that *CsrB* overexpression results in translation of *pgaA-D* and thus enhanced biofilm formation in UPECs. Indeed, *in vitro* attachment and biofilm production decreased upon deletion of *pgaA-D* similar to MG1655 (17, 20). In contrast, the *pgaA-D* deletion had no effect on bacterial burden despite persistence in the bladder of mice for up to 21 days. This *in vivo* phenotype of the *pgaA-D* mutant was unexpected, since several upstream components required for enhanced PGA synthesis or PGA itself, increased virulence/persistence of UPECs or closely related species (12, 28, 53-57, 62, 63). However, none of the studies investigated the function of UPEC *pgaA-D* during cystitis. For example, the transcriptional regulator of *pgaA-D* (NhaR) was recently determined to be a virulence factor during *Proteus mirabilis* UTIs (62). Furthermore, it was shown that antibodies against *Staphylococcus aureus* PGA were protecting mice from lethal *E. coli* infections (53, 64). Whether PGA affects survival, persistence and recurrence of UTIs after more than 21 days has to be determined. Moreover, histological sections of the bladder should be included, as the lack of *pgaA-D* might affect the structure of IBCs or the recruitment of immune cells.

5.6.2 Sub-MICs of translation inhibitors affect attachment of most UPECs

Sub-MICs of translation inhibitors have been shown to stimulate PGA dependent biofilm formation in MG1655 (20) and in UTI89 (this study). Most newly isolated UPECs did not form biofilms without the overexpression of *csrB* or sub-MICs of translation inhibitors *in vitro*, similar to UTI89. Boehm *et al.* showed in detail that the effect of translation inhibitors on ribosomes results in a cascade that signals ribosomal stress to the PgaA-D machinery. This cascade depends on SpoT-mediated hydrolysis of the alarmone ppGpp as well as the DGC YdeH (20). Since lack of ppGpp strongly boosted PGA dependent biofilm formation in UTI89, we propose a conserved ppGpp signalling mechanism for most UPECs. However, in the isolate clin571, sub-MICs of translation inhibitors are sufficient to stimulate attachment in the absence of *csrB* overexpression. One can hypothesise that exposure of clin571 to sub-MICs during treatment uncoupled PGA dependent biofilms from the status of the Csr system. It needs to be demonstrated if attachment of clin571 is mediated by *pgaA-D*. Another interesting finding in the present study is the clin591 strain, which attached independent of *pgaA-D*. As discussed later, we want to characterize the alternative biofilm matrix component, which appears to be independent of the Csr system and dominant over PGA. In summary, clin591 appears to be an aberrant UPEC that is interesting to study but does not represent a subgroup of UPECS.

5.6.3 c-di-GMP increases attachment of UPECs

The second messenger c-di-GMP is important in the signalling network that contributes to PGA dependent biofilm formation in MG1655 and UPECs. Similar to the effects of *csrB* overexpression in different UPECs, modulation of c-di-GMP levels has not the same impact on attachment of all UPECs. Nevertheless, once the Csr system was derepressed the c-di-GMP mediated stimulation of biofilm production was reproduced in all strains upon DgcA overexpressed.

In a screening of MG1655 mutants each lacking one DGC (GGDEF domain), PDE (EAL domain), or composite protein (GGDEF and EAL domain) at a time, only the *ydeH* (DGC) deletion mutant showed reduced attachment (20). We analysed DNA sequences in different UPECs and found that the amount and diversity of DGCs, PDEs, and composite proteins is similar to MG1655 (data not shown). Considering the similar availability of c-di-GMP related proteins in UPECs and MG1655 as well as the conserved function of PGA and the Csr system, we assumed that YdeH must be one of the major contributors of c-di-GMP in UTI89. We confirmed this hypothesis by demonstrating a decreased attachment in a UTI89 $\Delta ydeH$ deletion mutant. This suggests that UPECs also use c-di-GMP synthesis to stimulate *pgaA-D* dependent biofilm formation. Importantly, we showed that PGA dependent attachment could still be modulated via alternative DGCs (e.g. *ycdT*) or PDEs (*c1116*) in the absence of YdeH.

A recent study has shown that *ycdT* of *E. coli* is a DGC which is under positive selection in UPECs (28). However, did not find altered activity of the *ycdT* deletion in UPECs, indicating that *ycdT* is a weak diguanylate cycles in both MG1655 and UTI89. We observed that deletion of YdeH and YcdT together reduced the attachment more than deletion of YdeH alone. Despite of the missing ci-di-GMP measurements, we conclude that YcdT behaves like an active but weak DGC in UTI89. From the phenotypic comparison between UTI89 $\Delta ydeH$ and UTI89 $\Delta ycdT$ it appears that the strong DGC (YdeH) compensates for the lack of c-di-GMP upon deletion of the weak DGC (YcdT). On the other hand, weak DGCs might not be able to complement the reduced production of c-di-GMP of a strong DGC mutant (YdeH). We speculate that strong DGCs like YdeH serve to promote major physiological adaptations, e.g. by stimulating PGA production, while weak DGCs (e.g. YcdT) have a modulatory function. This would allow hierarchical roles of DGCs (and PDEs) depending on transcriptional, translational (e.g. via CsrA), post-translational levels but also via protein activity (e.g. dimerisation) and stability. Additionally, the hierarchy must be influenced by the availability of external and internal signals that activate specific DGCs (or PDEs) via their signal input

domains. This would allow bacteria to change their lifestyle when strong DGCs or PDEs are activated. Evidence for this assumption is demonstrated by ribosomal stress affecting PGA dependent biofilm formation in a ppGpp and YdeH dependent manner (20). On the contrary, the signals of a weak DGCs (e.g. YcdT) or PDEs would be inferior and only marginally affect bacterial physiology. To predict the interplay of different c-di-GMP metabolising DGCs and PDCs, their activity and abundance needs to be assessed *in vivo*. Furthermore, animal experiments would be helpful to investigate the overall effects of c-di-GMP on the UPEC pathogenesis. Ideally, this could be achieved by overexpression of either strong DGCs or PDEs, under a constitutive promoter from the chromosome. To fully test our established attachment model, the phenotypes of UTI89 deletion mutants affecting the Csr system (e.g. BarA/UvrY, *csrB*, *csrC* or *CsrD*) also need to be investigated *in vivo*.

5.6.4 Biofilm formation in clin591 is different than in UTI89

Clin591 was originally included in this study because of its aberrant behaviour in biofilm formation compared to all the other UPECs that form PGA dependent biofilms. As already discussed above, the attachment of a *pgaA-D* mutant in clin591 depended on an alternative matrix component. Interestingly, clin591 attachment responded variably upon overexpression of *csrB* from different plasmids (*pcj30 csrB* vs. *pCsrB*). While the induction of *pcj30 csrB* resulted in a stimulation of biofilm, *pCsrB* induction had no effect on attachment. The difference might be caused by sequences around the two insertion sites of *csrB* on the two plasmids as well as the different transcriptional start sites in both vectors. Furthermore, the copy number of *pcj30* and *pME6032* per cell might be different influencing the level of plasmid derived *csrB* molecules per cell. From this we conclude that clin591 is more susceptible to fluctuations of *csrB* levels than other UPECs. The different attachment behaviour of clin591 could thus be attributed to altered sensitivity toward the Csr system. To test this idea, all known components of the Csr system (*barA*, *uvrY*, *csrB*, *csrC*, *csrD* and if possible *csrA*) have to be deleted in clin591 and phenotypically characterised in attachment assays. If any component affects clin591 attachment, they should be sequenced and compared to other UPECs.

It is known that c-di-GMP positively activates many different forms of biofilm matrices (65-67), arguing that elevated levels of c-di-GMP could still boost this non-PGA dependent biofilm formation of clin591. Overexpression of *DgcA*, as well as the deletion of *ydeH* showed the expected responsiveness of this strain to c-di-GMP. As this responsiveness only became apparent upon overexpression of *csrB* it can be argued that the non-PGA matrix component

remains dependent on the Csr cascade and c-di-GMP. Alternatively, it could be hypothesised that *clin591* forms biofilms, which are composed of two matrix components other than type I fimbriae (data not shown) and PGA. In such a situation, one matrix component is always activated while the other one requires elevated levels of *csrB* and c-di-GMP to be induced. This hypothesis would also account for the fact that sub-MICs of translation inhibitors do not stimulate *clin591* attachment, since this induction depends on *pgaA-D*. A transposon mutagenesis screen in *clin591* might lead to the identification of the matrix components.

5.6.5 YdeH_{UTI89} and YdeH₈₃₉₇₂ alleles do not complement YdeH_{MG1655}

YdeH was shown to be the DGC with the strongest attachment phenotype in MG1655 (20) and UTI89 (this study). Other than *ycdT* this DGC is quite conserved among UPECs and other *E. coli* species (data not shown). Compared to MG1655 the allele of UTI89 contains three non-silent SNPs that are located evenly dispersed throughout the protein. According to the structure of YdeH (F. Zaehring; unpublished data) these three SNPs localize in the dimerization interphase of the sensory domain, in the GGDEF domain that comprises the active site and in the loop connecting the two domains. Based on their localisation it was impossible to deduce the significance of any SNPs. Therefore, two different *ydeH* alleles (*ydeH_{UTI89}* and *ydeH₈₃₉₇₂*) were investigated in the genetic background of MG1655 *csrA*⁻. We found that their effects on intracellular c-di-GMP levels and *pgaA-D* dependent attachment were different. The attachment and the intracellular c-di-GMP concentrations of MG1655 *csrA*⁻ *ydeH₈₃₉₇₂* together indicate a low activity of *ydeH₈₃₉₇₂*. Despite its elevated level of c-di-GMP determined for *ydeH_{UTI89}*, this allele resulted in an attachment similar to a *ydeH* deletion mutant (AB959). Though counterintuitive these results have been observed in hyperactive *ydeH* alleles (A. Boehm, personal communication) indicating that maximal attachment can only occur in a specific margin of c-di-GMP levels. Thus hyperactivity of YdeH_{UTI89} could explain the observed phenotypes. A step by step modification of *ydeH_{MG1655}* towards *ydeH_{UTI89}* through insertion of one SNP at a time followed by a biochemical comparison of the different alleles would be very helpful in understanding which of the SNP / SNPs is / are responsible for the potentially more active *ydeH* of UTI89.

In conclusion, the *in vitro* effect of PGA and c-di-GMP on biofilm formation of UPECs seems to be comparable to the model established in MG1655 (20); however, animal studies did not yet reveal the impact of PGA or c-di-GMP during chronic cystitis and requires further investigations.

5.7 Figure Legend

Figure 1: Congo red binding in UPEC strains

The ability of UPECs to bind congo red was compared to the laboratory MG1655 wild type strain, MG1655 *csrA*⁻ (AB958) and MG1655 *csrA*⁻ Δ *ydeH* (AB959). **A)** Congo red binding on LB plates containing 0.1 % congo red. **B)** Congo red binding of selected UPEC strains on LB plates containing 0.04 % congo red and 20 μ g / ml coomassie brilliant blue (35). These Images of colonies reveal more subtle differences compared to colonies in **A)**. illumination from above.

Figure 2: Motility of UPEC strains

Motility of UPEC strains on 0.3 % TB swarm agar plates was compared to the laboratory MG1655 strain, MG1655 *csrA*⁻ (AB958) and MG1655 *csrA*⁻ Δ *ydeH* (AB959). All motility plates were simultaneously scanned on a Microtek ScanMaker i800 scanner. The insets of 83972 and PIII-4 are images of the same plates taken through a binocular (Wild; Heerbrugg M3Z) at a magnification of 24 x with a Nikon Coolpix 990. All images were processed with Photoshop CS5.

Figure 3: Attachment of UPEC strains

Comparative analysis of biofilm formation between different *E. coli* strains **A)** The attachment of MG1655 *csrA*⁻ is compared to the attachment of MG1655 upon overexpression of *csrB* from plasmid (pcj30 *csrB*) or its control vector pcj30, respectively. **B)** Attachment of different UPEC strains and the effects of *csrB* overexpression from pcj30 *csrB*: Attachment values are shown as (surface-attached biomass divided by optical density of total cells). White bars show the attachment of strains with the empty vector (pcj30), black bars show attachment of strains carrying pcj30 *csrB*. **C)** Illustrates the effects of artificially increased cyclic-di-GMP levels on attachment. All data sets in **C)** have been normalised to the *csrB* induced biofilm of each wild type strain. The values are normalised as follows: ((surface-attached biomass divided by optical density of total cells) in percentage of wild type pCsrB). The pME6032 plasmid is used as vector control for pME6032 *csrB*. Increased c-di-GMP values are achieved through overexpression of the diguanylate cyclase DgcA from pBAD18. Black bars represent data obtained for UTI89, data for 591 is illustrated in white, light grey

shows data for 83972 and dark grey illustrates attachment of PIII-4. All errors are standard errors of the mean and are calculated from at least 6 wells per strain.

Figure 4: Influence of DGCs and *csrB* on motility of UTI89

The influence of *csrB* (pcj30 *CsrB*), DgcA (pAB551), the point mutant DgcA D164N (pAC551), and WspR (pME6010 *WspR*) on motility of UTI89 upon overexpression from plasmid was analysed on 0.3 % TB swarm agar and compared to the motility of UTI89 without plasmids and UTI89 with control plasmids. If necessary, TB swarm plates were supplemented with ampicillin (pcj30, and pBAD18) or tetracyclin (pME6032) and induced with 100 μ M IPTG or 0.2 % arabinose. After 6h of growth at 37° C, swarm plates were scanned on a Microtek ScanMaker i800 scanner and images were processed with Photoshop CS5.

Figure 5: The role of poly-GlcNAc, and diguanylate cyclases on UTI89 attachment

Poly-GlcNAc and c-di-GMP contribute to efficient biofilm formation in UTI89: **A)** Bars are shown as percentage of UTI89 wild type pcj30 *csrB* attachment calculated as (surface-attached biomass divided by optical density of total cells). Data obtained for the control plasmid pcj30 is shown in white, data for pcj30 *csrB* is shown in black. Error bars are standard errors of the mean calculated over at least three independent assays. **B – F):** Electron micrographs of biofilms grown statically on glass slides for 24 h at 37°C in the presence of pcj30 *csrB* induced with 100 μ M IPTG. Scale bars are indicated in each micrograph taken at a magnification of ~1000x. **B)** UTI89 wild type. **C)** UTI89 $\Delta ycdT$. **D)** UTI89 $\Delta ydeH$. **E)** UTI89 $\Delta pgaA$ **F)** UTI89 $\Delta ycdT \Delta ydeH$.

Figure 6: The role of poly-GlcNAc, and diguanylate cyclases on clin591 attachment

Poly-GlcNAc and c-di-GMP do not majorly contribute to efficient biofilm formation in clin591: The data is shown as percentage of clin591 wild type pcj30 *csrB* attachment corrected for growth (surface-attached biomass divided by optical density of total cells). Data obtained for the control plasmid pcj30 is shown in white, data for pcj30 *csrB* is shown in black. Error bars are standard errors of the mean.

Figure 7: Effects of translation inhibitors on clin591 biofilms at sub-MICs

Biofilms of clin591 were grown in the presence of sub-MICs of (A) tetracycline, (B) streptomycin and (C) chloramphenicol. The concentrations used for each antibiotic are indicated on the x-axis of each graph. Bars indicate quantified attachment (left y-axis). Bacterial growth is indicated as curves on the right y-axis and was measured at an OD₆₀₀. Error bars are standard errors of the mean. The left graphs illustrate the absolute attachment (OD₆₀₀ of crystal violet staining) of clin591 while the right graphs show the relative attachment (OD₆₀₀ of crystal violet staining / OD₆₀₀ of growth).

Figure 8: Effects of tetracyclin on clin571 biofilm at sub-MICs

Biofilms of clin571 were grown in the presence of sub-MICs of tetracycline. The concentrations of tetracycline are indicated on the x-axis of the graph. Bars indicated the quantified attachment (left y-axis). Bacterial growth is indicated as curves on the right y-axis and was measured at an OD₆₀₀. Error bars are standard errors of the mean. The left graph illustrates the absolute attachment (OD₆₀₀ of crystal violet staining) of clin571 while the right graph shows the relative attachment (OD₆₀₀ of crystal violet staining / OD₆₀₀ of growth).

Figure 9: Induction of UTI89 biofilms by sub-MICs of translation inhibitors and the importance of *csrB* overexpression

UTI89 pcj30 *csrB* biofilms were exposed to sub-MICs of (A) tetracycline, (B) streptomycin and (C) chloramphenicol. The respective antibiotic concentrations are indicated on the x-axis of each graph. Uninduced UTI89 pcj30 *csrB* (black) was compared to UTI89 pcj30 *csrB* induced with 10 µM IPTG (light grey) and UTI89 pcj30 *csrB* induced with 100 µM IPTG (dark grey). Bars indicate the quantified attachment (left y-axis). Bacterial growth is indicated as curves on the right y-axis and was measured at an OD₆₀₀. Error bars are standard errors of the mean. On the left side, bacterial biomass is quantified as absolute values (OD₆₀₀ of crystal violet staining) while the right graphs show relative attachment (OD₆₀₀ of crystal violet staining / OD₆₀₀ of growth).

Figure 10: Biofilm induction by sub-MICs of tetracycline and the importance of *pgaA-D*

UTI89 strains were exposed to sub-MICs of tetracycline for 24 h after which cell density (growth) and bacterial surface attachment was quantified. The antibiotic concentrations used

Figure Legend

are indicated on the x-axis of each graph. UTI89 pcj30 is shown in light grey, UTI89 pcj30 *csrB* in black and UTI89 Δ *pgaA-D* pcj30 *csrB* is shown in dark grey. Bars indicate the quantified attachment (left y-axis). Bacterial growth is indicated as curves on the right y-axis and was measured at an OD₆₀₀. Error bars are standard errors of the mean. On the left side, bacterial biomass is quantified as absolute values (OD₆₀₀ of crystal violet staining) while the right graph shows the relative attachment (OD₆₀₀ of crystal violet staining / OD₆₀₀ of growth).

Figure 11: The importance of the Csr cascade, c1116 and ppGpp on UTI89 attachment

Data is shown as percentage of UTI89 pCsrB attachment of (surface-attached biomass divided by optical density of total cells). Data obtained for the control vector pME6032 is shown in white, data for pCsrB is shown in black. Error bars are standard errors of the mean. **A)** Effects of *csrB*, *csrC* and *csrD* on poly-GlcNAc dependent attachment. The data was calculated as average over three independent attachment assays. Bars are calculated from $n \geq 10$ wells. **B)** Attachment data of an UPEC specific PDE *c1116* and its adjacent gene *c1117*. The data shown in the graph was calculated as average over two independent attachment assays and at least 7 wells. **C)** Attachment of a ppGpp⁰ UTI89 strain. The attachment was calculated over 6 wells per strain and plasmid and corrected for growth.

Figure 12: SNPs between YdeH of MG1655 and UTI89

The positions of non-silent SNPs found between MG1655 and UTI89 are shown on the structure of the MG1655 YdeH (Zaehring et. al, manuscript in process). **A)** Structure of a YdeH dimer of MG1655. The protein comprises a signal input domain in the C-terminus and a DGC domain which comprised the active site (A-site) of the enzyme as well as the I-site of the protein. The two domains are connected via a linker that contains one of the three non-silent SNPs (N130S). The position of this SNP is marked with a red circle. **B)** Visualization of the DGC domain containing both the A-site and I-site of the protein. A217T is a SNP which is located on a loop in proximity of the I-site. A217 is encircled in red. **C)** Representations of the signal input domain of YdeH. The third SNP (H31R) is encircled in red in both representations. In the left illustration, the viewer looks down the dimerization interface of the protein. On the right side, the protein is tilted by 90° and thus shows the signal input domain of the protein.

Figure 13: *ydeH* allelic exchange in MG1655

Figure Legend

The attachment assay was performed at **(A)** 37° C and **(B)** 30° C to account for the fact that UTI89 adheres better at 37°C while MG1655 adheres better at 30°C. In UTI89 the pME6032 *csrB* plasmid was overexpressed and in MG1655 strains the CsrA was inactivated (*csrA*⁻). Bars are calculated as (surface-attached biomass divided by optical density of total cells) and then normalised to the attachment of MG1655 *csrA*⁻ (100 %). Error bars are standard errors of the mean. **C)** Intracellular c-di-GMP concentrations of MG1655 with *ydeH* alleles of UTI89 and 83972. The c-di-GMP levels have been measured as triplicates via HPLC-MS/MS. Levels are indicated as total µM c-di-GMP concentration per bacterial cell.

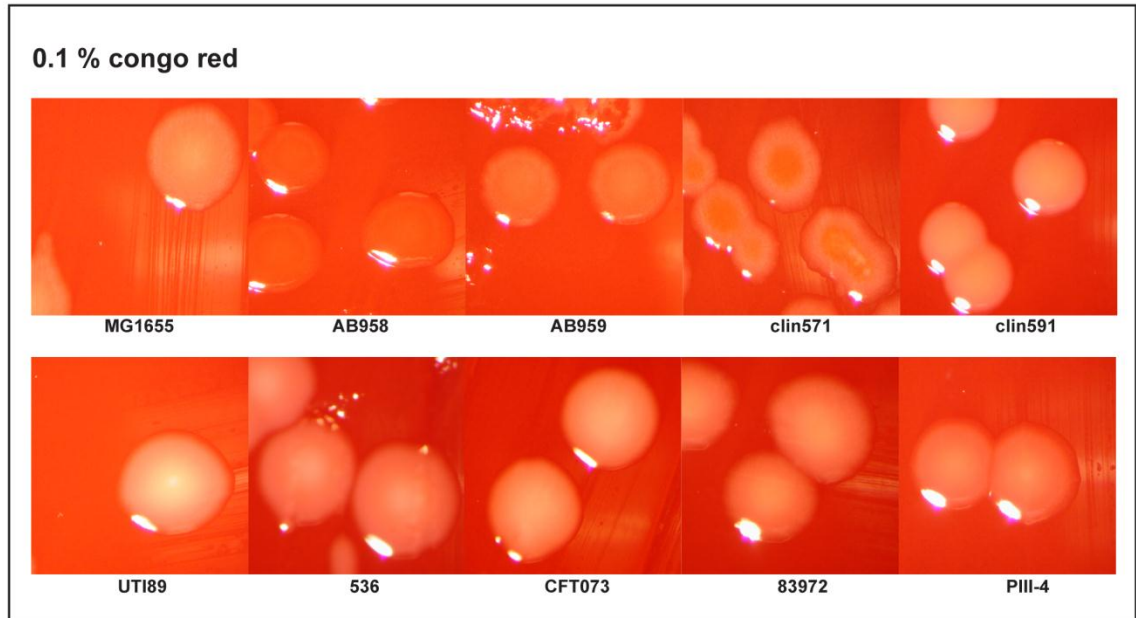
Figure 14: Murine cystitis model

For each experiment, 6 mice were infected with 1.5×10^9 bacteria concentrated in 30-45 µl sterile 0.9 % saline solution and observed for 1, 2, 3, 7, 14 or 21 days prior sacrifice. The data is represented as CFU / g of bladder with the median and the interquartile range over all animals (between 6 and 18 mice per strain and time point). CFU counts per animal are averaged from several plates of one bladder dilution series. None of the infected mice suffered from severe weight loss, died, or had to be sacrificed in advance, indicating that the wellbeing of the animals was never endangered during the experiment. The detection limit of 10 CFU / g of organ is shown as a dotted line. **A)** UTI89 (●), UTI89 $\Delta pgaA-D$ (○) and UTI89 $\Delta fimA-H$ (●). **B)** UTI89 (■), UTI89 $\Delta fimA-H$ (▲), MG1566 (▼) or PBS (◆), respectively. Values below the detection limit of 10 CFU per ml are indicated on the dotted line.

5.8 Figures

Figure 1

A



B

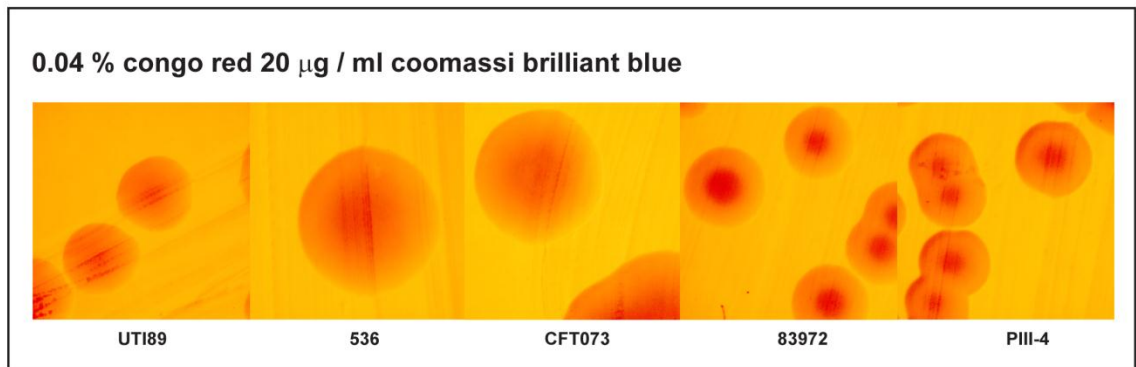


Figure 2

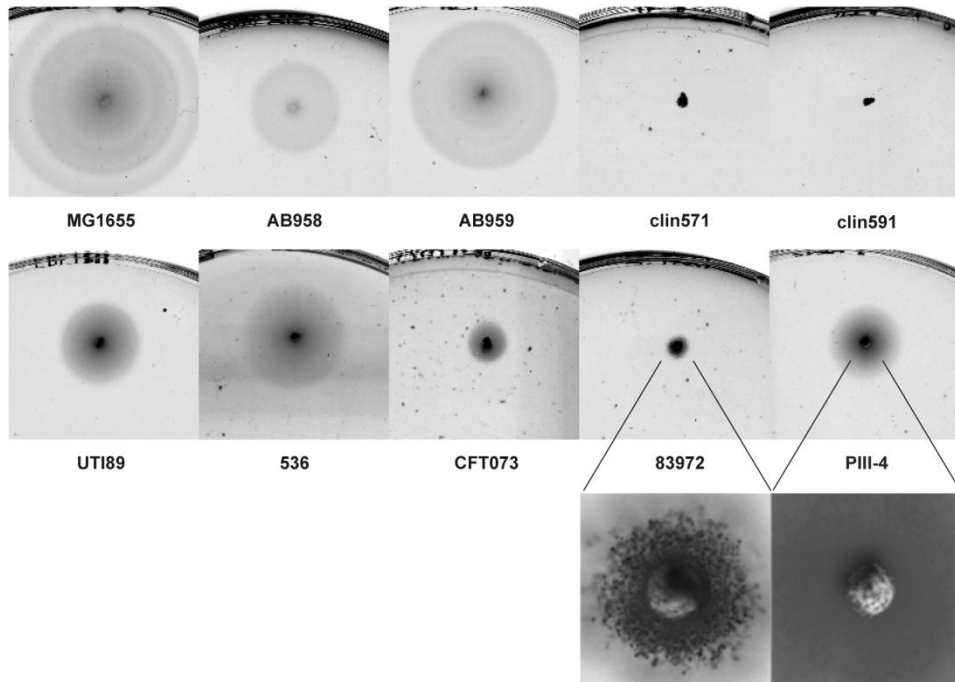


Figure 3

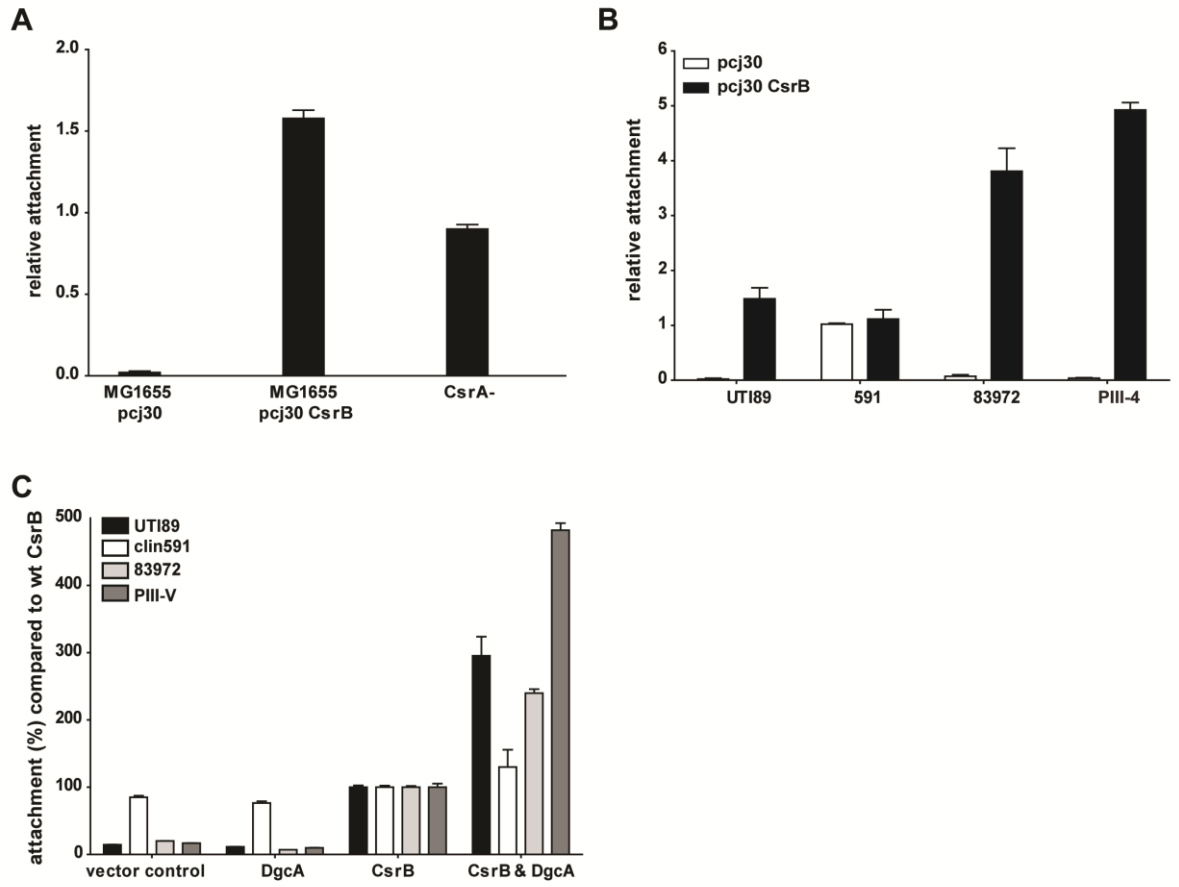


Figure 4

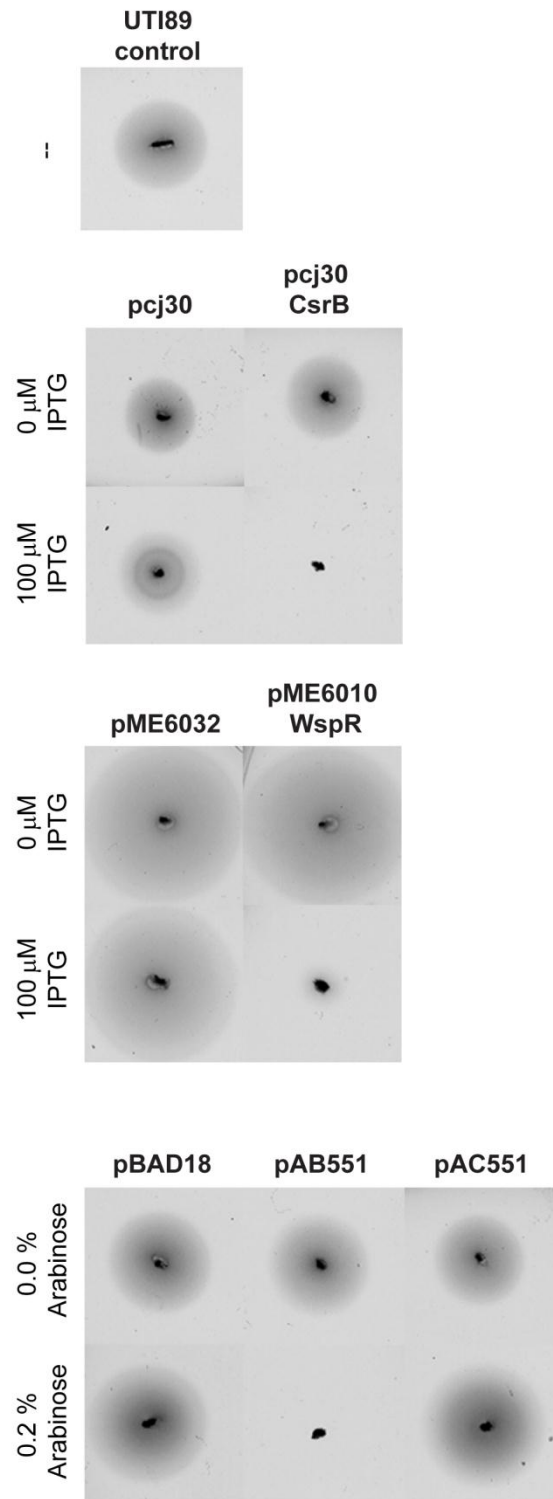


Figure 5

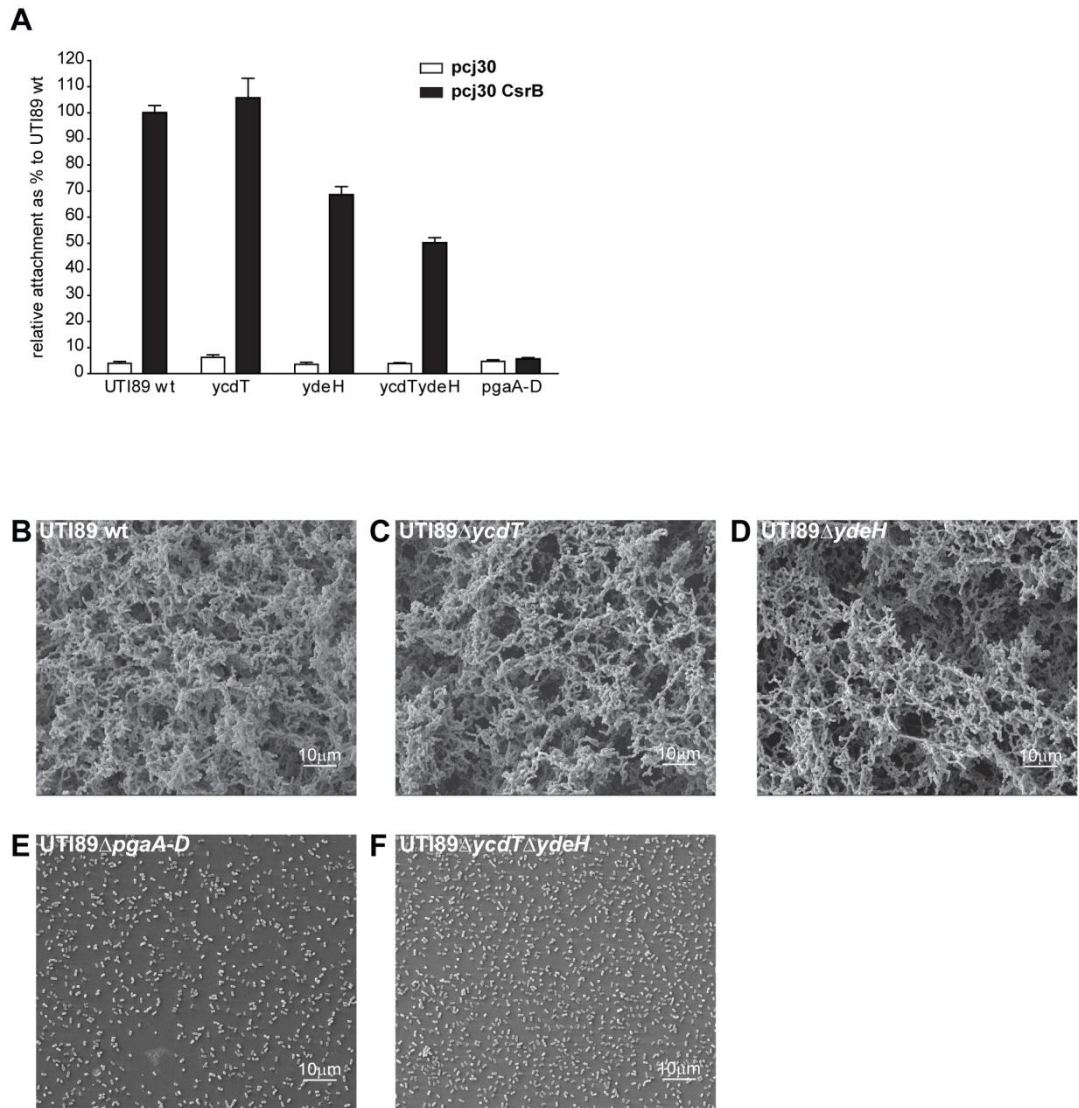


Figure 6

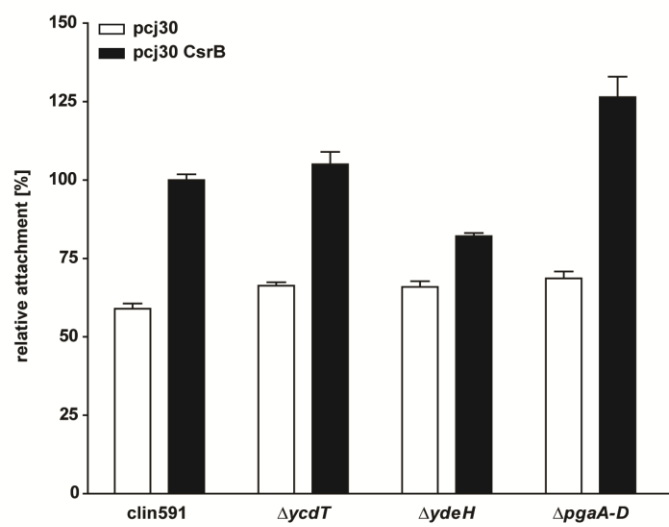


Figure 7

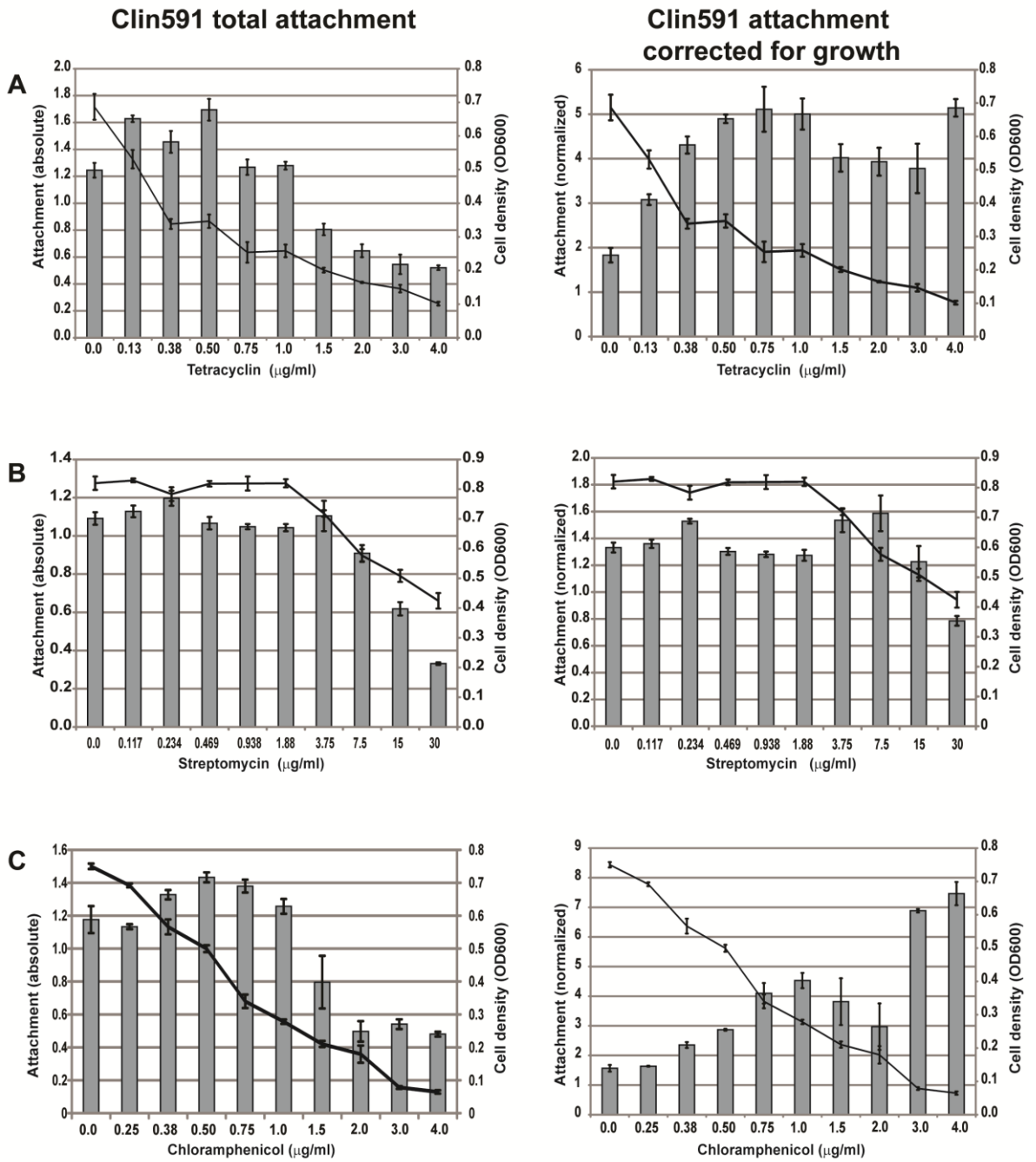


Figure 8

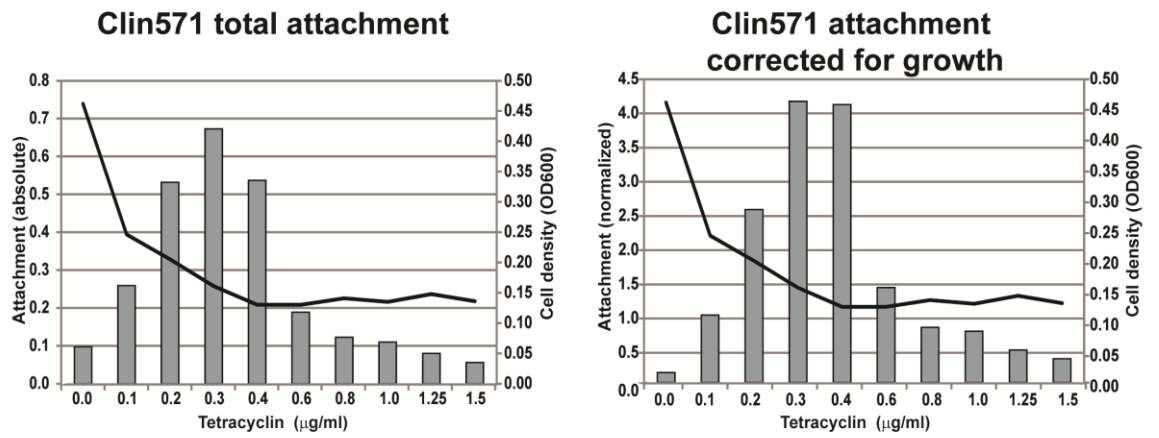


Figure 9

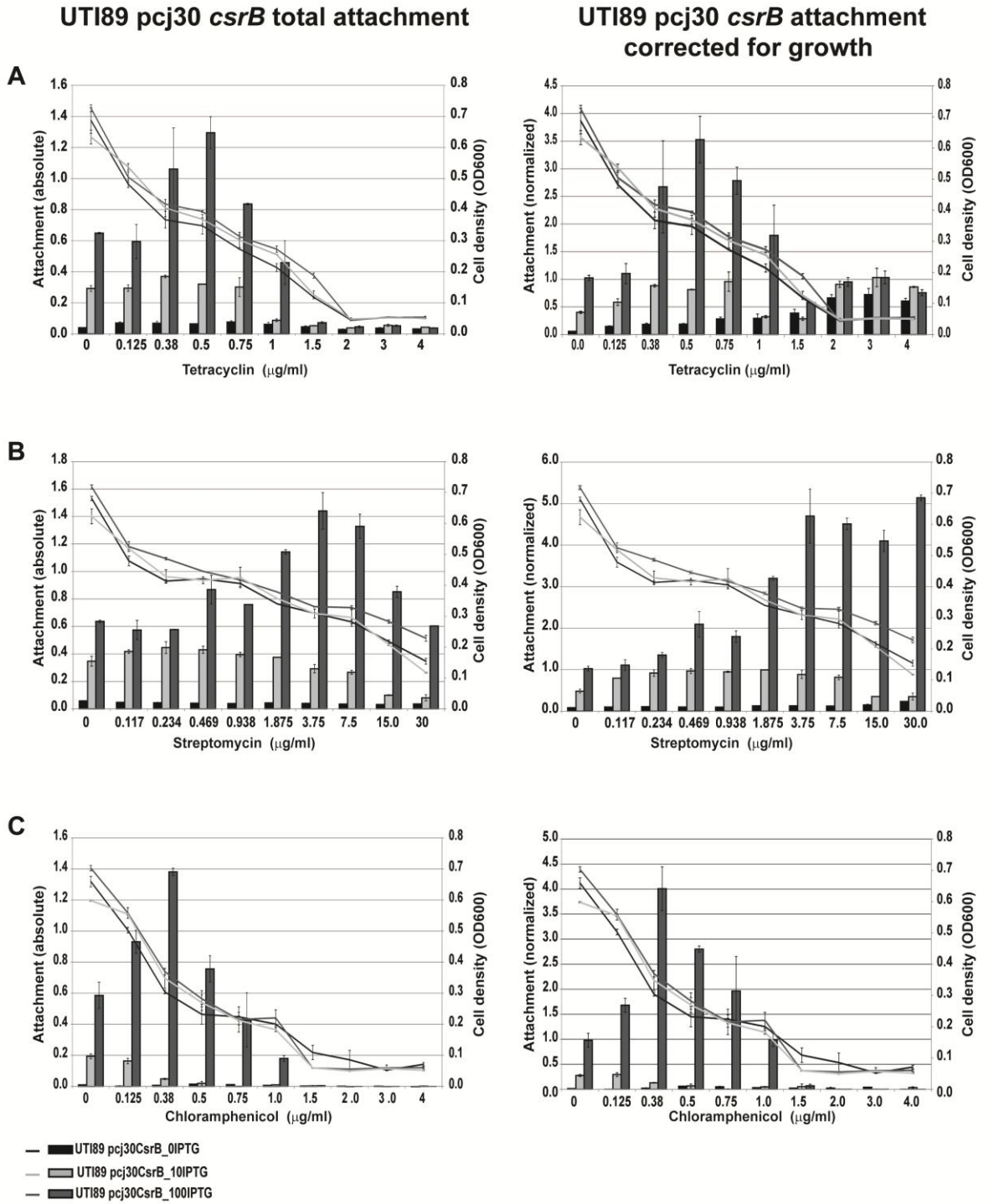


Figure 10

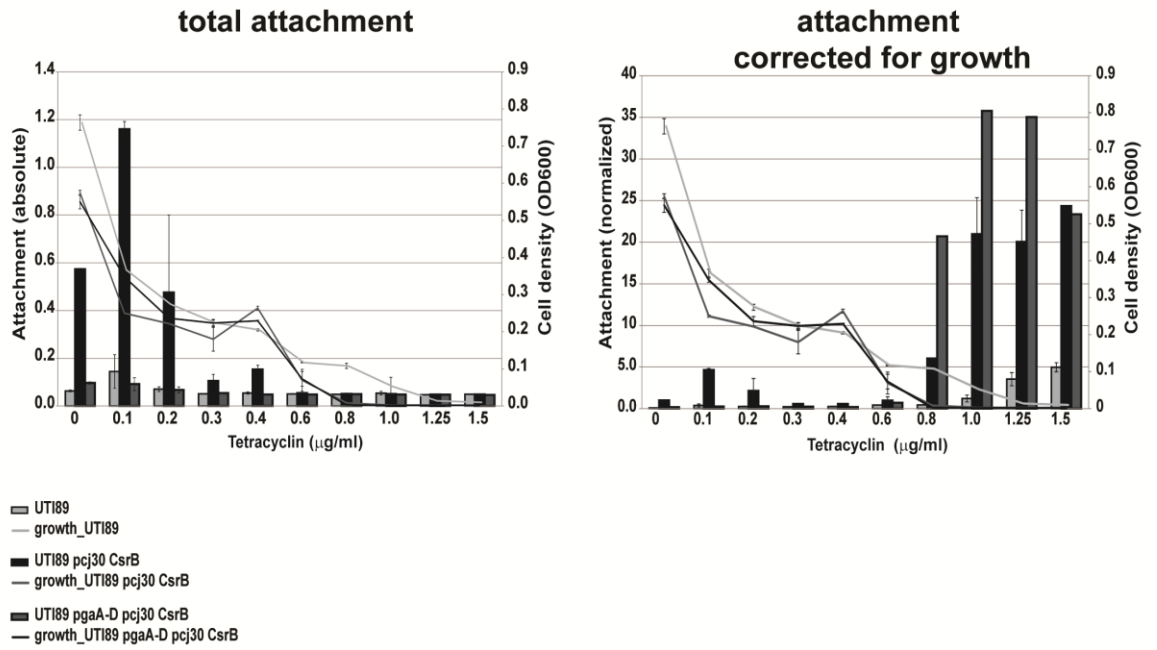


Figure 11

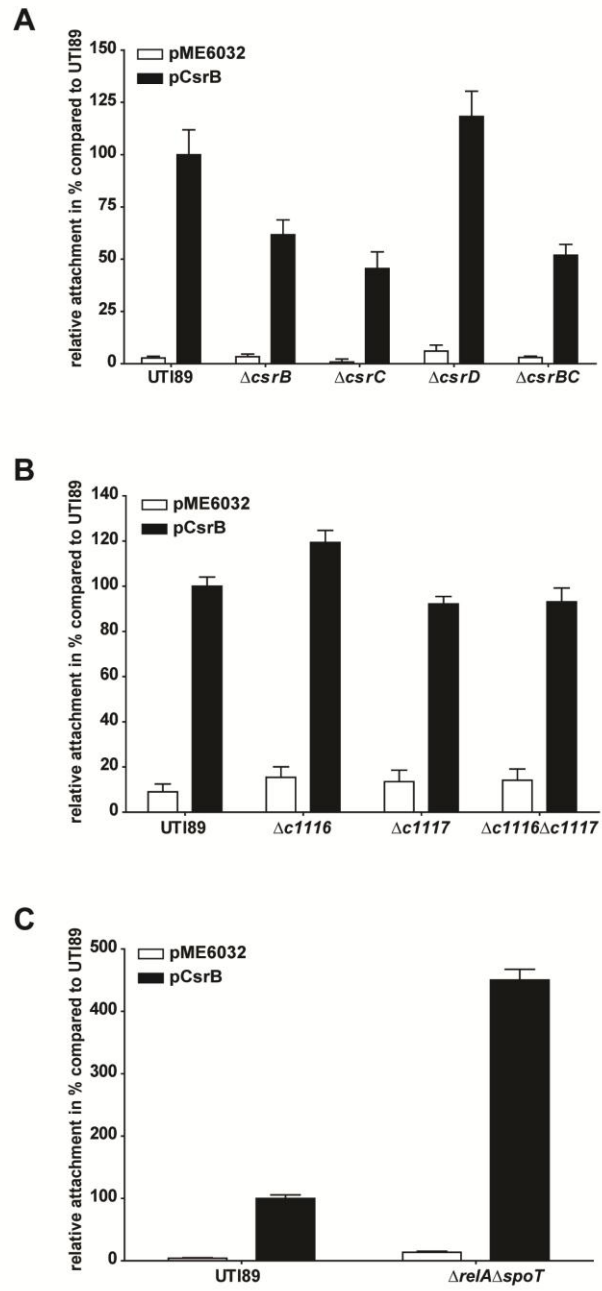


Figure 12

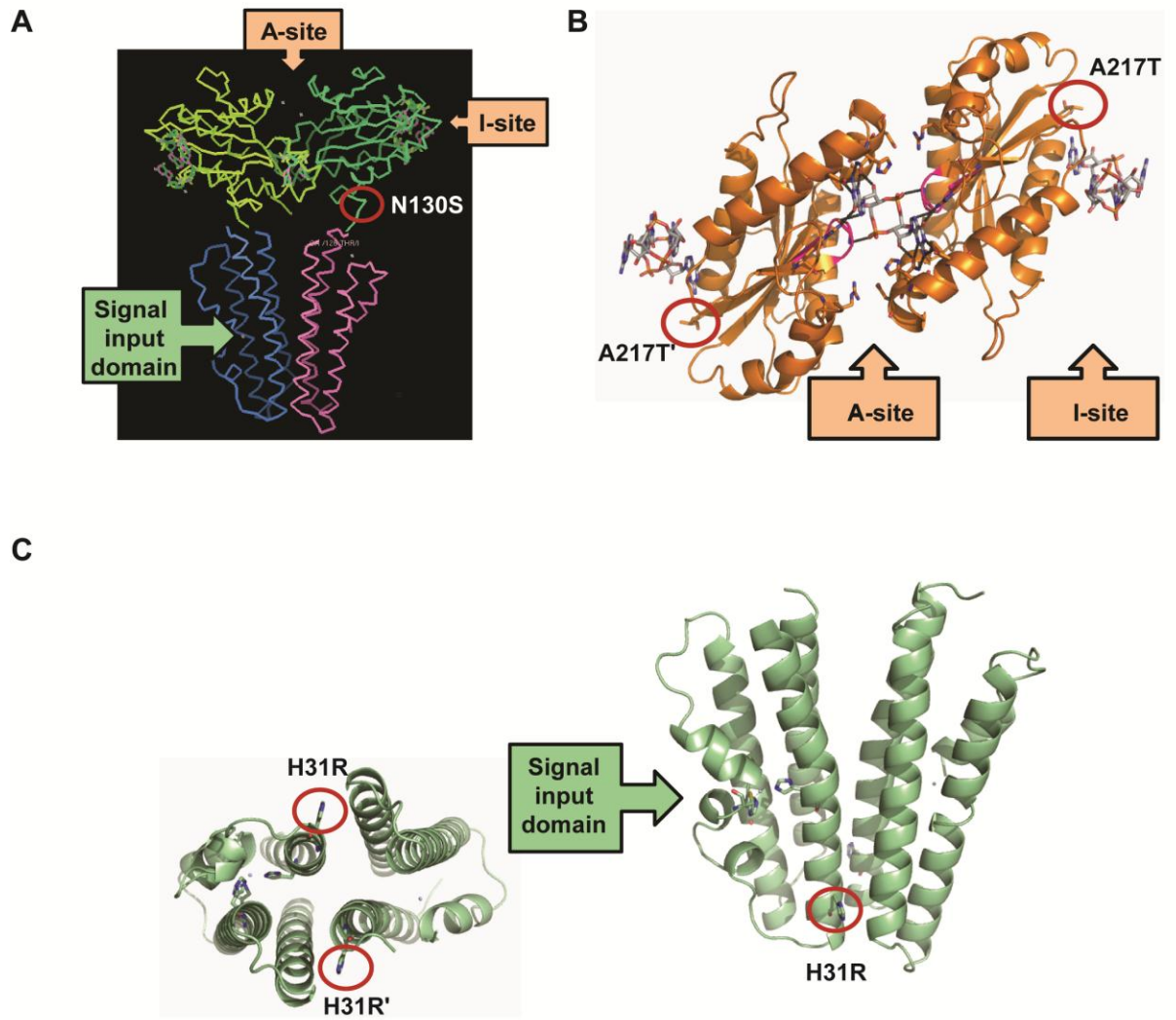


Figure 13

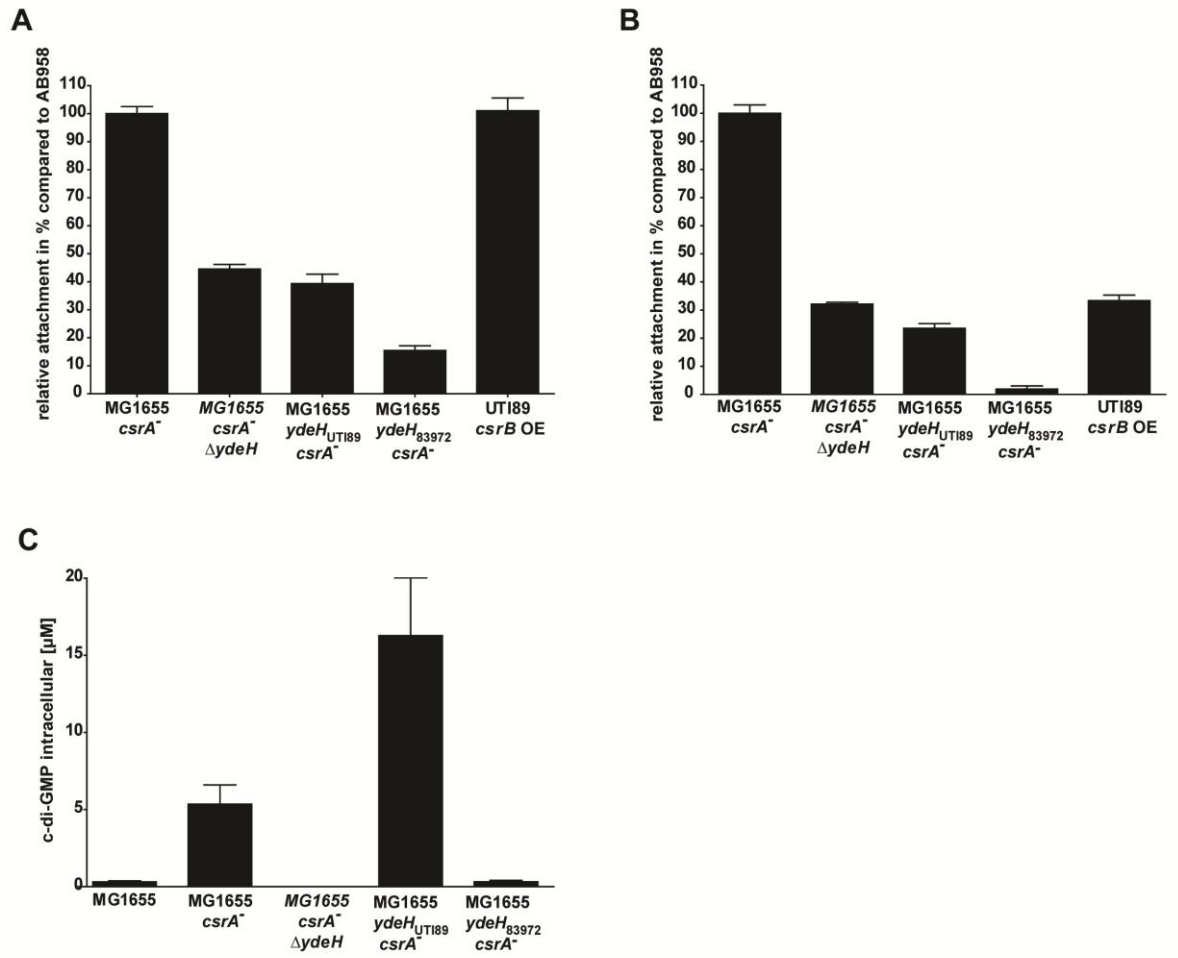
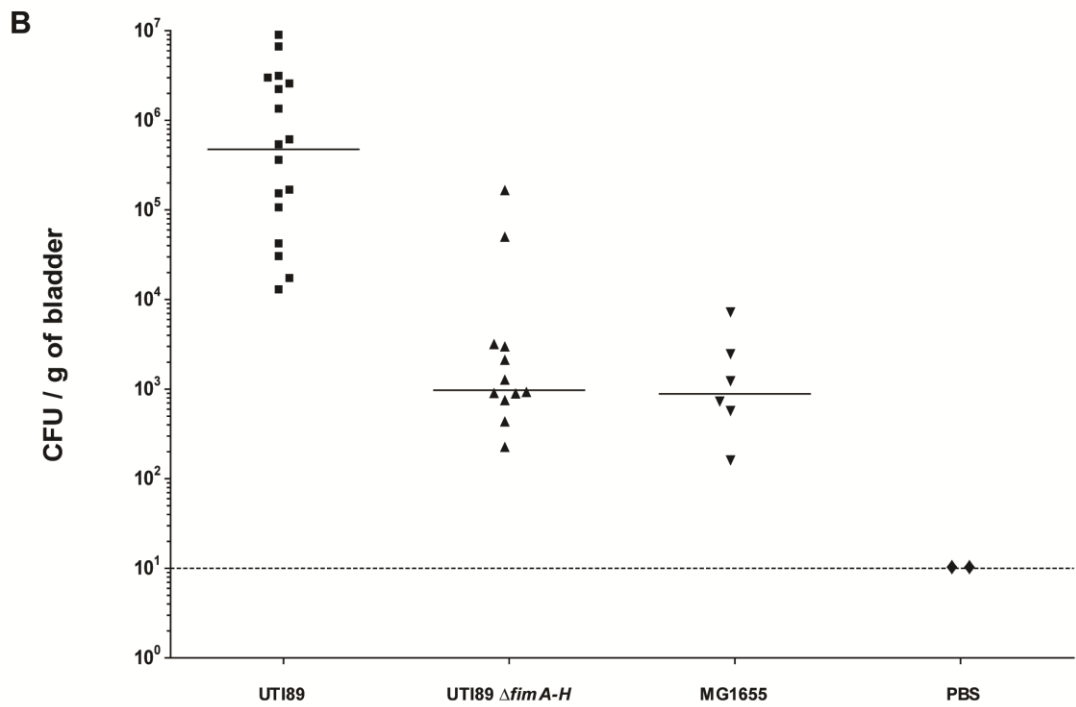
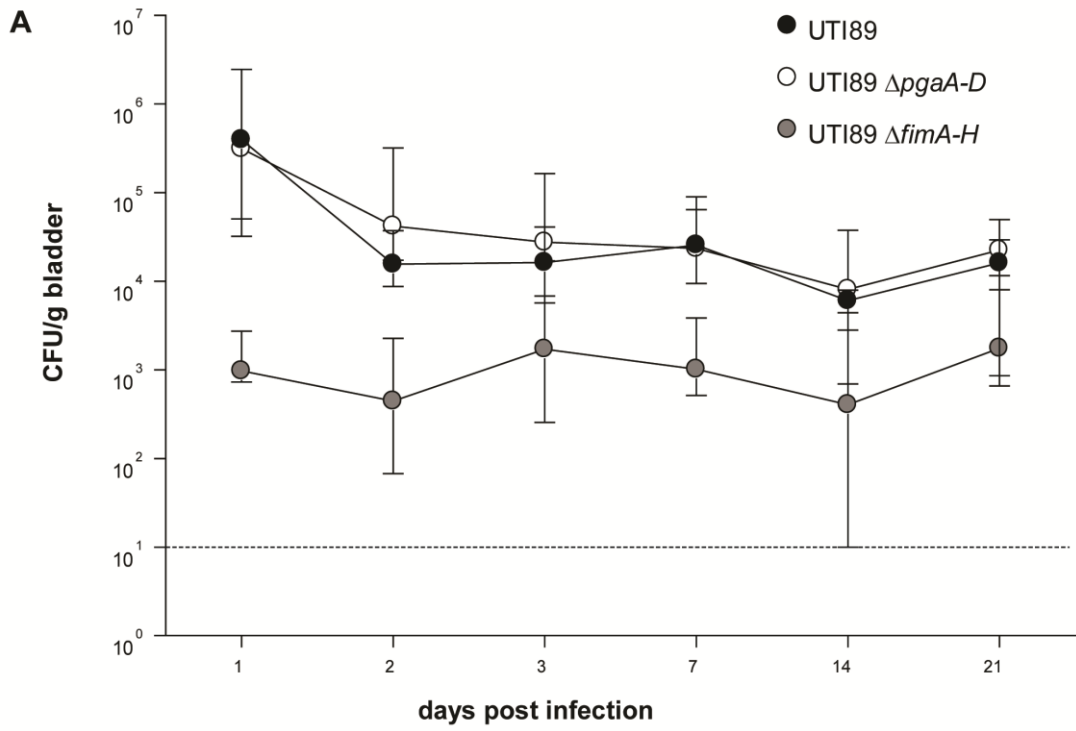


Figure 14



5.9 Tables

Table 1: Strains used in this study

Strain	Genotypes	Pathogenesis	Reference
MG1655 wt	sequenced wild type	non-pathogenic	Blatter <i>et al.</i> , 1997 (68)
AB958	<i>csrA</i> ::Tn5	N.A	Boehm <i>et al.</i> , 2009 (20)
AB959	<i>csrA</i> ::Tn5	N.A	Boehm <i>et al.</i> , 2009 (20)
AB1295	<i>ydeH</i> :: <i>ccdB</i> kan pKD46	N.A	this study
AB1295 <i>csrA</i> ⁻ <i>ydeH</i> _{UTI89}	<i>csrA</i> ::Tn5 <i>ydeH</i> :: <i>ccdB</i> :: <i>ydeH</i> _{UTI89}	N.A	this study
AB1295 <i>csrA</i> ⁻ <i>ydeH</i> ₈₃₉₇₂	<i>csrA</i> ::Tn5 <i>ydeH</i> :: <i>ccdB</i> :: <i>ydeH</i> ₈₃₉₇₂	N.A	this study
536 wt	sequenced wild type	Pyelonephritis	Hochhut <i>et al.</i> , 2006 (30)
clin571 wt	wild type	Cystitis	this study
clin591 wt	wild type	Catheter Associated UTI	this study
clin591 $\Delta ycdT$	<i>ycdT</i> :: <i>kan</i>	N.A	this study
clin591 $\Delta ydeH$	<i>ydeH</i> :: <i>kan</i>	N.A	this study
clin591 $\Delta pgaA-D$	<i>pgaA-D</i> :: <i>kan</i>	N.A	this study
83972 wt	sequenced wild type	Asymptomatic bacteriuria	Andersson <i>et al.</i> , 1991 (31) Lindberg <i>et al.</i> , 1975 (32)
CFT073 wt	sequenced wild type	Pyelonephritis	Welch <i>et al.</i> , 2002 (29)
P111-4	83972 re-isolate	Asymptomatic bacteriuria	Zdziarski <i>et al.</i> , 2008 (69)
UTI89	sequenced wild type	Cystitis	Mulvey <i>et al.</i> , 2001 (27) Chen <i>et al.</i> , 2006 (28)
UTI89 $\Delta ycdT$	<i>ycdT</i> :: <i>FRT</i>	N.A	this study
UTI89 $\Delta ydeH$	<i>ydeH</i> :: <i>FRT</i>	N.A	this study
UTI89 $\Delta ycd \Delta ydeH$	<i>ycdT</i> :: <i>FRT</i> <i>ydeH</i> :: <i>cat</i>	N.A	this study
UTI89 $\Delta pgaA-D$	<i>pgaA-D</i> :: <i>FRT</i>	N.A	this study
UTI89 $\Delta csrB$	<i>csrB</i> :: <i>FRT</i>	N.A	this study
UTI89 $\Delta csrC$	<i>csrC</i> :: <i>FRT</i>	N.A	this study
UTI89 $\Delta csrBC$	<i>csrBC</i> :: <i>FRT</i>	N.A	this study
UTI89 $\Delta csrD$	<i>csrD</i> :: <i>FRT</i>	N.A	this study
UTI89 $\Delta c1116$	<i>c1116</i> :: <i>FRT</i>	N.A	this study
UTI89 $\Delta c1117$	<i>c1117</i> :: <i>FRT</i>	N.A	this study
UTI89 $\Delta c1116 \Delta c1117$	<i>c1116</i> :: <i>FRT</i> <i>c1117</i> :: <i>FRT</i>	N.A	this study
UTI89 $\Delta relA \Delta spoT$	<i>relA</i> :: <i>FRT</i> <i>spoT</i> :: <i>kan</i>	N.A	this study
UTI89 $\Delta fimA-H$	<i>fimA-H</i> :: <i>FRT</i>	N.A	Abgottsporn <i>et al.</i> , 2010 (37)

Table 2: Plasmids used in this study

Plasmid name	Relevant genotype	Comments	Reference
pcj30	<i>lac^P bla⁺</i> (Amp ^R)	IPTG inducible expression vector	Bibikov <i>et al.</i> , 1997 (70)
pcj30 <i>csrB</i>	pcj30:: <i>csrB</i> (Amp ^R)	IPTG inducible expression vector; overexpression of <i>csrB</i>	this study
pME6032	pVS1 derived shuttle vector (Tet ^R)	IPTG inducible expression vector	Heeb <i>et al.</i> , 2000 (71)
pME6010 WspR	pME6010:: <i>wspR</i> (Tet ^R)	IPTG inducible expression vector; overexpression of WspR	Malone <i>et al.</i> , 2007 (72)
pCsrB	pME6032:: <i>csrB</i> (Tet ^R)	IPTG inducible expression vector; overexpression of <i>csrB</i>	this study
pBAD18	<i>araC⁺ bla⁺</i> (Amp ^R)	Arabinose inducible expression vector	Guzman <i>et al.</i> , 1995 (73)
pAB551	pBAD18:: <i>dgcA</i> (Amp ^R)	Arabinose inducible expression vector, overexpression of DgcA (cc3285) from <i>C. crescentus</i> ;	Boehm <i>et al</i> 2009 (20) Christen <i>et al.</i> , 2006 (74)
pAC551	pBAD18:: <i>dgcA</i> -D164N (Amp ^R)	Arabinose inducible expression vector, overexpression of DgcA D164N point mutant from <i>C. crescentus</i> ;	This study & Master thesis A. Casanova
pKM208	<i>lac^P</i> (Amp ^R)	IPTG inducible, temperature sensitive replication; λRED-mediated recombinogenic plasmid	Murphy <i>et al.</i> , 2003 (38)
pKD46	<i>araC⁺</i> (Amp ^R)	Arabinose inducible, temperature sensitive replication; λRED-mediated recombinogenic plasmid	Datsenko <i>et al.</i> , 2000 (39)
pCP20	<i>flp⁺</i> (Amp ^R) (CM ^R)	temperature-sensitive replication with inducible FLP recombinase	Cherepanov <i>et al.</i> , 1995 (75)

Table 3: Newly isolated UPECs from urine of hospitalised patients screened for sub-MIC induction of biofilm

Name	TET ^{R/S}	Biofilm*	Tetracycline induction#	Characteristics; comments	Age Patient	Gender Patient
536	S	--	--	Sequenced pyelonephritis isolate	N.A	N.A
UTI89	S	--	--	Sequenced cystitis isolate	N.A	F
clin76	S	--	--	Patient had chemo due to metastatic rectum cancer	74	F
clin56	S	--	--	Patient carried a DJ-Catheter	65	F
clin162	S	--	*	Patient had urethral complications and cerebral lymphoma	77	F
clin172	S	--	*	permanent catheter; patient had a spinal cord injury and UTI	94	F
clin181	S	--	--	N.A	45	F
clin184	R	--	--	N.A	75	F
clin197	S	--	--	Patient suffered from <i>Campylobacter</i> gastroenteritis	94	M
clin211	R	--	--	Patient with a permanent catheter	54	M
clin217	S	--	*	N.A	91	M
clin225	R	--	--	Isolate was identified as ESBL; Patient was catheterised	75	F
clin238	S	--	--	Patient with chronic obstructive pulmonary disease	83	F
clin241	R	--	--	N.A	64	F
clin248	S	--	--	Patient suffered from an infra-renal rupture of an aortic aneurysm	68	M
clin257	R	--	--	permanent catheter	83	M
clin287	S	--	--	N.A	59	M
clin295	S	--	--	N.A	88	M
clin310	S	--	--	permanent catheter	51	M
clin334	R	--	--	permanent catheter; patient suffered from an acute lymphatic leukaemia	61	F
clin340	S	--	--	permanent catheter	86	F
clin342	S	--	--	N.A	35	F
clin343	S	--	--	N.A	34	F
clin344	S	--	--	N.A	73	F
clin551	S	--	--	N.A	78	F
clin559	S	--	--	permanent catheter	91	F
clin565	S	--	--	permanent catheter	78	M
clin567	S	--	--	N.A	37	F
clin571	S	--	***	N.A	82	F
clin575	S	--	--	N.A	89	M
clin580	S	--	--	N.A	74	F
clin591	S	***	**	Isolate from Urine of a patient carrying a D-J catheter	76	F
clin594	S	--	--	N.A	30	F
clin601	S	--	--	N.A	81	F
clin602	S	--	--	N.A	76	F
clin619	S	--	--	Patient was catheterised	87	F
clin623	S	--	--	N.A	23	F
clin624	S	--	--	N.A	69	M

Tables

clin626	S	--	--	N.A	90	F
clin650	S	--	--	N.A	58	F
clin652	S	--	--	N.A	86	F
clin661	S	--	--	N.A	81	M
clin695	S	--	--	N.A	79	F
clin701	S	--	--	N.A	50	F
clin702	S	--	--	N.A	89	F
clin709	R	--	--	Patient was catheterised	54	F
clin712	R	--	--	N.A	26	F
clin717	S	--	--	N.A	64	F
clin719	R	--	--	Isolate was identified as ESBL	87	F
clin721	S	--	--	N.A	74	F
clin722	S	--	--	N.A	66	F
clin724	R	--	--	N.A	40	F
clin726	S	--	--	N.A	51	F
clin758	R	--	--	Patient was catheterised	63	F
clin769	S	--	--	N.A	29	F
clin787	S	--	--	Patient was catheterised	83	F

-- No biofilm or no biofilm induction by sub-MIC of tetracycline

* Biofilm was quantified in LB with wild type strains and without sub-MIC of tetracycline (Csr components were left at steady state)

Biofilm was quantified in LB with wild type strains and sub-MIC of tetracycline (Csr components were left at steady state)

N.A Data not available

Table 4: Primer List

Primer name	Primer Sequence
1143_csrB_KO_P1	CTTGTAAGACTTCGCGAAAAAGACGATTCTATCTTCGTCGACAGGTGTGTAGGCTGGAGCTGCTTCG
1144_csrB_KO_P2	CATAAAGCAACCTCAATAAGAAAACTGCCGCGAAGGATAGCAGGCATATGAATATCCTCCTTA
1145_csrC_KO_P1	TGGCGGTTGATTGTTTGTAAAGCAAAGGCGTAAAGTAGCACCCCTGTGTAGGCTGGAGCTGCTTCG
1146_csrC_KO_P2	GCCGTTTTATTAGTATAGATTTGCGGCGGAATCTAACAGAAAGCCATATGAATATCCTCCTTA
1545-ycdP_KO_P2	GTGCAGAGCCCCGGGCGAACCAGGCTTTGTTTTGGGTGTTTATGCCCGTCACATATGAATATCCTCCTTA
1546-ycdS-KO-P1	TAATTAGATACAGAGAGAGATTTTGGCAATACATGGAGTAATACAGGTGTGTAGGCTGGAGCTGCTTC
1651-ydeH_test_fwd	GCCGGACCAGATGATCAACATTAGTGG
1652-ydeH_test_rev	TGACTAATGAACGGAGATAATCCCTCACC
2125-spoT_KO_P1	TGCTGAAGTTCGTCGTTAATCACAAAGCGGGTCGCCCTTGTATCTGTTTTGTAGGCTGGAGCTGCTTCG
2126-spoT_KO_P2	GTTGGGTTCAAAAACATTAATTTTCGGTTTCGGGTGACTTTAATCACATATGAATATCCTCCTTAG
2145-fimA_KO_P1	GCCCATGTCGATTTAGAAATAGTTTTTGAAGGAAAGCAGCATGAAAATTGTAGGCTGGAGCTGCTTCG
2146-fimH_KO_P2	GTAATATTGCGTACCAGCATTAGCAATGTCCTGTGATTTCTTTATTGATACATATGAATATCCTCCTTAG
2400-ydeH_KO_P1	TAGAATAGCGCGACAAGGAAGTGTAAAAAGGAGTGGCAATGATCAAGTGTAGGCTGGAGCTGCTTCG
2401-ydeH_KO_P2	CACAGTAGCATCAGTTTTCTCAATGAATGTTAAACGGAGCTTAACTCGCATATGAATATCCTCCTTAG
2402_ycdT_seq_fwd1	TCATCATCGGTATTGTTTGTGGGCGG
2762_ycdT_KO_P2	CCGGGGGATGAGAAGCCCCAGGCGGAGGTCGACAACACTAGCGACAGACTGCCGCTTTATGGTGACTCAC
2878_c1116_KO_P1	CTTCTGGTCGGGAGGGGCTCATATTTCCGGAGGAGTAATGTCAGGGGCATGTGTAGGCTGGAGCTGCTTCG
2879_c1116_KO_P2	GAACATAAATGCTGGCTGCTGACAAGTCTGTGAAAAAGGATTATCCATGCAGCATATGAATATCCTCCTTAG
3547_c1117_KO_P1	GGAATAAATTGTAGTGAAAAGTCGAAGTTTACCGGATGACTGATGCGCTGTGTAGGCTGGAGCTGCTTCG
3548_c1117_KO_P2	GTCTTTCTGCAACTACTGCTTTCAACAAGTCAGGCATTTACACTTTATGACATATGAATATCCTCCTTAG
3880_CsrD_KO_P1	GCTAGTATGCCGCTTCCTCACTATCGGAGTTAACACAAGGATGAGATGTGTAGGCTGGAGCTGCTTCG
3881_CsrD_KO_P2	GCAGCGCGGTTATTCTACGTGAAAACGGATTAACGGCAGGTTAAACCGACATATGAATATCCTCCTTAG
3927_relA_test_rev	CAATAATTAATTTGCCATCC
3927_relA_test_rev	CAATAATTAATTTGCCATCC
3928_relA_test_fwd	ATAAACTGGAACCTATTCCG
3928_relA_test_fwd	ATAAACTGGAACCTATTCCG

5.10 Acknowledgements

We would like to thank Franziska Zähringer for providing us structural images of MG1655 YdeH. Special thanks go to the ZMB facility of the Biozentrum Basel for excellent service.

5.11 References

1. Croxen MA & Finlay BB (2010) Molecular mechanisms of Escherichia coli pathogenicity. *Nat Rev Microbiol* 8(1):26-38.
2. Justice SS, *et al.* (2004) Differentiation and developmental pathways of uropathogenic Escherichia coli in urinary tract pathogenesis. *Proc Natl Acad Sci U S A* 101(5):1333-1338.
3. Hunstad DA & Justice SS (2010) Intracellular lifestyles and immune evasion strategies of uropathogenic Escherichia coli. *Annu Rev Microbiol* 64:203-221.
4. Foxman B (2003) Epidemiology of urinary tract infections: incidence, morbidity, and economic costs. *Dis Mon* 49(2):53-70.
5. Litwin MS, *et al.* (2005) Urologic diseases in America Project: analytical methods and principal findings. *J Urol* 173(3):933-937.
6. Anderson G, *et al.* (2003) Intracellular bacterial biofilm-like pods in urinary tract infections. *Science* 301(5629):105-107.
7. Kau AL, Hunstad DA, & Hultgren SJ (2005) Interaction of uropathogenic Escherichia coli with host uroepithelium. *Current Opinion in Microbiology* 8(1):54-59.
8. Russo TA, Stapleton A, Wenderoth S, Hooton TM, & Stamm WE (1995) Chromosomal restriction fragment length polymorphism analysis of Escherichia coli strains causing recurrent urinary tract infections in young women. *J Infect Dis* 172(2):440-445.
9. Branda SS, Vik S, Friedman L, & Kolter R (2005) Biofilms: the matrix revisited. *Trends Microbiol* 13(1):20-26.
10. Lewis K (2007) Persister cells, dormancy and infectious disease. *Nat Rev Microbiol* 5(1):48-56.
11. Romeo T, Gong M, Liu M, & Brun-Zinkernagel A (1993) Identification and molecular characterization of csrA, a pleiotropic gene from Escherichia coli that affects glycogen biosynthesis, gluconeogenesis, cell size, and surface properties. *J Bacteriol* 175(15):4744-4755.
12. Lucchetti-Miganeh C, Burrowes E, Baysse C, & Ermel G (2008) The post-transcriptional regulator CsrA plays a central role in the adaptation of bacterial pathogens to different stages of infection in animal hosts. *Microbiology* 154(Pt 1):16-29.
13. Chavez RG, Alvarez AF, Romeo T, & Georgellis D (2010) The physiological stimulus for the BarA sensor kinase. *J Bacteriol* 192(7):2009-2012.
14. Suzuki K, *et al.* (2002) Regulatory circuitry of the CsrA/CsrB and BarA/UvrY systems of Escherichia coli. *J Bacteriol* 184(18):5130-5140.
15. Pannuri A, *et al.* (2012) Translational Repression of NhaR, a Novel Pathway for Multi-Tier Regulation of Biofilm Circuitry by CsrA. *J Bacteriol* 194(1):79-89.
16. Itoh Y, *et al.* (2008) Roles of pgaABCD genes in synthesis, modification, and export of the Escherichia coli biofilm adhesin poly-beta-1,6-N-acetyl-D-glucosamine. *J Bacteriol* 190(10):3670-3680.
17. Wang X, Preston JF, & Romeo T (2004) The pgaABCD locus of Escherichia coli promotes the synthesis of a polysaccharide adhesin required for biofilm formation. *J Bacteriol* 186(9):2724-2734.
18. Daley DO, *et al.* (2005) Global topology analysis of the Escherichia coli inner membrane proteome. *Science* 308(5726):1321-1323.
19. Timmermans J & Van Melderen L (2009) Conditional essentiality of the csrA gene in Escherichia coli. *J Bacteriol* 191(5):1722-1724.
20. Boehm A, *et al.* (2009) Second messenger signalling governs Escherichia coli biofilm induction upon ribosomal stress. *Mol Microbiol* 72(6):1500-1516.
21. Jenal U (2004) Cyclic di-guanosine-monophosphate comes of age: a novel secondary messenger involved in modulating cell surface structures in bacteria? *Curr Opin Microbiol* 7(2):185-191.
22. Galperin MY (2005) A census of membrane-bound and intracellular signal transduction proteins in bacteria: bacterial IQ, extroverts and introverts. *BMC Microbiol* 5:35.
23. Hengge R (2009) Principles of c-di-GMP signalling in bacteria. *Nat Rev Microbiol* 7(4):263-273.
24. Jenal U & Malone J (2006) Mechanisms of cyclic-di-GMP signaling in bacteria. *Annu Rev Genet* 40:385-407.

References

25. Jonas K, *et al.* (2008) The RNA binding protein CsrA controls cyclic di-GMP metabolism by directly regulating the expression of GGDEF proteins. *Mol Microbiol* 70(1):236-257.
26. Suzuki K, Babitzke P, Kushner SR, & Romeo T (2006) Identification of a novel regulatory protein (CsrD) that targets the global regulatory RNAs CsrB and CsrC for degradation by RNase E. *Genes Dev* 20(18):2605-2617.
27. Mulvey MA, Schilling JD, & Hultgren SJ (2001) Establishment of a persistent *Escherichia coli* reservoir during the acute phase of a bladder infection. *Infect Immun* 69(7):4572-4579.
28. Chen S, *et al.* (2006) Identification of genes subject to positive selection in uropathogenic strains of *Escherichia coli*: a comparative genomics approach. *Proc Natl Acad Sci U S A* 103(15):5977-5982.
29. Welch RA, *et al.* (2002) Extensive mosaic structure revealed by the complete genome sequence of uropathogenic *Escherichia coli*. *Proc Natl Acad Sci U S A* 99(26):17020-17024.
30. Hochhut B, *et al.* (2006) Role of pathogenicity island-associated integrases in the genome plasticity of uropathogenic *Escherichia coli* strain 536. *Mol Microbiol* 61(3):584-595.
31. Andersson P, *et al.* (1991) Persistence of *Escherichia coli* bacteriuria is not determined by bacterial adherence. *Infect Immun* 59(9):2915-2921.
32. Lindberg U, *et al.* (1975) Asymptomatic bacteriuria in schoolgirls. II. Differences in *Escherichia coli* causing asymptomatic bacteriuria. *Acta Paediatr Scand* 64(3):432-436.
33. Hull R, *et al.* (2000) Urinary tract infection prophylaxis using *Escherichia coli* 83972 in spinal cord injured patients. *J Urol* 163(3):872-877.
34. Zdziarski J, *et al.* (2010) Host imprints on bacterial genomes--rapid, divergent evolution in individual patients. *PLoS Pathog* 6(8):e1001078.
35. Moscoso JA, Mikkelsen H, Heeb S, Williams P, & Filloux A (2011) The *Pseudomonas aeruginosa* sensor RetS switches Type III and Type VI secretion via c-di-GMP signalling. *Environ Microbiol* 13(12):3128-3138.
36. Lindberg U, Claesson I, Hanson LA, & Jodal U (1978) Asymptomatic bacteriuria in schoolgirls. VIII. Clinical course during a 3-year follow-up. *J Pediatr* 92(2):194-199.
37. Abgottspon D, *et al.* (2010) Development of an aggregation assay to screen FimH antagonists. *J Microbiol Methods* 82(3):249-255.
38. Murphy KC & Campellone KG (2003) Lambda Red-mediated recombinogenic engineering of enterohemorrhagic and enteropathogenic *E. coli*. *BMC Mol Biol* 4:11.
39. Datsenko KA & Wanner BL (2000) One-step inactivation of chromosomal genes in *Escherichia coli* K-12 using PCR products. *Proc Natl Acad Sci U S A* 97(12):6640-6645.
40. Baba T, *et al.* (2006) Construction of *Escherichia coli* K-12 in-frame, single-gene knockout mutants: the Keio collection. *Mol Syst Biol* 2:2006.0008.
41. O'Toole GA, *et al.* (1999) Genetic approaches to study of biofilms. *Methods Enzymol* 310:91-109.
42. Miller J (1992) *A short course in bacterial genetics: a laboratory manual and handbook for E. coli and related bacteria.*
43. Garofalo C, *et al.* (2007) *Escherichia coli* from urine of female patients with urinary tract infections is competent for intracellular bacterial community formation. *Infect Immun* 75(1):52-60.
44. Wei BL, *et al.* (2001) Positive regulation of motility and flhDC expression by the RNA-binding protein CsrA of *Escherichia coli*. *Mol Microbiol* 40(1):245-256.
45. Jonas K, *et al.* (2008) The RNA binding protein CsrA controls cyclic di-GMP metabolism by directly regulating the expression of GGDEF proteins. *Mol Microbiol* 70(1):236-257.
46. Craig WA (1998) Pharmacokinetic/pharmacodynamic parameters: rationale for antibacterial dosing of mice and men. *Clin Infect Dis* 26(1):1-10; quiz 11-12.
47. Sjöström AE, *et al.* (2009) The SfaXII protein from newborn meningitis *E. coli* is involved in regulation of motility and type 1 fimbriae expression. *Microb Pathog* 46(5):243-252.
48. Sjöström AE, *et al.* (2009) Analysis of the *sfaX(II)* locus in the *Escherichia coli* meningitis isolate IHE3034 reveals two novel regulatory genes within the promoter-distal region of the main S fimbrial operon. *Microb Pathog* 46(3):150-158.
49. Kau A, Hunstad D, & Hultgren S (2005) Interaction of uropathogenic *Escherichia coli* with host uroepithelium. *Curr Opin Microbiol* 8(1):54-59.

References

50. Rachid S, Ohlsen K, Witte W, Hacker J, & Ziebuhr W (2000) Effect of subinhibitory antibiotic concentrations on polysaccharide intercellular adhesin expression in biofilm-forming *Staphylococcus epidermidis*. *Antimicrob Agents Chemother* 44(12):3357-3363.
51. Hoffman LR, *et al.* (2005) Aminoglycoside antibiotics induce bacterial biofilm formation. *Nature* 436(7054):1171-1175.
52. Linares JF, Gustafsson I, Baquero F, & Martinez JL (2006) Antibiotics as intermicrobial signaling agents instead of weapons. *Proc Natl Acad Sci U S A* 103(51):19484-19489.
53. Anderson GG, Martin SM, & Hultgren SJ (2004) Host subversion by formation of intracellular bacterial communities in the urinary tract. *Microbes Infect* 6(12):1094-1101.
54. Cerca N, *et al.* (2007) Protection against *Escherichia coli* infection by antibody to the *Staphylococcus aureus* poly-N-acetylglucosamine surface polysaccharide. *Proc Natl Acad Sci U S A* 104(18):7528-7533.
55. Hancock V & Klemm P (2007) Global gene expression profiling of asymptomatic bacteriuria *Escherichia coli* during biofilm growth in human urine. *Infect Immun* 75(2):966-976.
56. Roos V & Klemm P (2006) Global gene expression profiling of the asymptomatic bacteriuria *Escherichia coli* strain 83972 in the human urinary tract. *Infect Immun* 74(6):3565-3575.
57. Tomenius H, *et al.* (2006) The *Escherichia coli* BarA-UvrY two-component system is a virulence determinant in the urinary tract. *BMC Microbiol* 6:27.
58. Palaniyandi S, *et al.* (2012) BarA-UvrY Two-Component System Regulates Virulence of Uropathogenic *E. coli* CFT073. *PLoS One* 7(2):e31348.
59. Goller CC & Seed PC (2010) Intracellular bacterial biofilm-like pods in urinary tract infections (vol 301, pg 105, 2003). *Virulence* 1(4):333-337.
60. Anderson GG, Dodson KW, Hooton TM, & Hultgren SJ (2004) Intracellular bacterial communities of uropathogenic *Escherichia coli* in urinary tract pathogenesis. *Trends Microbiol* 12(9):424-430.
61. Babitzke P & Romeo T (2007) CsrB sRNA family: sequestration of RNA-binding regulatory proteins. *Curr Opin Microbiol* 10(2):156-163.
62. Timmermans J & Van Melderen L (2010) Post-transcriptional global regulation by CsrA in bacteria. *Cell Mol Life Sci* 67(17):2897-2908.
63. Himpsl SD, Lockett CV, Hebel JR, Johnson DE, & Mobley HL (2008) Identification of virulence determinants in uropathogenic *Proteus mirabilis* using signature-tagged mutagenesis. *J Med Microbiol* 57(Pt 9):1068-1078.
64. Goller C, Wang X, Itoh Y, & Romeo T (2006) The cation-responsive protein NhaR of *Escherichia coli* activates pgaABCD transcription, required for production of the biofilm adhesin poly-beta-1,6-N-acetyl-D-glucosamine. *J Bacteriol* 188(23):8022-8032.
65. Maira-Litrán T, Kropec A, Goldmann DA, & Pier GB (2005) Comparative opsonic and protective activities of *Staphylococcus aureus* conjugate vaccines containing native or deacetylated Staphylococcal Poly-N-acetyl-beta-(1-6)-glucosamine. *Infect Immun* 73(10):6752-6762.
66. Chen SL, *et al.* (2006) Identification of genes subject to positive selection in uropathogenic strains of *Escherichia coli*: a comparative genomics approach. *Proc Natl Acad Sci U S A* 103(15):5977-5982.
67. Malone JG, *et al.* (2010) YfiBNR mediates cyclic di-GMP dependent small colony variant formation and persistence in *Pseudomonas aeruginosa*. *PLoS Pathog* 6(3):e1000804.
68. Byrd MS, *et al.* (2011) Direct evaluation of *Pseudomonas aeruginosa* biofilm mediators in a chronic infection model. *Infect Immun* 79(8):3087-3095.
69. Yildiz FH & Visick KL (2009) *Vibrio* biofilms: so much the same yet so different. *Trends Microbiol* 17(3):109-118.
70. Blattner FR, *et al.* (1997) The complete genome sequence of *Escherichia coli* K-12. *Science* 277(5331):1453-1462.
71. Bibikov SI, Biran R, Rudd KE, & Parkinson JS (1997) A signal transducer for aerotaxis in *Escherichia coli*. *J Bacteriol* 179(12):4075-4079.
72. Heeb S, *et al.* (2000) Small, stable shuttle vectors based on the minimal pVS1 replicon for use in gram-negative, plant-associated bacteria. *Mol Plant Microbe Interact* 13(2):232-237.
73. Malone JG, *et al.* (2007) The structure-function relationship of WspR, a *Pseudomonas fluorescens* response regulator with a GGDEF output domain. *Microbiology* 153(Pt 4):980-994.
74. Guzman LM, Belin D, Carson MJ, & Beckwith J (1995) Tight regulation, modulation, and high-level expression by vectors containing the arabinose PBAD promoter. *J Bacteriol* 177(14):4121-4130.

References

75. Christen B, *et al.* (2006) Allosteric control of cyclic di-GMP signaling. *J Biol Chem* 281(42):32015-32024.
76. Cherepanov PP & Wackernagel W (1995) Gene disruption in *Escherichia coli*: TcR and KmR cassettes with the option of Flp-catalyzed excision of the antibiotic-resistance determinant. *Gene* 158(1):9-14.

6 Inverse regulation of poly-GlcNAc and fimbriae adhesins in uropathogenic *E. coli*

(Manuscript in preparation)

Lucie Hosch¹, Alexander Boehm^{1,2}, Urs Jenal^{1*}

Focal Area of Infection Biology, Biozentrum, University of Basel, Switzerland ¹

Institut für Molekulare Infektionsbiologie, Julius-Maximilians-Universität Würzburg,
Germany ²

Keywords: Uropathogenic *E. coli*, type I fimbriae, phase variation, poly-GlcNAc, PGA, biofilm, *csrB*

* Correspondance: Urs.Jenal@unibas.ch

6.1 Statement of Work

All strains constructed for this manuscript and all experiments reported in this manuscript have been performed by me. Fabienne Hamburger has helped me clone the *csrB* overexpressing plasmids and Meike Scharenberg has assisted me with the flow cytometric analysis of fluorescently labelled type I fimbriae.

6.2 Abstract

The successful establishment of acute and chronic urinary tract infections by uropathogenic *E. coli* strongly depends on the expression of type I fimbriae. Chronic bladder infections are mostly associated with sessile bacteria that persist in the host as multicellular communities for up to 3 years. These persister cells are encased in a self-produced matrix composed of varying components that include proteinacious structures e.g. type I fimbriae, or exopolysaccharides like poly β -1,6-*N*-acetylglucosamine (PGA). This *in vitro* study shows that expression of type I fimbriae p negatively interfere with PGA dependent biofilm formation in the cystitis isolate UTI89. To avoid interference UTI89 inversely regulates the expression of the two adhesins in a process that depends on the carbon storage regulator (Csr) system. Important players include *csrB*, the invertible element *fimS* as well as the recombinase FimE. We conclude that the inversed regulation by the Csr pathway, known to stimulate the PGA expression, simultaneously affects phase variation of type I fimbriae and pushes *fimS* into an OFF orientation. The studies unravel a novel regulatory feature of the global Csr system as mediator of an inverse regulation of two important surface adhesins, possibly to mediate the switch from an acute, type I fimbriae dependent infection to a persistent PGA-dependent sessile state of infection.

6.3 Introduction

Uropathogenic *Escherichia coli* (UPEC) are the primary cause of human urinary tract infections (UTI) and are responsible for a remarkable progression of disease. Once in the bladder the pathogen adheres to the urothelium, internalises into superficial facet cells where it rapidly multiplies before shifting into a sessile biofilm-like state, which can persist for up to 3 years (1-4). Functioning as a reservoir of bacteria, these intracellular biofilm-like structures are believed to be the source for recurring UTIs (2, 5-8). The initial step during UPEC pathogenesis depends on a virulence factor, which enables bacteria to adhere to eukaryotic cells. This is a long linear polymer termed type I fibrillum, which protrudes from the surface of the bacterium and is encoded by the *fimAICDFGH* (*fimA-H*) genes (9). With these hair-like structures, UPECs are capable to overcome possible repulsive forces between the bacterial and eukaryotic surfaces and thereby initiate host contact (10). Type I fimbriae are composed of a pilus rod (FimA) and a tip fibrillum consisting of three monomeric proteins, FimF, FimG and the distal tip adhesin FimH. FimH binds to surface exposed mannosylated host proteins, including $\beta 1$ and $\alpha 3$ integrins or the uroplakin UP1a (11-14). If Fim-mediated contact is missing, the virulence of UPECs massively decreases (15). The expression of type I fimbriae underlies a complex and tightly controlled regulatory network that governs the directionality of a DNA element (*fimS*) preceding the structural genes of type I fimbriae (*fimA-H*). The *fimS* switch-region is an invertible element of 314 bp that is flanked by inverted repeats (IRs) and contains the promoter of *fimA-H* and a multitude of binding sites for factors that influence the orientation of *fimS* (16). If the promoter located on *fimS* is oriented toward *fimA* bacteria express type I fimbriae (ON phase), but if the promoter is directed away from *fimA* bacteria are non-fimbriated (OFF phase). The directionality or phase of *fimS* is determined by three recombinases, FimB, FimE, and FimX, which belong to the λ integrase family of site-specific recombinases (16-18). While FimB and FimE have long been identified, FimX, which is not part of the *fimA-H* operon, was only recently determined as a FimB homolog in UPECs, where it was reported to be highly active *in vivo* but not *in vitro* (19). Importantly, the recombinases determining *fimS* orientation act independently (18, 20-23) and their directional preferences for *fimS* switching are different (16, 22, 24). FimE catalyses the inversion from ON to OFF, while FimB and its homolog FimX, although capable of catalysing the inversion of *fimS* in both directions, show a slight bias for the OFF to ON direction. Furthermore, the inversion frequencies triggered by FimB are markedly lower than the ones of FimE (21, 25). The inversion frequencies of FimX have not yet been investigated or compared to the ones of FimB and FimE. As the regulation of *fimB*, *fimX* and/or *fimE* expression is multifactorial as well and their action can be influenced by several factors that facilitate or hinder their recombineering action (16, 26), the equilibrium residing over the

phase of *fimS* is complex and difficult to predict. Despite this complexity, the regulation of *fimS* in the bladder appears to favour the fimbriated state of bacteria and hence bacterial adherence, infection of superficial facet cells, and ultimately the formation of intracellular bacterial communities (IBCs) and bacterial reservoirs (2, 3). Bacterial reservoirs or other chronic and recurrent infections are generally associated with the formation of bacterial biofilms, for example in cystic fibrosis, periodontitis or many others (27-30). The formation of biofilms is a complex process, which is highly regulated on both temporal and spatial levels. Bacteria within biofilms are encased in a self-produced matrix of proteinaceous adhesins and exopolysaccharide structures, which protects cells from assaults by the host immune system and from chemical threats. Interestingly, type I fimbriae of UPECs have also been implicated in the successful establishment of IBC formation during cystitis, where they are presumed to promote bacterial inter-adhesion (31) and thus biofilm formation. However, the exact involvement of type I fimbriae in *E. coli* biofilms during pathogenesis remains unclear (32-34).

Several Gram-positive (*Staphylococcus aureus* and *Staphylococcus epidermidis* (35-38)) and Gram-negative bacteria (*E. coli*, *Actinobacillus actinomycetemcomitans* and *Actinobacillus pleuropneumoniae* (39, 40)) utilise poly β -1,6-*N*-acetylglucosamine (poly-GlcNAc or PGA) as major exopolysaccharide component of their biofilm matrix. These PGA polymer components of the matrix have been implicated in cell-cell adhesion and bacterial attachment to surfaces and are reported in different studies as virulence factors (41). In *E. coli* the PGA synthesising machinery is encoded by the *pgaABCD* operon (40). It encodes four proteins that localise to the cell envelope where they catalyse the biosynthesis and export of PGA. PgaA, a porin spanning the outer membrane and PgaB, an *N*-acetylglucosamine deacetylase, are both required for export of the polymer (42). PgaC is an inner membrane glycosyltransferase that recognises UDP-activated GlcNAc monomer precursors and catalyses their polymerization. Finally, PgaD, although being essential for PGA formation, has a function that is not fully understood (40, 42, 43). The expression of PGA is tightly controlled by a variety of factors. Most importantly, the *pgaA-D* genes are repressed by the global **C**arbon **S**torage **R**egulator **A** (CsrA), which binds to the 5' UTR of many mRNAs involved in motility, cyclic-di-GMP signalling, carbon metabolism, virulence or other (44, 45). As for the regulation of contributing to the PGA synthesis CsrA not only binds to the transcripts of *pgaA-D* itself (46) but also controls *nhaR*, the transcriptional regulator of *pgaA-D* (47). This post-transcriptional repression by CsrA is counteracted by two small regulatory RNAs called *csrB* and *csrC*, which bind to CsrA and titrate it away from its target mRNAs (48). This ultimately leads to the derepression of several targets including the *pgaA-D* mRNA. The expression of *csrB* and *csrC* is regulated by the BarA/UvrY two-component system (TCS) (49), which responds to metabolic signals (50, 51). The additional auto-

regulatory loop between CsrA and the BarA/UvrY TCS further imposes a stringent regulation of the Csr system by positively affecting *csrB* and *csrC* expression (52). Finally, *csrB* and *csrC* stability is regulated by CsrD (YhdA), which targets both RNAs for degradation by RNase E. Although the precise activity of CsrD is unclear it requires its degenerate GGDEF and EAL domains, which usually metabolise c-di-GMP, to mediate degradation of *csrB* and *csrC* (53, 54).

Another readout controlled by the Csr system of *E. coli* is bis-(3'-5')-cyclic dimeric GMP (c-di-GMP) (45), a ubiquitous bacterial second messenger, which functions as a switch between a free-living, planktonic and a sessile, biofilm forming lifestyle in bacteria (55). This signalling molecule is synthesised by diguanylate cyclases (DGC) via their catalytic GGDEF domains (56-58) and degraded by phosphodiesterases (PDE) via catalytic EAL or HD-GYP domains (59-62). In response to internal and external cues, the DGCs and PDEs modulate the cellular concentration of c-di-GMP (63). The diversity of DGCs and PDEs in domain architecture and the abundance of these proteins in many bacteria accounts for the plethora of cellular processes that are controlled by c-di-GMP. These include motility (64), synthesis of exopolysaccharides (55, 65, 66) cell cycle progression (67), the expression of toxins (68), virulence factors (69-76) and many more. CsrA controls at least two DGCs (*ydeH* and *ycdT*) (45). Moreover, elevated levels of c-di-GMP stimulate PGA-dependent biofilm formation post-translationally (65).

This study reports that PGA dependent biofilm formation in UPECs is negatively affected by the expression of type I fimbriae *in vitro*. The basis for this negative effect of type I fimbriae on PGA biofilms was further investigated. It was elucidated that the regulatory mechanisms, which govern the expression of type I fimbriae and PGA are linked through their dependence on the Csr regulation system. It is shown that this novel function of the Csr system in modulating type I fimbriae expression affects the orientation of the switchable element *fimS*. Furthermore it is demonstrated that the Csr system acts on the site-specific recombinase FimE to exert its effects on *fimS* and requires CsrD to do so. It is demonstrated that the Csr system inversely controls PGA biogenesis and the expression of type I fimbriae, suggesting that this regulatory network is designed to separate the production of two surface adhesins that have distinct roles and negatively interfere with each other.

6.4 Material and Methods

6.4.1 Strains and plasmids used in this study

All strains used in this study are listed in Table 1, the plasmids are listed in Table 2.

6.4.2 Construction of isogenic deletion mutants

The strains used in this study are the sequenced clinical UPEC isolates UT189 (7, 77), and isogenic mutants thereof. Construction of isogenic deletion mutants was performed as previously published (78). Briefly, the strain to be mutated was transformed with the temperature sensitive plasmid pKM208 (Addgene; plasmid 13077) containing the λ RED recombination genes (79). To generate mutants, the UPEC strain carrying pKM208 was grown in LB medium without NaCl, supplemented with ampicillin (100 μ g/ml), and grown at 30 °C to late logarithmic phase (OD₆₀₀ 0.9). Thereafter, λ RED gene expression was induced for 30 min with 1 mM IPTG at 37 °C. Bacteria were then subjected to a 15 min heat shock at 42 °C, rapidly cooled in ice slurry, before washing twice with sterile 1×PBS and concentrating 100-fold in cold 10 % glycerol. The kanamycin and chloramphenicol resistance cassettes were used to replace the gene to be deleted. They were PCR amplified from pKD4 or pKD3 (80) with primers designed specifically to delete the desired region in the genome of UT189. These λ RED primers are composed of two parts, in their 3' regions they prime to the regions in pKD3 and pKD4 that contain the resistance cassettes and therefore remain constant in all primers: In the forward primer (P1) this constant region is TGTAGGCTGGAGCTGCTTCG and in the reverse primer (P2) it is CATATGAATATCCTCCTTAG. The 5' region of λ RED primers consists of roughly 50 nt of homology regions (HR) flanking the gene to be deleted and include the first 2-3 (HR1) respectively the last 2-3 codons (HR2) of the ORF to be deleted. In the end the λ RED primers have the following composition: 5'-HR1-P1-3' respectively 5'-HR2-P2-3'. The sequences of primers used to make genomic deletion are listed in Table 3. The linear DNA used to delete *pgaA-D* was amplified with primers 1546-ycdS-KO-P1 and 1545-ycdP_KO_P2. To delete *fimA-H* primers 2145-*fimA*_KO_P1 and 2146-*fimH*_KO_P2 were used. Similarly, deletion of *ydeH* was achieved with DNA amplified from primer 2400-*ydeH*_KO_P1 and 2401-*ydeH*_KO_P2. Deletion of *fimH* was enabled with DNA amplified with primers 3156-*fimH*_KO_P1 and 2146-*fimH*_KO_P2. Primers 2125-*spoT*_KO_P1 and 2126-*spoT*_KO_P2 amplified DNA used to delete *spoT* in a Δ *relA* strain. Linear DNA used to delete *fimX* was produced with primers 3541-*fimX*_KO_P1 and 3542-*fimX*_KO_P2. In some cases, the DNA used to delete genes was not amplified from

pKD3 or pKD4 but was amplified from a pre-existing mutant of the comprehensive `Keio-collection` (81) using simple test primers. This was the case for the DNA used to delete *ycdT* (primer: 2402_ycdT_seq_fwd1 and 2762_ycdT_KO_P2) as well as for *relA* (primer: 3927_relA_test_rev and 3928_relA_test_fwd) and *yhjH* (primer: 1658_yhjH_test_fwd_new and 1659_yhjH_test_rev_new). After amplification of the linear DNA by PCR, all PCR fragments were gel purified (MN Nucleospin Extract II, Machery Nagel, Oensingen, Switzerland) and 10–100 ng purified DNA was mixed to 65 µl recombination competent bacterial cells followed by electroporation in 1 mm Gene Pulser cuvettes using a Gene Pulser (BioRad, Reinach, Switzerland) set to 1.75 V, 25 µF and 400 Ω. Electro-shocked cells were mixed with cold (4 °C) salt optimised broth (2 % (w/v) bacto trypton; 0.5 % (w/v) yeast extract; 10 mM NaCl and 2.5 mM KCl), incubated for 1.5 h at 37 °C and plated out on LB agar plates containing 50 µg/ml kanamycin or 20 µg/ml chloramphenicol, respectively. Resistant clones were colony purified on LB medium containing kanamycin or chloramphenicol and tested by PCR for correct insertion of the resistance cassette. Finally, the resistance cassette of all deletion mutants was removed via Flp recombinase-mediated site-specific recombination upon transformation of mutants with pCP20 as described by Datsenko and Wanner (80, 141). The loss of the resistance cassette was checked once more by PCR.

6.4.3 Construction of p_{fimA-H}^{ON} Locked strains (p_{fimA-H}^{ON} and p_{fimA-H}^{OFF})

In order to have strains, which are blind to FimB, FimE, FimX mediated inversion of *fimS*, several p_{fimA-H}^{ON} and p_{fimA-H}^{OFF} strains were constructed. In these strain the invertible element (*fimS*) preceding the structural genes of type I fimbriae (*fimA-H*) can no longer be inverted. To engineer these construct, *fimS* was amplified in the ON-phase by colony PCR from UT189 wild type with primers 3509_ *fimS*_ON_fwd and 3510_ *fimS*_ON_rev, both of which could only bind to the ON orientation of *fimS* (p_{fimA-H}^{ON}). Similarly, *fimS* in the OFF-orientation (p_{fimA-H}^{OFF}) was amplified with primers 3511_ *fimS*_OFF_fwd and 3512_ *fimS*_OFF_rev. Another PCR was performed on pKD4 with primers 3513_ *FimBE*_KO_P1 and 3514_ *FimBE*_KO_P2, which amplified the kanamycin cassette described by Datsenko *et al.* (80). The latter DNA fragment had flanking regions around the kanamycin cassette, which were homologous to *fimBE* and could thus be used to delete *fimBE* (*fimBE::kan*). These two PCR products (*fimBE::kan* and p_{fimA-H}^{OFF} or p_{fimA-H}^{ON}) were than fused by splice overlap extension PCR (SOE-PCR) as described by Higuchi *et al.* (82). The resulting PCR fragments were termed Δ *fimBE::kan* p_{fimA-H}^{ON} and *fimBE::kan* p_{fimA-H}^{OFF} , respectively. Next, these two DNA fragments were used to construct chromosomal UT189

$\Delta fimBE::kan p_{fimA-H}^{ON}$ and a UTI89 $\Delta fimBE::kan p_{fimA-H}^{OFF}$ mutants via λ RED. The orientation of *fimS* as well as the absence of undesired point mutations was checked by sequencing the corresponding region in UTI89 $\Delta fimBE::kan p_{fimA-H}^{ON}$ and UTI89 *fimBE::kan p_{fimA-H}^{OFF}*. One of the sequenced UTI89 *fimBE::kan p_{fimA-H}^{OFF}* clones had an additional point mutant inside one of the inverted repeats bordering *fimS*. This point mutant (TTGGGGCCAA in wild type vs. TTAGGGCCAA in $\Delta fimBE p_{fimA-H}^{OFF}$) further ensures that the *fimS* remains in the OFF confirmation. It was thus used as a negative control for phase variation of the two p_{fimA-H}^{Locked} strains (UTI89 $\Delta fimBE::kan p_{fimA-H}^{ON}$ and UTI89 *fimBE::kan p_{fimA-H}^{OFF}*) and was named *fimBE::kan p_{fimA-H}^{OFF*}*. In all three p_{fimA-H}^{Locked} strains the kanamycin cassette was removed by Flp recombinase-mediated site-specific recombination (80, 141). Additionally, the third reported recombinase of UTI89 (*fimX*) (19) was deleted in all three p_{fimA-H}^{Locked} strains, resulting in UTI89 $\Delta fimX\Delta fimBE::FRT p_{fimA-H}^{ON}$, UTI89 $\Delta fimX\Delta fimBE::kan p_{fimA-H}^{OFF}$ and UTI89 $\Delta fimX\Delta fimBE::kan p_{fimA-H}^{OFF*}$. The resistance cassette of all these p_{fimA-H}^{Locked} strains was again removed as previously described (141).

6.4.4 Construction of *fimA::gfp* and *fimH-gfp* reporter constructs

Fluorescent reporter strains were constructed to effectively study phase variation of the *fimA-H* operon. GFP was inserted in two distinct loci whose expression depends on the orientation of *fimS*: (i) in *fimA*, causing inactivation of the entire *fimA-H* operon and (ii) in the 3' UTR of *fimH*, leaving all structural *fimA-H* genes intact. In both reporters, the GFP construct was amplified by PCR from SDFR3 (a Salmonella mutant provided to us by Dirk Bumann). In SDFR3 the *gfp* sequence is linked to a kanamycin cassette, which can be removed by Flp recombinase-mediated site-specific recombination (141). In UTI89 *fimA::gfp* the reporter fragment used for λ RED was amplified from SDFR3 with primers 3187_*FimA_GFP_repl_P1* and 3188_*FimA_GFP_repl_P2*. Since the polycistronic mRNA of *fimAICDFGH* is disrupted by the gene replacement, this reporter is non-fimbriated. In order to have a fimbriated reporter UTI89 *fimH-gfp* was constructed, where GFP is expressed as a function of the fimbrial promoter together with *fimA-H*. This construct was made with primers 3916_*fimH-reporter_rev* and 3917_*fimH-gfp_fwd*, to amplify DNA that inserts the *gfp* at the 3' end of *fimH*. Noteworthy, primer 3917_*fimH-gfp_fwd* contains a Shine-Dalgarno sequence, which ensures that translation and the transcription of the *fimA-H* continues after *fimH* and includes *gfp*. The linear DNA used to construct both reporter strains was further used to create p_{fimA-H}^{Locked} reporter strains. To do so both reporter DNA fragments were introduced via λ RED into the p_{fimA-H}^{Locked} strains, where they should either report 100 % or 0 % GFP signal or fimbriation, respectively. *FimA::gfp* was inserted into all 6 locked strains ($\Delta fimBE \Delta fimA::gfp$

p_{fimA-H}^{OFF} , $\Delta fimBE \Delta fimA::gfp$ p_{fimA-H}^{ON} , $\Delta fimBE \Delta fimA::gfp$ p_{fimA-H}^{OFF*} $\Delta fimX\Delta fimBE \Delta fimA::gfp$ p_{fimA-H}^{OFF} , $\Delta fimX\Delta fimBE \Delta fimA::gfp$ p_{fimA-H}^{ON} and $\Delta fimX\Delta fimBE \Delta fimA::gfp$ p_{fimA-H}^{OFF*}) while *fimH-gfp* was only inserted into the locked strains where all three recombinases have been deleted. These strains were called $\Delta fimX\Delta fimBE fimH-gfp$ p_{fimA-H}^{OFF} , $\Delta fimX\Delta fimBE fimH-gfp$ p_{fimA-H}^{ON} and $\Delta fimX\Delta fimBE fimH-gfp$ p_{fimA-H}^{OFF*} . In all UTI89 *fimA::gfp* strains as well as UTI89 *fimH-gfp* strains the resistance cassette have been removed, as previously reported (141).

6.4.5 Construction of deletion mutants in UTI89 *fimH-gfp*

To test any potential involvement of selected genes implicated in c-di-GMP signalling or elements of the carbon-storage-regulation system on phase variation of the *fim* operon, the reporter construct from above (*fimH-gfp*) was combined with several additional mutations. First, the *fimH-gfp* reporter was transformed with pKM208 and then used as parent strain to construct several deletion mutants. The strains constructed from *fimH-gfp* and the corresponding deletion primers are listed in Table 3 and hereafter: *fimH-gfp* $\Delta fimB$ (3182_FimB_KO_P1 and 3183_FimB_KO_P2), *fimH-gfp* $\Delta fimE$ (3184_FimE_KO_P1 and 3185_FimE_KO_P2), *fimH-gfp* $\Delta csrD$ (3880_CsrD_KO_P1 and 3881_CsrD_KO_P2), *fimH-gfp* $\Delta csrB$ (1143_csrB_KO_P1 and 1144_csrB_KO_P2), *fimH-gfp* $\Delta csrC$ (1145_csrC_KO_P1 and 1146_csrC_KO_P2), *fimH-gfp* $\Delta c1116$ (2878_c1116_KO_P1 and 2879_c1116_KO_P2), *fimH-gfp* $\Delta c1117$ (3547_c1117_KO_P1 and 3548_c1117_KO_P2), *fimH-gfp* $\Delta fimBE$ (3185_FimE_KO_P2 and 3182_FimB_KO_P1), *fimH-gfp* $\Delta fimX$ (3541_fimX_KO_P1 and 3542_fimX_KO_P2), *fimH-gfp* $\Delta ycgR$ (1456-ycgR_KO_P1 and 1457-ycgR_KO_P2), *fimH-gfp* $\Delta csgD$ (1680-csgD_KO_P1 and 1681-csgD_KO_P2), *fimH-gfp* $\Delta bcsA$ (3560_BcsA_KO_P1 and 3561_BcsA_KO_P2), *fimH-gfp* $\Delta ydeH$ (2400-ydeH_KO_P1 and 2401-ydeH_KO_P2), *fimH-gfp* $\Delta pgaA-D$ (1546-ycdS-KO-P1 and 1545-ycdP_KO_P2). Furthermore, *fimH-gfp* $\Delta yhjH$ (1658_yhjH_test_fwd_new and 1659_yhjH_test_rev_new) as well as *fimH-gfp* $\Delta ycdT$ (2402_ycdT_seq_fwd1 and 2762_ycdT_KO_P2) were constructed but other than the above mutants these two strains were made by amplifying the DNA from the $\Delta yhjH$ and $\Delta ycdT$ strains of the 'Keio-collection' (81) rather than pKD3 or pKD4. Finally, the reporter was inserted into $\Delta relA\Delta spoT$, resulting in *fimH-gfp* $\Delta relA\Delta spoT$. In this strain the *fimH-gfp* containing DNA fragment was introduced into the $\Delta relA\Delta spoT$ double mutant by λ RED. Also, in all mentioned mutants, the resistance cassette was eliminated before characterising the mutants (141).

6.4.6 Preparation of guinea pig erythrocytes for aggregometry

Guinea pig erythrocytes (GPE) were isolated from fresh guinea pig blood (Charles River Laboratories, Sulzfeld, Germany) and prepared as previously described (78). Briefly, an equal volume of guinea pig blood was carefully pored over Histopaque (density of 1.077 g/ml at 24 °C, Sigma-Aldrich, Buchs, Switzerland) and then centrifuged at 4 °C for 30 min at 400 g. After elimination of the supernatant, the purified erythrocytes were adapted in sterile 1×PBS to a final OD₆₀₀ of 2, 4 or 8.

6.4.7 Aggregometry

Bacterial mediated aggregation of GPE was measured and quantified on an APACT 4004 aggregometer (Endotell AG, Allschwil, Switzerland) as previously described (78). Bacteria were statically grown in 10 ml LB in a 50 ml falcon tube for 24 h at 37 °C. Cells were then collected by centrifugation (1 min at 8000 rpm), washed twice in sterile 1x PBS and adapted to an OD₆₀₀ of 2 or 4. Prior to each measurement, the instrument was calibrated by defining the two parameters PPP and PRP. PPP stands for protein poor plasma and defines 100 % aggregation while PRP stands for protein rich plasma and defines 0 % aggregation. Pure 1x PBS was used to define 100% aggregation and pure erythrocytes (adapted to an OD₆₀₀ of 2, 4, 8) to define 0 % aggregation. The aggregation measurements of bacteria were performed after the addition of 50 µl bacteria to 250 µl GPE and continuously measured at OD₇₄₀ nm over 10 min at 37 °C. To avoid sedimentation, the bacterial solutions in the cuvettes were continuously stirred at 1000 rpm.

6.4.8 Biofilm assay

Freshly grown LB overnight cultures were diluted 1:40 into 200 µl LB medium in 96-well polystyrene microtiter plates (Falcon, ordering number 353072). When appropriate bacteria were grown with the following concentrations of antibiotics to select for plasmids: 15.5 µg/ml tetracycline (pME6032 plasmids) or 100 µg/ml ampicillin (pcj30 and pPKL4) and were induced with 100 µM IPTG unless mentioned otherwise. The 96-well plates were incubated for 24 h at 37 °C without shaking and cell density was recorded at 600 nm on a plate reader. Subsequently, the medium with the non-attached cells was discarded through vigorous washing of the microtiter plates with deionised water from the hose. Once dry, wells were filled with 200 µl crystal violet solution [0.1 % (W/V) crystal violet (Sigma Aldrich, Article No.

C-3886), 1.7 % (W/V) 1-propanol, 1.67 % (W/V) methanol (96.7:1.66:1.66)] and stained on a platform shaker for 15 min at room temperature (RT). The staining solution was discarded and wells were washed, and then dried. Retained crystal violet stained biomass was dissolved in 200 µl acetic acid (20 %) and quantified at 600 nm on a plate reader. If measurements were outside the dynamic range of the plate reader, crystal violet solutions were further diluted in 20 % acetic acid. Bacterial biofilms were then quantified as the amount of biomass attached to the plastic surface of 96-well plates, essentially as described (65, 83). The relative attachment values are ratios of the optical density of dissolved crystal violet (corresponding to the attached biomass) divided by the cell density (total growth). The attached bacterial biomass is always illustrated in percentage of the biomass of UTI89 overexpressing *csrB* and corrected for growth (relative attachment). The values plotted into histograms are then compared to the values of UTI89 wild type carrying the *csrB* overexpressing plasmid pME6032 *csrB* (pCsrB) or pcj30 *csrB*, which is set to 100%. Single data points represent the mean of at least six wells. Error bars were calculated as the standard errors of the mean.

6.4.9 Scanning electron microscopy

For the acquisition of micrographs, bacteria were prepared essentially as described in chapter 6.4.8 for the attachment assay (65). Instead of using 96-well plates biofilms were prepared in 24 well plates. Each well contained 2 ml of LB supplemented with 100 µg/ml ampicillin and 100 µM IPTG (to select and induced pcj30 *csrB*) as well as a sterile glass slide. After biofilm formation for 24 h, the glass slides were removed, carefully washed with 1×PBS and fixed at room temperature in 1×PBS containing 2.5 % glutaraldehyde. After 1 h the glutaraldehyde was removed by washing with 1×PBS and then the glass slide was gradually dehydrated with an acetone step gradient (30%, 50%, 70%, 90%, 100%; 10 min each). Finally samples were critical point-dried and sputter-coated with a 3–5 nm Pt layer. Micrographs were recorded on a Hitachi S-4800 field emission scanning electron microscope with an acceleration voltage between 1.5 and 5 kV.

6.4.10 Phase variation PCR

The orientation of the invertible element *fimS* was evaluated in a three primer based PCR as described in (84). 2296_*fimA* is the primer, which binds to *fimA* and 2295_*fimE* binds to *fimE*. These two primers amplify a DNA fragment of 1221 bp, which is always produced.

The third primer (2297_inv) binds inside the invertible element. Depending on the orientation of *fimS*, 2297_inv amplifies the ON product of 450 bp together with primer 2296_ *fimA* or the OFF product of 750 bp together with primer 2295_ *fimE*. After amplification, the PCR products were then visualised on a 1 % agarose gel and the intensities of the OFF and ON bands were determined using ImageJ 1.43 (NIH, USA). After background subtraction, a ratio between the intensity of the OFF and ON bands were calculated for at least 10 replicas per strain and conditions. Outlayer values were excluded from further processing. The mean intensity ratios were plotted as dot blots with their interquartile range and compared to wild type UTI89. Statistical significance was calculated with GraphPad Prism 4 with $P > 0.05$ being significant.

6.4.11 Analysis of *fimA::gfp* and *fimH-gfp* by flow cytometry

Phase variation and reported fimbriation of strains carrying the *fimA::gfp* and *fimH-gfp* reporter constructs was analysed by of flow cytometry. The reporter strains were grown under different conditions as indicated in the results section, collected by centrifugation (1 min; 8000 rpm), washed twice with sterile filtered 1×PBS and fixed in a final concentration of 1 % Roti Histofix (Roth, ordering number A146.4). Fixed bacteria were stored at 4° C until sample acquisition in a Canto II FACS (BD Bioscience) cytometer. Unless mentioned otherwise, 50'000 events per sample were recorded and analysed with FlowJo version 9.3.3. The Alexa-Fluor488-H (Ex488_LP_525_BP_542/27-H) filter was used to record GFP and the PE-H (Ex405_LP_495_BP_514/30-H) filter to control the level of background fluorescence. The recorded data was then plotted according to the size distribution in a forward (FSC-H) vs. sideward scatter (SSC-H). In this plot contaminating particles (e.g. bacterial debris) was separated from bacterial cells by gating all events into four quadrants (Q1-Q4), where Q2 contains bacteria. Events in Q2 were then further analysed for their GFP signal (Alexa-Fluor 488-H). GFP signals were plotted as fluorescence intensity histograms. To distinguish bacteria, which express GFP from those that do not, the histogram of a UTI89 wild type control strain (no GFP signal) was overlaid with histograms of strains expressing GFP. Then, the GFP-positive events were separated from GFP-negative events by dividing the histogram into two sections. The fraction of GFP negative and GFP positive bacteria are indicated in each histogram.

6.4.12 Fluorescent staining of surface-exposed type I fimbriae via indirect immunofluorescence

Being surface exposed structures, type I fimbriae can be labelled with an antibody against FimA-H (85). To label bacteria, they were statically grown in LB for 24 hours, harvested by centrifugation (8000 rpm for 10 min at 4 °C), washed twice in sterile 1x PBS and adapted to an OD₆₀₀ of 2. From this solution 150 µl per strain were aliquoted into wells of a 96 well plate and centrifuged at 3800 rpm for 10 min at 24 °C. After removal of the supernatant, the pellet was resuspended in 40 µl 1x PBS containing a 1:250 dilution of the anti-type-1-Pili rabbit serum and 2 % BSA (gift of Beat Ernst's laboratory at the Pharmacentrum in Basel). The samples were incubated for one hour at 4 °C with the primary antibody, than washed twice by centrifugation. After incubation for one hour with the secondary anti-rabbit antibody (Invitrogen) (1:200 in 1x PBS containing 2 % BSA) cells were washed 3 x by centrifugation in 1x PBS and resuspended in a final volume of 300 µl 1x PBS and the Alexa 647 signal was analysed by flow cytometry on a CyAn (Beckman Coulter) in the APC filter. The scatter properties of the bacteria were first visualised in a forward (FS Log: FS) sideward (FS Log: SS) scatter. In this plot, bacteria were gated by subdividing the scatter into quadrants Q1-Q4, bacteria being in Q2. Next, the events from Q2 were plotted into a histogram that indicates the signal intensity obtained in the APC channel. All non-fimbriated strains ($\Delta fimA-H$, $\Delta fimX\Delta fimBE$ p_{fimA-H}^{OFF} and $\Delta fimX\Delta fimBE$ p_{fimA-H}^{OFF*}) were used to identify the section of the histogram where non-fimbriated bacteria localise. Every event with intensities higher than the one defined as non-fimbriated was defined as being fimbriated.

6.5 Results

6.5.1 Type I fimbriae interfere with PGA-mediated attachment

Lack of type I fimbriae greatly reduces the survival of UPEC cells in a cystitis mouse model (8, 13, 14, 31, 86-91). Thus, a *fim* mutant strain was originally constructed in the UTI89 background as a negative control to investigate the role of PGA in a murine model of cystitis (Hosch *et al.*, unpublished manuscript). The Δ *fimA-H* mutant used in this study was constructed by λ RED-mediated gene replacement (78) resulting in a clean deletion of all structural genes (*fimAEFGH*) as well as their assembly machinery (*fimCD*) and *fimI*. To fully characterise this strain it was included in all our *in vitro* assays.

FimH-mediated attachment to mannosylated receptors can be easily quantified by aggregometry. Scoring of guinea pig erythrocyte (GPE) aggregation is a measure for the expression and functionality of type I fimbriae (78). This aggregation assay was used to reconfirm that the aggregation of GPE is impaired in a UTI89 Δ *fimA-H* as well as in a UTI89 Δ *fimH* mutant strain (Figure 1A). Aggregation of both mutants was fully restored in the presence of a plasmid constitutively expressing the *fimA-H* genes in trans from pPKL4 (92). We next assayed the role of type I fimbriae in PGA dependent biofilm formation of UTI89 ((65) and Hosch *et al.*, unpublished manuscript). Under laboratory conditions PGA dependent biofilm formation is repressed by CsrA, which binds to the *pgaA-D* mRNA and hinders translation. However, PGA dependent biofilm formation can be induced in non-pathogenic *E. coli* K12 strains and in the uropathogenic strain UTI89 either by inactivating *csrA* (65) or as done in this work by overexpressing the small RNA *csrB* from plasmid (Hosch *et al.*, unpublished manuscript) (Figure 1B). Surprisingly, a UTI89 Δ *fimA-H* showed a significantly increased surface attachment (260%) compared to wild type. Like in wild type, attachment of the mutant was fully dependent on PGA (Figure 1B). The increased attachment of the Δ *fimA-H* mutant was reduced to wild type levels in the presence of fimbriae expressed from plasmid (Figure 1C). Interestingly, fimbriae expressed from plasmid also reduced attachment in the UTI89 wild type arguing that type I fimbriae structurally or functionally interfere with PGA-dependent biofilm formation in this model system.

6.5.2 Type I fimbriae functionally interfere with PGA dependent attachment

The interference of type I fimbriae with PGA-mediated attachment prompted us to analyse the biofilm morphology of wild type and mutant strains using scanning electron

Results

microscopy. Low magnification images showed denser and more protruding biofilm structures for the mutant lacking fimbriae as compared to wild type and confirmed the absence of biofilm in a *pgaA-D* mutant (Figure 2A). Images were also taken at higher magnifications to visualise extracellular structures (Figure 2B). In UTI89 wild type biofilms two distinct surface structures were observed: small knob-like protrusions and long, thin, hair-like structures extending into the medium and onto neighbouring bacteria (Figure 3C). The knobs were recently identified in *E. coli* MG1655 as surface aggregates of PGA, which serve as glue to stick bacteria together and allow adhesion to a surface (65). In agreement with this, these structures were observed on cell surfaces of UTI89 wild type and the Δ *fimA-H* mutant, but not in a Δ *pgaA-D* mutant (Figure 2B and C; black arrows). The thin hair-like structures are absent in the Δ *fimA-H* mutant, arguing that they represent type I fimbriae (Figure 2B and C white arrows). Interestingly, type I fimbriae and PGA knobs did not seem to be equally distributed on the surfaces of all bacterial cells within a biofilm. While PGA knobs were abundant on most wild type cells, type I fimbriae were commonly found only on a few closely grouped bacteria. As for the Δ *pgaA-D* mutant, the amount of attached bacteria was too little to identify those bacteria that express type I fimbriae. Moreover, the majority of cells expressing type I fimbriae on their surface exhibited very few or no PGA knobs (Figure 2B and C). This indicated that type I fimbriae are rarely expressed under the conditions used for biofilm formation and that the type I fimbriae and PGA adhesins may not be present on individual bacteria at the same time.

The structural studies above together with the observation that type I fimbriae interfere with PGA-mediated biofilm formation prompted us to test, if a regulatory mechanism to temporally uncouple the two surface adhesins exists. The regulation of *fimA-H* gene expression not only depends on promoter activity but primarily on the orientation of *fimS*, the invertible DNA cassette preceding the structural genes of type I fimbriae and which contains the *fim* promoter (16, 17, 93). To test if the regulatory pathway governing PGA-dependent biofilm formation in UTI89 affects *fimS*, a three primer based PCR method (84) was used to elucidate if plasmid-based overexpression of *csrB* (*pcj30 csrB*) influences phase variation. Comparison of colonies with induced versus non-induced *csrB* expression showed that the OFF ratio was significantly increased in a *csrB* dependent manner in all tested mutant strains (Figure 3). This finding suggests that conditions, which derepress the global Csr regulon and induce PGA-mediated biofilm formation, preferentially switch *fimS* to the OFF phase. From the observation that *csrB* overexpression equally affects the OFF to ON ratios in the wild type and the tested mutants known to affect PGA dependent attachment, it was concluded that the effects observed are independent of *ycdT*, *ydeH* and *pgaA-D*. These findings might provide the regulatory background of the functional interference observed between type I fimbriae and PGA surface adhesins.

6.5.3 *csrB* overexpression has no effects on fimbriation if *fimS* switching is impaired.

The results shown above indicate that the Csr cascade might affect fimbriation by influencing the orientational bias of *fimS* or alternatively affect the frequency or efficiency of *fimS* inversion. If so, *csrB* should no longer be capable of influencing fimbriation in strains that have *fimS* locked in the ON or OFF phase. To test this, mutants were constructed that have *fimS* locked in the ON or OFF phase, respectively (Figure 4A). In all these strains, either the recombinases FimB and FimE or the recombinases FimB, FimE, and FimX have been deleted and *fimS* was inserted in the ON or OFF orientation, respectively. Some strains, described as p_{fimA-H}^{OFF*} additionally carried a mutation in one of the inverted repeats of *fimS* (see Materials & Methods). First, we analysed overall attachment upon *csrB* overexpression. As shown in Figure 4B, strains with a locked OFF copy of *fimS* showed increased attachment (135.8 % \pm 6.6% for $\Delta fimBE p_{fimA-H}^{OFF}$; 117.6% \pm 3.8% for $\Delta fimBE p_{fimA-H}^{OFF*}$; 124.1% \pm 5.4% for $\Delta fimX\Delta fimBE p_{fimA-H}^{OFF}$; 108.9% \pm 4.4% for $\Delta fimX\Delta fimBE p_{fimA-H}^{OFF*}$) compared to the wild type. Thus, the phase of *fimS* and lack of recombinases affects PGA dependent attachment. However, none of the strains with *fimS* in the OFF phase reached the attachment levels of a $\Delta fimA-H$ mutant (190% \pm 8.8%). This suggests that *fimS* in an OFF orientation alone is not sufficient for the increase in attachment of the $\Delta fimA-H$ mutant, arguing that also lack of the fimbrial genes (*fimA-H*) somehow affect PGA dependent attachment. This hypothesis could be tested by expressing type I fimbriae in strains where *fimS* is locked OFF in *trans* and check if attachment decreases thereafter. In contrast, strains with *fimS* locked in the ON phase showed decreased attachment compared to wild type (41.7% \pm 2.2% for $\Delta fimBE p_{fimA-H}^{ON}$ and 30.4% \pm 2.5% for $\Delta fimX\Delta fimBE p_{fimA-H}^{ON}$). Interestingly, deletion of *fimX* caused a decrease in attachment by roughly 10% in all strains as compared to the parent strains lacking FimB and FimE alone, again suggesting that the orientation of *fimS* affects the attachment of UTI89 and that FimX acts as recombinase to convert *fimS* into the ON position.

The experiments described above indicated that *csrB* negatively regulates UTI89 fimbriation by influencing *fimS* phase variation. To verify these results, we analysed the potential of the triple recombinase mutants ($\Delta fimX\Delta fimBE p_{fimA-H}^{Locked}$) to aggregate GPE. Bacteria were statically grown overnight to maximise type I fimbrial expression (78) and adapted to an OD₆₀₀ of 4 while GPE were set to an OD₆₀₀ of 8. As shown in Figure 4C, aggregation was absent in the strain that lacks type I fimbriae ($\Delta fimA-H$) as well as strains with *fimS* in the OFF phase ($\Delta fimX\Delta fimBE p_{fimA-H}^{OFF}$ (1.0% of wild type) and $\Delta fimX\Delta fimBE p_{fimA-H}^{OFF*}$ (1.3%)). In contrast, the strain with locked ON *fimS* ($\Delta fimX\Delta fimBE p_{fimA-H}^{ON}$

Results

(148.3%)) caused an increased aggregation compared to wild type. Importantly, overexpression of *csrB* decreased the ability of UT189 wild type to aggregate GPE by 95% as compared to the vector control (Figure 4C), supporting the hypothesis that elevated levels of *csrB* negatively affect fimbriation. In mutants lacking fimbriae or mutants carrying *fimS* in the OFF state overexpression of *csrB* showed no effect. This is hardly surprising, as the aggregation of these strains is already at the detection limit and cannot be further decreased. Importantly, aggregation of a strain with *fimS* locked in the ON phase resulted in a minor and statistically non-significant decreased upon overexpression of *csrB* (Figure 4C), indicating that *csrB* impacts on fimbriation through its effects on the inversion of *fimS*.

The switch state of *fimS* is heritable over multiple generations allowing a given population to grow while stably maintaining fimbriated (*fim+*) or non-fimbriated (*fim-*) sub-populations (94). However, synthesised type I fimbriae may remain intact on the surface of bacteria even when *fimS* is switched OFF and thus fimbriae might not represent the phase of *fimS*. Therefore, a method, which directly reports the orientation of *fimS* might be more direct than the above assays. For this purpose two types of reporter strains were designed, which both express GFP as a function of the fimbrial promoter located on *fimS* (Figure 5A). One reporter had GFP inserted into the ORF of *fimA*, the first gene of *fimA-H* operon (*fimA::gfp*), and hence this reporter had a disrupted polycistronic *fimAICDFGH* operon. The other reporter had GFP inserted downstream of *fimH* (*fimH-gfp*), leaving *fimAICDFGH* operon intact. These two reporter strains were used to directly analyse the effects of *csrB* on the fimbrial switch. Figure 5B illustrates how individual *fimA::gfp* and *fimH-gfp* populations recorded by flow cytometry were gated in order to obtain the fraction of a bacterial population, which represents fimbriated bacteria (for details see Materials and Methods). In both reporter strains expression of GFP was observed. However, despite the same growth conditions, the fraction of the *fim+* population in *fimA::gfp* and *fimH-gfp* was significantly different (Figure 5B).

GPE aggregation assays indicated that the UT189 strain containing the *fimH-gfp* reporter behaved like wild type (Figure 6A). In agreement with this, biofilm formation of the *fimH-gfp* strain was not increased as compared to wild type (Figure 6B). Likewise, fimbriation of the *fimH-gfp* reporter strain was similar to UT189 wild type, as reported by flow cytometry upon staining cells with an anti-FimH primary and a fluorescently labelled secondary antibody (Alexa 647) (Figure 6C). The fluorescence distribution within the histogram was subdivided into a fimbriated and a non-fimbriated population using the APC signal derived from Alexa 647 of the Δ *fimA-H* mutant (data not shown), which defined the non-pilated baseline. As seen in Figure 6C, the results obtained were in agreement with previous our results. Although the signal was slightly more scattered in the GFP reporter strain, the

Results

majority of cells co-localised to the same area as in wild type (Figure 6C) and the percentage of FimH positive cells was similar in the two strains (88.4% for UTI89 wild type and 81.3% for the *fimH-gfp* reporter strain). In summary, it was concluded that this reporter strain behaves like wild type and expresses functional type I fimbriae, which phenotypically operate like type I fimbriae of the UTI89 wild type. In contrast, the *fimA::gfp* reporter strain is unable to form functional fimbriae due to its disrupted *fimAICDFGH* mRNA and thus this strain's phenotypes were not included in this study.

We next used the GFP reporter strains to assay the dynamics of fimbriation during growth in LB, both in static, non-shaken (conditions routinely used for biofilm formation and fimbrial aggregation) and in aerated, shaken cultures. As indicated already above, the *fimA::gfp* reporter strain showed only a small fraction of GFP positive cells (<5%) and only minor differences were observed for this strain when grown either statically or aerated (Figure 7A, B). When the same reporter was assayed in a strain background with the *fimS* locus locked in the ON orientation the whole population was reported as *fim+* while the whole population reported as *fim-* when *fimS* was locked in the OFF orientation (Figure 8A). These results were as expected, arguing that the *fimA::gfp* reporter allows to differentiate between distinct *fimS* phases. To assay fimbriation under conditions where the Csr system is derepressed the *fimA::gfp* reporter strain was assayed under *csrB* overexpressing conditions. Under these conditions, a small but significant reduction of GFP expression was observed (Figure 8B). Thus, *csrB* overexpression leads to a slight but significant reduction of reported fimbriated *fimA::gfp* cells, which supports our current hypothesis.

The most striking difference between the *fimA::gfp* (*fim-*) and *fimH-gfp* (*fim+*) reporter was the maximal level of GFP expression obtained for the two strains (Figures 7, 9). While the levels of GFP positive cells did not exceed 5% for the *fimA::gfp* reporter, the values for *fimH-gfp* were generally much higher (Figure 9 and Supplemental Figure 1 - 3). Importantly, the fraction of GFP positive cells from *fimH-gfp* was higher in static cultures as compared to aerated cultures. Noteworthy, the level of fimbriation measured between 18 and 24 hours of aerated conditions were very similar to the levels measured for the inoculum of the growth curve, which grew overnight under aerated conditions. Intriguingly, the fraction of GFP-positive *fimH-gfp* (*fim+*) cells was relatively low (5-10%) at low cell densities, but increased towards the end of the logarithmic growth phase and into the stationary phase. For *fimH-gfp* the increase in fimbriation over time was more pronounced during static growth where the fraction of *fim+* cells reached maximal levels of up to 50% (Figure 9B). Interestingly, a strain overexpressing *csrB* remained at a relatively low level of GFP positive cells (*fim+*) compared to wild type, even throughout the late stationary phase (Figure 9B). In aerated cultures fimbriation stagnated at a level of about 25% of GFP positive cells irrespective of *csrB*

overexpression (Figure 9A). To demonstrate that the observed effects of *csrB* on fimbriation indeed influence the orientation of *fimS* rather than modulating *fimA* promoter activity, the *fimH-gfp* reporter was analysed in strains carrying a locked copy of *fimS*. As shown in Figure 10 the fraction of GFP positive cells was very high in a strain with *fimS* locked in the ON phase, but at the detection limit in strains with *fimS* locked in the OFF phase. Likewise, strains with *fimS* locked in ON or OFF phase were unable to respond to increased levels of *csrB* (Figure 11), again arguing that the Csr system negatively influences type I fimbriation in UPECs by modulating *fimS*-mediated phase variation. Altogether, these data suggest that the expression of type I fimbriae is favoured under static, non-aerated conditions, especially in late stationary phase. This behaviour can be counteracted efficiently by artificially increasing *csrB* levels.

6.5.4 Deletion of FimE and CsrD influences the *csrB*- effects on the *fimS* orientation

To decipher the components involved in *csrB* dependent phase variation of *fimS* a series of mutant strains containing the *fimH-gfp* reporter were constructed and analysed by flow cytometry. The data obtained for the initial mutant screen is shown in Supplemental Experiments, Supplemental Figure 7 and Supplemental Figure 8. The screen included the following deletions in UT189 *fimH-gfp*: $\Delta pgaA-D$, $\Delta ycdT$, $\Delta ydeH$, $\Delta csrB$, $\Delta csrC$, $\Delta fimB$, $\Delta fimE$, $\Delta fimBE$, $\Delta fimX$, $\Delta ycgR$, $\Delta csgD$, $\Delta yhjH$, $\Delta bcsA$, and $\Delta csrD$. Furthermore, an UPEC specific phosphodiesterase ($\Delta c1116$) as well as its adjacent gene ($\Delta c1117$) reported to influence type I fimbriae were also deleted. Both genes are part of the Sfa fimbrial cluster and are located on a pathogenicity island (95, 96). From the initial analysis of these mutants in static cultures, we found that fimbriation was most altered in the $\Delta fimB$, $\Delta fimE$, and $\Delta csrD$ mutants. Importantly, while *fimB* mutants remained predominantly in the OFF phase, the *fimE* mutant showed constitutively high levels of fimbriation that were insensitive to *csrB* overexpression (Figure 12B, C, D and Supplemental Figures 4 and 5). This strongly suggests that Csr mediated control operates through the regulation of *fimE* expression.

Finally, CsrD, a factor involved in the degradation of the small RNAs *csrB* and *csrC* (54) and reported to strongly increase PGA dependent attachment upon deletion (Hosch *et al.*, unpublished manuscript) showed a strong influence on fimbriation (Figure 12E and Supplemental Figure 6). While the fraction of GFP positive cells in the $\Delta csrD$ mutant constantly increased during growth in a similar manner like wild type, overexpression of *csrB* in this mutant background not only caused a strong growth defect (Figure 12A) but also changed the dynamics of the fimbrial ON switch. Fractions of fimbriated cells were slightly increased and peaked already early during growth, before moderately decreasing thereafter.

This argues that CsrD is required for proper fimbriation in the cell and is involved in correctly mediating the switch of *fimS* into the OFF phase once *csrB* levels are high. Interestingly, the reported GFP signal of the CsrD mutant constantly remained below the signal for the wild type reporter strain, suggesting that the decreased degradation of *csrB* (and *csrC*) in the CsrD mutant might already be sufficient to cause a decrease in fimbriation. Whether this decrease is significant or not would still need to be investigated. CsrD being a degenerate GGDEF/EAL composite protein that might function as a c-di-GMP effector protein allows us to further speculate that c-di-GMP levels might also be involved in the inversed regulation of the two adhesins. Although this study has identified *csrB*, FimE and CsrD as components involved in type I fimbriae regulation, the mechanism responsible for Csr-mediated down regulation of fimbrial expression remains to be uncovered.

6.5.5 PGA and type I fimbriae mediated bacterial self-aggregation can be distinguished by flow cytometry

So far it was concluded that overexpression of *csrB* negatively interferes with the expression of type I fimbriae, while stimulating PGA dependent inter-bacterial and bacterial surface interactions. Based on this conclusion we used a flow cytometric assay, which can differentiate between type I fimbriae dependent and PGA dependent aggregation of bacteria (Figure 13). This differentiation of aggregates is based on the fact that the size of particles or aggregates can be monitored by flow cytometry and visualised in a FSC-H vs. SSC-H scatter, as seen in rows 1 and 2 of Figure 13. Aggregates which are caused through the expression of type I fimbriae but not PGA result in an increased GFP signal derived from the *fimH-gfp* reporter, as seen for the wild type reporter (Figure 13, quadrants 3A) and the strain with *fimS* in a locked ON orientation (Figure 13, quadrants 3B). On the contrary, strains whose aggregates are mediated by PGA rather than type I fimbriae, have a reduced or absent GFP signal, like the strain with *fimS* in a locked OFF orientation (Figure 13, quadrants 3C). Quadrants 1D and 2D of Figure 13 further illustrate that PGA dependent aggregates only occur when *csrB* is overexpressed from plasmid (Figure 13, quadrants 4A). With these results in mind we can conclude that the aggregates observed in quadrants 2C of Figure 13 must be caused by PGA while the aggregates of quadrants 2B of Figure 13 represent a combination of type I fimbriae and PGA. Furthermore, columns B and C of Figure 13 once more show that *csrB* can only exert its effects on fimbriation when *fimS* remains invertible. From this assay it can thus again be concluded that *csrB* overexpression allows *pgaA-D* dependent attachment between bacteria, while reducing type I fimbrial interactions, in a mechanism that depends on the invertible element *fimS*. Furthermore, this assay shows that

Results

a $\Delta pgaA-D$ population under *csrB* overexpressed conditions contains very few aggregates which are mediated by type I fimbriae. This argues that type I fimbriae are present in biofilms that are dominated by the PGA adhesin and that therefore these two structures are not mutually exclusive. Thus *csrB* levels determine the equilibrium between PGA-dependent and fim-dependent aggregates in a given population. Alteration of the *csrB* levels can thus be used to push bacteria into *fimA-H* driven aggregation (low *csrB* levels) or PGA driven aggregation (high *csrB* levels), which proves that the state of the Csr system (repressed vs. derepressed) is crucial to determine which of the two adhesins will be expressed in a given situation.

6.6 Discussion

Several studies exist, which report a coordinated expression of adhesins in bacteria (16, 95-111): A prominent example is the co-regulatory effect of CsgD on the expression of curli and cellulose, which are both adhesive matrix components of *E. coli* biofilms (97, 111). This co-regulatory effect strengthens the matrix of a biofilm and thus enhances the biofilm's survival. Another example is the inverse expression of P fimbriae and type I fimbriae in UPECs. This crosstalk is shown to involve the regulator of pyelonephritis-associated pili (PapB) and is believed to prevent the expression of multiple types of fimbriae on a single cell (16, 98-100). Yet other studies introduce a regulatory link between the expression of type I and Sfa fimbriae in pathogenic *E. coli* (95, 96). In this current study we identified a regulatory mechanism which inversely affects the expression of type I fimbriae (which promote bacterial adherence to eukaryotic cells and enable UTIs) and the biofilm matrix component PGA (which promotes bacterial attachment and stabilises three-dimensional biofilms (15, 40, 42, 89, 112)). We show that conditions derepressing the Csr system favour PGA expression but disfavour the expression of type I fimbriae. On the contrary, a repressed Csr system favours the expression of type I fimbriae but disfavors the expression of PGA. While the signalling cascade linking the Csr system to PGA expression is known and involves post-transcriptional control by CsrA (40, 42, 47, 113), the mechanism responsible for the downregulation of type I fimbriae still needs to be unravelled. Our work has identified several components that are required for this regulatory mechanism. These include the small RNA *csrB*, the recombinase FimE and the CsrD regulator involved in *csrB* stability control. Furthermore, we show that the Csr system affects type I fimbriae through the switchable element *fimS*, presumably by post-transcriptionally affecting the activity of the recombinase FimE via CsrA. This regulatory crosstalk between type I fimbriae and PGA expression raises several interesting questions with respect to its role *in vitro* or during the progression of urinary tract associated infections: Why would the expression of the two surface adhesins need to be spatially and/or temporally uncoupled?

The most important role of type I fimbriae in UPECs is to promote bacterial entry into urothelial cells, which ultimately leads to cystitis (10). With respect to our model, this suggests that the conditions in urine and/or the epithelial cells of the bladder repress the Csr system. Consequently, PGA dependent biofilm formation is disfavoured while the expression of type I fimbriae is favoured. Contrary to UPECs, the closely related ABU strains are attenuated in their expression of type I fimbriae (114). In the ABU strain 83972, this attenuation is due to a large deletion in the *fim* operon described as *fimB'::DFGH+*, which results in the loss of *fimA*, *fimI* and *fimC* (115). In order to survive in the bladder 83972 had to

Discussion

adapt and find a way to persist without functional type I fimbriae. This is achieved by either fast growth or the formation of biofilms (116, 117). This argues that the nutritional state and the environment, which favour type I fimbriae expression in pathogenic UPECs might favour PGA expression in ABU strains. Moreover, it suggests that the model established in this work could be in place in pathogenic as well as ABU strains but have the opposite effects on adhesin expression, despite the same environmental conditions. Interestingly it was shown that *csrB* and *csrC* levels of 83972 are elevated upon patient colonisation or growth in urine (118, 119), which argues for an involvement of the Csr system in the bladder. This finding also allows speculating that the Csr system of 83972 is derepressed in ABU strains and repressed in cystitis isolates in the absence of physiological BarA/UvrY stimuli. It would be interesting to search for SNPs between pathogenic UPECs and ABU strains in the whole Csr system and all those components required for the inversed regulation of type I fimbriae and PGA. Maybe these SNPs can explain why UPECs express type I fimbriae and ABU strains form biofilms in the same host environment. Furthermore, it would be interesting to overexpress type I fimbriae from plasmid or delete the *pgaA-D* genes in ABU strains and see if their ability to survive within bladder is affected. This would be expected if our model is applicable to ABU strains.

After successful adherence of pathogenic UPECs (e.g. UTI89) to urothelial cells, they are internalised into superficial facet cells where they start to form dense sessile biofilm-like structures (IBCs) (1-4). *In vitro*, type I fimbriae have been implicated in the initial attachment of bacteria to abiotic or biotic surfaces (32, 120-122). It is possible that these structures are expressed by UPECs in the cytoplasm during the initial phase of intracellular growth and are thereafter stably maintained in mature IBCs but without *de novo* synthesis. It was reported that expression of the *pgaA-D* promoter constantly increases during the 14 hours tested (123). So contrary to type I fimbriae, polysaccharide adhesins including PGA are expressed in the matrix of mature three-dimensional biofilms and hence appear to be temporally separated from the expression of type I fimbriae (28, 34, 122-124). Based on these *in vitro* studies it might be that the expression of type I fimbriae and PGA are temporally separated in the development of chronic UTI: type I fimbriae being synthesised in the initial phase of IBC development and PGA only being expressed in mature IBCs or long term persisting QIRs. Initial data obtained for the UTI89 *pgaA-D* mutant in a murine cystitis model (Hosch *et al.*, unpublished manuscript) does not support this hypothesis and rather suggests that PGA is not important during cystitis. However, this study might not be fully conclusive, as the three weeks tested might not be sufficient to investigate phenotypical differences between persisting UTI89 wild type and UTI89 Δ *pgaA-D*. Furthermore, a phenotype for the UTI89 Δ *pgaA-D* might only manifest itself once mice have suffered from recurring UTIs. This idea is supported by another study, which suggested that the *pgaA-D* genes of UPECs are

expressed *in vivo* and might contribute to virulence, (125). It would be interesting to monitor the expression of type I fimbriae and PGA simultaneously in a murine cystitis model using a double *fimH-gfp pgaD-gfp_uv* reporter strain. With this construct, it would be possible to differentiate the expression of *fimA-H* (GFP) from *pgaA-D* (GFP-UV) during infection without disrupting the UTI89 wild type disease progression. The use of such a double reporter strain would reveal if the inversed effects imposed by the Csr system occur *in vivo* and result in spatially and/or temporally separated expression of the two adhesins. In the end, the spatial and/or temporal separated expression of type I fimbrial and PGA expression has to occur in accordance with the environment and thus be regulated somehow. How can the identified components impose a signalling cascade, which inversely affects type I fimbriae and PGA? Why are type I fimbriae negatively regulated by the Csr system? Is CsrA the central component of the inversed regulation of the adhesin? Does CsrA directly regulate the expression of *fimE*, or are other *fim* components and unidentified factors necessary in the signalling cascade?

6.6.1 The inverse effect of the Csr system on type I fimbriae and PGA involves *csrB*, CsrD, FimE and the phase variation of *fimS*.

The results presented in this study provide evidence that the interference of type I fimbriae and PGA expression is predominantly functional, although an additional structural interference might still exist. The identified factors required to inversely regulate the two adhesins allow speculating on the hierarchy in the signalling cascade (Figure 14): We showed that the centre of the signalling cascade is composed of the Csr system. Modifications in the environmental composition require bacteria to quickly adapt, e.g. through the formation of PGA dependent biofilms and downregulation of type I fimbriae. The involvement of a global regulator, such as CsrA, is a reliable way to this. Upon environmental stimuli, it allows a controlled transition from fimbriated to non-fimbriated, PGA expressing bacteria. With respect to what is known about the mechanisms implied by the Csr system it can be assumed that the effects of *csrB* overexpression on type I fimbria are mediated through the mRNA binding protein CsrA, similar to the mechanism reported for PGA repression (49, 126). As a Δ *fimE* mutant is irresponsive to alterations of *csrB* levels, it can be concluded that FimE must be downstream of *csrB* and CsrA in the signalling cascade. However, it remains to be elucidated, if CsrA really is involved, and acts on *fimE* or whether a novel role for *csrB*, which is independent of CsrA, was identified. A suggested interaction of CsrA with *fimE* mRNA could be indirect via inhibition of a positive regulator. Alternatively CsrA could exert a direct negative effect on the function of FimE by binding to and

Discussion

destabilising the *fimE* mRNA. The construction of a *fimE::lacZ* transcriptional reporter with β -galactosidase activity could be used under *csrB* or CsrA overexpressing conditions, to elaborate the effect of the Csr system on *fimE*. Furthermore, direct binding of CsrA to the *fimE* mRNA could be investigated via gel shift assays. The direct interaction of CsrA with *fimE* mRNA would thus put another output system (type I fimbriae) under the direct control of CsrA.

The third factor involved in the Csr mediated inversed effect on type I fimbriae and PGA expression was CsrD, a protein reported to ensure homeostatic levels of *csrB* and *csrC*. CsrD targets *csrB* and *csrC* for RNaseE degradation and hence affects their stability and cytoplasmic levels. Regarding its function in the Csr system it is expected that the deletion of CsrD resulted in a decreased level of fimbriation, even without the overexpression of *csrB*. Fimbriation of a *csrD* mutant was indeed decreased compared to wild type but only marginally. Likely this marginal decrease in fimbriation is due to enhanced stabilisation of *csrB* and *csrC* and hence a partial derepression of the Csr system. But as the levels of *csrB* and *csrC* are low under Csr repressed conditions the effects of a *csrD* mutant must be marginal. As for the overexpression of *csrB* in a *csrD* mutant, we speculate that the Csr system is completely deregulated, which impairs bacteria to express fimbriae in response to their environmental and metabolic state. Besides its effects on type I fimbriae, the deletion of *csrD* and simultaneous overexpression of *csrB* represents a stressful condition that results in a growth deficit and a massive increase in PGA dependent biofilm formation (Hosch et al., unpublished manuscript). This argues that CsrD ensures a balanced level of type I fimbrial expression and PGA production, which is adapted to the environmental conditions surrounding the bacteria. Being part of the Csr system, it is likely that the environmental cues, which modulate the levels of the two adhesins signal through the BarA/UvrY two component system. Unfortunately, the literature on environmental factors influencing the Csr system, fimbriation or PGA expression is scarce and based on these studies it is difficult to hypothesise, which environmental signals are at the basis of the inversed adhesin regulation. However, some of these studies could serve as guidelines in determining which environmental cues integrate into this regulatory mechanism. For example, it has previously been shown that oxygen limiting conditions, which are found during stationary growth (e.g. during static growth) enrich for fimbriated bacteria (127). This is in agreement with our findings that fimbriation is highest in a stationary phase culture statically grown and deprived of oxygen. Thus the observation that *csrB* overexpression only downregulates fimbriation under static conditions suggests that the described regulatory network is oxygen-sensitive. Moreover, an Affymetrix array hybridisation study suggested that the environmental pH might influence the translation of type I fimbriae, *csrB*, many metabolic genes, as well as the diguanylate cyclase YdeH (128). And yet another study has reported that the short chain

fatty acids acetate and formate, both fermented under carbon limiting conditions, get sensed by the BarA/UvrY two-component system and result in a derepressed Csr system (50). Moreover, it is known that glycogen synthesis, which is under the control of the Csr system as well, starts to increase upon entry into stationary phase (46, 129-133). It is thus plausible to speculate that glycogen availability, oxygen, pH and/or short chain fatty acids contribute to the Csr-dependent regulation of the two adhesins. Hence, it would be worthwhile to test the impact of these stimuli on the dual adhesin system using the *fimH-gfp* or a *fimH-gfp pgaD-gfp_uv* double reporter strain. Of course, this construct could be used *in vitro* and *in vivo* to identify other metabolic components or other physiological signals that activate the Csr cascade and by that adapt the expression pattern of the two adhesins. An *in vitro* transposon screen performed on the double reporter strain should further help to identifying the remaining bacterial components that are involved in the regulatory mechanism underlying the inversed adhesin regulation that trigger the inversed regulation via the BarA/UvrY TCS.

6.6.2 During biofilm formation type I fimbriae and PGA expression are separated

The inverse regulation of type I fimbriae and PGA expression indicates that the expression of both adhesins must be separated in some way, and that their expression is favoured in some but not in other environments. Thus far, it seems that the expression of either of the adhesins occurs in response to environmental signals sensed by the Csr system. This raises the question whether any signal is strong enough to completely turn off the expression of one adhesin and stimulate the expression of the other or whether the signal only serves to modulate the abundance of the two structures. Biofilms visualised on electron micrographs showed us that the two extracellular adhesin structures do not get co-expressed on the surface of a single bacterium. Furthermore, the adhesin abundance was different over the whole population, arguing for a spatial separation of adhesin-expression over the entire population and a clear preference for PGA over the entire population. Importantly however, this also suggests that type I fimbriae are not completely absent under conditions that favour PGA dependent attachment, as few UTI89 wild type bacteria in a biofilm expressed type I fimbriae despite elevated *csrB* levels. Similarly, overexpression of type I fimbriae under conditions which stimulate PGA dependent biofilm formation (overexpression of *csrB*) still allowed the formation of a residual biofilm. Also, we found that attachment of UTI89 wild type lays between the attachment of the locked ON and locked OFF strains, arguing that bacteria can still form residual PGA dependent biofilms when type I fimbriae are highly present. In conclusion it seems that the abundance of both adhesins cannot be equal on the surface of a bacterial population but do not necessarily exclude one

Discussion

another. Thus, signals interacting with the BarA/UvrY TCS are not strong enough to completely abrogate the expression of the other adhesin. Presumably the different environments encountered by UPECs during pathogenesis have exerted a selective pressure on bacteria to only expression one of the adhesins. As a result, UPECs, and maybe also other bacteria, were able to adapt to several environments by imposing regulatory networks which govern over dual adhesin systems.

Furthermore, we observed that the absence of type I fimbrial expression in a *fimS* locked OFF mutant, does not fully account for the enhanced attachment of a strain, which lacks all structural genes ($\Delta fimA-H$). This result was unexpected and will need to be elaborated in the future. Possible explanations include the following scenarios: i) maybe the deletion of *fimA-H* results in a polar effect in which the fimbrial promoter is brought into proximity of the *uxuA* gene downstream of *fimH*. Interestingly, UxuA is involved in the carbon metabolism where it interconverts pentose and glucuronate. Thus an *uxuA* deletion might result in a metabolic flux which favours attachment by affecting the Csr signalling. To study this “polar effect”, the phenotype of a *uxuA* deletion mutant in attachment would have to be investigated in attachment assays. ii) The increased attachment in a *fimA-H* mutant compared to the locked OFF strains could also be caused by the action of one of the recombinases (FimB, FimX or FimE), as their genes are deleted in the locked OFF strains but not in UT189 wt or the *fimA-H* mutant. To test this hypothesis, the recombinases would have to be deleted in the *fimA-H* mutant and the attachment would have to be compared to UT189 and the recombinase mutants. iii) Alternatively, the difference in attachment might result from residual read-through of an upstream promoter into the *fim* genes. The easiest way to test this is by investigating GFP expression of the *fimH-gfp* reporter strain, which has a locked OFF phase of *fimS* under repressed and derepressed Csr signalling and compare it to the results obtained from a *fimH-gfp* $\Delta fimA-H$. Regardless of the underlying cause the difference in attachment between $\Delta fimA-H$ and *fimS* locked OFF mutant remains an intriguing result, which suggests that any genetic alteration of the *fimBE-fimS-fimAICDFGH* or *fimX* locus has an effect in PGA dependent attachment. Furthermore, this result again raises the question whether the inversed regulatory effect exerted by the Csr system is sufficient for all phenotypes observed, or whether an additional structural interference of the two adhesins may further contribute to the observed interference.

6.6.3 Disruption of the *fimAICDFGH* operon reduces the signal reporting fimbrial expression

Besides the novel inversed regulation of type I fimbriae and PGA, this study demonstrates that our *fimA::gfp* reporter strain does not properly represent wild type fimbriation. The improperly reported fimbriation must be due to the disruption of the *fimAICDFGH* operon. Similar to other studies (24, 94), *fimA::gfp* reported very few *fim*⁺ UTI89 bacteria under the conditions, which usually maximise fimbriation. This result is not in agreement with the wild type fimbriation measured by other methods (e.g. aggregometry). A possible explanation for the discrepancy in fimbriation levels could be that the expression of type I fimbriae underlies a positive feedback mechanism that depends on the correct expression of *fimA-H*. Different studies have reported that the outer membrane composition is remodelled once type I fimbriae are inserted into the membrane and interact with abiotic surfaces. These remodelling actions affect the protein composition and the physiochemical characteristics of the membrane (122, 134, 135). Interestingly, one protein whose abundance alters upon insertion of type I fimbriae into the outer membrane was OmpX. Deletion of this protein was shown to cause an increase in type I fimbriae mediated interactions with abiotic surfaces (136). This suggests that the levels of surface exposed type I fimbria and OmpX must be controlled by a feedback mechanisms, which signals into the cell and affects the expression of type I fimbriae or *ompX*, respectively. Regarding our dual adhesin system, a similar situation could contribute to the inverse effects of the Csr system. The fimbrial proteins are secreted through the SecYEG translocon and only get folded once they reached the periplasm. Therefore, it is very unlikely that the structural *fim* proteins act upon their own upregulation. The presence of this hypothesised feedback loop could easily be confirmed by overexpressing type I fimbriae from plasmid in the *fimA::gfp* reporter strain and test if the GFP levels reporting fimbriation get complemented to the levels reported for *fimH-gfp*. An interesting candidate involved in the hypothesised feedback loop is FimI, found downstream of FimA on the polycistronic *fimA-H* operon. In *E. coli* and *S. typhimurium*, FimI was shown to be essential for proper fimbriation. It contains a signal sequence, which directs the protein to the outer membrane (77, 137, 138). In *S. typhimurium* FimI was further suggested to anchor type I fimbriae to the cell membrane (138). The precise function of FimI and its location outside the cytoplasm could not yet be determined in *E. coli*. We speculate that FimI might be involved in a mechanism, which feeds back from the outer membrane to the regulators that affect the expression of type I fimbriae in the periplasm. This function of FimI would be novel but it would not contradict previous results. Presumably, a comprehensive search for components involved in the overall interference of type I fimbriae and PGA, e.g. via transposon screen based on the dual reporter, would identify FimI or the other components involved in the mechanism underlying the inversed regulation of type I fimbriae and PGA.

Discussion

In conclusion, this study performed in UPECs has identified a regulatory link between the expression of type I fimbriae, which contribute to virulence during UTIs, and the well-established exopolysaccharide PGA involved in biofilm formation. This regulatory link depends on the Csr system which integrates environmental signals to inversely affect the two adhesins through post-transcriptional control by CsrA. Repression of the Csr system hinders PGA dependent biofilm formation while a derepressed Csr system decreases fimbriation by affecting the orientation of *fimS*, in a process that requires the recombinase FimE. Our model further suggests that CsrD is required for the regulatory mechanism leading to a balanced dual adhesin expression, which is in accordance with the environmental state. Furthermore we hypothesise that the localisation of type I fimbriae to the outer membrane leads to membrane modifications, which result in a signalling cascade that further interferes with PGA expression and additionally boosts fimbriation. This hypothetical feedback mechanism might be integrated into the Csr signalling cascade that affects the expression of type I fimbriae via FimE.

6.7 Figure Legend

Figure 1: Phenotypes of type I fimbriae in UTI89.

The phenotypes of type I fimbriae have been investigated in isogenic $\Delta fimA-H$ or $\Delta fimH$ mutants using UTI89 as parent strain. Complementation of all type I fimbrial phenotypes was performed by overexpressing type I fimbriae from plasmid (pPKL4). Error bars of all assays are standard errors of the mean. **A) Deletion of type I fimbriae abolishes GPE aggregation:** Bacteria were grown for 24 h statically and then adapted to an OD₆₀₀ of 4, GPE were adapted to an OD₆₀₀ of 4 as well. Aggregation was measured over 10 min and was normalised to 0 % aggregation (GPE solution) and 100 % aggregation (PBS). The histogram indicates the percentage of aggregated GPE compared to UTI89 wild type (100 %). Strains without pPKL4 are shown in white; strains carrying pPKL4 are shown in black. In some strains, aggregation was not detectable, these strains are indicated as n.d. **B) Type I fimbriae are detrimental for PGA dependent attachment:** Cell density and surface attachment was measured as OD₆₀₀ after static growth for 24 h. Overexpression of *csrB* was performed to derepress the translation of the *pgaA-D* mRNA required for PGA synthesis. Bars represent biofilm formation (surface-attached biomass divided by optical density of total cells) compared to UTI89 *pcj30 csrB*. Data for *pcj30 csrB* is depicted in black bars; data for the control plasmid *pcj30* is depicted in white bars. **C) Complementation of type I fimbriae lowers PGA dependent attachment of UTI89:** Cell density and surface attachment was determined at 600 nm after static growth for 24 h. Bars represent biofilm formation (surface-attached biomass divided by optical density of total cells) compared to UTI89 *pCsrB* (white bars). Black bars indicate data obtained from strains carrying *pCsrB* and *pPKL4*. Data is shown with standard errors of the mean.

Figure 2: Scanning electron micrographs of biofilms.

Electron micrographs of biofilms were taken from strains statically grown on glass slides for 24 h in a 24-well plate at 37° C. All strains were grown in the presence of induced *pcj30 csrB*. Scale bars are indicated in each micrograph. Biofilm formation of UTI89 wild type is compared to biofilm formation of $\Delta fimA-H$ and $\Delta pgaA-D$. **A)** Images were taken at the following magnifications: 2000x for UTI89 and UTI89 $\Delta pgaA-D$ and 1700x for UTI89 $\Delta fimA-H$. **B)** Images were taken at the following magnifications: 10'000x for UTI89 wt and UTI89 $\Delta fimA-H$ and 6700x for UTI89 $\Delta pgaA-D$. Black arrows points out PGA knobs, the white arrows indicate type I fimbriae. The fibrillar structures present in UTI89 $\Delta fimA-H$ are thicker

than the hair like structures observed in UTI89 and most likely represent flagella. The close up images shown in **C)** are sections of representative images taken from bacteria within biofilms that express both type I fimbriae and PGA knobs.

Figure 3: Effects of *csrB* on the phase of the invertible element *fimS*.

The *fim* OFF to ON ratio was calculated from DNA band intensities of the three primer based PCR-products. Determination of this ratio was performed with ImageJ as follows: ((OFF band intensity – background intensity) / (ON band intensity – background intensity)). The data in each box-plot represent the average of at least 8 clones per strain and condition. The boxes represent the second and third quartile, the line in the box indicates the mean over all clones. The boundaries of the first and fourth quartile are indicated as lines. White bars indicate ratios determined from strains carrying noninduced pCsrB [Ratios: UTI89 wild type (2.9 ± 0.7), $\Delta pgaA-D$ (3.3 ± 1.0), $\Delta ycdT$ (2.3 ± 1.0) and $\Delta ydeH$ (2.7 ± 0.9)]. Data shown for the induced pCsrB is shown in gray [The calculated ratios were as follows: UTI89 wild type (5.1 ± 1.3), $\Delta pgaA-D$ (5.9 ± 2.0) $\Delta ycdT$ (3.8 ± 1.6) and $\Delta ydeH$ (4.4 ± 0.6)]. The degree of significance between noninduced and induced colonies are indicated at the top of the graph and were calculated in an unpaired t-test ($P > 0.05$).

Figure 4: Structure and phenotypes of p_{fimA-H}^{Locked} constructs:

A: structure of p_{fimA-H}^{Locked} constructs: The wild type locus of type I fimbriae is located at the top. The second line illustrates the UTI89 $\Delta fimA-H$ construct. In the lower two constructs, the recombinases *fimB* and *fimE* are deleted and the orientation of *fimS* (red) is artificially fixed (see Material and Methods). To ensure that *fimS* remains fixed, *fimX* was additionally deleted in the pre-existing p_{fimA-H}^{Locked} strains, as illustrated in the fourth construct. The red arrow indicates that the invertible element *fimS* can still be switched and thus the promoter of fimbriae can be found in two orientations. In the lower two constructs the arrow heads of *fimS* are missing since the phase of p_{fimA-H}^{Locked} constructs is fixed in either the ON or the OFF configuration. White boxes indicate unmodified areas while grey boxes indicate deleted genes. **B): Attachment of p_{fimA-H}^{Locked} strains:** Cell density and surface attachment was measured and quantified at 600 nm after 24 h static growth. Bars represent biofilm formation (surface-attached biomass divided by optical density of total cells) compared to UTI89 pcj30 *csrB* with standard errors of the mean. (Data obtained with the empty vector is not shown) **C): Aggregation of p_{fimA-H}^{Locked} strains under *csrB* overexpressing conditions:** The capacity of the p_{fimA-H}^{Locked} mutants to aggregate GPE is quantified as

Figure Legend

percentage compared to UT189 wild type mediated aggregation. Data obtained for the empty plasmid (pME6032) is shown in white; aggregation of strains with pCsrB is shown in black. GPEs were adapted to an OD₆₀₀ of 8; bacteria to an OD₆₀₀ of 4. Standard errors of the mean are calculated from three measurements of the same culture. The effect of *csrB* in $\Delta fimX \Delta fimBE$ $p_{fimA-H}^{Locked ON}$ has been calculated as being non-significant (n.s) in an unpaired t-test ($P > 0.05$).

Figure 5: Construction of p_{fimA-H} GFP reporter constructs to monitor fimbrial phase variation.

Two distinct fimbrial reporter constructs were made. **A) structure of p_{fimA-H} reporter constructs:** The top line illustrates the wild type locus of type I fimbriae. The green boxes indicate the position at which the GFP reporter was inserted. The red arrowheads of *fimS* indicate that phase variation is still possible. White boxes represent genes, which have not been modified. Grey boxes indicate that these genes are still present but not expressed due to disruption of the polycistronic *fimAICDFGH* mRNA through GFP insertion into *fimA*. In *fimH-gfp* the GFP was inserted at the 3' end of *fimH* and thus this strain remains fimbriated. Expression of GFP is ensured through the insertion of a Shine Dalgarno sequence between *fimH* and *gfp*. **B) Flow cytometric measurement of fimbriation:** For each strain we captured 50`000 events with a flow cytometer and plotted them according to their size (indicated in the left pannel). This plot was subdivided into four quadrants (Q1- Q4), bacteria being in the upper right quadrant (Q2). Next, the GFP signal (Alexa-Fluor 488-H) of all events in Q2 was plotted against the red channel (PE-H) to exclude a possible increases in background fluorescence. Also, the GFP signal of all bacteria in Q2 was plotted in a histogram to investigate the distribution of signal intensities. Based on the negative control (UT189 wild type) the intensity plot was subdivided into a GFP minus (*fim-*) section (left) and a GFP positive (*fim+*) section (right). The percentages of events, which localise in the *fim+* and *fim-* section, are indicated in the histogram.

Figure 6: Characterisation of the *fimH-gfp* reporter strain.

A) Aggregation of *fimH-gfp*: Aggregation of *fimH-gfp* was measured after setting the GPE and bacteria to an OD₆₀₀ of 4. The values in the histogram are shown as the mean of three measurements and the standard errors thereof. **B) Attachment of *fimH-gfp*:** Cell density and surface attachment was measured as OD₆₀₀ after static growth for 24 h. Bars represent biofilm formation (surface-attached biomass divided by optical density of total cells)

Figure Legend

compared to UTI89 pCsrB. Bars in white indicate attachment measured for strains carrying the pME6032 control plasmid. The data of pCsrB is shown in black. The standard error of the mean is included for all data sets. **C) Fimbriation patterns of *fimH-gfp***: In the upper panel, fimbriation of each strain is shown as pseudocolored, size-dependent distribution in a forward-sideward scatter and was measured using a type I fimbriae specific antibody. The lower panel depicts histograms showing the Alexa 647 signal distribution measured in the APC channel. Histograms have been subdivided into two populations using UTI89 $\Delta fimA-H$ to determine the non-fimbriated population (Data not shown). The left section of the histograms represents non-fimbriated bacteria; the right section represents fimbriated bacteria. The percentage of non-fimbriated respectively fimbriated bacteria is indicated in each histogram.

Figure 7: Growth dependent analysis of fimbriation in *fimA::gfp*.

GFP expression of the *fimA::gfp* reporter strain was measured over time and under aerated (**B**) as well as static (**A**) conditions. Samples were taken at the beginning of the growth curve as well as after 1, 2, 3, 5, 8 and 24 hours. To measure fimbriation bacteria were fixed and processed for flow cytometric analysis. The upper panels in **A** and **B** illustrate the size distribution of the 10`000 events measured for each sample. The upper right quadrant in each SSC-H vs. FCS-H scatter contains bacteria. The GFP signal intensities for all bacteria recorded in the upper right quadrant are illustrated in histograms (lower panels). The left peak in the histogram corresponds to the signal intensities determined for the negative control and thus represents events without GFP signal (*fim*⁻). The second peak, at the right side of the histograms, corresponds to the fraction of bacteria, which express GFP (*fim*⁺). The fractions of *fim*⁻ and *fim*⁺ are indicated in each histogram.

Figure 8: Flow cytometric analysis of *fimA::gfp* p_{fimA-H}^{Locked} strains.

The flow cytometric patterns of the p_{fimA-H}^{Locked} strains are shown in **A**): The first column shows the flow cytometric pattern of the wild type *fimA::gfp* construct. The second column shows flow cytometric patterns of *fimA::gfp* $\Delta fimBE$ p_{fimA-H}^{ON} , where *fimS* was locked in the ON phase. The last two columns show the data of *fimA::gfp* $\Delta fimBE$ P_{fimA-H}^{OFF} respectively *fimA::gfp* $\Delta fimBE$ P_{fimA-H}^{OFF*} where *fimS* is locked in the OFF phase. Subdivision into *fim*⁻ and *fim*⁺ bacteria was performed as previously described and the fraction of *fim*⁻ and *fim*⁺ bacteria is indicated in each histogram. **Figure 8B**) shows the effects of *csrB* overexpression on the *fim*⁺ fraction in the *fimA::gfp* reporter stain. As the effect of *csrB* on fimbriation in

Figure Legend

fimA::gfp was minor the histograms only considers the fraction of bacteria, which were *fim*⁺ according to the GFP-signal intensity distribution (histogram of the Alexa-Fluor 488-H signal). Per strain, 3 independently grown clones were measured and their mean as well as the standard error thereof was calculated. The significance was calculated with an unpaired t-test ($P > 0.05$).

Figure 9: Growth dependent analysis of fimbriation in *fimH-gfp* strains.

The left y-axis indicates the fraction of the bacterial population, which expresses GFP (*fim*⁺), the right y-axis indicates the optical density of the bacterial culture at the time the sample was taken. The data of the growth curve is shown as empty circles, GFP data from flow cytometry is indicated as filled squares. Strains without plasmid are shown in a continuous line, strains with the pME6032 control plasmid are shown as discontinued line and strains with pCsrB are shown as dotted line. The negative control (UTI89 wt) is shown in gray. All data points are calculated as the mean \pm standard error of the mean of three independent samples grown in parallel in 250 ml glass flasks. At each time point, samples were collected and processed for flow cytometry. Once all samples were collected, they were transferred into a 96 well plate and analysed with a HTS sampler by flow cytometry. **A) Fimbriation under aerated conditions:** Samples were taken at the start of the growth culture, after 30 min, 1 h, 2 h, 3 h, 4 h, 5h, 6 h, 7 h, 8 h and 24 h. **B) Fimbriation under static conditions:** Samples were taken at the start of the growth culture and then after 1 h, 2 h, 3 h, 4 h, 5h, 6 h, 7 h, 8 h, 9 h, 10 h, 12 h, 14 h, 16 h, 18 h, 20 h, 22 h and 24 h. The values of three time points (Start, 10 h and 24 h) are calculated from 6 independent samples.

Figure 10: Flow cytometric analysis of *fimH-gfp* p_{fimA-H}^{Locked} strains.

The flow cytometric patterns of the p_{fimA-H}^{Locked} strains in the *fimH-gfp* reporter construct. Data was obtained from cultures, which grew statically for 24 h. The data for the wild type *fimH-gfp* construct is illustrated in the left column. The *fimH-gfp* p_{fimA-H}^{ON} data is shown in the second column from the left. The two last columns show the data of *fimH-gfp* p_{fimA-H}^{OFF} and *fimH-gfp* p_{fimA-H}^{OFF*} the ladder of which contains a point mutant in one of the two inverted repeats of *fimS*. Subdivision into *fim*⁻ and *fim*⁺ bacteria was performed as described above and the *fim*⁺ and *fim*⁻ fractions are indicated in each graph.

Figure 11: Effects of *csrB* in *fimH-gfp* p_{fimA-H}^{Locked} strains

Figure Legend

The data obtained in this figure comes from cultures, which grew statically for 18 h in 50 ml falcon tubes. The data for the *fimH-gfp* carrying the pME6032 control plasmid is illustrated in **A**). The data for the pCsrB overexpressing plasmid is illustrated in **B**). The gating was performed as described in Materials and Methods or **Figure 6B**. Subdivision into *fim*⁻ and *fim*⁺ bacteria was performed as described above and the *fim*⁺ and *fim*⁻ fractions are indicated in each graph.

Figure 12: Growth dependent fimbriation in Δ *fimB*, Δ *fimE* and Δ *csrD* mutants.

The mutants *fimH-gfp* Δ *fimB*, *fimH-gfp* Δ *fimE* and *fimH-gfp* Δ *csrD* were statically grown. The first sample was taken after 10 h, thereafter samples were collected every two hours up to 24 h. The data illustrated corresponds to the *fim*⁺ fraction of the bacterial *fimH-gfp* population. Data obtained from strains without plasmid is shown as filled line, data of pME6062 is shown as dashed line and the data of pCsrB is shown as dotted line. The growth curves of wild type *fimH-gfp* as well as the three *fimH-gfp* mutants are shown in **A**). GFP expression profiles of *fimH-gfp* is shown in **B**), those of *fimH-gfp* Δ *fimB* in **C**) *fimH-gfp* Δ *fimE* in **D**) and *fimH-gfp* Δ *csrD* in **E**). After sample collection and processing for flow cytometry, the samples were stored at 4 °C and all analysed at once in a 96-well plate. Data points are the average of three independent clones grown in parallel. Error bars are shown as standard errors of the mean.

Figure 13: Flow cytometric differentiation between *fimA-H* and *pgaA-D* mediated aggregates.

GFP expression was determined by flow cytometry from cultures which grew in 50 ml falcon tubes for 18 h under static conditions. **Row 1** and **row 2** represent size dependent distributions of bacteria in a forward-sideward-scatter. The GFP signal of all the bacteria in the upper right quadrant (Q2) of each FSC-H vs. SSC-H plot are represented as intensity distributions in **lane 3** and **lane 4**. **Lanes 1** and **lane 3** represent strains carrying the pME6032 control vector, **row 2** and **row 4** are data obtained from strains with pCsrB. The histograms of **row 3** and **row 4** are subdivided into a GFP negative (*fim*⁻) and a GFP positive section (*fim*⁺). **Column A** shows the data obtained for the *fimH-gfp* wild type, **column B** and **column C** are data for the $p_{\text{fimA-H}}^{\text{ON}}$ and $p_{\text{fimA-H}}^{\text{OFF}}$ reporter strains, respectively. The data for Δ *pgaA-D* is shown in **column D**.

Figure 14: Concluding model of inversed adhesin regulation.

The model illustrates the inversed regulation of PGA and type I fimbrial expression by the Csr system (red). Factors affected by CsrA which are not involved in the inversed regulation of the two adhesins are not illustrated here. Neither are factors affecting phase variation of *fimS*. Formate, acetate and most certainly other signals derepress the Csr cascade through stimulating the BarA/UvrY two component system (TCS). Upon stimulation of the TCS, the small RNAs *csrB* and *csrC* get synthesised, bind to CsrA and titrate it away from its confirmed target mRNAs (*nhaR*, *pgaA-D*, *ydeH*, *ycdT*) and its postulated target mRNAs (*fimE* or a positive regulator thereof). As a consequence PGA dependent biofilm formation occurs and FimE switches *fimS* into the OFF phase, discontinuing the expression of type I fimbriae and counteracting the activity of FimE. CsrD serves as a control, which balances the expression of the two adhesins, according to environmental cues. Additional known feedback loops of the Csr system are illustrated in the model and also serve to stabilise the system.

6.8 Figures

Figure 1

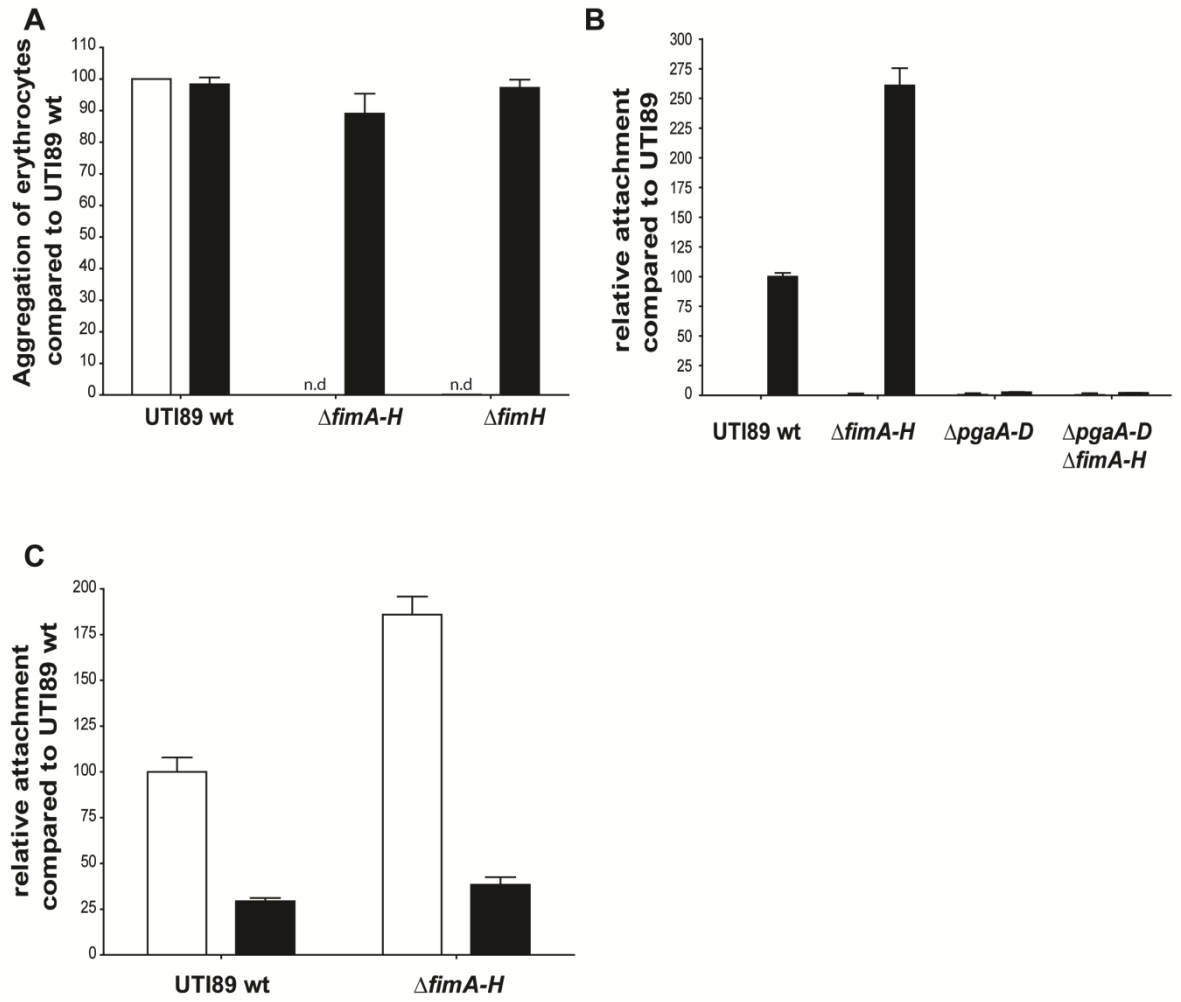


Figure 2

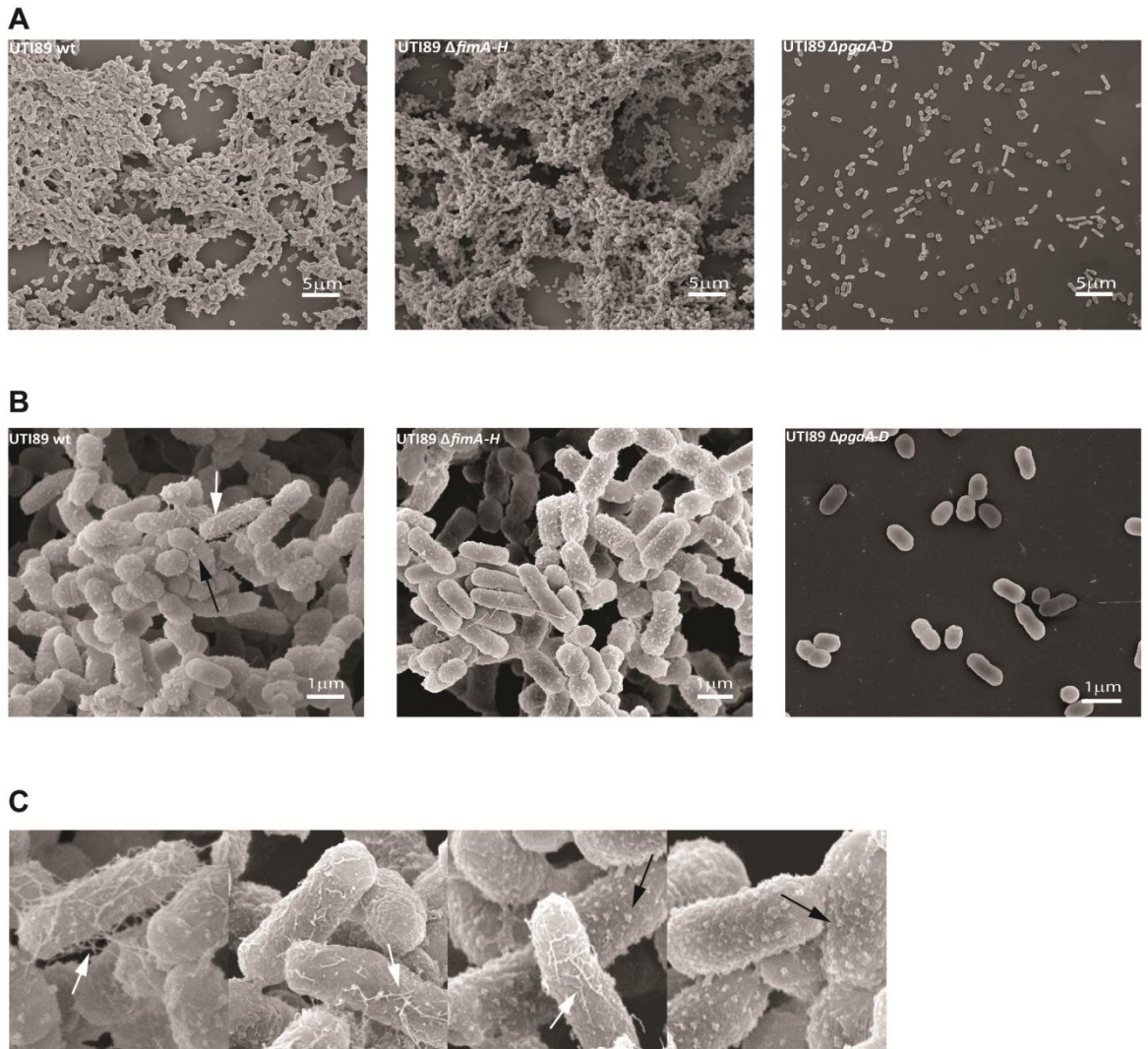


Figure 3

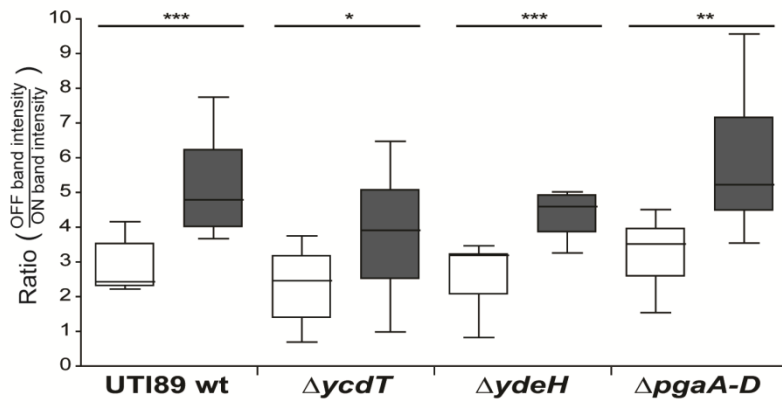
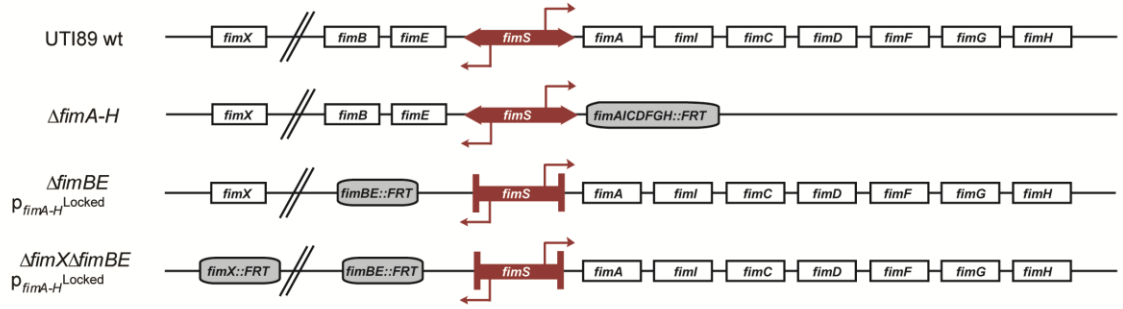
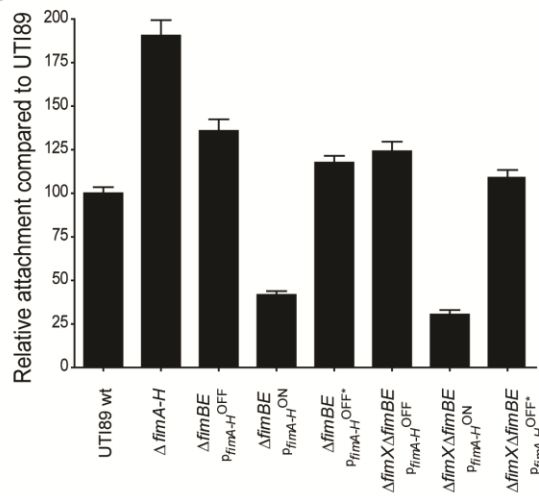


Figure 4

A



B



C

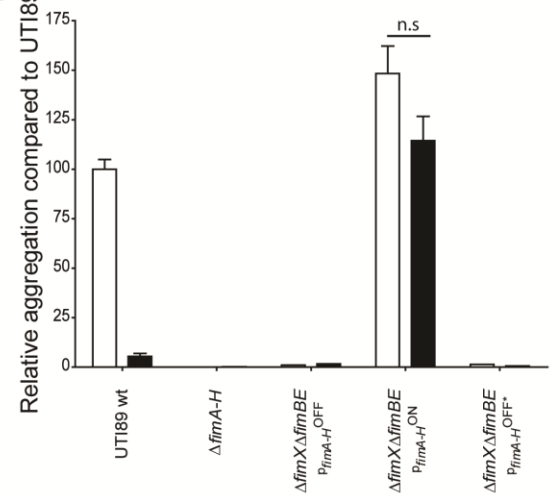
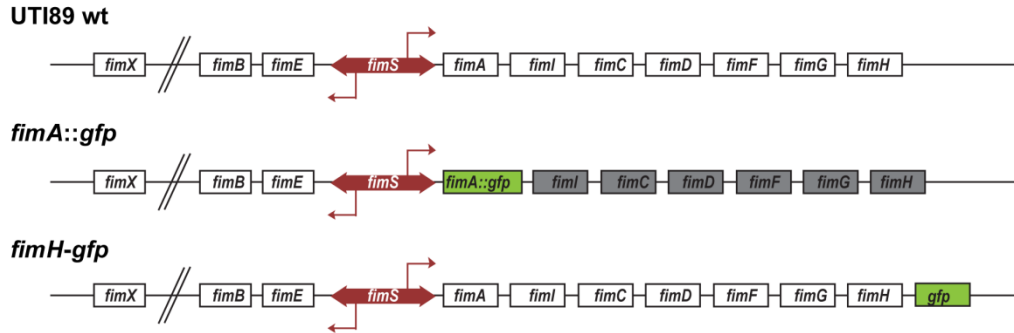


Figure 5

A



B

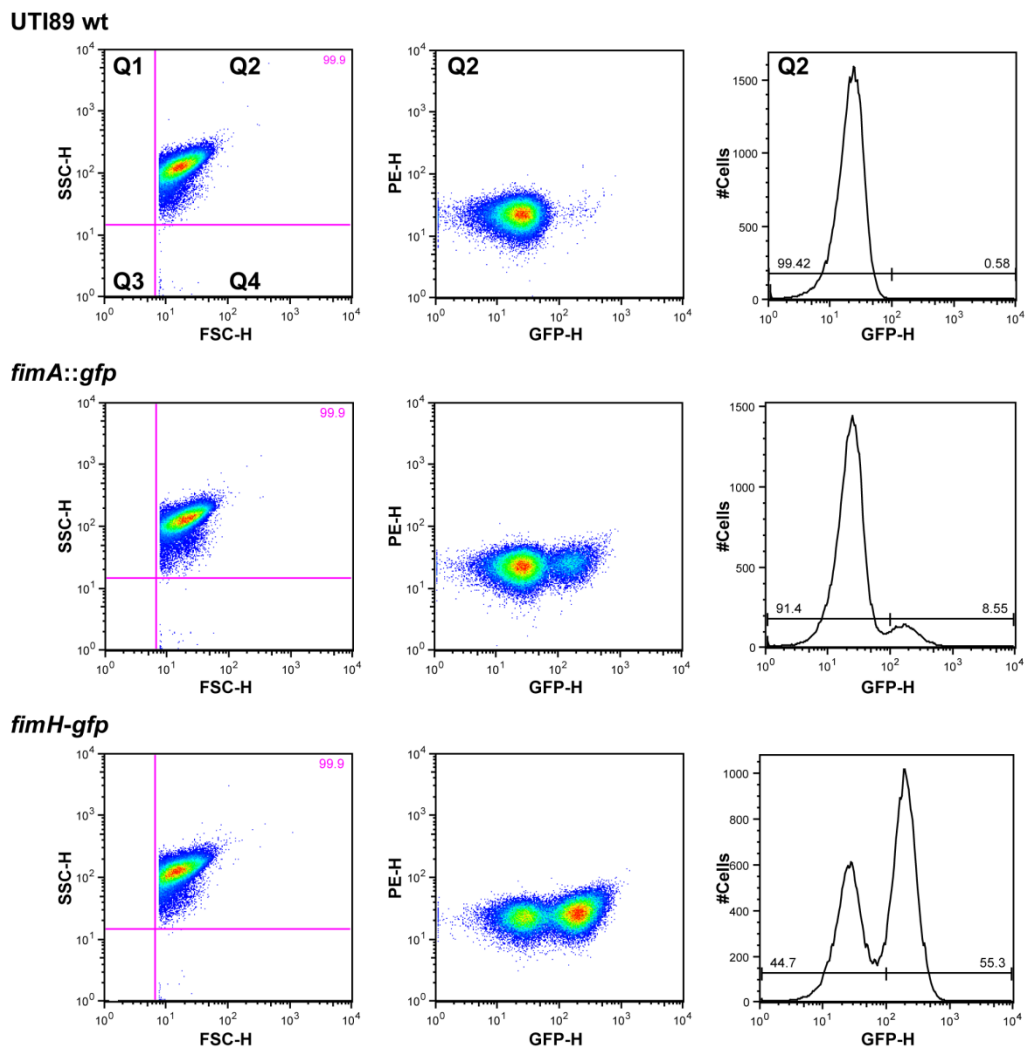


Figure 6

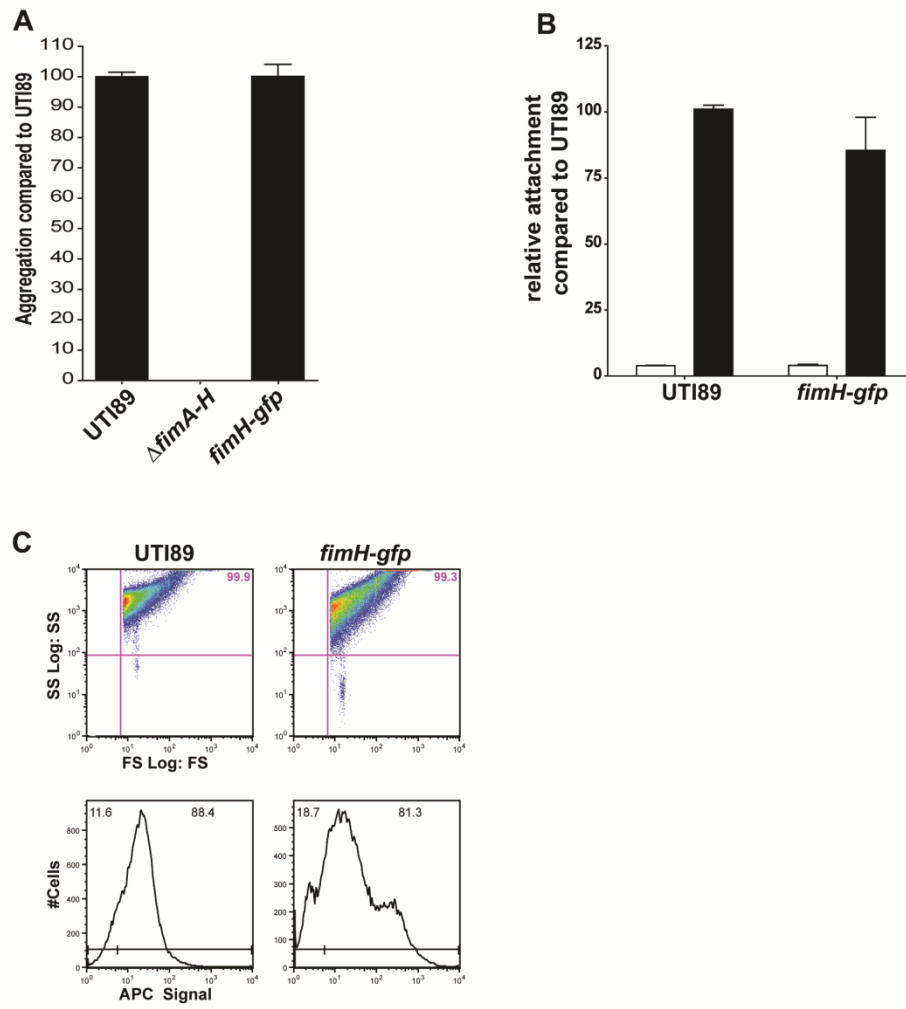
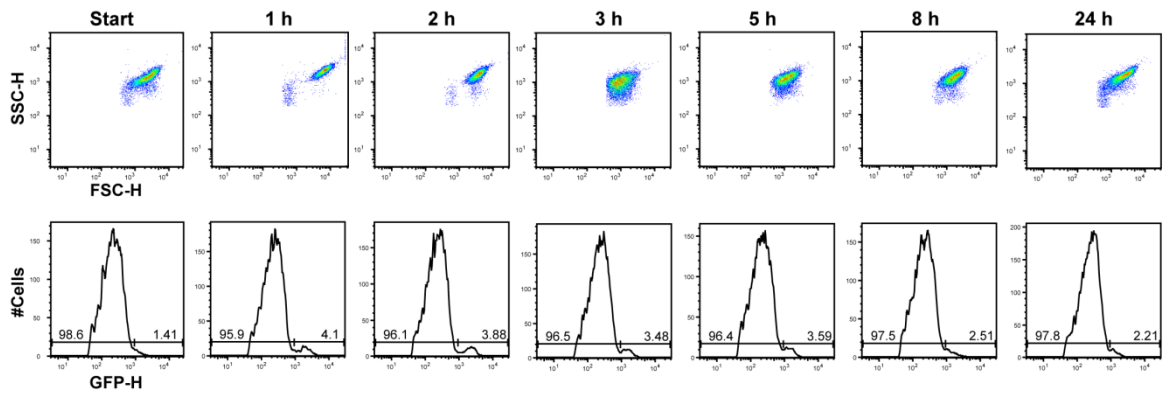


Figure 7

A

fimA::gfp (rotated)



B

fimA::gfp (static)

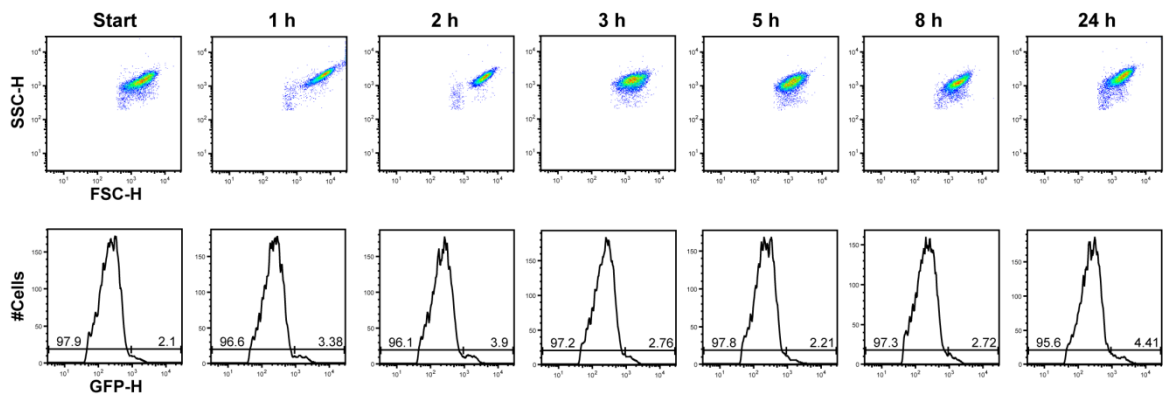
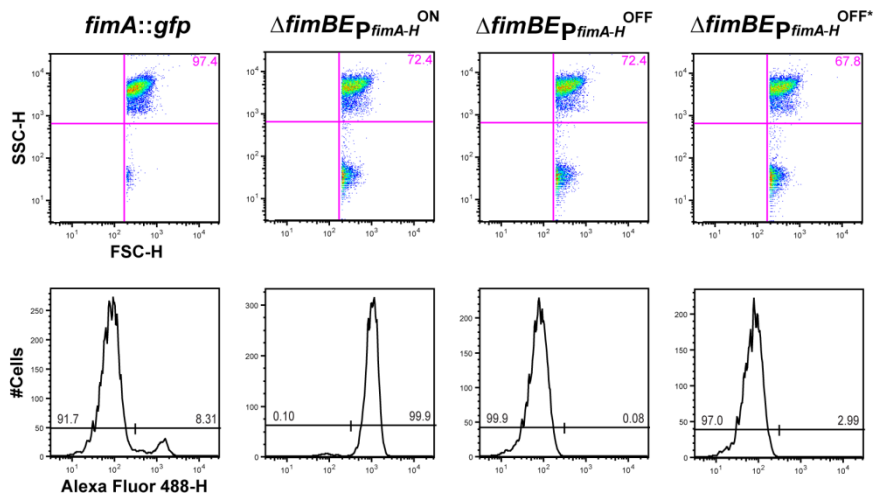


Figure 8

A



B

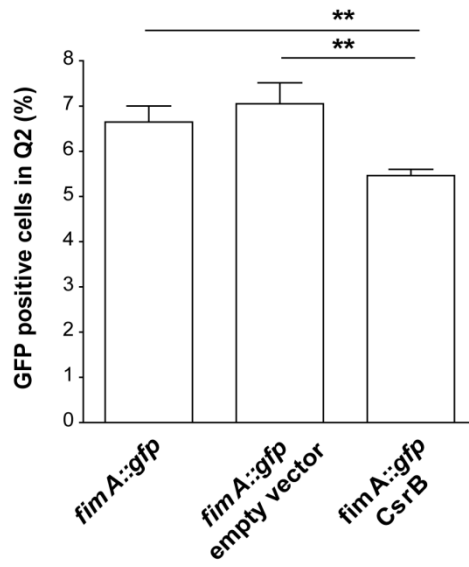
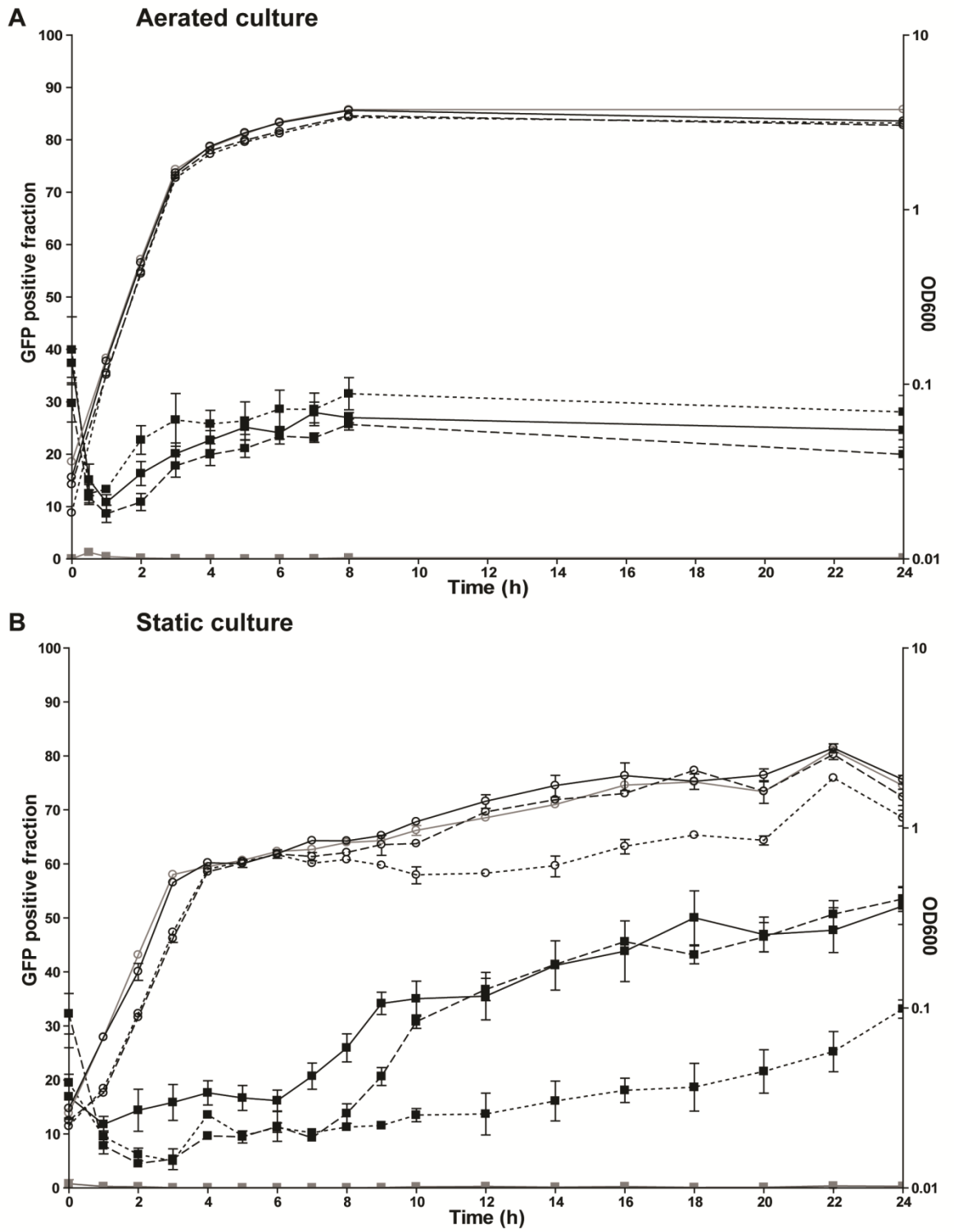
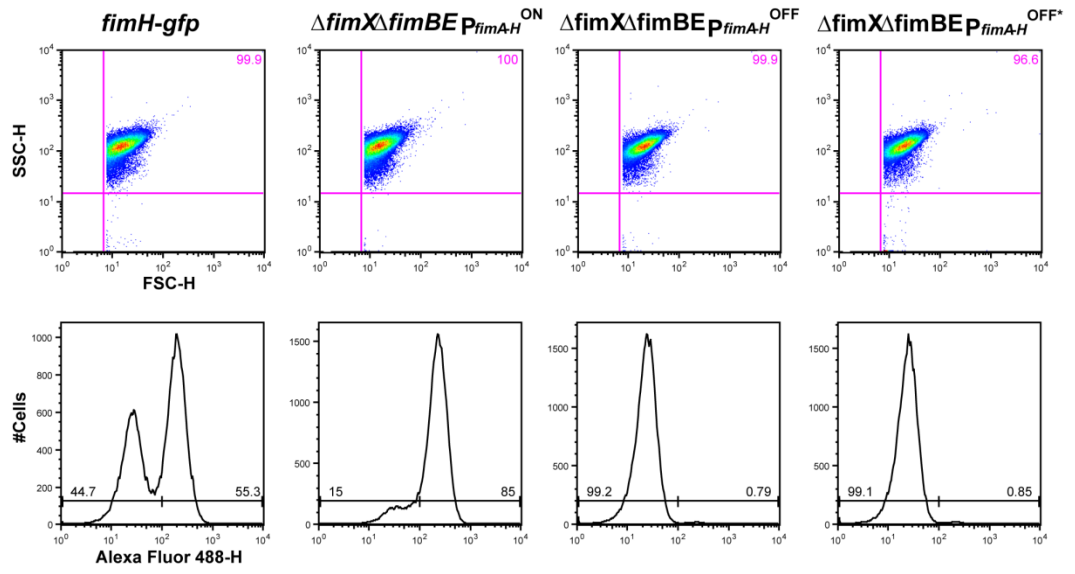


Figure 9



Figures

Figure 10



Figures

Figure 11

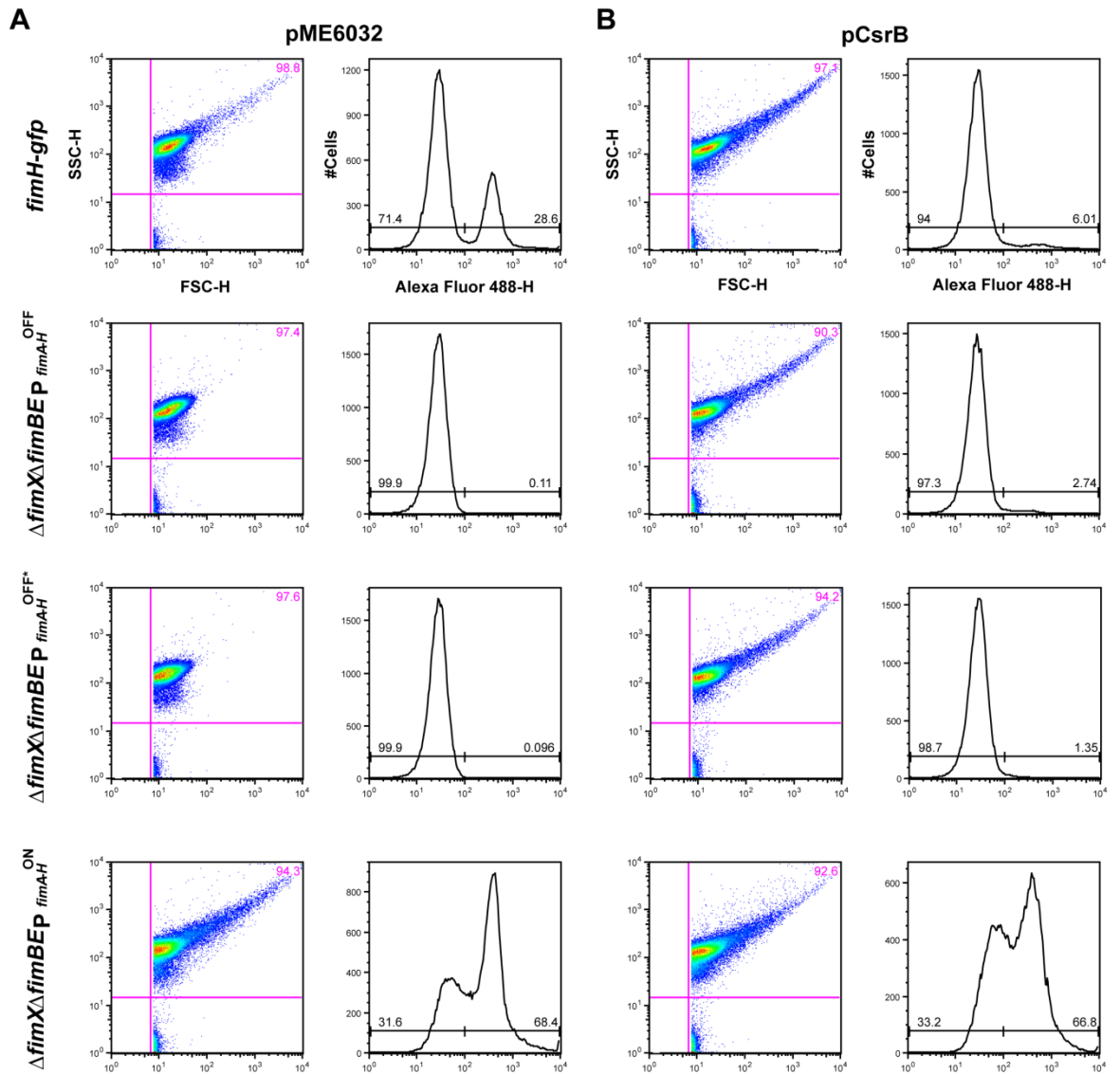


Figure 12

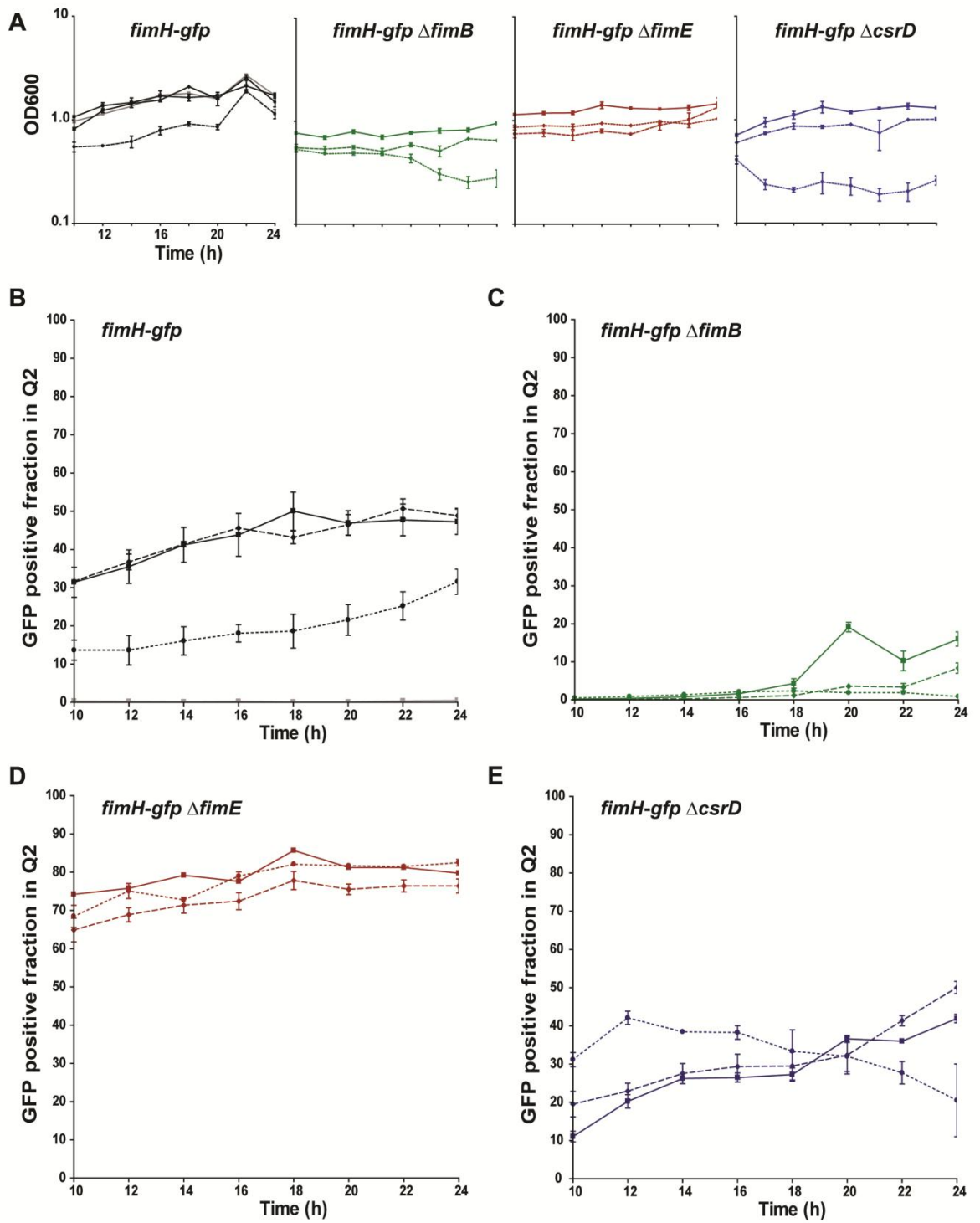


Figure 13

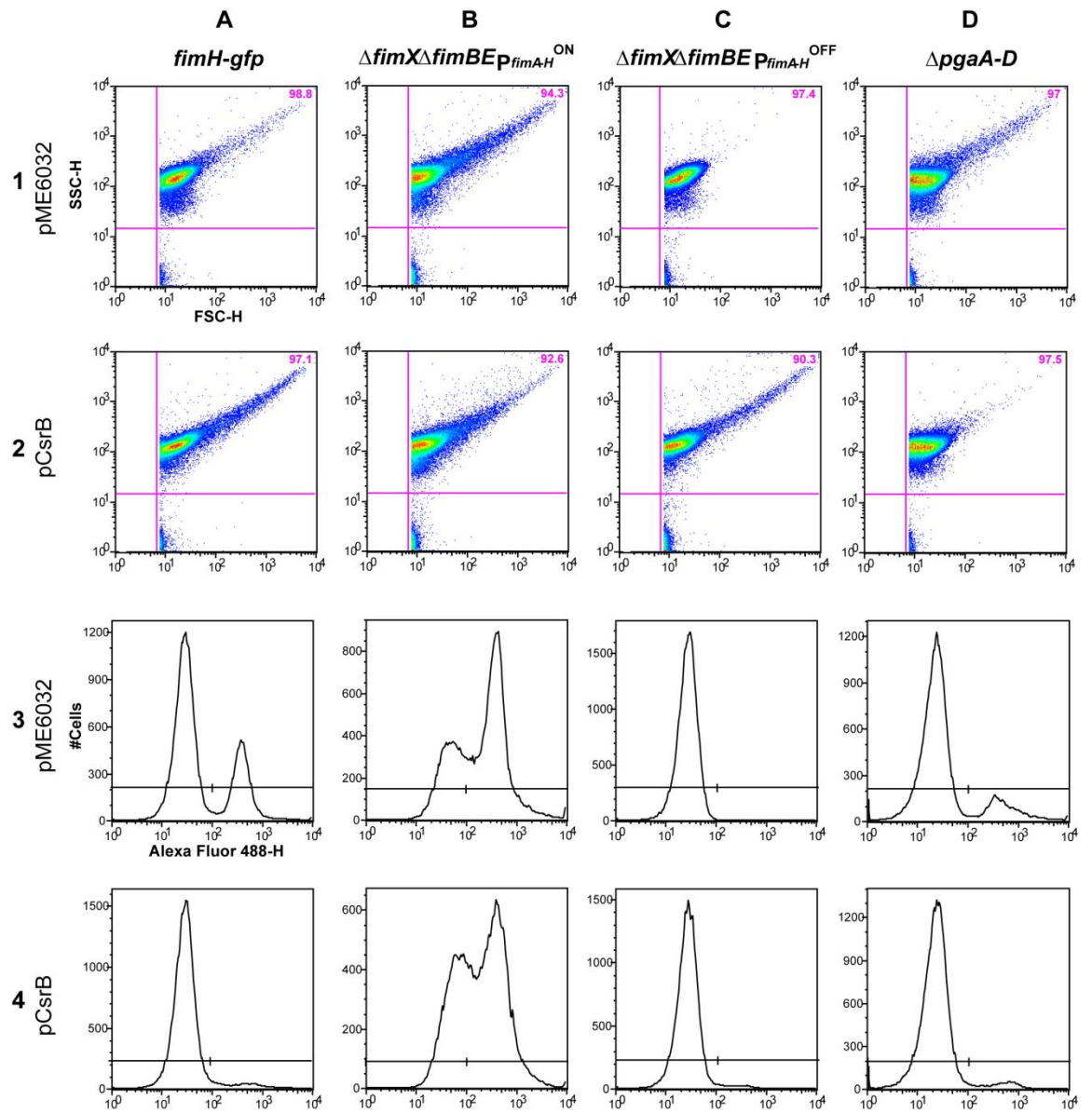
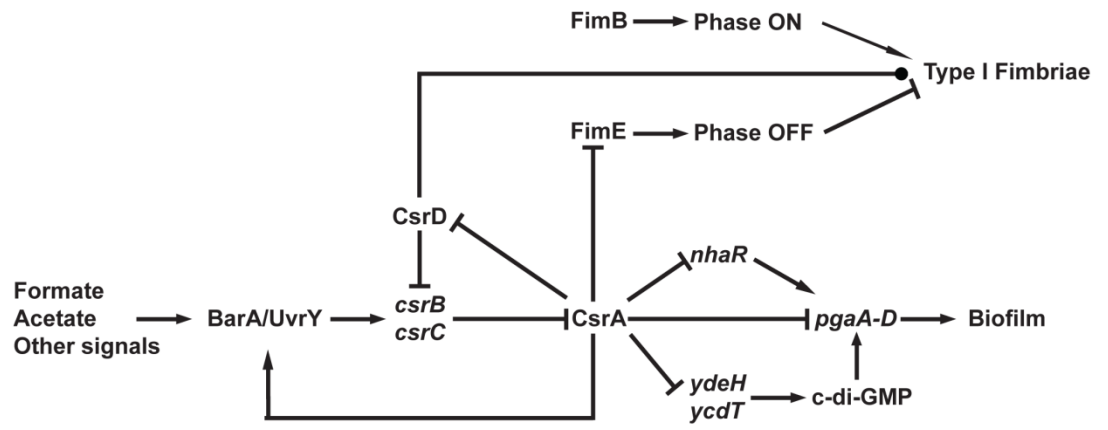


Figure 14



6.9 Tables

Table 1: Strain used in this study

Strain Ref.	Strain Name	Strain Characterisation	Reference
UTI89	UTI89 wild type	Wild type strain and parent of all mutants	(7, 77).
LH022	$\Delta ycdT$	clean deletion of <i>ycdT</i>	Hosch <i>et al.</i> , unpublished
LH023	$\Delta ydeH$	clean deletion of <i>ydeH</i>	Hosch <i>et al.</i> , unpublished
LH024	$\Delta pgaA-D$	clean deletion of <i>pgaA-D</i>	Hosch <i>et al.</i> , unpublished
LH026	$\Delta fimA-H$	clean deletion of <i>fimAICDFGH</i>	(78), this study
LH055	$\Delta fimA::gfp$	fimbrial reporter strain where <i>gfp</i> replaces the ORF of <i>fimA</i>	this study
LH064	$\Delta fimBE$ p_{fimA-H}^{OFF}	clean deletion of <i>fimBE</i> and a fixed orientation of <i>fimS</i> in the OFF orientation	this study
LH065	$\Delta fimBE$ p_{fimA-H}^{ON}	clean deletion of <i>fimBE</i> and a fixed orientation of <i>fimS</i> in the ON orientation	this study
LH066	$\Delta fimBE$ p_{fimA-H}^{OFF*}	clean deletion of <i>fimBE</i> and a fixed orientation of <i>fimS</i> in the OFF orientation with an additional point mutation (TTGGGGCCAA in wild type vs. TTAGGGCCAA in $\Delta fimBE$ p_{fimA-H}^{OFF*}) in one of the two inverted repeats of <i>fimS</i>	this study
LH109	$\Delta fimBEX$	clean deletion of <i>fimBE</i> and <i>fimX</i>	this study
LH116	$\Delta fimBE$ $\Delta fimA::gfp$ p_{fimA-H}^{OFF}	Insertion of the <i>fimA::gfp</i> reporter construct into the clean deletion of <i>fimBE</i> and a fixed orientation of <i>fimS</i> in the OFF orientation	this study
LH117	$\Delta fimBE$ $\Delta fimA::gfp$ p_{fimA-H}^{ON}	Insertion of the <i>fimA::gfp</i> reporter construct into the clean deletion of <i>fimBE</i> and a fixed orientation of <i>fimS</i> in the ON orientation	this study
LH118	$\Delta fimBE$ $\Delta fimA::gfp$ p_{fimA-H}^{OFF*}	Insertion of the <i>fimA::gfp</i> reporter construct into the clean deletion of <i>fimBE</i> and a fixed orientation of <i>fimS</i> in the OFF orientation with an additional point mutation (TTGGGGCCAA in wild type vs. TTAGGGCCAA in $\Delta fimBE$ p_{fimA-H}^{OFF*}) in one of the two inverted repeats of <i>fimS</i>	this study
LH149	$\Delta fimX\Delta fimBE$ $\Delta fimA::gfp$ p_{fimA-H}^{OFF}	Insertion of the <i>fimA::gfp</i> reporter construct into the clean deletion of <i>fimBE</i> and <i>fimX</i> and a fixed orientation of <i>fimS</i> in the OFF orientation	this study
LH150	$\Delta fimX\Delta fimBE$ $\Delta fimA::gfp$ p_{fimA-H}^{ON}	Insertion of the <i>fimA::gfp</i> reporter construct into the clean deletion of <i>fimBE</i> and <i>fimX</i> and a fixed orientation of <i>fimS</i> in the ON orientation	this study
LH151	$\Delta fimX\Delta fimBE$ $\Delta fimA::gfp$ p_{fimA-H}^{OFF*}	Insertion of the <i>fimA::gfp</i> reporter construct into the clean deletion of <i>fimBE</i> and <i>fimX</i> and a fixed orientation of <i>fimS</i> in the OFF orientation with an additional point mutation (TTGGGGCCAA in wild type vs. TTAGGGCCAA in $\Delta fimBE$ p_{fimA-H}^{OFF*}) in one of the two inverted repeats of <i>fimS</i>	this study
LH155	$\Delta fimX\Delta fimBE$ p_{fimA-H}^{OFF}	clean deletion of <i>fimBE</i> and <i>fimX</i> and a fixed orientation of <i>fimS</i> in the OFF orientation	this study
LH156	$\Delta fimX\Delta fimBE$ p_{fimA-H}^{ON}	clean deletion of <i>fimBE</i> and <i>fimX</i> and a fixed orientation of <i>fimS</i> in the ON orientation	this study
LH157	$\Delta fimX\Delta fimBE$ p_{fimA-H}^{OFF*}	clean deletion of <i>fimBE</i> and <i>fimX</i> and a fixed orientation of <i>fimS</i> in the OFF orientation with an additional point mutation in one of the two inverted repeats of <i>fimS</i>	this study
LH196	<i>fimH-gfp</i>	fimbrial reporter strain where GFP is inserted downstream of <i>fimH</i>	this study
LH218	<i>fimH-gfp</i> $\Delta relA\Delta spoT$	Insertion of <i>fimH-gfp</i> into $\Delta relA\Delta spoT$ (Strain still is kan ^R)	this study
LH227	<i>fimH-gfp</i> $\Delta csrB$	Insertion of $\Delta csrB$ into <i>fimH-gfp</i>	this study
LH228	<i>fimH-gfp</i> $\Delta csrC$	Insertion of $\Delta csrC$ into <i>fimH-gfp</i>	this study
LH229	<i>fimH-gfp</i> $\Delta csrD$	Insertion of $\Delta csrD$ into <i>fimH-gfp</i>	this study
LH230	<i>fimH-gfp</i> $\Delta ycdT$	Insertion of $\Delta ycdT$ into <i>fimH-gfp</i>	this study
LH231	<i>fimH-gfp</i> $\Delta c1116$	Insertion of $\Delta c1116$ into <i>fimH-gfp</i>	this study
LH232	<i>fimH-gfp</i> $\Delta c1117$	Insertion of $\Delta c1117$ into <i>fimH-gfp</i>	this study

Tables

LH233	<i>fimH-gfp ΔfimB</i>	Insertion of <i>ΔfimB</i> into <i>fimH-gfp</i>	this study
LH234_2	<i>fimH-gfp ΔfimE</i>	Insertion of <i>ΔfimE</i> into <i>fimH-gfp</i>	this study
LH235	<i>fimH-gfp ΔfimBE</i>	Insertion of <i>ΔfimBE</i> into <i>fimH-gfp</i>	this study
LH236	<i>fimH-gfp ΔfimX</i>	Insertion of <i>ΔfimX</i> into <i>fimH-gfp</i>	this study
LH237	<i>fimH-gfp ΔycgR</i>	Insertion of <i>ΔycgR</i> into <i>fimH-gfp</i>	this study
LH238	<i>fimH-gfp ΔcsgD</i>	Insertion of <i>ΔcsgD</i> into <i>fimH-gfp</i>	this study
LH239	<i>fimH-gfp ΔyhjH</i>	Insertion of <i>ΔyhjH</i> into <i>fimH-gfp</i>	this study
LH240	<i>fimH-gfp ΔbcsA</i>	Insertion of <i>ΔbcsA</i> into <i>fimH-gfp</i>	this study
LH242	<i>fimH-gfp ΔydeH</i>	Insertion of <i>ΔydeH</i> into <i>fimH-gfp</i>	this study
LH243	<i>fimH-gfp ΔpgaA-D</i>	Insertion of <i>ΔpgaA-D</i> into <i>fimH-gfp</i>	this study
LH244	<i>ΔfimXΔfimBE p_{fimA-H}^{OFF} fimH-gfp</i>	Insertion of the <i>fimH-gfp</i> reporter construct into the clean deletion of <i>fimBE</i> and <i>fimX</i> and a fixed orientation of <i>fimS</i> in the OFF orientation	this study
LH245	<i>ΔfimXΔfimBE p_{fimA-H}^{ON} fimH-gfp</i>	Insertion of the <i>fimH-gfp</i> reporter construct into the clean deletion of <i>fimBE</i> and <i>fimX</i> and a fixed orientation of <i>fimS</i> in the ON orientation	this study
LH246	<i>ΔfimXΔfimBE p_{fimA-H}^{OFF*} fimH-gfp</i>	Insertion of the <i>fimH-gfp</i> reporter construct into the clean deletion of <i>fimBE</i> and <i>fimX</i> and a fixed orientation of <i>fimS</i> in the OFF orientation with an additional point mutation (TTGGGGCCAA in wild type vs. TTAGGGCCAA in <i>ΔfimBE p_{fimA-H}^{OFF*}</i>) in one of the two inverted repeats of <i>fimS</i>	this study

Table 2: Plasmids used in this study

Plasmid name	Relevant genotype	Comments	Reference
pcj30	<i>lacI^P bla⁺ (amp^R)</i>	IPTG inducible expression vector	Bibikov <i>et al.</i> , 1997; (139)
pcj30 <i>csrB</i>	pcj30:: <i>csrB</i> (<i>amp^R</i>)	IPTG inducible expression vector	this study; Hosch <i>et al.</i> , unpublished manuscript
pME6032	pVS1 derived shuttle vector (<i>tet^R</i>)	IPTG inducible expression vector	Heeb <i>et al.</i> , 2000; (140)
pCsrB	pME6032:: <i>csrB</i> (<i>tet^R</i>)	IPTG inducible expression vector	this study; Hosch <i>et al.</i> , unpublished manuscript
pKM208	<i>lacI^P (amp^R)</i>	Temperature sensitive replication; λ RED-mediated recombinogenic plasmid; IPTG inducible	Murphy <i>et al.</i> , 2003; (79)
pCP20	<i>flp⁺ (amp^R) (CM^R)</i>	temperature-sensitive replication and induction of FLP (recombinase)	Cherepanov <i>et al.</i> , 1995; (141)
pPKL4	pBR322 derivatate (<i>amp^R</i>)	contains the entire <i>fim</i> gene cluster from <i>E. coli</i> K-12	Krogfelt <i>et al.</i> , 1988; (92)

Table 3: Primers used in this study

Primer name	Primer Sequene
1545-ycdP_KO_P2	GTGCAGAGCCCGGGCGAACCGGGCTTTGTTTTGGGTGTTTATGCCCGTCACATATGAATATCCTCCTTAG
1546-ycdS-KO-P1	TAATTAGATACAGAGAGAGATTTTGGCAATACATGGAGTAATACAGGTGTGTAGGCTGGAGCTGC TTC
2145-fimA_KO_P1	GCCCATGTGCGATTTAGAAATAGTTTTTTGAAAGGAAAGCAGCATGAAAATTGTAGGCTGGAGCTGC TTCG
2146-fimH_KO_P2	GTAATATTGCGTACCAGCATTAGCAATGTCTGTGATTTCTTTATTGATACATATGAATATCCTCCT TAG
2295_fimE	GCAGGCGGTTTGTACGGGG
2296_fimA	GATGCGGTACGAACCTGTCC
2297_inv	GAGGTGATGTGAAATTAATTTAC
2400-ydeH_KO_P1	TAGAATAGCGCGCACAAAGGAAGTGTAAAAAGGAGTGGCAATGATCAAGTGTAGGCTGGAGCTG CTTCCG
2401-ydeH_KO_P2	CACAGTAGCATCAGTTTTCTCAATGAATGTTAAACGGAGCTTAAACTCGCATATGAATATCCTCCTT AG
2402_ycdT_seq_fwd1	TCATCATCGGTATTGTTTGTGGGCGG
2762_ycdT_KO_P2	CCGGGGGGATGAGAAGCCCCAGGCGGAGGTGACAACTAGCGACAGACTGCCGCTTTATGGTG ACTCAC
3156_fimH_KO_P1	CACCTATACCTACAGCTGAACCCAAAGAGATGATTGTAATGAAACGAGTTTGTAGGCTGGAGCTG CTTCCG
3182_FimB_KO_P1	GCACAGCTAGTGCGCGTCTGTAATTATAAGGGAAAACGATGAAGAATAAGTGTGTAGGCTGGAGC TGCTTCG
3183_FimB_KO_P2	GTAGTTTTTAACACCATCCCTGGTATCTCAACTATCTCTATAAAAACAGCCATATGAATATCCTCCTT AG
3184_FimE_KO_P1	GTATTCATTCAAATATATCTCAGTCAGGAGTACTACTATTGTGAGTAAACGTTGTGTAGGCTGGAG CTGCTTCG
3185_FimE_KO_P2	GTATTTATTTGTTTTTTAACTTTATTATCAATTAGTTAAATCAAGCTTCTCCATATGAATATCCTCCT TAG
3187_FimA_GFP_repl_P1	CGACTGCCCATGTGCGATTTAGAAATAGTTTTTTAAAGGAAAGCAGCATGAGTAAAGGAGAAGAAC TTTTCA
3188_FimA_GFP_repl_P2	CGCACAAAGGGTGGGCATCCCTGCCCGTAATGACGTCCCTGAACCTGGGTAGGGTGTAGGCTGGA GCTGCTTC
3509_fimS_ON_fwd	GTTAAAAAACAAATAAATACAAGACAATTGGGGCCAAACTGTCTATATC
3510_fimS_ON_rev	CAACTGTCACAGTTTTCCCCAAAAGATGAAACATTTGGGGCCATTTGACTCATAGAGGAAAGC ATCGC
3511_fimS_OFF_fwd	GTTAAAAAACAAATAAATACAAGACAATTGGGGCCATTTGACTCATAG
3512_fimS_OFF_rev	CCAACACTGCACAGTTTTCCCCAAAAGATGAAACATTTGGGGCCAAACTGTCTATATCATAAATA AGTTACG
3513_FimBE_KO_P1	CCAGCACAGCTAGTGCGCGTCTGTAATTATAAGGGAAAACGATGAAGTGTGTAGGCTGGAGCTGC TTCG
3514_FimBE_KO_P2	CTTGATTTTATTTGTTTTTAACCTTTATTATCAATTAGTTAAATCAAGCTTCATATGAATATCCTCCTT AG
3541_fimX_KO_P1	GATTACATCGATAACGTTCTGATTGCAGGCATACTTATCTGGGTGTGCTGTGTAGGCTGGAGCTG CTTCCG
3542_fimX_KO_P2	GGAAAACGTAGGAATCTGACATTTTGAATCAGAAGGACTGTTTTAACGAGGCATATGAATATCCT CCTTAG
3880_CsrD_KO_P1	GCTAGTATGCCCGCTTCCCTCACTATCGGAGTTAACACAAGGATGAGATGTGTAGGCTGGAGCTGC TTCG
3881_CsrD_KO_P2	GCAGCGCGGTTATTCTACGTGAAAACGGATTAACGGCAGGTTAAACCGACATATGAATATCCT CCTTAG
3916_3'fimH-reporter_rev	GCTTCAGGTAATATTGCGTACCTGCATTAGCAATGCCCTGTGATTTCTGTGTAGGCTGGAGCTGCT TCG
3917_3'fimH-GFP_fwd	GACTGCAGGGAATGTGCAATCGATTATTGGCGTGACTTTTGTTTATCAATAAAAGGAGATATACAT ATGAGTAAAGGAGAAGAAC
3927_relA_test_rev	CAATAATTAATTTGCCATCC
3928_relA_test_fwd	ATAAAACTGGAACCTATTCG
1143_csrB_KO_P1	CTTGTAAGACTTCGCGAAAAAGACGATTCTATCTTCGTCGACAGGTGTGTAGGCTGGAGCTGCTT CG
1144_csrB_KO_P2	CATAAAGCAACCTCAATAAGAAAACTGCCGCGAAGGATAGCAGGCATATGAATATCCTCCTTAG
1145_csrC_KO_P1	TGGCGGTTGATTGTTTGTAAAGCAAAGGCGTAAAGTAGCACCTGTGTAGGCTGGAGCTGCTT CG

Tables

1146_csrC_KO_P2	GCCGTTTTATTTCAGTATAGATTTGCGGCGGAATCTAACAGAAAGCCATATGAATATCCTCCTTAG
2878_c1116_KO_P1	CTTCTGGTCGGGAGGGGCTCATATTTCCGGAGGAGTAATGTCAGGGGCATGTGTAGGCTGGAGC TGCTTCG
2879_c1116_KO_P2	GAACATAAATGCTGGCTGCTGACAAGTCTGTGAAAAAGGATTATCCATGCAGCATATGAATATCCT CCTTAG
3547_c1117_KO_P1	GGAATAAATTGTAGTGGAAGTCAAGTTTACCGGATGACTGATGCGCTGTGTAGGCTGGAGCTG CTTCG
3548_c1117_KO_P2	GTCTTTCTGCAACACTACTGCTTTCAACAAGTCAGGCATTTACACTTTATGACATATGAATATCCT CCTTAG
3541_fimX_KO_P1	GATTACATCGATAACGTTCTGATTGCAGGCATACTTATCTGGGTGTGCTGTGTAGGCTGGAGCTG CTTCG
3542_fimX_KO_P2	GGAAAACGTAGGAATCTGACATTTTGAATCAGAAGGACTGTTTTAACGAGGCATATGAATATCCT CCTTAG
1456-ycgR_KO_P1	AGACAGTTTGTGAGTCAGGAGTTTTTCCGCGTGAGTCATTGTGTAGGCTGGAGCTGCTTC
1457-ycgR_KO_P2	AAACTTGAGCAGGCACTGGACGCGATGTAAATCAGTCGCGTCACATATGAATATCCTCCTTAG
1680-csgD_KO_P1	GCGATCAATAAAAAAGCGGGTTTCATCATGTTTAATTGTGTAGGCTGGAGCTGCTTCG
1681-csgD_KO_P2	CACAAATCCAGCGTAAATAACGTTTCATGGCTTTATCGCCTCATATGAATATCCTCCTTAG
1658_yhjH_test_fwd_new	TCATGCATTCGCCAATCACGGC
1659_yhjH_test_rev_new	CGCGTGGCAAATGCACCATCG
3560_BcsA_KO_P1	GTGCCTGTTAAACTATTCCGGGCTGAAAATGCCAGTCGGGAGTGCATCATGAGTATCTGTGTAGG CTGGAGCTGCTTCG
3561_BcsA_KO_P2	CCAGAGCCACTGCACAAATCCAGAATATTTTCTTTTCATCGCGTTATCATCATTGTTGCATATGAA TATCCTCCTTAG
3927_relA_test_rev	CAATAATTAATTTGCCATCC
3928_relA_test_fwd	ATAAACTGGAACCTATTCG
2125-spoT_KO_P1	TGCTGAAGGTCGTCGTTAATCACAAAGCGGGTCGCCCTTGATCTGTTTTGTAGGCTGGAGCTGC TTCG
2126-spoT_KO_P2	GTTGGGTTCATAAAACATTAATTTTCGGTTTCGGGTGACTTTAATCACATATGAATATCCTCCTTAG

6.10 Acknowledgements

We would like to thank Ulrich Dobrindt for providing us the pPKL4 plasmid and the group of Beat Ernst for letting us use the aggregometer, providing us with fresh guinea pig erythrocytes and the anti Fim antibody. Special thanks also go to Prof. Dirk Bumann with his FACS facility staff and the ZMB facility of the Biozentrum Basel for excellent service.

6.11 References

1. Goller CC & Seed PC (2010) Intracellular bacterial biofilm-like pods in urinary tract infections (vol 301, pg 105, 2003). *Virulence* 1(4):333-337.
2. Justice SS, *et al.* (2004) Differentiation and developmental pathways of uropathogenic *Escherichia coli* in urinary tract pathogenesis. *Proc Natl Acad Sci U S A* 101(5):1333-1338.
3. Anderson GG, Dodson KW, Hooton TM, & Hultgren SJ (2004) Intracellular bacterial communities of uropathogenic *Escherichia coli* in urinary tract pathogenesis. *Trends Microbiol* 12(9):424-430.
4. Hunstad DA & Justice SS (2010) Intracellular lifestyles and immune evasion strategies of uropathogenic *Escherichia coli*. *Annu Rev Microbiol* 64:203-221.
5. Mysorekar IU & Hultgren SJ (2006) Mechanisms of uropathogenic *Escherichia coli* persistence and eradication from the urinary tract. *Proc Natl Acad Sci U S A* 103(38):14170-14175.
6. Schilling JD, Lorenz RG, & Hultgren SJ (2002) Effect of trimethoprim-sulfamethoxazole on recurrent bacteriuria and bacterial persistence in mice infected with uropathogenic *Escherichia coli*. *Infect Immun* 70(12):7042-7049.
7. Mulvey MA, Schilling JD, & Hultgren SJ (2001) Establishment of a persistent *Escherichia coli* reservoir during the acute phase of a bladder infection. *Infect Immun* 69(7):4572-4579.
8. Mulvey MA, Schilling JD, Martinez JJ, & Hultgren SJ (2000) Bad bugs and beleaguered bladders: interplay between uropathogenic *Escherichia coli* and innate host defenses. *Proc Natl Acad Sci U S A* 97(16):8829-8835.
9. Geibel S & Waksman G (2011) Crystallography and electron microscopy of chaperone/usher pilus systems. *Adv Exp Med Biol* 715:159-174.
10. Axner O, *et al.* (2011) Assessing bacterial adhesion on an individual adhesin and single pili level using optical tweezers. *Adv Exp Med Biol* 715:301-313.
11. Mulvey MA (2002) Adhesion and entry of uropathogenic *Escherichia coli*. *Cell Microbiol* 4(5):257-271.
12. Jones CH, *et al.* (1995) FimH adhesin of type 1 pili is assembled into a fibrillar tip structure in the Enterobacteriaceae. *Proc Natl Acad Sci U S A* 92(6):2081-2085.
13. Eto DS, Jones TA, Sundsbak JL, & Mulvey MA (2007) Integrin-mediated host cell invasion by type 1-piliated uropathogenic *Escherichia coli*. *PLoS Pathog* 3(7):e100.
14. Zhou G, *et al.* (2001) Uroplakin Ia is the urothelial receptor for uropathogenic *Escherichia coli*: evidence from in vitro FimH binding. *J Cell Sci* 114(Pt 22):4095-4103.
15. Martinez JJ, Mulvey MA, Schilling JD, Pinkner JS, & Hultgren SJ (2000) Type 1 pilus-mediated bacterial invasion of bladder epithelial cells. *EMBO J* 19(12):2803-2812.
16. Holden N, *et al.* (2007) Comparative analysis of FimB and FimE recombinase activity. *Microbiology* 153(Pt 12):4138-4149.
17. Abraham JM, Freitag CS, Clements JR, & Eisenstein BI (1985) An invertible element of DNA controls phase variation of type 1 fimbriae of *Escherichia coli*. *Proc Natl Acad Sci U S A* 82(17):5724-5727.
18. Klemm P (1986) Two regulatory fim genes, fimB and fimE, control the phase variation of type 1 fimbriae in *Escherichia coli*. *EMBO J* 5(6):1389-1393.
19. Hannan TJ, *et al.* (2008) LeuX tRNA-dependent and -independent mechanisms of *Escherichia coli* pathogenesis in acute cystitis. *Mol Microbiol* 67(1):116-128.
20. Blakely G, *et al.* (1993) Two related recombinases are required for site-specific recombination at dif and cer in *E. coli* K12. *Cell* 75(2):351-361.
21. Blomfield IC, McClain MS, Princ JA, Calie PJ, & Eisenstein BI (1991) Type 1 fimbriation and fimE mutants of *Escherichia coli* K-12. *J Bacteriol* 173(17):5298-5307.
22. Gally DL, Leathart J, & Blomfield IC (1996) Interaction of FimB and FimE with the fim switch that controls the phase variation of type 1 fimbriae in *Escherichia coli* K-12. *Mol Microbiol* 21(4):725-738.
23. McClain MS, Blomfield IC, & Eisenstein BI (1991) Roles of fimB and fimE in site-specific DNA inversion associated with phase variation of type 1 fimbriae in *Escherichia coli*. *J Bacteriol* 173(17):5308-5314.
24. Leathart JB & Gally DL (1998) Regulation of type 1 fimbrial expression in uropathogenic *Escherichia coli*: heterogeneity of expression through sequence changes in the fim switch region. *Mol Microbiol* 28(2):371-381.

References

25. Gally DL, Bogan JA, Eisenstein BI, & Blomfield IC (1993) Environmental regulation of the fim switch controlling type 1 fimbrial phase variation in *Escherichia coli* K-12: effects of temperature and media. *J Bacteriol* 175(19):6186-6193.
26. Corcoran CP & Dorman CJ (2009) DNA relaxation-dependent phase biasing of the fim genetic switch in *Escherichia coli* depends on the interplay of H-NS, IHF and LRP. *Mol Microbiol* 74(5):1071-1082.
27. Heitz-Mayfield LJ & Lang NP (2010) Comparative biology of chronic and aggressive periodontitis vs. peri-implantitis. *Periodontol 2000* 53:167-181.
28. Hall-Stoodley L, Costerton JW, & Stoodley P (2004) Bacterial biofilms: from the natural environment to infectious diseases. *Nat Rev Microbiol* 2(2):95-108.
29. Lewis K (2007) Persister cells, dormancy and infectious disease. *Nat Rev Microbiol* 5(1):48-56.
30. Häussler S (2010) Multicellular signalling and growth of *Pseudomonas aeruginosa*. *Int J Med Microbiol* 300(8):544-548.
31. Wright KJ, Seed PC, & Hultgren SJ (2007) Development of intracellular bacterial communities of uropathogenic *Escherichia coli* depends on type 1 pili. *Cell Microbiol* 9(9):2230-2241.
32. Pratt LA & Kolter R (1998) Genetic analysis of *Escherichia coli* biofilm formation: roles of flagella, motility, chemotaxis and type I pili. *Mol Microbiol* 30(2):285-293.
33. Van Houdt R & Michiels CW (2005) Role of bacterial cell surface structures in *Escherichia coli* biofilm formation. *Res Microbiol* 156(5-6):626-633.
34. Beloin C, Roux A, & Ghigo JM (2008) *Escherichia coli* biofilms. *Curr Top Microbiol Immunol* 322:249-289.
35. Mack D, *et al.* (1996) The intercellular adhesin involved in biofilm accumulation of *Staphylococcus epidermidis* is a linear beta-1,6-linked glucosaminoglycan: purification and structural analysis. *J Bacteriol* 178(1):175-183.
36. Rupp ME, Fey PD, Heilmann C, & Götz F (2001) Characterization of the importance of *Staphylococcus epidermidis* autolysin and polysaccharide intercellular adhesin in the pathogenesis of intravascular catheter-associated infection in a rat model. *J Infect Dis* 183(7):1038-1042.
37. Götz F (2002) *Staphylococcus* and biofilms. *Mol Microbiol* 43(6):1367-1378.
38. Maira-Litrán T, *et al.* (2002) Immunochemical properties of the staphylococcal poly-N-acetylglucosamine surface polysaccharide. *Infect Immun* 70(8):4433-4440.
39. Kaplan JB, *et al.* (2004) Genes involved in the synthesis and degradation of matrix polysaccharide in *Actinobacillus actinomycetemcomitans* and *Actinobacillus pleuropneumoniae* biofilms. *J Bacteriol* 186(24):8213-8220.
40. Wang X, Preston JF, & Romeo T (2004) The pgaABCD locus of *Escherichia coli* promotes the synthesis of a polysaccharide adhesin required for biofilm formation. *J Bacteriol* 186(9):2724-2734.
41. Agladze K, Wang X, & Romeo T (2005) Spatial periodicity of *Escherichia coli* K-12 biofilm microstructure initiates during a reversible, polar attachment phase of development and requires the polysaccharide adhesin PGA. *J Bacteriol* 187(24):8237-8246.
42. Itoh Y, *et al.* (2008) Roles of pgaABCD genes in synthesis, modification, and export of the *Escherichia coli* biofilm adhesin poly-beta-1,6-N-acetyl-D-glucosamine. *J Bacteriol* 190(10):3670-3680.
43. Daley DO, *et al.* (2005) Global topology analysis of the *Escherichia coli* inner membrane proteome. *Science* 308(5726):1321-1323.
44. Edwards AN, *et al.* (2011) Circuitry linking the Csr and stringent response global regulatory systems. *Mol Microbiol* 80(6):1561-1580.
45. Jonas K, *et al.* (2008) The RNA binding protein CsrA controls cyclic di-GMP metabolism by directly regulating the expression of GGDEF proteins. *Mol Microbiol* 70(1):236-257.
46. Romeo T, Gong M, Liu M, & Brun-Zinkernagel A (1993) Identification and molecular characterization of *csrA*, a pleiotropic gene from *Escherichia coli* that affects glycogen biosynthesis, gluconeogenesis, cell size, and surface properties. *J Bacteriol* 175(15):4744-4755.
47. Pannuri A, *et al.* (2012) Translational Repression of NhaR, a Novel Pathway for Multi-Tier Regulation of Biofilm Circuitry by CsrA. *J Bacteriol* 194(1):79-89.
48. Romeo T (1998) Global regulation by the small RNA-binding protein CsrA and the non-coding RNA molecule CsrB. *Mol Microbiol* 29(6):1321-1330.
49. Lucchetti-Miganeh C, Burrowes E, Baysse C, & Ermel G (2008) The post-transcriptional regulator CsrA plays a central role in the adaptation of bacterial pathogens to different stages of infection in animal hosts. *Microbiology* 154(Pt 1):16-29.

References

50. Chavez RG, Alvarez AF, Romeo T, & Georgellis D (2010) The physiological stimulus for the BarA sensor kinase. *J Bacteriol* 192(7):2009-2012.
51. Pernestig A, *et al.* (2003) The Escherichia coli BarA-UvrY two-component system is needed for efficient switching between glycolytic and gluconeogenic carbon sources. *J Bacteriol* 185(3):843-853.
52. Suzuki K, *et al.* (2002) Regulatory circuitry of the CsrA/CsrB and BarA/UvrY systems of Escherichia coli. *J Bacteriol* 184(18):5130-5140.
53. Suzuki K, Babitzke P, Kushner SR, & Romeo T (2006) Identification of a novel regulatory protein (CsrD) that targets the global regulatory RNAs CsrB and CsrC for degradation by RNase E. *Genes Dev* 20(18):2605-2617.
54. Suzuki K, Babitzke P, Kushner SR, & Romeo T (2006) Identification of a novel regulatory protein (CsrD) that targets the global regulatory RNAs CsrB and CsrC for degradation by RNase E. *Genes Dev* 20(18):2605-2617.
55. Jenal U & Malone J (2006) Mechanisms of cyclic-di-GMP signaling in bacteria. *Annu Rev Genet* 40:385-407.
56. Ausmees N, *et al.* (2001) Genetic data indicate that proteins containing the GGDEF domain possess diguanylate cyclase activity. *FEMS Microbiol Lett* 204(1):163-167.
57. Christen M, Christen B, Folcher M, Schauerte A, & Jenal U (2005) Identification and characterization of a cyclic di-GMP-specific phosphodiesterase and its allosteric control by GTP. *J Biol Chem* 280(35):30829-30837.
58. Paul R, *et al.* (2004) Cell cycle-dependent dynamic localization of a bacterial response regulator with a novel di-guanylate cyclase output domain. *Genes Dev* 18(6):715-727.
59. Bobrov AG, Kirillina O, & Perry RD (2005) The phosphodiesterase activity of the HmsP EAL domain is required for negative regulation of biofilm formation in Yersinia pestis. *FEMS Microbiol Lett* 247(2):123-130.
60. Ryan RP, *et al.* (2006) Cell-cell signaling in Xanthomonas campestris involves an HD-GYP domain protein that functions in cyclic di-GMP turnover. *Proc Natl Acad Sci U S A* 103(17):6712-6717.
61. Tamayo R, Tischler AD, & Camilli A (2005) The EAL domain protein VieA is a cyclic diguanylate phosphodiesterase. *J Biol Chem* 280(39):33324-33330.
62. Schmidt AJ, Ryjenkov DA, & Gomelsky M (2005) The ubiquitous protein domain EAL is a cyclic diguanylate-specific phosphodiesterase: enzymatically active and inactive EAL domains. *J Bacteriol* 187(14):4774-4781.
63. Galperin MY (2006) Structural classification of bacterial response regulators: diversity of output domains and domain combinations. *J Bacteriol* 188(12):4169-4182.
64. Boehm A, *et al.* (2010) Second messenger-mediated adjustment of bacterial swimming velocity. *Cell* 141(1):107-116.
65. Boehm A, *et al.* (2009) Second messenger signalling governs Escherichia coli biofilm induction upon ribosomal stress. *Mol Microbiol* 72(6):1500-1516.
66. Hengge R (2009) Principles of c-di-GMP signalling in bacteria. *Nat Rev Microbiol* 7(4):263-273.
67. Abel S, *et al.* (2011) Regulatory cohesion of cell cycle and cell differentiation through interlinked phosphorylation and second messenger networks. *Mol Cell* 43(4):550-560.
68. Tischler AD & Camilli A (2005) Cyclic diguanylate regulates Vibrio cholerae virulence gene expression. *Infect Immun* 73(9):5873-5882.
69. Fazli M, *et al.* (2011) The CRP/FNR family protein Bcam1349 is a c-di-GMP effector that regulates biofilm formation in the respiratory pathogen Burkholderia cenocepacia. *Mol Microbiol* 82(2):327-341.
70. Malone JG, *et al.* (2010) YfiBNR mediates cyclic di-GMP dependent small colony variant formation and persistence in Pseudomonas aeruginosa. *PLoS Pathog* 6(3):e1000804.
71. Kozlova EV, Khajanchi BK, Sha J, & Chopra AK (2011) Quorum sensing and c-di-GMP-dependent alterations in gene transcripts and virulence-associated phenotypes in a clinical isolate of Aeromonas hydrophila. *Microb Pathog* 50(5):213-223.
72. Bobrov AG, *et al.* (2011) Systematic analysis of cyclic di-GMP signalling enzymes and their role in biofilm formation and virulence in Yersinia pestis. *Mol Microbiol* 79(2):533-551.
73. Lee HS, Gu F, Ching SM, Lam Y, & Chua KL (2010) CdpA is a Burkholderia pseudomallei cyclic di-GMP phosphodiesterase involved in autoaggregation, flagellum synthesis, motility, biofilm formation, cell invasion, and cytotoxicity. *Infect Immun* 78(5):1832-1840.

References

74. Lory S, Merighi M, & Hyodo M (2009) Multiple activities of c-di-GMP in *Pseudomonas aeruginosa*. *Nucleic Acids Symp Ser (Oxf)* (53):51-52.
75. Lim B, Beyhan S, & Yildiz FH (2007) Regulation of *Vibrio* polysaccharide synthesis and virulence factor production by CdgC, a GGDEF-EAL domain protein, in *Vibrio cholerae*. *J Bacteriol* 189(3):717-729.
76. Kulasakara H, *et al.* (2006) Analysis of *Pseudomonas aeruginosa* diguanylate cyclases and phosphodiesterases reveals a role for bis-(3'-5')-cyclic-GMP in virulence. *Proc Natl Acad Sci U S A* 103(8):2839-2844.
77. Chen S, *et al.* (2006) Identification of genes subject to positive selection in uropathogenic strains of *Escherichia coli*: a comparative genomics approach. *Proc Natl Acad Sci U S A* 103(15):5977-5982.
78. Abgottspon D, *et al.* (2010) Development of an aggregation assay to screen FimH antagonists. *J Microbiol Methods* 82(3):249-255.
79. Murphy KC & Campellone KG (2003) Lambda Red-mediated recombinogenic engineering of enterohemorrhagic and enteropathogenic *E. coli*. *BMC Mol Biol* 4:11.
80. Datsenko KA & Wanner BL (2000) One-step inactivation of chromosomal genes in *Escherichia coli* K-12 using PCR products. *Proc Natl Acad Sci U S A* 97(12):6640-6645.
81. Baba T, *et al.* (2006) Construction of *Escherichia coli* K-12 in-frame, single-gene knockout mutants: the Keio collection. *Mol Syst Biol* 2:2006.0008.
82. Higuchi R, Krummel B, & Saiki RK (1988) A general method of in vitro preparation and specific mutagenesis of DNA fragments: study of protein and DNA interactions. *Nucleic Acids Res* 16(15):7351-7367.
83. O'Toole GA, *et al.* (1999) Genetic approaches to study of biofilms. *Methods Enzymol* 310:91-109.
84. Schwan WR, Seifert HS, & Duncan JL (1992) Growth conditions mediate differential transcription of fim genes involved in phase variation of type 1 pili. *J Bacteriol* 174(7):2367-2375.
85. Stahlhut SG, *et al.* (2009) Comparative structure-function analysis of mannose-specific FimH adhesins from *Klebsiella pneumoniae* and *Escherichia coli*. *J Bacteriol* 191(21):6592-6601.
86. Anderson G, *et al.* (2003) Intracellular bacterial biofilm-like pods in urinary tract infections. *Science* 301(5629):105-107.
87. Snyder JA, Lloyd AL, Lockett CV, Johnson DE, & Mobley HL (2006) Role of phase variation of type 1 fimbriae in a uropathogenic *Escherichia coli* cystitis isolate during urinary tract infection. *Infect Immun* 74(2):1387-1393.
88. Song J, *et al.* (2009) TLR4-mediated expulsion of bacteria from infected bladder epithelial cells. *Proc Natl Acad Sci U S A* 106(35):14966-14971.
89. Hultgren SJ, Porter TN, Schaeffer AJ, & Duncan JL (1985) Role of type 1 pili and effects of phase variation on lower urinary tract infections produced by *Escherichia coli*. *Infect Immun* 50(2):370-377.
90. Langermann S, *et al.* (1997) Prevention of mucosal *Escherichia coli* infection by FimH-adhesin-based systemic vaccination. *Science* 276(5312):607-611.
91. Bahrani-Mougeot FK, *et al.* (2002) Type 1 fimbriae and extracellular polysaccharides are preeminent uropathogenic *Escherichia coli* virulence determinants in the murine urinary tract. *Mol Microbiol* 45(4):1079-1093.
92. Krogfelt KA & Klemm P (1988) Investigation of minor components of *Escherichia coli* type 1 fimbriae: protein chemical and immunological aspects. *Microb Pathog* 4(3):231-238.
93. Burns LS, Smith SG, & Dorman CJ (2000) Interaction of the FimB integrase with the fimS invertible DNA element in *Escherichia coli* in vivo and in vitro. *J Bacteriol* 182(10):2953-2959.
94. Adiciptaningrum AM, Blomfield IC, & Tans SJ (2009) Direct observation of type 1 fimbrial switching. *EMBO Rep* 10(5):527-532.
95. Sjöström AE, *et al.* (2009) Analysis of the *sfaX(II)* locus in the *Escherichia coli* meningitis isolate IHE3034 reveals two novel regulatory genes within the promoter-distal region of the main S fimbrial operon. *Microb Pathog* 46(3):150-158.
96. Sjöström AE, *et al.* (2009) The SfaXII protein from newborn meningitis *E. coli* is involved in regulation of motility and type 1 fimbriae expression. *Microb Pathog* 46(5):243-252.
97. Römling U (2005) Characterization of the *rdar* morphotype, a multicellular behaviour in Enterobacteriaceae. *Cell Mol Life Sci* 62(11):1234-1246.
98. Xia Y, Gally D, Forsman-Semb K, & Uhlin BE (2000) Regulatory cross-talk between adhesin operons in *Escherichia coli*: inhibition of type 1 fimbriae expression by the PapB protein. *EMBO J* 19(7):1450-1457.

References

99. Lane MC & Mobley HL (2007) Role of P-fimbrial-mediated adherence in pyelonephritis and persistence of uropathogenic *Escherichia coli* (UPEC) in the mammalian kidney. *Kidney Int* 72(1):19-25.
100. Holden NJ, *et al.* (2006) Demonstration of regulatory cross-talk between P fimbriae and type 1 fimbriae in uropathogenic *Escherichia coli*. *Microbiology* 152(Pt 4):1143-1153.
101. Hanna A, Berg M, Stout V, & Razatos A (2003) Role of capsular colanic acid in adhesion of uropathogenic *Escherichia coli*. *Appl Environ Microbiol* 69(8):4474-4481.
102. Schembri MA & Klemm P (2001) Coordinate gene regulation by fimbriae-induced signal transduction. *EMBO J* 20(12):3074-3081.
103. Schembri MA, Ussery DW, Workman C, Hasman H, & Klemm P (2002) DNA microarray analysis of fim mutations in *Escherichia coli*. *Mol Genet Genomics* 267(6):721-729.
104. Schembri MA, Dalsgaard D, & Klemm P (2004) Capsule shields the function of short bacterial adhesins. *J Bacteriol* 186(5):1249-1257.
105. Reisner A, Haagensen JA, Schembri MA, Zechner EL, & Molin S (2003) Development and maturation of *Escherichia coli* K-12 biofilms. *Mol Microbiol* 48(4):933-946.
106. Holden NJ & Gally DL (2004) Switches, cross-talk and memory in *Escherichia coli* adherence. *J Med Microbiol* 53(Pt 7):585-593.
107. Beloin C, *et al.* (2006) The transcriptional antiterminator RfaH represses biofilm formation in *Escherichia coli*. *J Bacteriol* 188(4):1316-1331.
108. Landini P & Zehnder AJ (2002) The global regulatory hns gene negatively affects adhesion to solid surfaces by anaerobically grown *Escherichia coli* by modulating expression of flagellar genes and lipopolysaccharide production. *J Bacteriol* 184(6):1522-1529.
109. Ulett GC, Webb RI, & Schembri MA (2006) Antigen-43-mediated autoaggregation impairs motility in *Escherichia coli*. *Microbiology* 152(Pt 7):2101-2110.
110. Melican K, *et al.* (2011) Uropathogenic *Escherichia coli* P and Type 1 fimbriae act in synergy in a living host to facilitate renal colonization leading to nephron obstruction. *PLoS Pathog* 7(2):e1001298.
111. Pesavento C, *et al.* (2008) Inverse regulatory coordination of motility and curli-mediated adhesion in *Escherichia coli*. *Genes Dev* 22(17):2434-2446.
112. Mulvey MA, *et al.* (1998) Induction and evasion of host defenses by type 1-piliated uropathogenic *Escherichia coli*. *Science* 282(5393):1494-1497.
113. Wang X, *et al.* (2005) CsrA post-transcriptionally represses pgaABCD, responsible for synthesis of a biofilm polysaccharide adhesin of *Escherichia coli*. *Mol Microbiol* 56(6):1648-1663.
114. Klemm P, Roos V, Ulett GC, Svanborg C, & Schembri MA (2006) Molecular characterization of the *Escherichia coli* asymptomatic bacteriuria strain 83972: the taming of a pathogen. *Infect Immun* 74(1):781-785.
115. Zdziarski J, Svanborg C, Wullt B, Hacker J, & Dobrindt U (2008) Molecular basis of commensalism in the urinary tract: low virulence or virulence attenuation? *Infect Immun* 76(2):695-703.
116. Andersson P, *et al.* (1991) Persistence of *Escherichia coli* bacteriuria is not determined by bacterial adherence. *Infect Immun* 59(9):2915-2921.
117. Hull R, *et al.* (2000) Urinary tract infection prophylaxis using *Escherichia coli* 83972 in spinal cord injured patients. *J Urol* 163(3):872-877.
118. Hancock V & Klemm P (2007) Global gene expression profiling of asymptomatic bacteriuria *Escherichia coli* during biofilm growth in human urine. *Infect Immun* 75(2):966-976.
119. Roos V & Klemm P (2006) Global gene expression profiling of the asymptomatic bacteriuria *Escherichia coli* strain 83972 in the human urinary tract. *Infect Immun* 74(6):3565-3575.
120. Duncan MJ, *et al.* (2005) The distinct binding specificities exhibited by enterobacterial type 1 fimbriae are determined by their fimbrial shafts. *J Biol Chem* 280(45):37707-37716.
121. Rodrigues DF & Elimelech M (2009) Role of type 1 fimbriae and mannose in the development of *Escherichia coli* K12 biofilm: from initial cell adhesion to biofilm formation. *Biofouling* 25(5):401-411.
122. Chao Y & Zhang T (2011) Probing Roles of Lipopolysaccharide, Type 1 Fimbria, and Colanic Acid in the Attachment of *Escherichia coli* Strains on Inert Surfaces. *Langmuir* 27(18):11545-11553.
123. Cerca N & Jefferson KK (2008) Effect of growth conditions on poly-N-acetylglucosamine expression and biofilm formation in *Escherichia coli*. *FEMS Microbiol Lett* 283(1):36-41.
124. Monds RD & O'Toole GA (2009) The developmental model of microbial biofilms: ten years of a paradigm up for review. *Trends Microbiol* 17(2):73-87.

References

125. Cerca N, *et al.* (2007) Protection against *Escherichia coli* infection by antibody to the *Staphylococcus aureus* poly-N-acetylglucosamine surface polysaccharide. *Proc Natl Acad Sci U S A* 104(18):7528-7533.
126. Timmermans J & Van Melderen L (2010) Post-transcriptional global regulation by CsrA in bacteria. *Cell Mol Life Sci* 67(17):2897-2908.
127. Lane MC, Li X, Pearson MM, Simms AN, & Mobley HL (2009) Oxygen-limiting conditions enrich for fimbriate cells of uropathogenic *Proteus mirabilis* and *Escherichia coli*. *J Bacteriol* 191(5):1382-1392.
128. Hayes ET, *et al.* (2006) Oxygen limitation modulates pH regulation of catabolism and hydrogenases, multidrug transporters, and envelope composition in *Escherichia coli* K-12. *BMC Microbiol* 6:89.
129. Baker CS, Morozov I, Suzuki K, Romeo T, & Babitzke P (2002) CsrA regulates glycogen biosynthesis by preventing translation of glgC in *Escherichia coli*. *Mol Microbiol* 44(6):1599-1610.
130. Liu MY, Yang H, & Romeo T (1995) The product of the pleiotropic *Escherichia coli* gene *csrA* modulates glycogen biosynthesis via effects on mRNA stability. *J Bacteriol* 177(10):2663-2672.
131. Sabnis NA, Yang H, & Romeo T (1995) Pleiotropic regulation of central carbohydrate metabolism in *Escherichia coli* via the gene *csrA*. *J Biol Chem* 270(49):29096-29104.
132. Timmermans J & Van Melderen L (2009) Conditional essentiality of the *csrA* gene in *Escherichia coli*. *J Bacteriol* 191(5):1722-1724.
133. Yang H, Liu MY, & Romeo T (1996) Coordinate genetic regulation of glycogen catabolism and biosynthesis in *Escherichia coli* via the CsrA gene product. *J Bacteriol* 178(4):1012-1017.
134. Orndorff PE, *et al.* (2004) Immunoglobulin-mediated agglutination of and biofilm formation by *Escherichia coli* K-12 require the type 1 pilus fiber. *Infect Immun* 72(4):1929-1938.
135. Otto K, Norbeck J, Larsson T, Karlsson KA, & Hermansson M (2001) Adhesion of type 1-fimbriated *Escherichia coli* to abiotic surfaces leads to altered composition of outer membrane proteins. *J Bacteriol* 183(8):2445-2453.
136. Otto K & Hermansson M (2004) Inactivation of *ompX* causes increased interactions of type 1 fimbriated *Escherichia coli* with abiotic surfaces. *J Bacteriol* 186(1):226-234.
137. Valenski ML, Harris SL, Spears PA, Horton JR, & Orndorff PE (2003) The Product of the *fimI* gene is necessary for *Escherichia coli* type 1 pilus biosynthesis. *J Bacteriol* 185(16):5007-5011.
138. Rossolini GM, Muscas P, Chiesurin A, & Satta G (1993) Analysis of the *Salmonella* *fim* gene cluster: identification of a new gene (*fimI*) encoding a fimbrin-like protein and located downstream from the *fimA* gene. *FEMS Microbiol Lett* 114(3):259-265.
139. Bibikov SI, Biran R, Rudd KE, & Parkinson JS (1997) A signal transducer for aerotaxis in *Escherichia coli*. *J Bacteriol* 179(12):4075-4079.
140. Heeb S, *et al.* (2000) Small, stable shuttle vectors based on the minimal pVS1 replicon for use in gram-negative, plant-associated bacteria. *Mol Plant Microbe Interact* 13(2):232-237.
141. Cherepanov PP & Wackernagel W (1995) Gene disruption in *Escherichia coli*: TcR and KmR cassettes with the option of Flp-catalyzed excision of the antibiotic-resistance determinant. *Gene* 158(1):9-14.

7 Development of an aggregation assay to screen FimH antagonists

7.1 Statement of work

This work was mainly performed by the groups of Beat Ernst from the Institute of Molecular Pharmacy from the University of Basel, Switzerland and Andrey Trampuz from the Infectious Diseases Service of the University Hospital Basel and later the University of Lausanne, Switzerland. My contribution was the construction of UT189 $\Delta fimA-H$, which was used throughout this publication as negative control for the mannose-specific binding of *E. coli* to yeast cells and erythrocytes.



Development of an aggregation assay to screen FimH antagonists

Daniela Abgottspon^{a,b}, Gina Rölli^{a,b}, Lucie Hosch^c, Andrea Steinhuber^a, Xiaohua Jiang^a, Oliver Schwardt^a, Brian Cutting^a, Martin Smiesko^a, Urs Jenal^c, Beat Ernst^{a,*}, Andrej Trampuz^{b,d,*}

^a Institute of Molecular Pharmacy, Pharmacenter, University of Basel, Switzerland

^b Infectious Diseases Research Laboratory, Department of Biomedicine, University Hospital, Basel, Switzerland

^c Molecular Microbiology, Biozentrum, University of Basel, Switzerland

^d Infectious Diseases Service, Department of Internal Medicine, University Hospital and University of Lausanne, Switzerland

ARTICLE INFO

Article history:

Received 13 April 2010

Received in revised form 19 June 2010

Accepted 29 June 2010

Available online 8 July 2010

Keywords:

Aggregation

E. coli

FimH antagonist

Type 1 pili

Urinary tract infection (UTI)

ABSTRACT

α -D-Mannopyranosides are potent FimH antagonists, which inhibit the adhesion of *Escherichia coli* to highly mannosylated uroplakin Ia on the urothelium and therefore offer an efficient therapeutic opportunity for the treatment and prevention of urinary tract infection. For the evaluation of the therapeutic potential of FimH antagonists, their effect on the disaggregation of *E. coli* from *Candida albicans* and guinea pig erythrocytes (GPE) was studied.

The mannose-specific binding of *E. coli* to yeast cells and erythrocytes is mediated by type 1 pili and can be monitored by aggregometry. Maximal aggregation of *C. albicans* or GPE to *E. coli* is reached after 600 s. Then the FimH antagonist was added and disaggregation determined by light transmission over a period of 1400 s. A FimH-deleted mutant of *E. coli*, which does not induce any aggregation, was used in a control experiment. The activities of FimH antagonists are expressed as IC₅₀s, the half maximal inhibitory concentration of the disaggregation potential. *n*-Heptyl α -D-mannopyranoside (**1**) was used as a reference compound and exhibits an IC₅₀ of 77.14 μ M, whereas methyl α -D-mannopyranoside (**2**) does not lead to any disaggregation at concentrations up to 800 μ M. *o*-Chloro-*p*-[*N*-(2-ethoxy-3,4-dioxocyclobut-1-enyl)amino]phenyl α -D-mannopyranoside (**3**) shows a 90-fold and 2-chloro-4-nitrophenyl α -D-mannopyranoside (**4**) a 6-fold increased affinity compared to **1**. Finally, 4-nitrophenyl α -D-mannopyranoside (**5**) exhibits an activity similar to **1**. As negative control, D-galactose (**6**) was used.

The standardized aggregation assay generates concentration-dependent, reproducible data allowing the evaluation of FimH antagonists according to their potency to inhibit *E. coli* adherence and can therefore be employed to select candidates for experimental and clinical studies for treatment and prevention of urinary tract infections.

© 2010 Elsevier B.V. All rights reserved.

1. Introduction

Urinary tract infection (UTI) is one of the most common infections, affecting millions of people each year. Particularly affected are women, who have a 40–50% risk to experience at least one symptomatic UTI episode at some time during their life. Furthermore, more than half of them experience a relapse of the infection within 6 months (Fihn, 2003; Hooton, 2001).

Although UTI rarely cause severe disease such as pyelonephritis or urosepsis, it is associated with high morbidity and consumes

considerable healthcare resources (Wiles et al., 2008). Uropathogenic *Escherichia coli* (UPEC) is the primary cause of UTIs accounting for 70–95% of the reported cases. Symptomatic UTIs require antimicrobial treatment, often resulting in the emergence of resistant microbial flora. As a consequence, treatment of consecutive infections becomes increasingly difficult, since the number of antibiotics is limited and the resistance in *E. coli* is increasing, especially in patients with diabetes, urinary tract anomaly, paraplegia and those with permanent urinary catheter. Therefore, a new approach for the prevention and treatment of UTI with inexpensive, orally applicable therapeutics with a low potential for resistance would have a great impact on patient care, public healthcare and medical expenses.

UPEC strains express a number of well-studied virulence factors used for a successful colonization of their host (Gouin et al., 2009; Rosen et al., 2008; Wiles et al., 2008). One important virulence factor is located on type 1 pili, allowing UPEC to adhere and invade host cells within the urinary tract. It enables UPEC to attach to oligomannosides, which are part of the glycoprotein uroplakin Ia on the urinary bladder

* Corresponding authors. B. Ernst is to be contacted at Institute of Molecular Pharmacy, Pharmacenter, University of Basel, Klingelbergstrasse 50, CH-4056 Basel, Switzerland. Tel.: +41 61 267 1551; fax: +41 61 267 1552. Trampuz, Infectious Diseases Service, Department of Internal Medicine, University Hospital and University of Lausanne, Rue du Bugnon 46, CH-1011 Lausanne, Switzerland. Tel.: +41 21 314 3992; fax: +41 21 314 2876.

E-mail addresses: beat.ernst@unibas.ch (B. Ernst), andrej.trampuz@chuv.ch (A. Trampuz).

mucosa. This initial step prevents the rapid clearance of *E. coli* from the urinary tract by the bulk flow of urine and at the same time, enables the invasion of the host cells (Mulvey, 2002; Wiles et al., 2008).

Type 1 pili are the most prevalent fimbriae encoded by UPEC, consisting of the four subunits FimA, FimC, FimG and FimH, the latter located at the tip of the pili (Capitani et al., 2006). As a part of the FimH subunit, a carbohydrate-recognizing domain (CRD) is responsible for bacterial interactions with the host cells within the urinary tract (Mulvey, 2002). The crystal structure of the FimH-CRD was solved (Choudhury et al., 1999) and its complex with *n*-butyl α -D-mannopyranoside (Bouckaert et al., 2005) and Man α (1-3)[Man α (1-6)]Man (Wellens et al., 2008) recently became available.

Previous studies showed that vaccination with FimH adhesin inhibits colonization and subsequent *E. coli* infection of the urothelium in humans (Langermann et al., 1997; Langermann et al., 2000). In addition, adherence and invasion of host cells by *E. coli* can also be prevented by α -D-mannopyranosides, which are potent antagonists of type 1 pili interactions (Bouckaert et al., 2006). Whereas α -D-mannopyranosides efficiently prevent adhesion of *E. coli* to human urothelium, they are not exhibiting a selection pressure to provoke antimicrobial resistance. Furthermore, environmental contamination is less problematic compared to antibiotics (Sharon, 2006).

For the evaluation of the inhibitory potential of FimH antagonists various target-based (Bouckaert et al., 2005; Sperling et al., 2006) and function-based assays (Ofek and Beachey, 1978; Firon et al., 1987) were previously described. In this contribution, we present an advanced and validated approach to evaluate the antagonistic potential of α -mannopyranosides by a function-based aggregation assay. The FimH-dependent adhesion of *E. coli* to the urothelium can be mimicked by the interaction with mannan-presenting yeast cells (e.g. *Candida albicans*) or with the glycocalyx of guinea pig erythrocytes (GPE), respectively. Both interactions can be specifically inhibited with α -mannopyranosides (e.g. Giampapa et al., 1988; Gouin et al., 2009).

Originally, Ofek and Beachey, 1978 and Firon et al., 1982, monitored the aggregation of mannan-containing yeast cells and various strains of *E. coli* by aggregometry, i.e. as a function of the reduced turbidity caused by the aggregation event. They quantified the rate of aggregation by the steepest slope in the curve produced by increasing light transmission (Baumgartner and Born, 1968). In this communication, various parameters of the aggregometry assay were optimized and the potential of FimH antagonists quantified by the AUC (area under the curve) of the disaggregation curves. As a result, the hitherto predominantly visual examination of the aggregation event can now be quantitatively detected and reported by IC₅₀-values. The assay is standardized and allows the accurate, rapid and reproducible high-throughput screening of compound libraries to

identify FimH antagonists qualified for an evaluation in a disease model (Hvidberg et al., 2000).

2. Materials and methods

2.1. Test and control microorganisms

The clinical *E. coli* isolate UTI89 (Mulvey et al., 2001) and the *C. albicans* strain ATCC 60193 were used. Microorganisms were stored at -70°C and before experiment incubated at 37°C in 10 ml medium using 50 ml tubes. Prior to each experiment, the microorganisms were washed twice and re-suspended in phosphate buffered saline (PBS) at pH 7.4 to reach the desired concentration. Bacterial and yeast concentrations were determined by plating serial 1:10 dilutions on blood agar, followed by colony counting on plates with 20–200 colonies after overnight incubation at 37°C .

As control, a *E. coli* UTI89 *fimA-H:kan* mutant strain, lacking FimH-specific aggregation, was constructed. For this purpose, the parent *E. coli* UTI89 strain was transformed with the temperature sensitive plasmid pKM208 (Addgene plasmid 13077) containing the *red* recombination genes (Murphy and Campellone, 2003). Transformants carrying pKM208 were grown in LB medium without NaCl, supplemented with ampicillin (100 $\mu\text{g}/\text{ml}$) at 30°C to late logarithmic phase. The *red* gene expression was induced for 30 min with 1 mM IPTG at 37°C . Bacteria were subjected to a 15 min heat shock at 42°C and rapidly cooled in an ice slurry before washing twice with PBS and concentrating 100-fold in 10% glycerol. A kanamycin resistance cassette was PCR amplified from pKD3 (Datsenko and Wanner, 2000) with primer 2145-*fimA_KO_P1* (gcc cat gtc gat tta gaa ata gtt ttt tga aag gaa agc agc ATG AAA ATt gta ggc tgg agc tgc ttc g) and primer 2146-*fimH_KO_P2* (gta ata ttg cgt acc agc att agc aat gtc ctg tga ttt ctT TAT TGA TAc ata tga ata tcc tcc tta g). PCR fragments were gel purified (MN Nucleospin Extract II, Machery Nagel, Oensingen, Switzerland) and 10–100 ng purified DNA was mixed with 65 μl recombination competent UTI89 cells followed by electroporation in 1 mm Gene Pulser Cuvettes using a Gene Pulser (BioRad, Reinach, Switzerland) set to 1.75 V, 25 μF and 400 Ω . Shocked cells were mixed with cold (4°C) salt optimized broth (2% (w/v) bacto trypton; 0.5% (w/v) yeast extract; 10 mM NaCl and 2.5 mM KCl), incubated for 1.5 h at 37°C and plated out on LB agar plates containing 20 $\mu\text{g}/\text{ml}$ kanamycin. Resistant clones were colony purified on LB medium containing kanamycin, tested by PCR and sequenced for correct insertion of the resistance cassette into the *fimA-H* locus.

2.2. Nutrients and solutions

The following media were used to investigate the optimal growth conditions for the microorganisms: Luria-Bertani broth (LB),

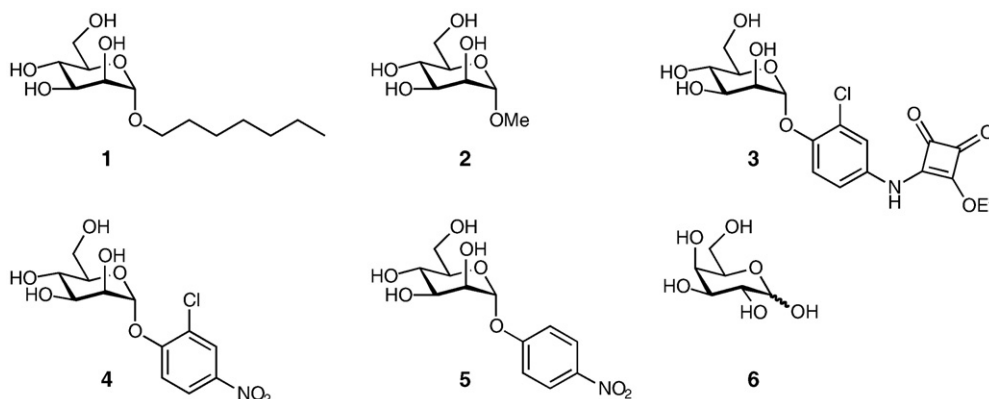


Fig. 1. Structures of the tested FimH antagonists 1–5 and the negative control D-galactose (6). *n*-Heptyl α -D-mannopyranoside (1), methyl α -D-mannopyranoside (2), *o*-chloro-*p*-[N-(2-ethoxy-3,4-dioxocyclobut-1-enyl)amino]phenyl α -D-mannopyranoside (3), 2-chloro-4-nitrophenyl α -D-mannopyranoside (4) and 4-nitrophenyl α -D-mannopyranoside (5).

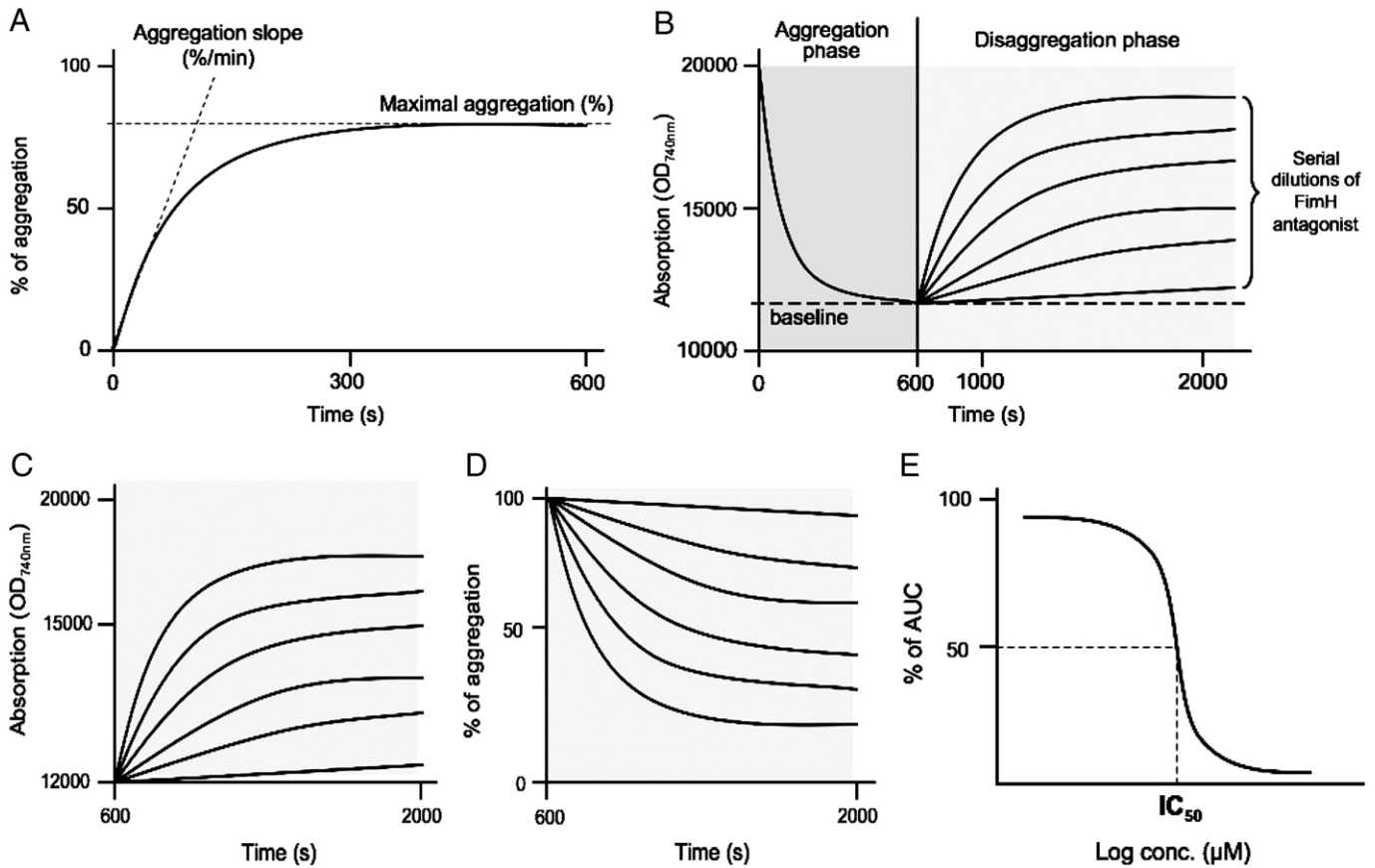


Fig. 2. Schematic overview of the evaluation process of the aggregometer data. (A) During measurements, the aggregometer software is plotting the aggregation curve as % of aggregation over time. For establishment of the method, the aggregation slope and the maximal aggregation were optimized. (B) The data exported from the aggregometer is plotted as absorbance (OD_{740nm}) over time. The aggregation phase is identical for all measurements whereas the disaggregation phase depends on the potency of FimH antagonists. For further evaluation only the disaggregation curves were taken into consideration. (C) Disaggregation curves of a serial dilution of a FimH antagonist after subtraction of the baseline. (D) For visualization purposes the disaggregation curves were inverted and normalized. At 100% of aggregation cells were maximally aggregated and disaggregation was monitored over 1400 s. (E) The AUC of the disaggregation curves are plotted against the concentration to determine the IC_{50} .

trypticase soy broth (TSB), Mueller-Hinton broth (MHB) and nutrient broth (NB). Media were dissolved in deionized water, autoclaved at 121 °C for 15 min and the pH was adjusted to 7.3. All media were purchased from Becton, Dickinson and Company (Le Pont de Claix, France). Autoclaved, endotoxin-free phosphate buffered saline (PBS), pH 7.4 was purchased from the Hospital Pharmacy at the University Hospital Basel, Switzerland.

2.3. Guinea pig erythrocytes (GPE)

Guinea pig blood was purchased from Charles River Laboratories, Sulzfeld, Germany. To separate GPE from other blood components, 1 ml of guinea pig blood was carefully added to 1 ml of Histopaque (density of 1.077 g/ml at 24 °C, Sigma-Aldrich, Buchs, Switzerland) and centrifuged at 24 °C for 30 min at 400 g. GPE were diluted in PBS to an OD_{600} of 4 and their number was determined using an automated cell counter (Invitrogen AG, Basel, Switzerland) resulting in 2.2×10^6 cells/ml.

2.4. Synthesis of the FimH antagonists

The FimH antagonists tested are listed in Fig. 1. The synthesis of *n*-heptyl α -D-mannopyranoside (1) is described in the supplementary content. Methyl α -D-mannopyranoside (2) was purchased from Fluka Chemie GmbH (Buchs, Switzerland). *o*-Chloro-*p*-[*N*-(2-ethoxy-3,4-dioxocyclobut-1-enyl)amino]phenyl α -D-mannopyranoside (3) and 2-chloro-4-nitrophenyl α -D-mannopyranoside (4) were synthesized as previously described (Sperling et al., 2006). 4-Nitrophenyl α -D-

mannopyranoside (5) and D-galactose (6) were purchased from Sigma (Buchs, Switzerland).

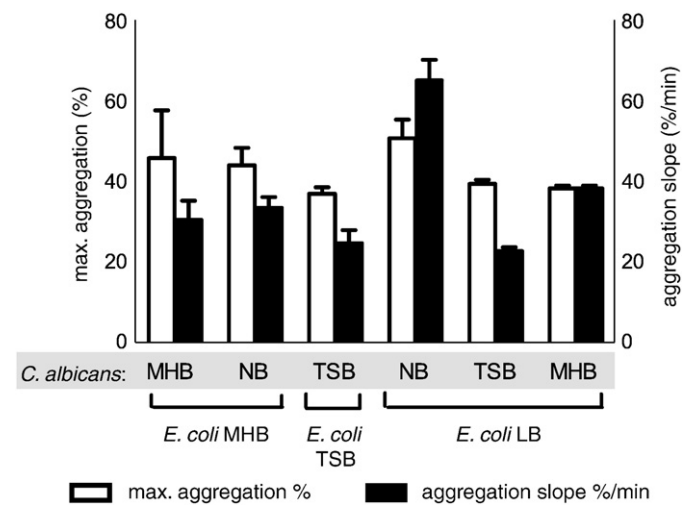


Fig. 3. Aggregation of *E. coli* with *C. albicans*, previously incubated in different cultivation media. Bars in black are representing the maximal aggregation (in %) and the white bars are showing the aggregation slope (in %/min). The bars represent means \pm SD. MHB, Mueller-Hinton broth; TSB, trypticase soy broth; LB, Luria-Bertani broth; NB, nutrient broth. The highest values for the aggregation phase were obtained with *C. albicans* grown in NB and *E. coli* in LB, resulting in a maximal aggregation slope of 64.15 %/min (± 6.0 %/min) and a maximal aggregation of 54.65 % (± 4.6 %).

Table 1
Influence of *E. coli* and *C. albicans* concentrations on aggregation measurements. The values represent means \pm SD of the maximal aggregation and the aggregation slope.

<i>E. coli</i>	<i>C. albicans</i>			
	OD ₆₀₀ of 2 ^a		OD ₆₀₀ of 3 ^b	
	Maximal aggregation (%)	Aggregation slope (%/min)	Maximal aggregation (%)	Aggregation slope (%/min)
OD ₆₀₀ 2 ^c	50.68 \pm 4.61	64.15 \pm 6.02	–	–
OD ₆₀₀ 3 ^d	40.99 \pm 5.11	53.34 \pm 22.19	41.77 \pm 2.41	65.95 \pm 6.53

^a OD₆₀₀ of 2 for *C. albicans* corresponds to 2×10^8 CFU/ml.

^b OD₆₀₀ of 3 for *C. albicans* corresponds to 3×10^8 CFU/ml.

^c OD₆₀₀ of 2 for *E. coli* corresponds to 9.6×10^7 CFU/ml.

^d OD₆₀₀ of 3 for *E. coli* corresponds to 1.4×10^8 CFU/ml.

2.5. Aggregation assay

The percentage of aggregation of *E. coli* with *C. albicans* or GPE was quantitatively determined by measuring the optical density at 740 nm, 37 °C under stirring at 1000 rpm using an ARACT 4004 aggregometer (Endotell AG, Allschwil, Switzerland). Bacteria and yeast were statically incubated overnight (12 h) in TSB at 37 °C. Prior to the measurements, the cell densities were adjusted to OD₆₀₀ of 2, corresponding to 9.6×10^7 CFU *E. coli*/ml and 2×10^8 CFU *C. albicans*/ml, respectively. For the calibration of the instrument, the aggregation of protein poor plasma (PPP) using PBS alone was set as 100% and the aggregation of protein rich plasma (PRP) as 0%. After calibration, measurements were performed with 250 μ l *C. albicans* or GPE and 50 μ l bacterial suspension and the aggregation monitored over 600 s. To optimize the assay, different bacterial and yeast growth conditions and measurement conditions were evaluated for the aggregation phase.

With the optimized assay parameters, the disaggregation potential of FimH antagonists was evaluated. After an aggregation phase of 600 s, 25 μ l of antagonist was added to each cuvette and disaggregation was monitored for 1400 s. A two-fold serial dilution of a stock solution of the FimH antagonists **1** to **5** and the negative control D-galactose (**6**), starting at 769 μ M, was tested in triplicates.

2.6. Data analysis

The data for the aggregation and the disaggregation phase were plotted using the ARACT 4 LPC software version 1.21c from Labor BioMedical Technologies (LABiTec GmbH, Ahrensburg, Germany). For the aggregation phase, the initial slope (in %/min) and the maximal aggregation (in %) were determined (Fig. 2A). Values for the absorption at 740 nm were measured with the aggregometer every 0.2 s. For the disaggregation phase, the baseline was determined by calculating the average value between 530 and 590 s and subtracted from the disaggregation curves (Fig. 2B and C). The curves were then inverted and the baseline before addition of the antagonist was set as 100% aggregation (Fig. 2D). For calculating the potency of FimH antagonists, the area under each disaggregation curve from 600 s until 2000 s (AUC_{600–2000 s}) was determined and plotted against the concentration of the antagonist to obtain the half maximal inhibitory concentration (IC₅₀) (Fig. 2E). Mean values, standard deviation (SD), AUC and the plots were calculated and plotted using GraphPad Prism 5.0a (GraphPad Software, La Jolla, CA).

Fig. 5. Disaggregation curves and corresponding IC₅₀ values, calculated using the AUC_{600–2000s} of the disaggregation curves. Values represent the mean \pm SD of triplicate measurements. (A) **1** shows an IC₅₀ of 77.14 μ M and represents the reference antagonist. (B) **2** does not exhibit a measurable disaggregation potency at concentrations up to 769 μ M, (C) **3** exhibits the best inhibitory potential of all measured FimH antagonists with an IC₅₀ of 0.87 μ M, (D) **4** has an IC₅₀ of 13.92 μ M, (E) **5** shows almost the same inhibitory potential as **2**, resulting in an IC₅₀ 62.96 μ M.

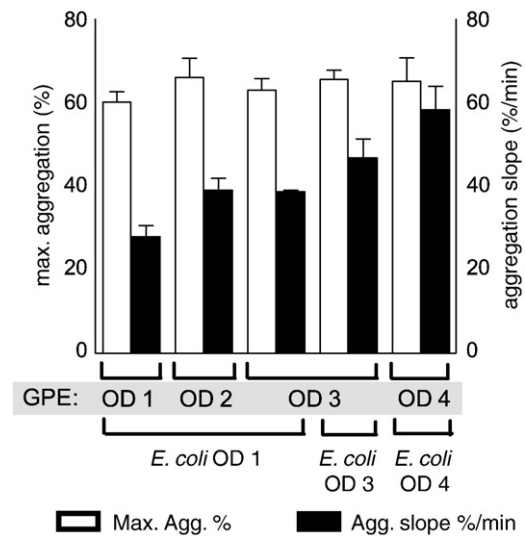


Fig. 4. Evaluation of the best aggregation conditions using *E. coli* and GPE at different concentrations, measured as OD₆₀₀. Bars in black are representing the maximal aggregation (in %) and the white bars are showing the aggregation slope (in %/min). The bars represent means \pm SD. For *E. coli*, OD₆₀₀ of 1 corresponds to 4.7×10^7 CFU/ml, OD₆₀₀ of 3 to 1.4×10^8 CFU/ml and OD₆₀₀ of 4 to 1.9×10^8 CFU/ml. For GPE, OD₆₀₀ of 1 corresponds to 5.5×10^5 cells/ml, OD₆₀₀ of 2 to 1.1×10^6 cells/ml, OD₆₀₀ of 3 to 1.7×10^6 cells/ml and OD₆₀₀ of 4 to 2.2×10^6 cells/ml.

3. Results

3.1. Optimization of the aggregation assay

3.1.1. Initial growth and measurement conditions

Bacteria and yeast were incubated overnight (12 h) in TSB at 37 °C without shaking, leading to a maximal aggregation slope for *E. coli* with *C. albicans* of 23.78 %/min (\pm 4.09 %/min) and a maximal aggregation of 36.89 % (\pm 1.63 %). With the *E. coli* Δ fimA-H mutant, virtually no aggregation was observed with *C. albicans*, resulting in a maximal aggregation slope of 0.25 %/min (\pm 0.29 %/min) and a maximal aggregation of 0.02 % (\pm 0.1 %) (Fig. 2A). After 600 s of measurement, a stable baseline was achieved, a prerequisite for a reliable determination of the disaggregation potency of FimH antagonists (Fig. 2B).

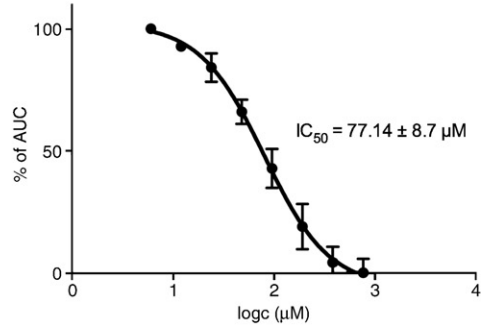
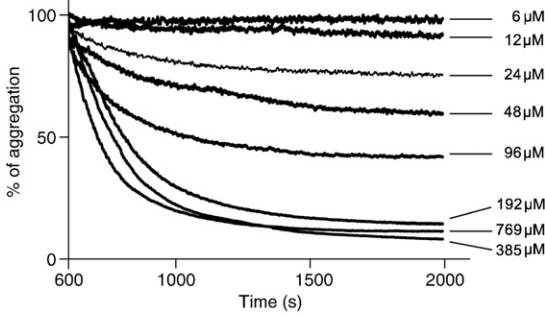
3.1.2. Shaking versus static incubation

Compared to static incubation (see above), *E. coli* and *C. albicans* incubated overnight under shaking conditions (250 rpm) exhibited a 13-fold lower aggregation slope of 1.82 %/min (\pm 0.61 %/min) and a 5-fold lower aggregation maximum of 8.38 % (\pm 0.69 %). In the optimized assay format, *E. coli* was therefore incubated overnight under static conditions whereas *C. albicans* was agitated at 250 rpm.

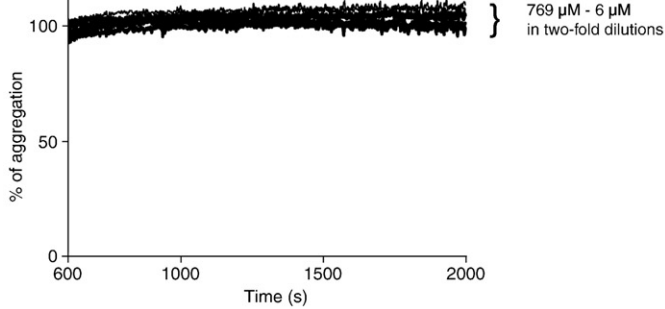
3.1.3. Bacterial and yeast growth media

In Fig. 3, the maximal aggregation (%) and the aggregation slope (%/min) of *E. coli* and *C. albicans* incubated in different growth media are presented. The best values were obtained when *E. coli* was cultivated in LB broth and *C. albicans* in NB medium, resulting in an aggregation slope of 64.15 %/min (\pm 6.0 %/min) and a maximal aggregation of 54.65 % (\pm 4.6 %). These conditions were therefore applied for all further measurements.

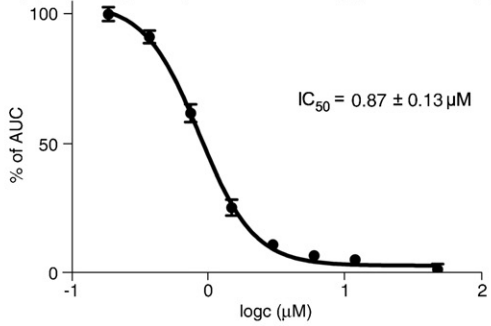
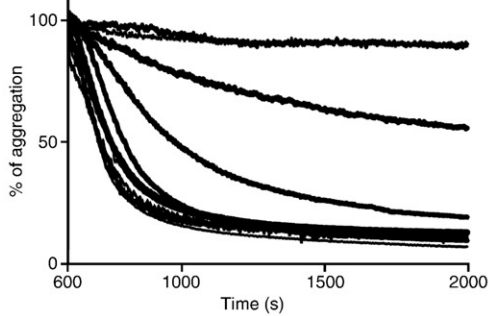
A: n-Heptyl α -D-mannopyranoside (1)



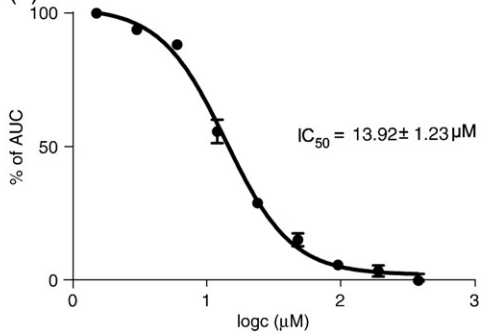
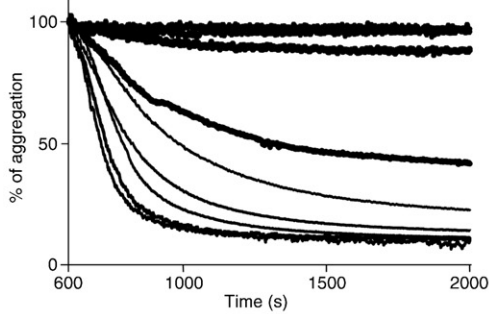
B: Methyl α -D-mannopyranoside (2)



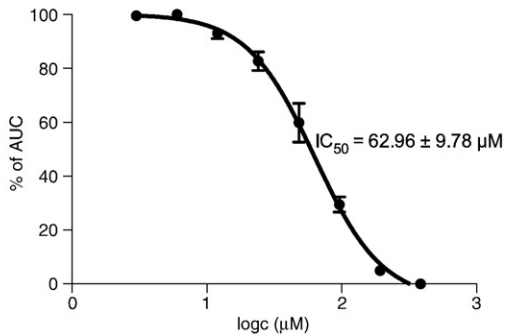
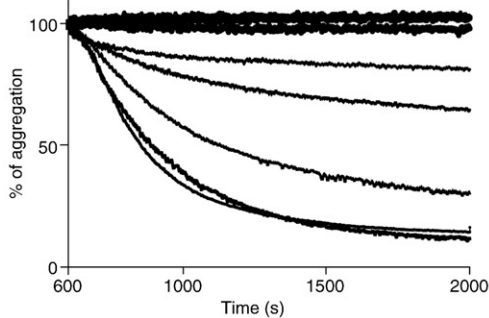
C: *o*-Chloro-*p*-[*N*-(2-ethoxy-3,4-dioxocyclobut-1-enyl)amino]phenyl α -D-mannopyranoside (3)



D: 2-Chloro-4-nitrophenyl α -D-mannopyranoside (4)



E: 4-Nitrophenyl α -D-mannopyranoside (5)



3.1.4. Concentration of *E. coli* and *C. albicans*

For both *E. coli* and *C. albicans*, the highest maximal aggregation of 50.68 % (± 4.61 %) was obtained at an OD₆₀₀ of 2 (Table 1). This concentration represents a bacteria to yeast ratio of 10:1 (4.8×10^6 CFU/50 μ l; 5×10^7 CFU/250 μ l). When the concentration of *E. coli* exceeds this ratio, a reduction of the maximal aggregation was observed.

3.1.5. Incubation time

For the optimization of the incubation time, cultures of *E. coli* and *C. albicans* incubated overnight, for 24 h and 48 h were compared. For *C. albicans*, the incubation time did not influence the aggregation behavior (data not shown). However, for *E. coli* the aggregation slope was increased by approx. 10 % and the maximal aggregation by approximately 5 % after incubation for 24 h compared to those incubated overnight. Incubation for 48 h resulted in a 16.1 % increase of the aggregation slope, but a 6.3 % reduction of the maximal aggregation. Since a 24 h incubation period resulted in the best maximal aggregation, it was applied for all further measurements.

3.1.6. Ratio of GPE and *E. coli*

To obtain an optimal aggregation phase, different ratios of *E. coli* and GPE were tested (Fig. 4). For both, an OD₆₀₀ of 4 showed the best aggregation potential [aggregation slope of 62.2 %/min (± 2.4 %/min) and a maximal aggregation of 65.1 % (± 5.6 %)]. This concentration represents a bacteria to GPE ratio of 17:1 (9.6×10^6 CFU/50 μ l; 5.8×10^5 cells/250 μ l).

Since the aggregation of *E. coli* with GPE showed less variability and a higher reproducibility than those of *E. coli* with *C. albicans* (data not shown), they were exclusively employed for evaluation of the disaggregation potential of FimH antagonists.

3.2. Disaggregation potential of FimH antagonists

The disaggregation potential of five α -D-mannopyranosides and D-galactose was determined with the optimized conditions (see section 3.1). Fig. 5 shows the disaggregation curves for two-fold serial dilutions of the antagonists and the corresponding IC₅₀ curves, calculated using the AUC_{600–2000 s}. The AUC of each curve was calculated and plotted against the concentration. The reference compound **1** exhibits an IC₅₀ of 77.14 ± 8.7 μ M. For compound **2** no disaggregation could be observed up to 769 μ M. Compounds **4** and **5** showed IC₅₀s of 13.92 ± 1.23 μ M and 62.96 ± 9.78 μ M, respectively. The best disaggregation potential was achieved with compound **3**, resulting in an IC₅₀ of 0.87 ± 0.13 μ M. Compound **6** was used as negative control and showed no disaggregation up to 769 μ M.

In order to optimize the measurement time, the effect of a shorter disaggregation period was evaluated. When the AUC for a disaggregation phase of 700 s (AUC_{600–1300 s}) and 1400 s (AUC_{600–2000 s}) were compared, no significant difference of the IC₅₀s (\pm SD) for the antagonists **1**, **3** and **4** was observed. However, for compound **5** (Fig. 5E), an approx. 50 % higher IC₅₀-value was obtained with a 700 s disaggregation phase, because the baseline is not reached at that time point (IC₅₀ of 92.86 μ M vs. 62.96 ± 9.78 μ M). Therefore, a standard disaggregation phase of 1400 s (AUC_{600–2000 s}) was applied.

4. Discussion

In the initially reported aggregometry assay by Ofek and Beachey in 1978, *E. coli* and yeast cells were used and the potential of FimH antagonists was evaluated and quantified based on the slope of the *E. coli*-yeast disaggregation curve. Since for our investigation a different assay set-up, other *E. coli* strains, and different aggregation cells were applied, the measurement settings had to be re-evaluated and validated.

Due to the suppression of type 1 pili expression under shaking incubation (Hultgren, 1986), a significant decrease in aggregation was

observed using *E. coli* cultures agitated overnight. *C. albicans* showed no reduction of aggregation after shaking incubation, indicating that the mannan-structures on the cell wall are constantly expressed. Due to a higher yield of microorganisms grown under shaking conditions, *C. albicans* was incubated at 250 rpm for all further experiments. With the Δ fimA-H deletion mutant of *E. coli*, we could demonstrate that the aggregation depends exclusively on type 1 pili mediated adherence to *C. albicans* and GPE, respectively.

To determine the optimal nutrient conditions for type 1 pili expression, various growth media were investigated. With *E. coli* incubated in LB broth and *C. albicans* grown in NB medium, the highest aggregation values were achieved (Hultgren, 1986; Ofek and Beachey, 1978). In addition, optimal aggregation conditions were obtained when *E. coli* and *C. albicans* samples with an OD₆₀₀ of 2 were used. As recommended (Blood and Curtis, 1995; Firon et al., 1983; Giampapa et al., 1988) the best results were obtained when the cultures were incubated for at least 24 h. Whereas overnight incubation led to less aggregation, similar values were obtained with cultures incubated for 48 h.

The majority of the disaggregation data reported in literature were obtained by a visual and therefore only semiquantitative interpretation of the disaggregation potential of the investigated FimH antagonists (e.g. Nagahori et al., 2002; Gouin et al., 2009). In addition, quantitative disaggregation data were also determined with an aggregometry assay reported by Ofek and Beachey, 1978 and Firon et al., 1983. In contrast, in this communication IC₅₀ values were determined from the AUCs of the disaggregation curves obtained of serially diluted antagonists. In addition, the various assay parameters as growth and measurement conditions, cell types were thoroughly optimized.

Optimization experiments clearly showed the advantages of blood cells (GPE, Fig. 4) over yeast (*C. albicans*, Fig. 3). With GPE the maximal aggregation is independent on the OD₆₀₀s within 60–66 %, whereas the aggregation slope is heavily depending on the OD₆₀₀ of both GPE and *E. coli*. The present format leads to a substantial improvement of the maximal aggregation (from 36.9 % to 65.1 %) and the ascending slope (from 23.8 %/min to 62.2 %/min).

The aggregometry assay was validated with five FimH antagonists (**1–5**) and a negative control (**6**) measured in serial dilutions starting with a concentration of 769 μ M (Table 2). The determination of the AUCs from the antagonist concentration (Fig. 5) leads to the IC₅₀-values. *n*-Heptyl α -D-mannopyranoside (**1**) was employed as reference compound. Methyl α -D-mannopyranoside (**2**) exhibited no disaggregation at a concentration up to 769 μ M. Furthermore, **3** showed the lowest IC₅₀ of all tested antagonists. **4** exhibited a slight improvement of activity compared to reference compound **1**, whereas **5** was equally active as **1**. With D-galactose (**6**) disaggregation could not be enforced and was therefore used as negative control (e.g. Clegg et al., 1984; Nagahori et al., 2002).

In Table 2 the IC₅₀-values are summarized and compared to those reported in literature. A direct comparison, however, is not possible, since the antagonistic potencies were measured in different assay formats and are reported relative to methyl α -D-mannopyranoside (**2**), which does not contribute to disaggregation up to a concentration of 769 μ M in our aggregometry assay. Since the literature values for the disaggregation potencies are expressed as relative inhibitory potentials (rIPs) compared to **2**, the IC₅₀s were transformed into rIPs (Table 2). Except for **5**, our rIPs correlate well with values found in literature. Whereas **5** showed equal activity than the reference compound **1** in the aggregometry assay, a 6-fold lower activity is reported in literature.

Compared to previously described aggregation- and hemagglutination assays (Firon et al., 1983; Nagahori et al., 2002; Gouin et al., 2009) the presented aggregometry assay was optimized and standardized allowing the accurate and reproducible high-throughput screening of FimH antagonists. Instead of a visual and therefore only semi-quantitative analysis of the disaggregation event, a

Table 2

IC₅₀ values determined with the aggregometry assay using *E. coli* with GPE. The relative IC₅₀ (rIC₅₀) of the reference compound 1 was defined as 1. The rIP of each substance was calculated by dividing the IC₅₀ of the reference compound 1 by the IC₅₀ of the compound of interest. This results in rIPs above 1.00 for derivatives binding better than 1 and rIPs below 1.00 for compounds with a lower affinity than 1. (n.d.: not determinable).

FimH antagonist	Aggregometry assay			Literature
	IC ₅₀ [μM]	rIC ₅₀	rIP	rIP
<i>n</i> -Heptyl α-D-mannopyranoside (1)	77.14 ± 8.7	1	1	440 ^a
Methyl α-D-mannopyranoside (2)	n.d.	n.d.	n.d.	1 ^{a,b,c}
<i>o</i> -Chloro- <i>p</i> -[<i>N</i> -(2-ethoxy-3,4-dioxocyclobut-1-enyl)amino]phenyl α-D-mannopyranoside (3)	0.87 ± 0.13	0.011	90	6900 ^b
2-Chloro-4-nitrophenyl α-D-mannopyranoside (4)	13.92 ± 1.23	0.18	6	717 ^c
4-Nitrophenyl α-D-mannopyranoside (5)	62.96 ± 9.8	0.82	1	70 ^c

^a RIP determined by surface plasmon resonance measurements (Bouckaert et al., 2005).

^b RIP determined by ELISA measurements (Sperling et al., 2006).

^c RIP determined by aggregometer measurements (Firon et al., 1987).

quantitative method to determine the inhibitory potential of FimH antagonists was developed. The results (IC₅₀) of this function-based assay can be applied to determine the therapeutic dosage for in vivo studies.

The potential of anti-virulence therapies for UTI is investigated for a long period of time (Collier and De Miranda, 1955; Old, 1972; Ofek and Beachey, 1978; Firon et al., 1983; Bouckaert et al., 2005; Ernst and Magnani, 2009) and is still actively pursued (Cegelski et al., 2008). The reported new assay format will hopefully contribute to this endeavor by supporting the identification of carbohydrate-derived FimH antagonists with a therapeutic potential.

Acknowledgments

This study was supported by the Swiss National Science Foundation (SNF interdisciplinary grant K-32 K1-120904). Part of the results were presented at the 49th Interscience Conference of Antimicrobial Agents and Chemotherapy, San Francisco, CA, September 12 to 15 2009 (B-040).

Appendix A. Supplementary data

Supplementary data associated with this article can be found, in the online version, at doi:10.1016/j.mimet.2010.06.015.

References

- Baumgartner, H.R., Born, G.V.R., 1968. Effect of 5-hydroxytryptamine on platelet aggregation. *Nature* 218, 137–141.
- Blood, R.M., Curtis, G.D., 1995. Media for 'total' Enterobacteriaceae, coliforms and *Escherichia coli*. *Int. J. Food Microbiol.* 26, 93–115.
- Bouckaert, J., Berglund, J., Schembri, M., De Genst, E., Cools, L., Wuhler, M., Hung, C.S., Pinkner, J., Slattegard, R., Zavalov, A., Choudhury, D., Langermann, S., Hultgren, S.J., Wyns, L., Klemm, P., Oscarson, S., Knight, S.D., De Greve, H., 2005. Receptor binding studies disclose a novel class of high-affinity inhibitors of the *Escherichia coli* FimH adhesin. *Mol. Microbiol.* 55, 441–455.
- Bouckaert, J., Mackenzie, J., de Paz, J.L., Chipwaza, B., Choudhury, D., Zavalov, A., Mannerstedt, K., Anderson, J., Pierard, D., Wyns, L., Seeberger, P.H., Oscarson, S., De Greve, H., Knight, S.D., 2006. The affinity of the FimH fimbrial adhesin is receptor-driven and quasi-independent of *Escherichia coli* pathotypes. *Mol. Microbiol.* 61, 1556–1568.
- Capitani, G., Eidam, O., Glockshuber, R., Grutter, M.G., 2006. Structural and functional insights into the assembly of type 1 pili from *Escherichia coli*. *Microbes Infect.* 8, 2284–2290.

- Cegelski, L., Marshall, G.R., Eldridge, G.R., Hultgren, S.J., 2008. The biology and future prospects of antivirulence therapies. *Nat. Rev. Microbiol.* 6, 17–27.
- Choudhury, D., Thompson, A., Stojanoff, V., Langermann, S., Pinkner, J., Hultgren, S.J., Knight, S.D., 1999. X-ray structure of the FimC–FimH chaperone–adhesin complex from uropathogenic *Escherichia coli*. *Science* 285, 1061–1066.
- Clegg, H., Guerina, N., Langermann, S., Kessler, T.W., Guerina, V., Goldmann, D., 1984. Pilus-mediated adherence of *Escherichia coli* K1 to human oral epithelial cells. *Infect. Immun.* 45, 299–301.
- Collier, W.A., De Miranda, J.C., 1955. Bacterial hemagglutination. III. Mannose inhibition of *E. coli* hemagglutination. *Antonie Leeuwenhoek* 21, 133–140.
- Datsenko, K.A., Wanner, B.L., 2000. One-step inactivation of chromosomal genes in *Escherichia coli* K-12 using PCR products. *Proc. Natl. Acad. Sci. USA* 97, 6640–6645.
- Ernst, B., Magnani, J.L., 2009. From carbohydrate leads to glycomimetic drugs. *Nat. Rev. Drug Discov.* 8, 661–677.
- Fihn, S.D., 2003. Clinical practice. Acute uncomplicated urinary tract infection in women. *N Engl J. Med.* 349, 259–266.
- Firon, N., Ofek, I., Sharon, N., 1982. Interaction of mannose-containing oligosaccharides with the fimbrial lectin of *Escherichia coli*. *Biochem. Biophys. Res. Commun.* 105, 1426–1432.
- Firon, N., Ofek, I., Sharon, N., 1983. Carbohydrate specificity of the surface lectins of *Escherichia coli*, *Klebsiella pneumoniae*, and *Salmonella typhimurium*. *Carbohydr. Res.* 120, 235–249.
- Firon, N., Ashkenazi, S., Mirelman, D., Ofek, I., Sharon, N., 1987. Aromatic alpha-glycosides of mannose are powerful inhibitors of the adherence of type 1 fimbriated *Escherichia coli* to yeast and intestinal epithelial cells. *Infect. Immun.* 55, 472–476.
- Giampapa, C.S., Abraham, S.N., Chiang, T.M., Beachey, E.H., 1988. Isolation and characterization of a receptor for type 1 fimbriae of *Escherichia coli* from guinea pig erythrocytes. *J. Biol. Chem.* 263, 5362–5367.
- Gouin, S.G., Wellens, A., Bouckaert, J., Kovensky, J., 2009. Synthetic multimeric heptyl mannoses as potent antiadhesives of uropathogenic *Escherichia coli*. *Chem. Med. Chem.* 4, 749–755.
- Hvidberg, H., Struve, C., Kroghfelt, K.A., Christensen, N., Rasmussen, S.N., Frimodt-Møller, N., 2000. Development of a long-term ascending urinary tract infection mouse model for antibiotic treatment studies. *Antimicrob. Agents Chemother.* 44, 156–163.
- Hooton, T.M., 2001. Recurrent urinary tract infection in women. *Int. J. Antimicrob. Agents* 17, 259–268.
- Hultgren, S.J., 1986. Regulation of production of type 1 pili among urinary tract isolates of *Escherichia coli*. *Infect. Immun.* 54, 613–620.
- Langermann, S., Palaszynski, S., Barnhart, M., Auguste, G., Pinkner, J.S., Burlein, J., Barren, P., Koenig, S., Leath, S., Jones, C.H., Hultgren, S.J., 1997. Prevention of mucosal *Escherichia coli* infection by FimH-adhesin-based systemic vaccination. *Science* 276, 607–611.
- Langermann, S., Mollby, R., Burlein, J.E., Palaszynski, S.R., Auguste, C.G., DeFusco, A., Strouse, R., Schenerman, M.A., Hultgren, S.J., Pinkner, J.S., Winberg, J., Guldevall, L., Soderhall, M., Ishikawa, K., Normark, S., Koenig, S., 2000. Vaccination with FimH adhesin protects cynomolgus monkeys from colonization and infection by uropathogenic *Escherichia coli*. *J. Infect. Dis.* 181, 774–778.
- Mulvey, M.A., 2002. Adhesion and entry of uropathogenic *Escherichia coli*. *Cell. Microbiol.* 4, 257–271.
- Mulvey, M.A., Schilling, J.D., Hultgren, S.J., 2001. Establishment of a persistent *Escherichia coli* reservoir during the acute phase of a bladder infection. *Infect. Immun.* 69, 4572–4579.
- Murphy, K.C., Campellone, K.G., 2003. Lambda Red-mediated recombinogenic engineering of enterohemorrhagic and enteropathogenic *E. coli*. *BMC Mol. Biol.* 4, 11.
- Nagahori, N., Lee, R.T., Nishimura, S., Page, D., Roy, R., Lee, Y.C., 2002. Inhibition of adhesion of type 1 fimbriated *Escherichia coli* to highly mannosylated ligands. *ChemBiochem* 3, 836–844.
- Ofek, I., Beachey, E.H., 1978. Mannose binding and epithelial cell adherence of *Escherichia coli*. *Infect. Immun.* 22, 247–254.
- Old, D.C., 1972. Inhibition of the interaction between fimbrial haemagglutinins and erythrocytes by d-mannose and other carbohydrates. *J. Gen. Microbiol.* 71, 149–157.
- Rosen, D.A., Hung, C.S., Kline, K.A., Hultgren, S.J., 2008. Streptozocin-induced diabetic mouse model of urinary tract infection. *Infect. Immun.* 76, 4290–4298.
- Sharon, N., 2006. Carbohydrates as future anti-adhesion drugs for infectious diseases. *Biochim. Biophys. Acta* 1760, 527–537.
- Sperling, O., Fuchs, A., Lindhorst, T.K., 2006. Evaluation of the carbohydrate recognition domain of the bacterial adhesin FimH: Design, synthesis and binding properties of mannoseidoligands. *Org. Biomol. Chem.* 4, 3913–3922.
- Wellens, A., Garofalo, C., Nguyen, H., Van Gerven, N., Slättergård, R., Hernalsteens, J.-P., Wyns, L., Oscarson, S., De Greve, H., Hultgren, S., Bouckaert, J., 2008. Intervening with urinary tract infections using anti-adhesives based on the crystal structure of the FimH oligomannose 3 complex. *PLoS ONE* 3, 4–13.
- Wiles, T.J., Kulesus, R.R., Mulvey, M.A., 2008. Origins and virulence mechanisms of uropathogenic *Escherichia coli*. *Exp. Mol. Pathol.* 85, 11–19.

8 Appendix

8.1 Supplemental Results and Discussion

8.1.1 Raw data for flow cytometric analysis of *fimH-gfp* construct

It was previously established that flow cytometry can be used to visualise the degree of bacterial aggregate formation. Repression of the Csr system was shown to produce type I fimbriae mediated aggregates while derepression of the Csr system primarily promotes PGA mediated aggregates. Supplemental Figures 1-6 contain the raw data acquired by flow cytometry during growth curves of *fimH-gfp*, *fimH-gfp ΔfimB*, *fimH-gfp ΔfimE*, and *fimH-gfp ΔcsrD*. The results of these figures are discussed in detail in chapter 6.5.4, they are averaged over three independent clones per strain and condition. The flow cytometric analysis of these supplemental figures is restricted to one out of three clones per *fimH-gfp* reporter strain and condition and are meant to illustrate the formation of type I fimbrial vs. PGA aggregates over time.

8.1.2 C-di-GMP and ppGpp affect the phase variation in *fimH-gfp*

The involvement of selected genes in the phase variable regulation of type I fimbriae was screened in the *fimH-gfp* reporter construct and analysed after 18 h of static growth. The aim was to identify components that are required for the dual adhesin regulation by the Csr system. All tested genes have previously been reported to i) affect the regulation of type I fimbriae, ii) belong to the Csr system, iii) contribute to c-di-GMP signalling or iv) be required for the synthesis of EPS matrix components. The results for this initial screen are subdivided into two Figures where Supplemental Figure 7 illustrates the difference in GFP expression between the wild type reporter strain and the mutant reporter strains. Supplemental Figure 8 illustrates the effect of *csrB* overexpression in the wild type reporter vs. the mutant reporter strains. All tested strains except the deletions of the small RNAs *csrB* and *csrC* affected GFP expression in the *fimH-gfp* reporter (Supplemental Figure 7). This result for *csrB* and *csrC* was not surprising, since both small RNAs are published to result in a modest compensatory increase in the levels of the other small RNA upon deletion, complementing any phenotype (139, 144). Most likely, an effect of the two small RNAs would require the construction of a *fimH-gfp ΔcsrB ΔcsrC* double reporter mutant. According to the established model, such a double mutant should have an increased fraction of GFP expressing bacteria compared to

wild type. Importantly, the results obtained for the *fimB* and *fimE* recombinases were as expected and confirmed their effect on fimbriation. Both recombinases have been investigated in detail in chapter 6. Interestingly, the construction of the *fimBE* mutant resulted in a strain, which expressed very low amounts of GFP, indicative of a very low level of fimbriation. In this mutant, fimbriation can only be controlled by the third known recombinase (FimX), which was reported to be very slow *in vitro* and predominantly switch *fimS* from the OFF to the ON phase (264). This could explain the residual fimbriation in the *fimBE* mutant. However, lack of FimB and FimE should result in a mutant strain, which is bi-stable and occur in either a predominant OFF or a predominant ON state. Thus, it would be worthwhile to simultaneously investigate and compare several clones of the *fimH-gfp ΔfimBE* mutant and see how often the OFF versus the ON versions occur. Such a comparison should give insight into the activity and directionality of the remaining recombinase FimX. Deletion of *fimX* resulted in a strain whose fimbriation depends on FimB and FimE. In a *fimX* mutant, the OFF to ON switching predominantly relies on FimB alone while the ON to OFF switching depends on the strong FimE. Since FimE was reported to be more active *in vitro* compared to FimB (245, 247, 249-251) the *fimX* mutant should have reduced ON to OFF switching and result in elevated levels of GFP expression, which was indeed the case. Interestingly, deletion of the PGA machinery *pgaA-D*, the curli master regulator *csgD* as well as the cellulose synthase *bcsA* all resulted in a slight decrease in GFP expression, similar to *ydeH*, *csrD* from the Csr cascade or the Sfa fimbrial gene *c1117*. However, to proof whether fimbriation is really affected by any of these genes, a more precise investigation over time is required. In agreement with a previous publication (285) the screening results obtained for the PDEs YhjH and C1116 as well as the DGC YcdT support the notion that fimbriation is enhanced under lower levels of c-di-GMP. Moreover, the PilZ containing c-di-GMP effector protein YcgR or a downstream component thereof was previously suggested to regulate the expression and/or activities of the Fim recombinases (285). This finding is compatible with the result obtained in this study. Interestingly, a study performed by Jonas *et al.*, has shown that overexpression of the DGC YdeH abolished the presence of fimbrial structures on the bacterial surface (213). However, *fimH-gfp ΔydeH* constructed in this study did not support this finding. However, it is necessary to follow up on this discrepancy by a more detailed investigation of *fimH-gfp ΔydeH* over time, as a single time point does not give a decisive result. Finally, the construction of a strain, which lacks the alarmone ppGpp (*fimH-gfp ΔrelA ΔspoT*; ppGpp⁰) resulted in a complete loss of GFP expression. This finding is very important, as ppGpp⁰ strains strongly induce PGA dependent biofilm formation (see chapter 5). In conclusion, the mutant screen performed in this study (Supplemental Figure 7) provides evidence that fimbriation under a repressed Csr system is strongly affected by the stress alarmone ppGpp and moderately affected by c-di-GMP, presumably through the

activities of YjhH, YcgR and YcdT. To follow up on the effect of c-di-GMP on fimbriation it would be interesting to see if overexpression of any strong DGC or PDE might cause an effect, or whether the effect observed is specific for the proteins investigated here.

The second aim of the mutant screen was to identify components, which are required to mediate the switching of *fimS* into the OFF phase upon derepression of the Csr system. The difference between the GFP signal derived from reporter mutants containing the empty vector or the *csrB* overexpressing plasmid was compared to the difference in the wild type *fimH-gfp* reporter (Supplemental Figure 8). If the deleted gene is involved in the Csr dependent switching of *fimS*, the effects of *csrB* overexpression in the wild type would have to be different than those observed in the mutant reporter. With this reasoning, we were able to show that *fimE* and *csrD* were both involved in the *csrB*-dependent switching of *fimS* OFF (see chapter 6.5.4 for detail). However, our results suggest that these two components are not the only ones, which are directly or indirectly involved in the *csrB*-dependent dual adhesin system affecting the phase of *fimS*. The initial screening results for *fimH-gfp ΔycgR* indicate that overexpression of *csrB* upon deletion of *ycgR* is impaired to reduce fimbriation, suggesting that this protein might serve as effector in the dual adhesin regulation as well. However, similar to CsrD its effect could also affect the correct timing of fimbriation during growth. It would thus be necessary to investigate fimbriation of *fimH-gfp ΔycgR* over time with and without *csrB* overexpression. For many mutants tested (*ΔydeH*, *ΔycdT*, *ΔyjhH*, *ΔpgaA-D*, *ΔbcsA* and *ΔcsgD*) the results obtained at the one time point were inconclusive. In order to properly investigate their involvement in the signalling cascade affecting phase variation of *fimS* these mutant strains would have to be investigated individually in more detail as well. Finally, the results obtained for *fimH-gfp Δc1116* and *fimH-gfp Δc1117* show that these two Sfa fimbrial proteins are not involved in the Csr mediated switching of *fimS*. In principle, this result would support the hypothesis that the effects of the Csr system on the phase of *fimS* is conserved among all *E. coli* strains and thus only involves factors, which are present in all strains of *E. coli* and does not involve factors encoded on genomic regions that are only found on pathogenic *E. coli*.

In the end, the obtained screening data can be integrated into the regulatory signalling mechanism, which gets triggered once uropathogenic UTI89 change from a planktonic lifestyle, capable of causing acute urinary tract infections, to a sessile lifestyle, during which bacteria persist as biofilms (Supplemental Figure 9). Under laboratory conditions, this lifestyle switch can occur when bacteria change from logarithmic to stationary growth. At this transition, nutrients and oxygen become limiting and bacteria initiate metabolic fluxes toward glycogen biosynthesis (130, 296). This is often associated with the derepression of the Csr system. Maybe a similar metabolic adaptation occurs upon entry of bacteria into the

bladder lumen or upon internalisation into urothelial cells. At this time, bacteria start to increase fimbriation if the Csr system is repressed, or prepare for PGA dependent biofilm formation if the Csr system is derepressed. Thus it is likely that environmental cues and consequently the state of the Csr system act as checkpoint deciding over the population's fate whether to become virulent (fimbriated) or become sessile (formation of PGA dependent biofilms). Most likely the checkpoint's decision between an acute and persistent lifestyle depends on the directionality of metabolic carbon fluxes (129, 132, 143, 297), similar to the *in vitro* situation. Furthermore, if external and internal signals favour a sessile lifestyle, c-di-GMP will accumulate and enhance biofilm formation within the host. On the other hand, elevated ribosomal stress, which results in ppGpp accumulation, should retain bacterial motility, which permits them to seek a more favourable environment (e.g. cytoplasm of urothelial cells). Thus the feedback loops between the dominant Csr system, the levels of c-di-GMP and ppGpp, continuously stabilize the population's lifestyle unless environmental signals reprogram the lifestyle of the bacterial cells.

8.2 Supplemental Figure Legends

Supplemental Figure 1: Aerated growth and fimbriation of UTI89 *fimH-gfp* (0h-8h & 24h)

GFP expression of the *fimH-gfp* reporter strain was measured over time under aerated conditions and analysed by flow cytometry. The data is shown for one out of three wild type *fimH-gfp* reporter clones tested in parallel (A) *fimH-gfp* without plasmid, (B) *fimH-gfp* with the empty vector (pME6032), (C) *fimH-gfp* overexpressing *csrB* (pME6032 *csrB*). The top row for each strain depicts the population's size distribution in a forward-sideward scatter. The forward scatter is shown on the x-axis and the sideward scatter on the y-axis. Both scales range from 0 to 10^4 . All events are gated into four quadrants, bacteria being in the upper right quadrant (Q2). The lower row for each strain depicts the GFP signal distribution. The intensity of the recorded GFP signal is shown on the x-axis (from 0 to 10^4), cell counts on the y-axis. In the histogram, only events in Q2 were considered. The left peak in each histogram corresponds to the fraction of events without GFP signal and the right peak to the fraction of events with GFP signal. For each sample 50'000 events were analysed. Time points during growth at which samples were analysed are indicated at the bottom of (C).

Supplemental Figure 2: Static growth and fimbriation of UTI89 *fimH-gfp* (0h-8h & 24h)

GFP expression of the *fimH-gfp* reporter strain was measured over time under static conditions and analysed by flow cytometry. The data is shown for one out of three wild type *fimH-gfp* reporter clones tested in parallel (A) *fimH-gfp* without plasmid, (B) *fimH-gfp* with the empty vector (pME6032), (C) *fimH-gfp* overexpressing *csrB* (pME6032 *csrB*). The top row for each strain depicts the population's size distribution in a forward-sideward scatter. The forward scatter is shown on the x-axis and the sideward scatter on the y-axis. Both scales range from 0 to 10^4 . All events are gated into four quadrants, bacteria being in the upper right quadrant (Q2). The lower row for each strain depicts the GFP signal distribution. The intensity of the recorded GFP signal is shown on the x-axis (from 0 to 10^4), cell counts on the y-axis. In the histogram, only events in Q2 were considered. The left peak in each histogram corresponds to the fraction of events without GFP signal and the right peak to the fraction of events with GFP signal. For each sample 50'000 events were analysed. Time points during growth at which samples were analysed are indicated at the bottom of (C).

Supplemental Figure 3: Static growth and fimbriation of UTI89 *fimH-gfp* (10h - 24h)

GFP expression of the *fimH-gfp* reporter strain was measured over time under static conditions and analysed by flow cytometry. The data is shown for one out of three wild type *fimH-gfp* reporter clones tested in parallel and compared to UTI89 as GFP negative control: (A) UTI89 wt as negative control (B) *fimH-gfp* without plasmid, (C) *fimH-gfp* with the empty vector (pME6032), (D) *fimH-gfp* overexpressing *csrB* (pME6032 *csrB*). The top row for each strain depicts the population's size distribution in a forward-sideward scatter. The forward scatter is shown on the x-axis and the sideward scatter on the y-axis. Both scales range from 0 to 10^4 . All events are gated into four quadrants, bacteria being in the upper right quadrant (Q2). The lower row for each strain depicts the GFP signal distribution. The intensity of the recorded GFP signal is shown on the x-axis (from 0 to 10^4), cell counts on the y-axis. In the histogram, only events in Q2 were considered. The left peak in each histogram corresponds to the fraction of events without GFP signal and the right peak to the fraction of events with GFP signal. For each sample 50'000 events were analysed. Time points during growth at which samples were analysed are indicated at the bottom of (D).

Supplemental Figure 4: Static growth and fimbriation of UTI89 Δ *fimB fimH-gfp* (10h - 24h)

GFP expression of the Δ *fimB fimH-gfp* reporter strain was measured over time under static conditions and analysed by flow cytometry. The data is shown for one out of three wild type Δ *fimB fimH-gfp* reporter clones tested in parallel and compared to UTI89 *fimH-gfp*. (A) UTI89 wt as negative control (B) Δ *fimB fimH-gfp* without plasmid, (C) Δ *fimB fimH-gfp* with the empty vector (pME6032), (D) Δ *fimB fimH-gfp* overexpressing *csrB* (pME6032 *csrB*). The top row for each strain depicts the population's size distribution in a forward-sideward scatter. The forward scatter is shown on the x-axis and the sideward scatter on the y-axis. Both scales range from 0 to 10^4 . All events are gated into four quadrants, bacteria being in the upper right quadrant (Q2). The lower row for each strain depicts the GFP signal distribution. The intensity of the recorded GFP signal is shown on the x-axis (from 0 to 10^4), cell counts on the y-axis. In the histogram, only events in Q2 were considered. The left peak in each histogram corresponds to the fraction of events without GFP signal and the right peak to the fraction of events with GFP signal. For each sample 50'000 events were analysed. Time points during growth at which samples were analysed are indicated at the bottom of (D).

Supplemental Figure 5: Static growth and fimbriation of UTI89 $\Delta fimE fimH-gfp$ (10h - 24h)

GFP expression of the $\Delta fimE fimH-gfp$ reporter strain was measured over time under static conditions and analysed by flow cytometry. The data is shown for one out of three wild type $\Delta fimE fimH-gfp$ reporter clones tested in parallel and compared to UTI89 $fimH-gfp$. (A) UTI89 wt as negative control (B) $\Delta fimE fimH-gfp$ without plasmid, (C) $\Delta fimE fimH-gfp$ with the empty vector (pME6032), (D) $\Delta fimE fimH-gfp$ overexpressing *csrB* (pME6032 *csrB*). The top row for each strain depicts the population's size distribution in a forward-sideward scatter. The forward scatter is shown on the x-axis and the sideward scatter on the y-axis. Both scales range from 0 to 10^4 . All events are gated into four quadrants, bacteria being in the upper right quadrant (Q2). The lower row for each strain depicts the GFP signal distribution. The intensity of the recorded GFP signal is shown on the x-axis (from 0 to 10^4), cell counts on the y-axis. In the histogram, only events in Q2 were considered. The left peak in each histogram corresponds to the fraction of events without GFP signal and the right peak to the fraction of events with GFP signal. For each sample 50'000 events were analysed. Time points during growth at which samples were analysed are indicated at the bottom of (D).

Supplemental Figure 6: Static growth and fimbriation of UTI89 $\Delta csrD fimH-gfp$ (10h - 24h)

GFP expression of the $\Delta csrD fimH-gfp$ reporter strain was measured over time under static conditions and analysed by flow cytometry. The data is shown for one out of three wild type $\Delta csrD fimH-gfp$ reporter clones tested in parallel and compared to UTI89 $fimH-gfp$. (A) UTI89 wt as negative control (B) $\Delta csrD fimH-gfp$ without plasmid, (C) $\Delta csrD fimH-gfp$ with the empty vector (pME6032), (D) $\Delta csrD fimH-gfp$ overexpressing *csrB* (pME6032 *csrB*). The top row for each strain depicts the population's size distribution in a forward-sideward scatter. The forward scatter is shown on the x-axis and the sideward scatter on the y-axis. Both scales range from 0 to 10^4 . All events are gated into four quadrants, bacteria being in the upper right quadrant (Q2). The lower row for each strain depicts the GFP signal distribution. The intensity of the recorded GFP signal is shown on the x-axis (from 0 to 10^4), cell counts on the y-axis. In the histogram, only events in Q2 were considered. The left peak in each histogram corresponds to the fraction of events without GFP signal and the right peak to the fraction of events with GFP signal. For each sample 50'000 events were analysed. Time points during growth at which samples were analysed are indicated at the bottom of (D).

Supplemental Figure 7: Knowledge based screen of *fimH-gfp* mutants under a repressed Csr system

Each histogram compares the GFP signal intensity distribution of a *fimH-gfp* mutant (blue) to the distribution of the *fimH-gfp* wild type reporter strain (red). The fraction of GFP expressing cells (*fim*+) for both strains is indicated at the right side of each graph and corresponds to the fraction associated to the right peak of the histogram. The left peak of each histogram corresponds to the non-GFP expressing events (*fim*-). A small vertical black line in each histogram indicates the border between *fim*+ and *fim*-. In each case, the mutant and the wild type samples were prepared simultaneously after 18 h of static growth. Per sample 50'000 events were recorded. The GFP signal intensity distribution was only calculated after gating each sample and selecting for bacteria. The x-axis of all histograms range from 0 to 10^4 and the y-axis range from 0 % to 100 % as indicated in the graph of the $\Delta ydeH$ mutant.

Supplemental Figure 8: Knowledge based screen of *fimH-gfp* mutants under a derepressed Csr system

Each histogram compares the GFP signal intensity distribution of a *fimH-gfp* mutant (orange and green) to the distribution of the *fimH-gfp* wild type reporter strain (blue and red). Green and red show data obtained with the pME6032 control vector while orange and blue show data obtained from strains overexpressing *csrB* (pCsrB). The fraction of GFP expressing cells (*fim*+) for all strains is indicated at the right side of each graph and corresponds to the fraction of events associated to the right peak of the histogram. The left peak of each histogram corresponds to the non-GFP expressing events (*fim*-). A small vertical black line in each histogram indicates the border between *fim*+ and *fim*-. In each case, the mutant and the wild type samples were prepared simultaneously after 18 h of static growth in LB supplemented with tetracycline and IPTG for plasmid induction. Also, the samples were taken together with those illustrated in Supplemental Figure 7. Per sample 50'000 events were recorded. The GFP signal intensity distribution was only calculated after gating each sample and selecting for bacteria. The x-axis of all histograms range from 0 to 10^4 and the y-axis range from 0 % to 100 % as indicated in the graph of the $\Delta ydeH$ mutant.

Supplemental Figure 9: Inversed effects of the Csr system, c-di-GMP and ppGpp on fimbriation and PGA dependent biofilm

Fimbriation is favoured when c-di-GMP levels are kept low, when the Csr system is repressed and FimE activity is high, and when ppGpp levels are elevated. On the contrary, PGA dependent biofilm formation is favoured when the Csr system is derepressed, lowering FimE activity, when c-di-GMP levels are high and when ppGpp levels are low. In the end, the state of the Csr system is a major factor deciding over fimbriation and PGA dependent biofilm formation, respectively. It affects both output systems (Fimbriation vs. PGA) depending on the presence or absence of nutrients and environmental signals. C-di-GMP and ppGpp levels inversely depend on the Csr system and might be used to boost the effects of the Csr system. In this model, CsrD is part of a feedback loop within the Csr system, which ensures homeostatic levels of fimbriation versus PGA expression and thus avoids stressful conditions. While the DGCs YdeH and YcdT have been shown to boost PGA dependent biofilm formation, the precise effect of the PDE YhjH and the c-di-GMP receptor YcgR on fimbriation remains to be elucidated. Also, it was not yet determined, whether the effects of ppGpp on Fimbriation are direct or indirect (e.g. via FimE) and whether CsrA directly or indirectly interferes with FimE activity, as indicated by the question mark.

8.3 Supplemental Figures

Figure 1

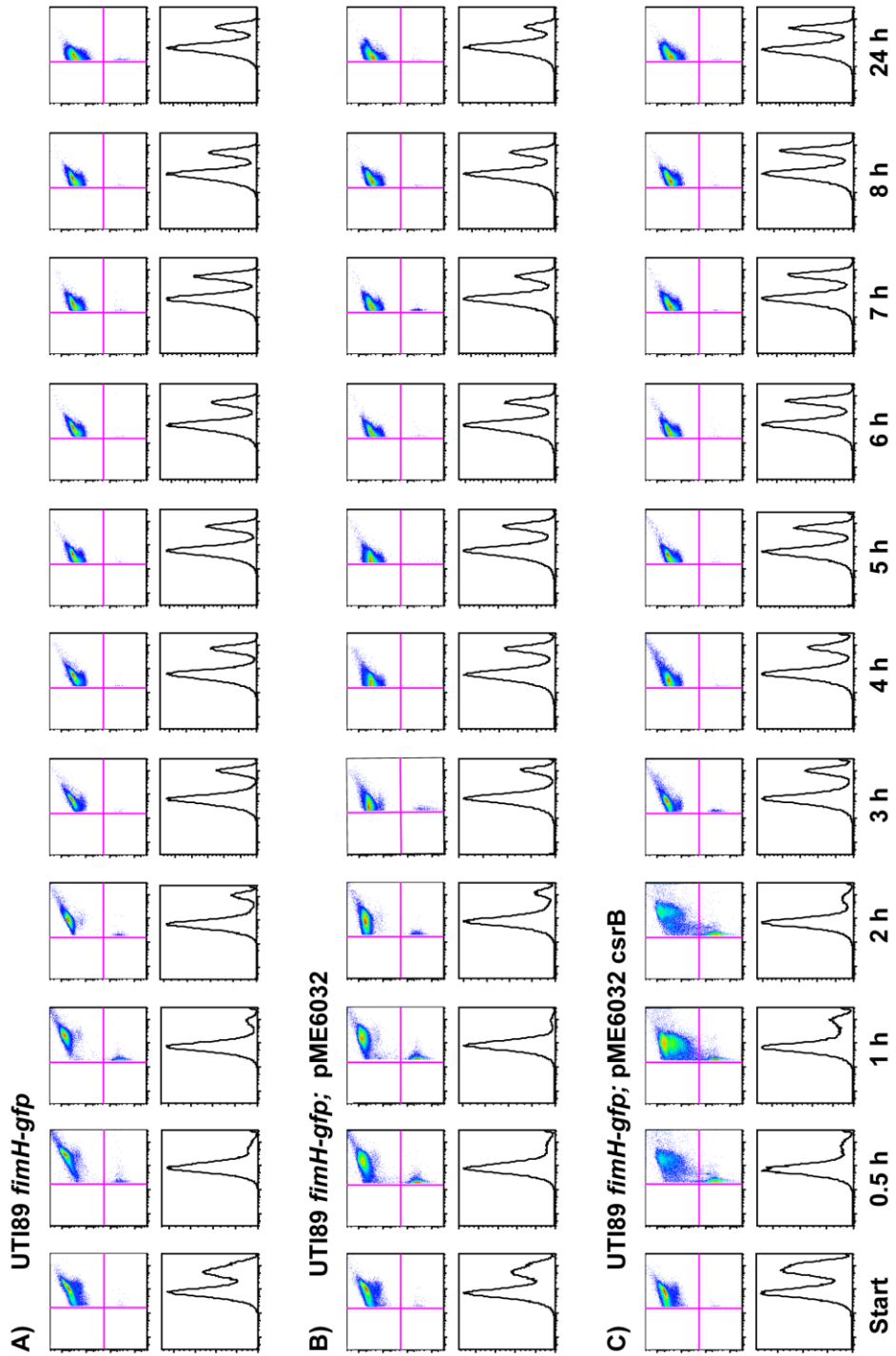


Figure 2

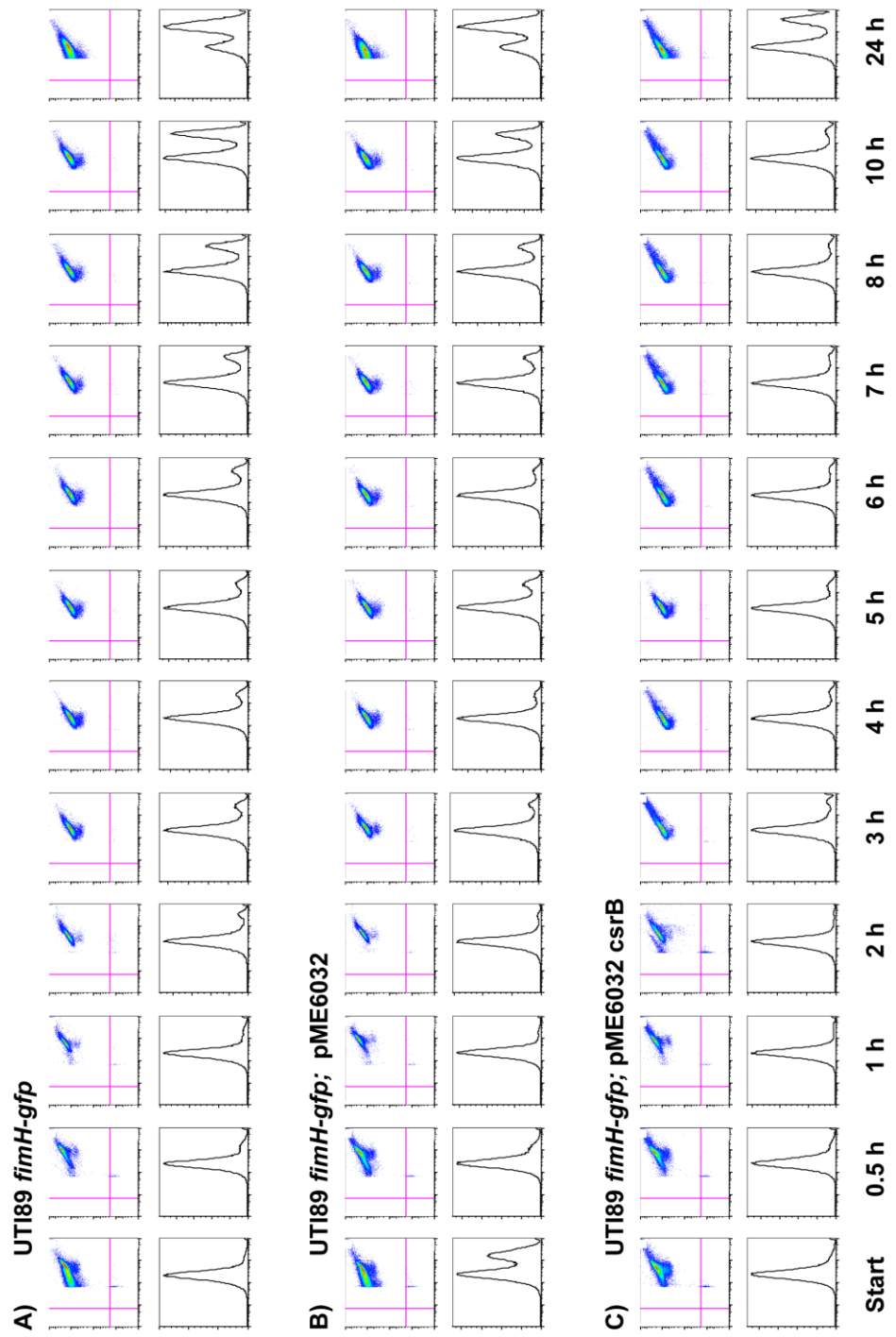


Figure 3

A) UTI89 wt

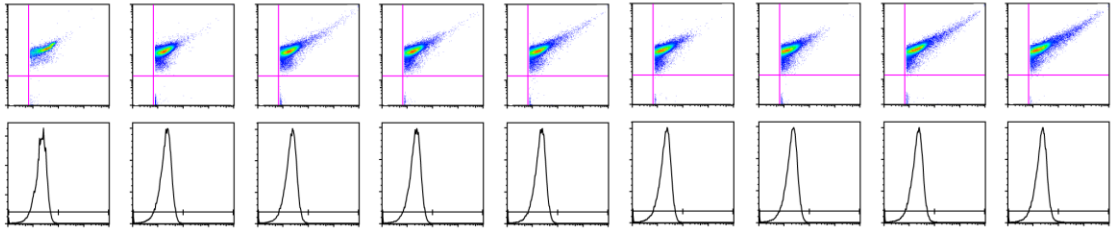
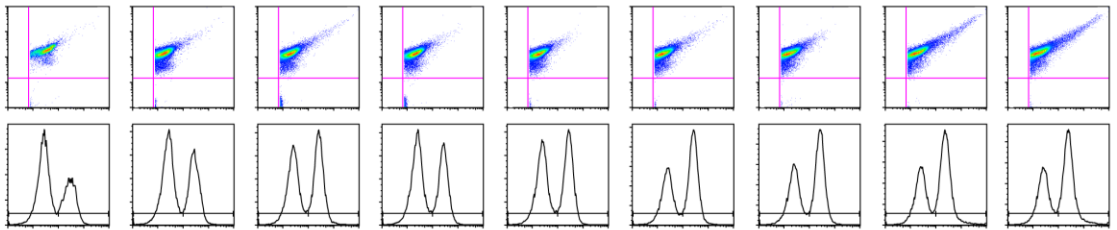
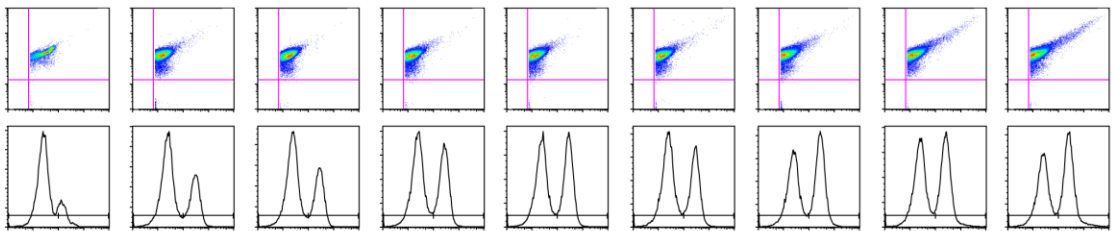
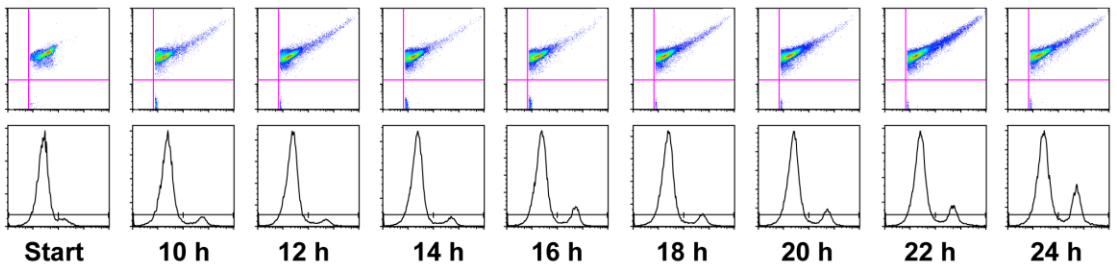
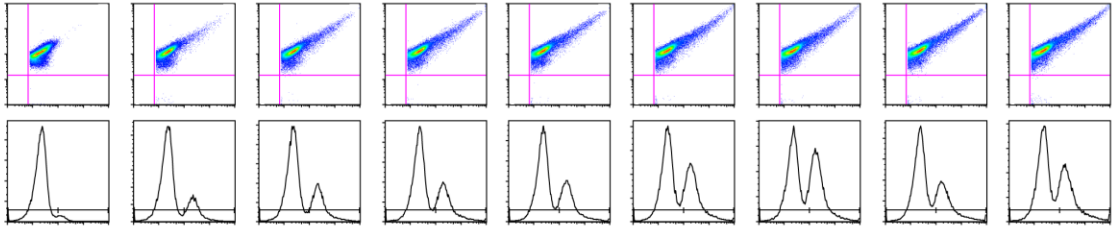
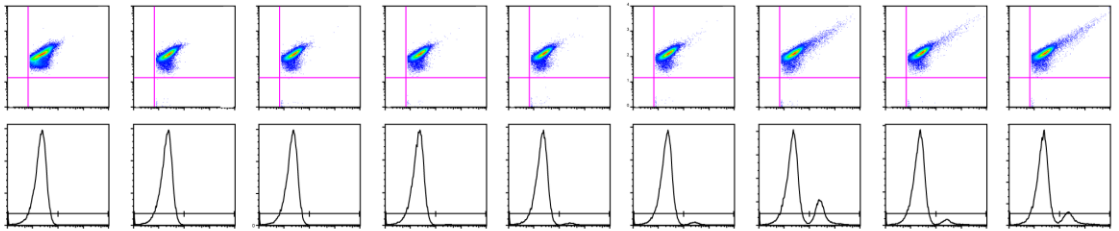
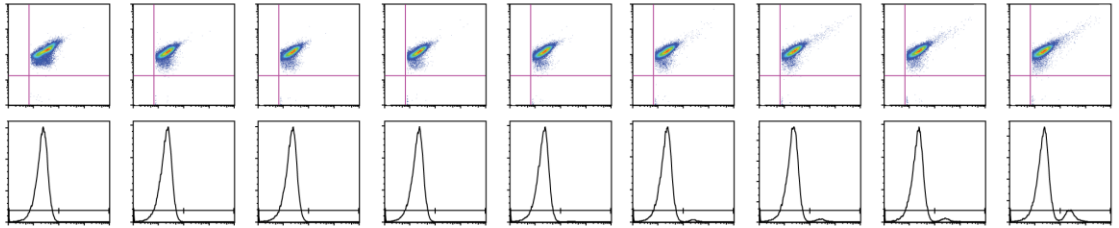
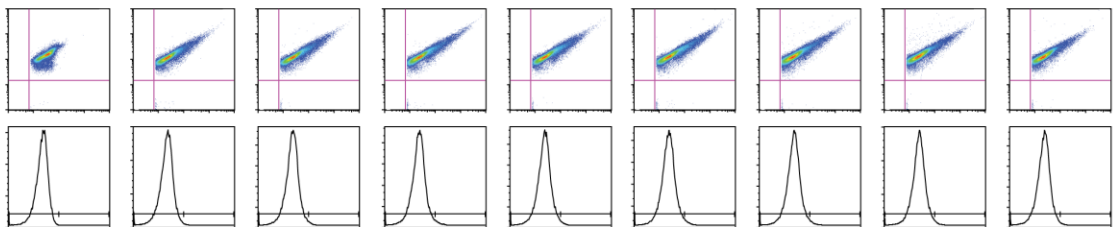
B) UTI89 *fimH-gfp*C) UTI89 *fimH-gfp*; pME6032D) UTI89 *fimH-gfp*; pME6032 *csrB*

Figure 4

A) UTI89 *fimH-gfp*B) Δ *fimB fimH-gfp*C) Δ *fimB fimH-gfp*; pME6032D) Δ *fimB fimH-gfp*; pME6032 *csrB*

Start

10 h

12 h

14 h

16 h

18 h

20 h

22 h

24 h

Figure 5

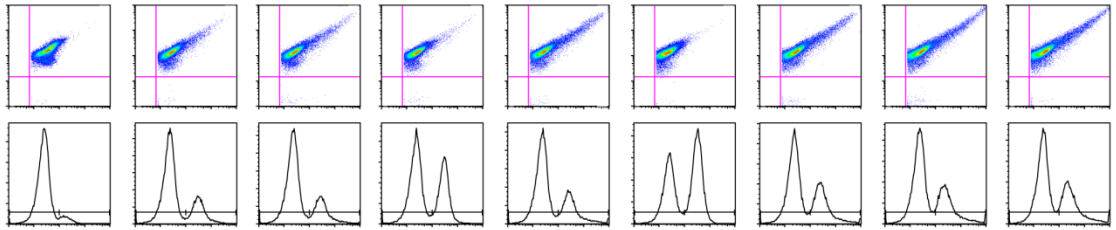
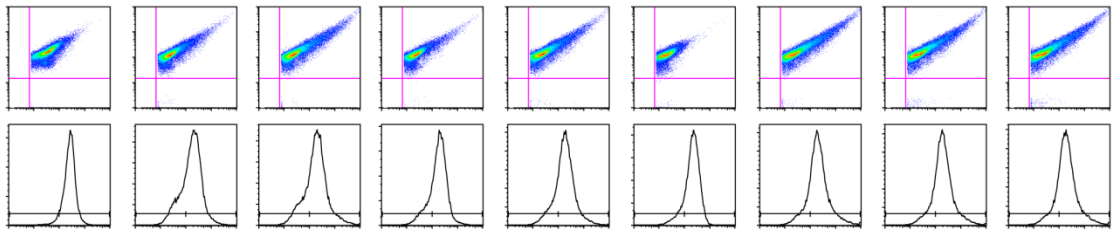
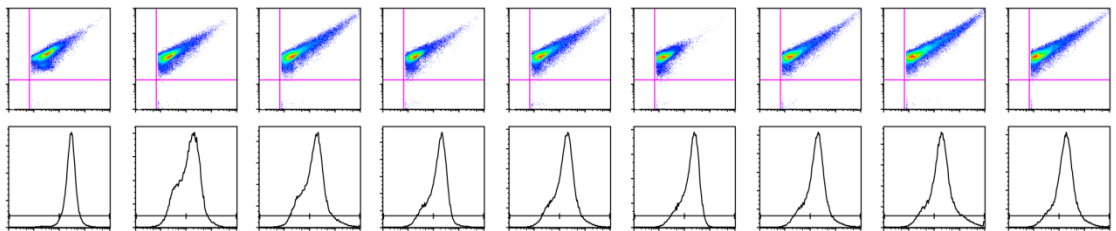
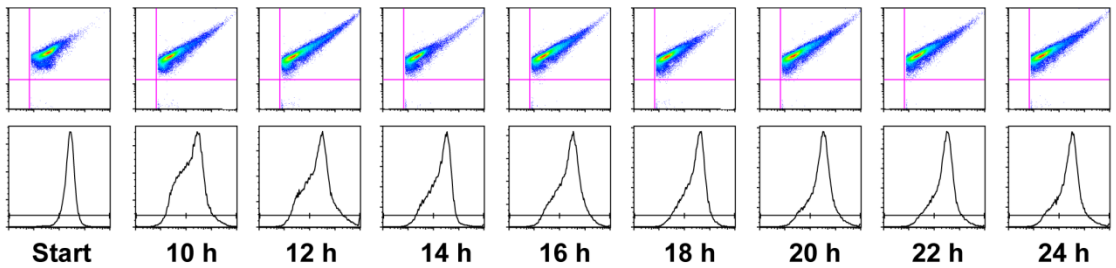
A) UT189 *fimH-gfp*B) Δ *fimE fimH-gfp*C) Δ *fimE fimH-gfp*; pME6032D) Δ *fimE fimH-gfp*; pME6032 *csrB*

Figure 6

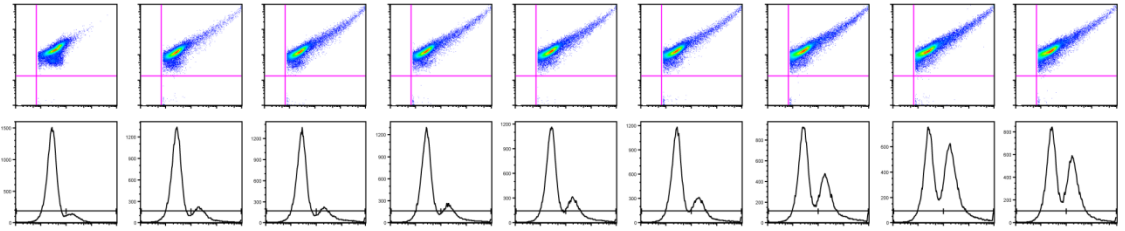
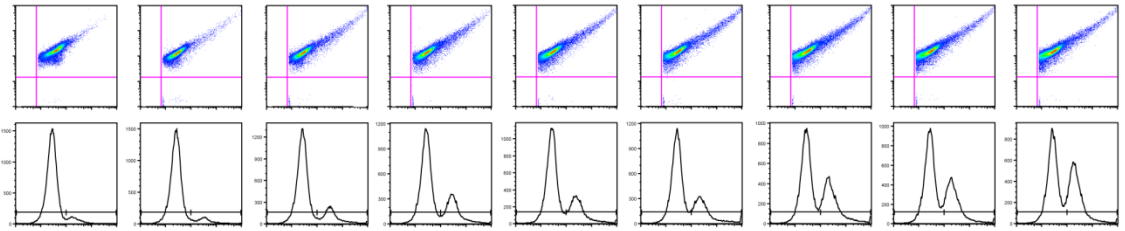
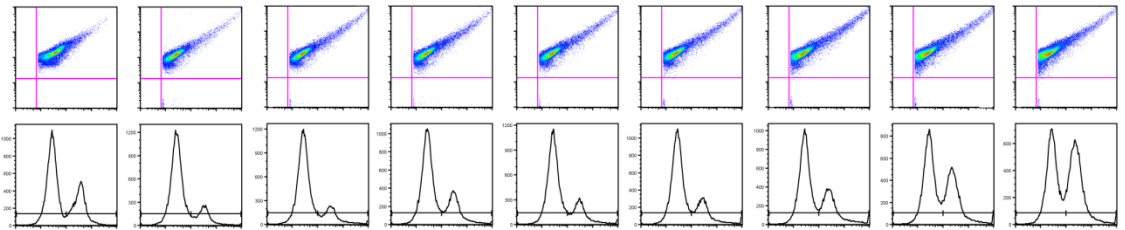
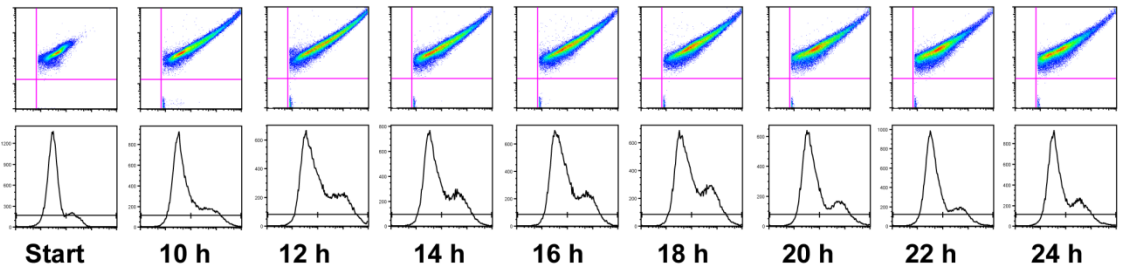
A) UT189 *fimH-gfp*B) Δ *csrD* *fimH-gfp*C) Δ *csrD* *fimH-gfp*; pME6032D) Δ *csrD* *fimH-gfp*; pME6032 *csrB*

Figure 7

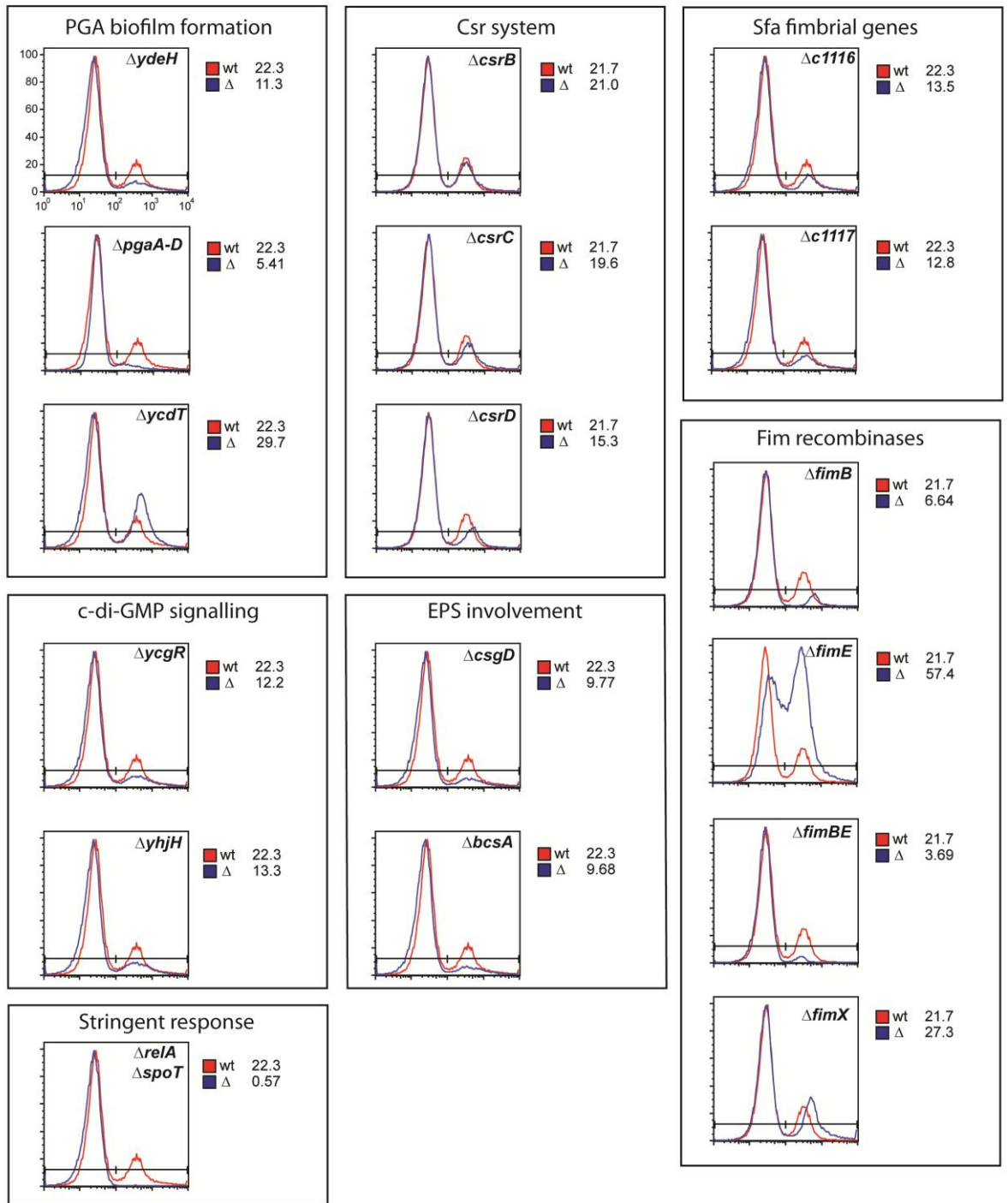


Figure 8

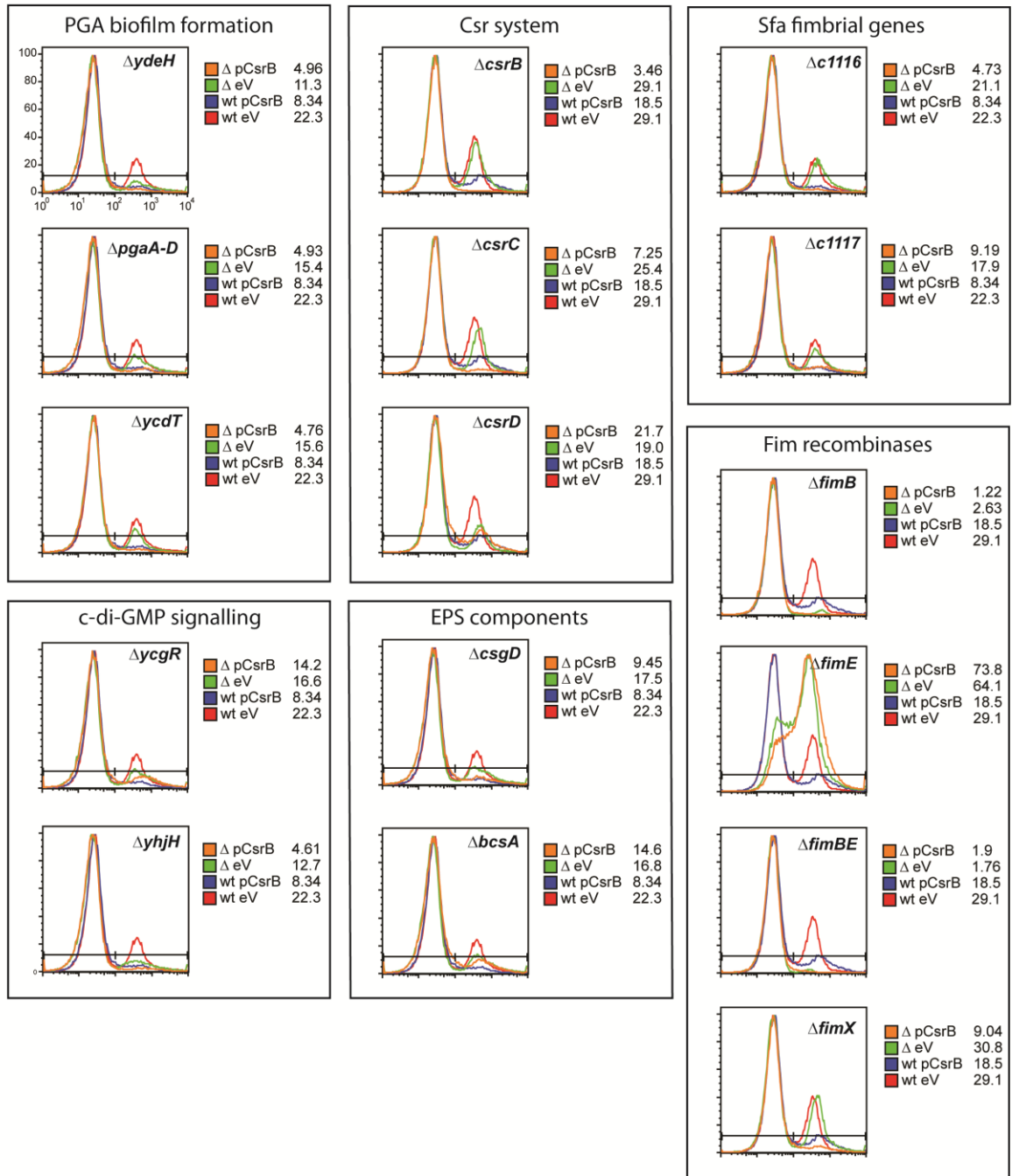
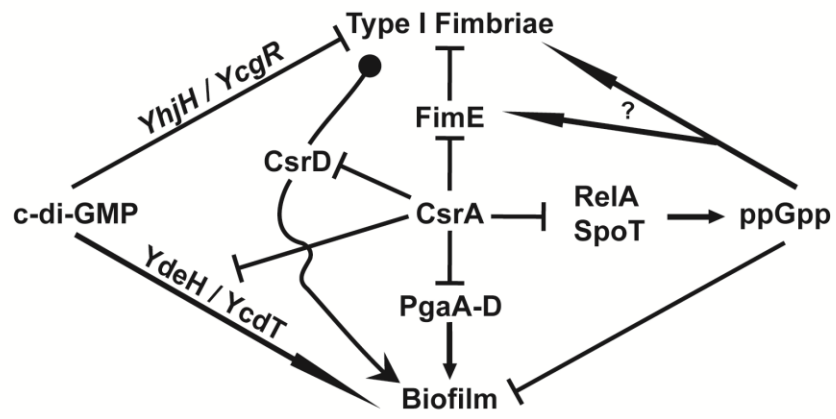


Figure 9



9 Outlook

In this work, the PGA dependent biofilm formation of uropathogenic *E. coli* was investigated and a novel regulatory link between the expression of type I fimbriae and the PGA adhesin was discovered. It shows that the mechanisms leading to PGA dependent biofilm formation in UPECs follow the same principles as in non-pathogenic *E. coli*: This biofilm formation requires a derepressed Csr system and gets stimulated by elevated levels of c-di-GMP or sub-MICs of translation inhibitors, latter of which is elicited by the ribosome via ppGpp signalling upon translational stress. This work shows that type I fimbriae negatively interfere with PGA dependent attachment on a regulatory level. Derepression of the Csr system enhances PGA dependent biofilm formation and simultaneously hinders type I fimbriae expression through the activity of the recombinase FimE. The involvement of the Csr system makes this regulatory link susceptible to environmental queues, which signal to the Csr system via the BarA/UvrY TCS and thus allow environmental adaptation of adhesin expression. Furthermore, this dual adhesin regulation is inversely affected by c-di-GMP and ppGpp, which appear to balance or modulated the expression profile of the two adhesins.

Also, this work hypothesizes a positive feedback loop between the correct surface exposure of type I fimbriae and the expression thereof. It is suggested that the correct insertion of type I fimbriae into the membrane signals back to the cell and results in enhanced fimbriation, which in turn causes decreased PGA expression. It is thus argued that this positive feedback integrates into the dual adhesin regulation by the Csr system. Future experiments should address the existence of such a feedback loop and investigate the role of FimI in it. It should be addressed how such a feedback would affect PGA expression by clarifying if it is integrated into the mechanism proposed here and whether FimI, or OmpX, are involved. Furthermore, the precise role and function of c-di-GMP and ppGpp in the dual adhesin regulation should be addressed in more detail. As previously mentioned, growthcurves of *fimH-gfp* ppGpp⁰, *fimH-gfp* $\Delta yhjH$ and *fimH-gfp* $\Delta ycgR$, or the expression of a strong DGC and PDE in *fimH-gfp* under Csr repressed and derepressed conditions would be a good starting point.

The discovered link between type I fimbriae and PGA dependent biofilm formation raises many questions especially regarding its importance and role *in vivo*. Most importantly, it has to be asked where, when and why the dual adhesin regulation is relevant during UTIs. Is the expression of type I fimbriae and PGA spatially and/or temporally separated during infections? If spatially separated, does it involve different organs e.g. type I fimbriae expression in the bladder and PGA expression in kidneys? Or does it involve different cell types within the urothelium, e.g. type I fimbriae for interacting with fully differentiated

Outlook

superficial facet cells and PGA expression for survival in undifferentiated cell layers susceptible for reservoir formation? Maybe PGA expression is not required for UTI but involved for survival in the gastrointestinal tract, from which UPECs often originate. On the other hand temporal separation of the two surface exposed adhesins would support the notion that type I fimbriae are required during the acute phase of infection allowing initial adherence of cells to the urothelium while PGA expression, usually occurring during maturation of biofilms, might only get synthesised intracellularly when UPECs start to form IBCs and QIR. Any temporal and/or spatial separated expression of the two adhesins poses the question why this is needed? Is wrongful expression of any adhesion during UTIs detrimental for the pathogen's fitness? Or is the dual adhesin regulation in place to save energy?

Importantly, the established model of inversed adhesin regulation is supported by the notion that ABU strains, which do not express type I fimbriae, usually display enhanced biofilm formation (16, 298, 299). The lack of expressed type I fimbriae and their excellent ability to cause long-term asymptomatic bacteriuria raises the question of where ABU strains reside within the bladder to persist. With regard to the inversed adhesin expression and the observation that ABU strains are strong biofilms formers it could be argued that non-fimbriated strains (including ABU strains or UTI89 $\Delta fimA-H$) might be able to colonise an alternative (intra- or extracellular) niche within the bladder. Likely, this alternative niche would get colonised through PGA dependent biofilms and thus harbour non-fimbriated bacteria. This hypothesis could also explain our results obtained for UTI89 $\Delta fimA-H$, which lack type I fimbriae but were shown to survive in the bladder over a period of 3 weeks at low titres. Interestingly, it was also shown that UPECs become non-fimbriated upon arrival into murine kidneys (300, 301), whose cells are reported to comprise very few mannose receptors (302). This argues that expression of type I fimbriae might not be favourable during pyelonephritis and raises the question whether PGA might be expressed in kidneys rather than bladders and thus contribute to pyelonephritis.

The majority of these scenarios with spatially and/or temporally separated expression of type I fimbriae and PGA could be investigated through the construction of a *fimH-gfp pgaD-gfp_uv* double reporter strain in the UTI89 background. Importantly the use of this double reporter strain would allow the simultaneous investigation of both adhesins without biasing the pathogenesis of the wild type strain. After infection of mice and establishment of cystitis or pyelonephritis, organs of interest could be prepared for histological analysis by fluorescence microscopy. Analysis of the fluorescent GFP and GFP_UV signals would aid in localising the bacteria within the organ and directly indicate which of the two adhesins dominates in a particular niche or organ. Flow cytometric analysis of organ homogenates

Outlook

could further be used to compare the fraction of a population, which expresses GFP versus the fraction that expresses GFP_{UV} and thus elucidate the abundance of both adhesins per organ. Finally, follow-up *in-vivo* experiments with different UTI89 double reporter mutants (e.g. $\Delta fimE$, $\Delta csrBC$, $\Delta csrD$, $\Delta ycgR$, $\Delta yhjH$, $\Delta fimA-H$ and $\Delta pgaA-D$) could be performed to investigate and confirm the established model *in vivo*.

Taken together the follow up experiments suggested here could reveal the importance of the dual adhesin regulation *in vitro* and *in vivo*. They could give detailed knowledge on the interlinked regulatory mechanisms as well as the expression and importance of each adhesin in relationship to the other one during UTI. This would take us a step closer in understanding how UPECs cause acute or chronic infections and may even reveal alternative targets for UTI therapies in the future.

10 Acknowledgements

First of all, I would like to thank my supervisor Professor Urs Jenal who has offered me the opportunity to work in his group and commence a new project on biofilm formation in uropathogenic *E. coli*. I have greatly appreciated the biweekly meetings with him during which we had many fruitful discussions, which have cultivated my critical thinking and helped me focus on my next steps. This supervision provided me with good advice but allowed me to elaborate many of my own ideas, a freedom which I highly appreciated.

I would especially like to thank Alex Boehm who was a great supervisor and mentor during the first two years of my PhD and who has always had rock solid advice for me. His frank comments, his patience regarding stupid questions, and his willingness to discuss science or non-related things were highly appreciated. His encyclopaedic memory was impressive to me and was very helpful in many instances. The legendary *E. coli* dinners with the “coli-group-members”, which he commenced were a very enjoyable enrichment for everyone, despite the consequent headaches and sleep deprivations.

As expert on uropathogenic *E. coli*, collaborator and member of my PhD committee also Professor Ulrich Dobrindt has played an irreplaceable role during my PhD. He has provided us with many UPEC strains, plasmids, methods, or eukaryotic cells and has thus greatly helped in getting my project up and running. In addition, he offered us the opportunity to test some UPEC strains in a murine cystitis models in Würzburg. I have greatly appreciated to work with Uli and his PhD student Roswitha Schiller as they have thought me how to perform a murine cystitis model and offered me a very enjoyable atmosphere during my stay in Würzburg. A special tanks also goes to Roswitha Schiller with whom I had a very short but intense, effective, and fun collaboration.

Professor Cécile Arrieumerlou has offered me the opportunity to perform cell-culture based infections in her laboratory and has supported me with a lot of professional advice and material. During this period her entire group, especially Christoph Schmutz, Isabel Sorg and Christoph Kasper have almost adopted me as group member and offered me a very nice atmosphere to work in.

Furthermore, I would like to mention Dirk Bumann, and his technicians, which were all very helpful to me with flow cytometry-related problems. Daniela Abgottspon, Meike Scharenberger and Professor Beat Ernst from the Institut für Molekulare Pharmazie at the University of Basel have offered me the opportunity to use their Aggregometer as well as their antibody against type I fimbriae. These experiments were very helpful in answering project related questions. My collaboration with them led to my first authorship on a paper

Acknowledgements

and I would like to thank them for this collaboration. Also they were always open for type I fimbriae related discussions and this was very helpful to me.

Isabel Hug, thank you very much for helpful corrections with the manuscript and for your contributions of fun in the Jenal lab... Matthias Schmalzer, I am still indebted to you. Your willingness and your helpful corrections greatly helped me AGAIN.

Finally, I would like to mention all current or former Jenal lab members, for contributing to many nice and relaxed moments after work. Fabienne, egg painting with Elli, and Tabitha at your place was great fun and relaxing. Imke (and Robin) your arrival into the Jenal group has been an enrichment in many ways. I am very thankful for providing me with frequent and very good dinners and letting me puzzle on things other than my dissertation. Tina, thanks for your thesis related inputs and corrections. And please know that the drawer really wasn't personal... Though frictions were not always avoidable I really have appreciate your presence and your willingness to help in any situation. I think we were a pretty good S2 team after all. Talking about S2; thanks Jake for your (mostly) very good music supply, and the talks about this and that while working in the S2 lab. Sämi: your interest in my project and the frequent *E. coli* related discussions in your lab were very helpful and reassuring to me. Marco, thanks for your help with bits and pieces, you are a great person. Christian... You are a funny guy and I still owe you a Coke desert (Pieks).

Marina Kuhn, Roger Sauder, Michaela Hahnisch, Claudia Erbel and the rest of the 4th floor staff as well as Daniel Oeschger, thank you for supporting my science "in the background". You all let me (and the other 4th floor scientists) focus on science, and provided me with a very nice atmosphere to work in, a contribution which is highly appreciated and which cannot be thanked for enough.

Last but not least, I would like to thank my parents and my sister who were always there for me, who in every instance have given me great mental support and who have helped me with so many trivial things.

11 References

1. Westall F, *et al.* (2001) Early Archean fossil bacteria and biofilms in hydrothermally-influenced sediments from the Barberton greenstone belt, South Africa. *Precambrian Research* 106:93–116.
2. Kaper JB, Nataro JP, & Mobley HL (2004) Pathogenic *Escherichia coli*. *Nat Rev Microbiol* 2(2):123-140.
3. Russo TA & Johnson JR (2000) Proposal for a new inclusive designation for extraintestinal pathogenic isolates of *Escherichia coli*: ExPEC. *J Infect Dis* 181(5):1753-1754.
4. Brzuszkiewicz E, *et al.* (2006) How to become a uropathogen: comparative genomic analysis of extraintestinal pathogenic *Escherichia coli* strains. *Proc Natl Acad Sci U S A* 103(34):12879-12884.
5. Marrs CF, Zhang L, & Foxman B (2005) *Escherichia coli* mediated urinary tract infections: are there distinct uropathogenic *E. coli* (UPEC) pathotypes? *FEMS Microbiol Lett* 252(2):183-190.
6. Mulvey MA, Schilling JD, & Hultgren SJ (2001) Establishment of a persistent *Escherichia coli* reservoir during the acute phase of a bladder infection. *Infect Immun* 69(7):4572-4579.
7. Chen S, *et al.* (2006) Identification of genes subject to positive selection in uropathogenic strains of *Escherichia coli*: a comparative genomics approach. *Proc Natl Acad Sci U S A* 103(15):5977-5982.
8. Hochhut B, *et al.* (2006) Role of pathogenicity island-associated integrases in the genome plasticity of uropathogenic *Escherichia coli* strain 536. *Mol Microbiol* 61(3):584-595.
9. Welch RA, *et al.* (2002) Extensive mosaic structure revealed by the complete genome sequence of uropathogenic *Escherichia coli*. *Proc Natl Acad Sci U S A* 99(26):17020-17024.
10. Andersson P, *et al.* (1991) Persistence of *Escherichia coli* bacteriuria is not determined by bacterial adherence. *Infect Immun* 59(9):2915-2921.
11. Lindberg U, *et al.* (1975) Asymptomatic bacteriuria in schoolgirls. II. Differences in *Escherichia coli* causing asymptomatic bacteriuria. *Acta Paediatr Scand* 64(3):432-436.
12. Klemm P, Hancock V, & Schembri M (2007) Mellowing out: adaptation to commensalism by *Escherichia coli* asymptomatic bacteriuria strain 83972. *Infect Immun* 75(8):3688-3695.
13. Klemm P, Roos V, Ulett GC, Svanborg C, & Schembri MA (2006) Molecular characterization of the *Escherichia coli* asymptomatic bacteriuria strain 83972: the taming of a pathogen. *Infect Immun* 74(1):781-785.
14. Roos V, Schembri MA, Ulett GC, & Klemm P (2006) Asymptomatic bacteriuria *Escherichia coli* strain 83972 carries mutations in the *foc* locus and is unable to express F1C fimbriae. *Microbiology* 152(Pt 6):1799-1806.
15. Hull R, *et al.* (2000) Urinary tract infection prophylaxis using *Escherichia coli* 83972 in spinal cord injured patients. *J Urol* 163(3):872-877.
16. Zdziarski J, *et al.* (2010) Host imprints on bacterial genomes--rapid, divergent evolution in individual patients. *PLoS Pathog* 6(8):e1001078.
17. Zdziarski J, Svanborg C, Wullt B, Hacker J, & Dobrindt U (2008) Molecular basis of commensalism in the urinary tract: low virulence or virulence attenuation? *Infect Immun* 76(2):695-703.
18. Foxman B (2003) Epidemiology of urinary tract infections: incidence, morbidity, and economic costs. *Dis Mon* 49(2):53-70.
19. Nielubowicz GR & Mobley HL (2010) Host-pathogen interactions in urinary tract infection. *Nat Rev Urol* 7(8):430-441.
20. Dobrindt U (2010) [Virulence factors of uropathogens]. *Urologe A* 49(5):598-605.
21. Franco AV (2005) Recurrent urinary tract infections. *Best Pract Res Clin Obstet Gynaecol* 19(6):861-873.
22. Stamey TA & Sexton CC (1975) The role of vaginal colonization with enterobacteriaceae in recurrent urinary infections. *J Urol* 113(2):214-217.
23. Litwin MS, *et al.* (2005) Urologic diseases in America Project: analytical methods and principal findings. *J Urol* 173(3):933-937.
24. Eschenbach DA, *et al.* (2001) Effects of vaginal intercourse with and without a condom on vaginal flora and vaginal epithelium. *J Infect Dis* 183(6):913-918.
25. Scholes D, *et al.* (2000) Risk factors for recurrent urinary tract infection in young women. *J Infect Dis* 182(4):1177-1182.

References

26. Andriole VT & Patterson TF (1991) Epidemiology, natural history, and management of urinary tract infections in pregnancy. *Med Clin North Am* 75(2):359-373.
27. Ronald A & Ludwig E (2001) Urinary tract infections in adults with diabetes. *Int J Antimicrob Agents* 17(4):287-292.
28. Nicolle LE (2005) Catheter-related urinary tract infection. *Drugs Aging* 22(8):627-639.
29. Reid G, Denstedt JD, Kang YS, Lam D, & Nause C (1992) Microbial adhesion and biofilm formation on ureteral stents in vitro and in vivo. *J Urol* 148(5):1592-1594.
30. Flanigan TP, *et al.* (1999) Self-reported bacterial infections among women with or at risk for human immunodeficiency virus infection. *Clin Infect Dis* 29(3):608-612.
31. Russo TA, Stapleton A, Wenderoth S, Hooton TM, & Stamm WE (1995) Chromosomal restriction fragment length polymorphism analysis of *Escherichia coli* strains causing recurrent urinary tract infections in young women. *J Infect Dis* 172(2):440-445.
32. Brauner A, Jacobson SH, & Kühn I (1992) Urinary *Escherichia coli* causing recurrent infections--a prospective follow-up of biochemical phenotypes. *Clin Nephrol* 38(6):318-323.
33. Cass AS & Ireland GW (1985) Antibacterial perineal washing for prevention of recurrent urinary tract infections. *Urology* 25(5):492-494.
34. Lane MC, Alteri CJ, Smith SN, & Mobley HL (2007) Expression of flagella is coincident with uropathogenic *Escherichia coli* ascension to the upper urinary tract. *Proc Natl Acad Sci U S A* 104(42):16669-16674.
35. Wright KJ, Seed PC, & Hultgren SJ (2005) Uropathogenic *Escherichia coli* flagella aid in efficient urinary tract colonization. *Infect Immun* 73(11):7657-7668.
36. Song J, *et al.* (2009) TLR4-mediated expulsion of bacteria from infected bladder epithelial cells. *Proc Natl Acad Sci U S A* 106(35):14966-14971.
37. Hagberg L, *et al.* (1984) Difference in susceptibility to gram-negative urinary tract infection between C3H/HeJ and C3H/HeN mice. *Infect Immun* 46(3):839-844.
38. Samuelsson P, Hang L, Wullt B, Irjala H, & Svanborg C (2004) Toll-like receptor 4 expression and cytokine responses in the human urinary tract mucosa. *Infect Immun* 72(6):3179-3186.
39. Song J, *et al.* (2007) A novel TLR4-mediated signaling pathway leading to IL-6 responses in human bladder epithelial cells. *PLoS Pathog* 3(4):e60.
40. Hedges S, Anderson P, Lidin-Janson G, de Man P, & Svanborg C (1991) Interleukin-6 response to deliberate colonization of the human urinary tract with gram-negative bacteria. *Infect Immun* 59(1):421-427.
41. Weichhart T, Haidinger M, Hörl WH, & Säemann MD (2008) Current concepts of molecular defence mechanisms operative during urinary tract infection. *Eur J Clin Invest* 38 Suppl 2:29-38.
42. Wright KJ, Seed PC, & Hultgren SJ (2007) Development of intracellular bacterial communities of uropathogenic *Escherichia coli* depends on type 1 pili. *Cell Microbiol* 9(9):2230-2241.
43. Snyder JA, Lloyd AL, Lockett CV, Johnson DE, & Mobley HL (2006) Role of phase variation of type 1 fimbriae in a uropathogenic *Escherichia coli* cystitis isolate during urinary tract infection. *Infect Immun* 74(2):1387-1393.
44. Wright KJ & Hultgren SJ (2006) Sticky fibers and uropathogenesis: bacterial adhesins in the urinary tract. *Future Microbiol* 1(1):75-87.
45. Zhou G, *et al.* (2001) Uroplakin Ia is the urothelial receptor for uropathogenic *Escherichia coli*: evidence from in vitro FimH binding. *J Cell Sci* 114(Pt 22):4095-4103.
46. Eto DS, Jones TA, Sundsbak JL, & Mulvey MA (2007) Integrin-mediated host cell invasion by type 1-piliated uropathogenic *Escherichia coli*. *PLoS Pathog* 3(7):e100.
47. Anderson GG, Dodson KW, Hooton TM, & Hultgren SJ (2004) Intracellular bacterial communities of uropathogenic *Escherichia coli* in urinary tract pathogenesis. *Trends Microbiol* 12(9):424-430.
48. Justice SS, *et al.* (2004) Differentiation and developmental pathways of uropathogenic *Escherichia coli* in urinary tract pathogenesis. *Proc Natl Acad Sci U S A* 101(5):1333-1338.
49. Hunstad DA & Justice SS (2010) Intracellular lifestyles and immune evasion strategies of uropathogenic *Escherichia coli*. *Annu Rev Microbiol* 64:203-221.
50. Eto DS, Sundsbak JL, & Mulvey MA (2006) Actin-gated intracellular growth and resurgence of uropathogenic *Escherichia coli*. *Cell Microbiol* 8(4):704-717.

References

51. Martinez JJ, Mulvey MA, Schilling JD, Pinkner JS, & Hultgren SJ (2000) Type 1 pilus-mediated bacterial invasion of bladder epithelial cells. *EMBO J* 19(12):2803-2812.
52. Anderson G, *et al.* (2003) Intracellular bacterial biofilm-like pods in urinary tract infections. *Science* 301(5629):105-107.
53. Justice SS, Hunstad DA, Cegelski L, & Hultgren SJ (2008) Morphological plasticity as a bacterial survival strategy. *Nat Rev Microbiol* 6(2):162-168.
54. Mysorekar IU & Hultgren SJ (2006) Mechanisms of uropathogenic *Escherichia coli* persistence and eradication from the urinary tract. *Proc Natl Acad Sci U S A* 103(38):14170-14175.
55. Schilling JD, Lorenz RG, & Hultgren SJ (2002) Effect of trimethoprim-sulfamethoxazole on recurrent bacteriuria and bacterial persistence in mice infected with uropathogenic *Escherichia coli*. *Infect Immun* 70(12):7042-7049.
56. Mulvey MA, Schilling JD, Martinez JJ, & Hultgren SJ (2000) Bad bugs and beleaguered bladders: interplay between uropathogenic *Escherichia coli* and innate host defenses. *Proc Natl Acad Sci U S A* 97(16):8829-8835.
57. Hvidberg H, *et al.* (2000) Development of a long-term ascending urinary tract infection mouse model for antibiotic treatment studies. *Antimicrob Agents Chemother* 44(1):156-163.
58. Rosen DA, *et al.* (2008) Utilization of an intracellular bacterial community pathway in *Klebsiella pneumoniae* urinary tract infection and the effects of FimK on type 1 pilus expression. *Infect Immun* 76(7):3337-3345.
59. Garofalo C, *et al.* (2007) *Escherichia coli* from urine of female patients with urinary tract infections is competent for intracellular bacterial community formation. *Infect Immun* 75(1):52-60.
60. Rosen D, Hooton T, Stamm W, Humphrey P, & Hultgren S (2007) Detection of intracellular bacterial communities in human urinary tract infection. *PLoS Med* 4(12):e329.
61. Fletcher M (1988) Attachment of *Pseudomonas fluorescens* to glass and influence of electrolytes on bacterium-substratum separation distance. *J Bacteriol* 170(5):2027-2030.
62. Danese PN, Pratt LA, Dove SL, & Kolter R (2000) The outer membrane protein, antigen 43, mediates cell-to-cell interactions within *Escherichia coli* biofilms. *Mol Microbiol* 37(2):424-432.
63. Donlan RM (2002) Biofilms: microbial life on surfaces. *Emerg Infect Dis* 8(9):881-890.
64. Pratt LA & Kolter R (1998) Genetic analysis of *Escherichia coli* biofilm formation: roles of flagella, motility, chemotaxis and type I pili. *Mol Microbiol* 30(2):285-293.
65. Prigent-Combaret C, Vidal O, Dorel C, & Lejeune P (1999) Abiotic surface sensing and biofilm-dependent regulation of gene expression in *Escherichia coli*. *J Bacteriol* 181(19):5993-6002.
66. Ghigo JM (2001) Natural conjugative plasmids induce bacterial biofilm development. *Nature* 412(6845):442-445.
67. Beloin C, Roux A, & Ghigo JM (2008) *Escherichia coli* biofilms. *Curr Top Microbiol Immunol* 322:249-289.
68. Van Houdt R & Michiels CW (2005) Role of bacterial cell surface structures in *Escherichia coli* biofilm formation. *Res Microbiol* 156(5-6):626-633.
69. Ben Nasr A, Olsén A, Sjöbring U, Müller-Esterl W, & Björck L (1996) Assembly of human contact phase proteins and release of bradykinin at the surface of curli-expressing *Escherichia coli*. *Mol Microbiol* 20(5):927-935.
70. Olsén A, Jonsson A, & Normark S (1989) Fibronectin binding mediated by a novel class of surface organelles on *Escherichia coli*. *Nature* 338(6217):652-655.
71. Molin S & Tolker-Nielsen T (2003) Gene transfer occurs with enhanced efficiency in biofilms and induces enhanced stabilisation of the biofilm structure. *Curr Opin Biotechnol* 14(3):255-261.
72. Amábile-Cuevas CF & Chicurel ME (1996) A possible role for plasmids in mediating the cell-cell proximity required for gene flux. *J Theor Biol* 181(3):237-243.
73. Hall-Stoodley L, Costerton JW, & Stoodley P (2004) Bacterial biofilms: from the natural environment to infectious diseases. *Nat Rev Microbiol* 2(2):95-108.
74. Sutherland I (2001) Biofilm exopolysaccharides: a strong and sticky framework. *Microbiology* 147(Pt 1):3-9.
75. Flemming HC & Wingender J (2010) The biofilm matrix. *Nat Rev Microbiol* 8(9):623-633.
76. de Beer D, Stoodley P, Roe F, & Lewandowski Z (1994) Effects of biofilm structures on oxygen distribution and mass transport. *Biotechnol Bioeng* 43(11):1131-1138.

References

77. Redfield RJ (2002) Is quorum sensing a side effect of diffusion sensing? *Trends Microbiol* 10(8):365-370.
78. Kulasakara H, *et al.* (2006) Analysis of *Pseudomonas aeruginosa* diguanylate cyclases and phosphodiesterases reveals a role for bis-(3'-5')-cyclic-GMP in virulence. *Proc Natl Acad Sci U S A* 103(8):2839-2844.
79. Levi A & Jenal U (2006) Holdfast formation in motile swarmer cells optimizes surface attachment during *Caulobacter crescentus* development. *J Bacteriol* 188(14):5315-5318.
80. Boles BR & McCarter LL (2002) *Vibrio parahaemolyticus* scrABC, a novel operon affecting swarming and capsular polysaccharide regulation. *J Bacteriol* 184(21):5946-5954.
81. Boehm A, *et al.* (2010) Second messenger-mediated adjustment of bacterial swimming velocity. *Cell* 141(1):107-116.
82. Ko M & Park C (2000) Two novel flagellar components and H-NS are involved in the motor function of *Escherichia coli*. *J Mol Biol* 303(3):371-382.
83. Perry RD, *et al.* (2004) Temperature regulation of the hemin storage (Hms+) phenotype of *Yersinia pestis* is posttranscriptional. *J Bacteriol* 186(6):1638-1647.
84. Aldridge P, Paul R, Goymer P, Rainey P, & Jenal U (2003) Role of the GGDEF regulator PleD in polar development of *Caulobacter crescentus*. *Mol Microbiol* 47(6):1695-1708.
85. Malone JG, *et al.* (2010) YfiBNR mediates cyclic di-GMP dependent small colony variant formation and persistence in *Pseudomonas aeruginosa*. *PLoS Pathog* 6(3):e1000804.
86. Goymer P, *et al.* (2006) Adaptive divergence in experimental populations of *Pseudomonas fluorescens*. II. Role of the GGDEF regulator WspR in evolution and development of the wrinkly spreader phenotype. *Genetics* 173(2):515-526.
87. Güvener ZT & McCarter LL (2003) Multiple regulators control capsular polysaccharide production in *Vibrio parahaemolyticus*. *J Bacteriol* 185(18):5431-5441.
88. Ude S, Arnold DL, Moon CD, Timms-Wilson T, & Spiers AJ (2006) Biofilm formation and cellulose expression among diverse environmental *Pseudomonas* isolates. *Environ Microbiol* 8(11):1997-2011.
89. Spiers AJ, Kahn SG, Bohannon J, Travisano M, & Rainey PB (2002) Adaptive divergence in experimental populations of *Pseudomonas fluorescens*. I. Genetic and phenotypic bases of wrinkly spreader fitness. *Genetics* 161(1):33-46.
90. Spiers AJ, Bohannon J, Gehrig SM, & Rainey PB (2003) Biofilm formation at the air-liquid interface by the *Pseudomonas fluorescens* SBW25 wrinkly spreader requires an acetylated form of cellulose. *Mol Microbiol* 50(1):15-27.
91. Branda SS, Vik S, Friedman L, & Kolter R (2005) Biofilms: the matrix revisited. *Trends Microbiol* 13(1):20-26.
92. Costerton JW, Stewart PS, & Greenberg EP (1999) Bacterial biofilms: a common cause of persistent infections. *Science* 284(5418):1318-1322.
93. Diderichsen B (1980) flu, a metastable gene controlling surface properties of *Escherichia coli*. *J Bacteriol* 141(2):858-867.
94. Kjaergaard K, Schembri MA, Hasman H, & Klemm P (2000) Antigen 43 from *Escherichia coli* induces inter- and intraspecies cell aggregation and changes in colony morphology of *Pseudomonas fluorescens*. *J Bacteriol* 182(17):4789-4796.
95. Henderson IR, Navarro-Garcia F, & Nataro JP (1998) The great escape: structure and function of the autotransporter proteins. *Trends Microbiol* 6(9):370-378.
96. Proft T & Baker EN (2009) Pili in Gram-negative and Gram-positive bacteria - structure, assembly and their role in disease. *Cell Mol Life Sci* 66(4):613-635.
97. Stewart PS & Franklin MJ (2008) Physiological heterogeneity in biofilms. *Nat Rev Microbiol* 6(3):199-210.
98. Kazmierczak BI, Lebron MB, & Murray TS (2006) Analysis of FimX, a phosphodiesterase that governs twitching motility in *Pseudomonas aeruginosa*. *Mol Microbiol* 60(4):1026-1043.
99. Huang B, Whitchurch CB, & Mattick JS (2003) FimX, a multidomain protein connecting environmental signals to twitching motility in *Pseudomonas aeruginosa*. *J Bacteriol* 185(24):7068-7076.
100. Hanna A, Berg M, Stout V, & Razatos A (2003) Role of capsular colanic acid in adhesion of uropathogenic *Escherichia coli*. *Appl Environ Microbiol* 69(8):4474-4481.
101. Prigent-Combaret C, *et al.* (2000) Developmental pathway for biofilm formation in curli-producing *Escherichia coli* strains: role of flagella, curli and colanic acid. *Environ Microbiol* 2(4):450-464.

References

102. Römling U (2002) Molecular biology of cellulose production in bacteria. *Res Microbiol* 153(4):205-212.
103. Wang X, Preston JF, & Romeo T (2004) The pgaABCD locus of *Escherichia coli* promotes the synthesis of a polysaccharide adhesin required for biofilm formation. *J Bacteriol* 186(9):2724-2734.
104. Götz F (2002) *Staphylococcus* and biofilms. *Mol Microbiol* 43(6):1367-1378.
105. Buckles EL, *et al.* (2004) Identification and characterization of a novel uropathogenic *Escherichia coli*-associated fimbrial gene cluster. *Infect Immun* 72(7):3890-3901.
106. Perna NT, *et al.* (2001) Genome sequence of enterohaemorrhagic *Escherichia coli* O157:H7. *Nature* 409(6819):529-533.
107. Dobrindt U, Hentschel U, Kaper JB, & Hacker J (2002) Genome plasticity in pathogenic and nonpathogenic enterobacteria. *Curr Top Microbiol Immunol* 264(1):157-175.
108. Dudley EG, *et al.* (2006) An IncI1 plasmid contributes to the adherence of the atypical enteroaggregative *Escherichia coli* strain C1096 to cultured cells and abiotic surfaces. *Infect Immun* 74(4):2102-2114.
109. Reisner A, Haagenen JA, Schembri MA, Zechner EL, & Molin S (2003) Development and maturation of *Escherichia coli* K-12 biofilms. *Mol Microbiol* 48(4):933-946.
110. McDougald D, Rice SA, Barraud N, Steinberg PD, & Kjelleberg S (2012) Should we stay or should we go: mechanisms and ecological consequences for biofilm dispersal. *Nat Rev Microbiol* 10(1):39-50.
111. Watnick P & Kolter R (2000) Biofilm, city of microbes. *J Bacteriol* 182(10):2675-2679.
112. O'Toole G, Kaplan HB, & Kolter R (2000) Biofilm formation as microbial development. *Annu Rev Microbiol* 54:49-79.
113. Stoodley P, Sauer K, Davies DG, & Costerton JW (2002) Biofilms as complex differentiated communities. *Annu Rev Microbiol* 56:187-209.
114. Jackson DW, *et al.* (2002) Biofilm formation and dispersal under the influence of the global regulator CsrA of *Escherichia coli*. *J Bacteriol* 184(1):290-301.
115. Romeo T (1998) Global regulation by the small RNA-binding protein CsrA and the non-coding RNA molecule CsrB. *Mol Microbiol* 29(6):1321-1330.
116. Agladze K, Wang X, & Romeo T (2005) Spatial periodicity of *Escherichia coli* K-12 biofilm microstructure initiates during a reversible, polar attachment phase of development and requires the polysaccharide adhesin PGA. *J Bacteriol* 187(24):8237-8246.
117. Wang X, *et al.* (2005) CsrA post-transcriptionally represses pgaABCD, responsible for synthesis of a biofilm polysaccharide adhesin of *Escherichia coli*. *Mol Microbiol* 56(6):1648-1663.
118. Daley DO, *et al.* (2005) Global topology analysis of the *Escherichia coli* inner membrane proteome. *Science* 308(5726):1321-1323.
119. Itoh Y, *et al.* (2008) Roles of pgaABCD genes in synthesis, modification, and export of the *Escherichia coli* biofilm adhesin poly-beta-1,6-N-acetyl-D-glucosamine. *J Bacteriol* 190(10):3670-3680.
120. Kaplan JB, *et al.* (2004) Genes involved in the synthesis and degradation of matrix polysaccharide in *Actinobacillus actinomycetemcomitans* and *Actinobacillus pleuropneumoniae* biofilms. *J Bacteriol* 186(24):8213-8220.
121. Mack D, *et al.* (1996) The intercellular adhesin involved in biofilm accumulation of *Staphylococcus epidermidis* is a linear beta-1,6-linked glucosaminoglycan: purification and structural analysis. *J Bacteriol* 178(1):175-183.
122. Rupp ME, Fey PD, Heilmann C, & Götz F (2001) Characterization of the importance of *Staphylococcus epidermidis* autolysin and polysaccharide intercellular adhesin in the pathogenesis of intravascular catheter-associated infection in a rat model. *J Infect Dis* 183(7):1038-1042.
123. Maira-Litrán T, *et al.* (2002) Immunochemical properties of the staphylococcal poly-N-acetylglucosamine surface polysaccharide. *Infect Immun* 70(8):4433-4440.
124. Cerca N, *et al.* (2007) Protection against *Escherichia coli* infection by antibody to the *Staphylococcus aureus* poly-N-acetylglucosamine surface polysaccharide. *Proc Natl Acad Sci U S A* 104(18):7528-7533.
125. Rahav-Manor O, *et al.* (1992) NhaR, a protein homologous to a family of bacterial regulatory proteins (LysR), regulates nhaA, the sodium proton antiporter gene in *Escherichia coli*. *J Biol Chem* 267(15):10433-10438.
126. Goller C, Wang X, Itoh Y, & Romeo T (2006) The cation-responsive protein NhaR of *Escherichia coli* activates pgaABCD transcription, required for production of the biofilm adhesin poly-beta-1,6-N-acetyl-D-glucosamine. *J Bacteriol* 188(23):8022-8032.

References

127. Himpsl SD, Lockett CV, Hebel JR, Johnson DE, & Mobley HL (2008) Identification of virulence determinants in uropathogenic *Proteus mirabilis* using signature-tagged mutagenesis. *J Med Microbiol* 57(Pt 9):1068-1078.
128. Pannuri A, *et al.* (2012) Translational Repression of NhaR, a Novel Pathway for Multi-Tier Regulation of Biofilm Circuitry by CsrA. *J Bacteriol* 194(1):79-89.
129. Romeo T, Gong M, Liu M, & Brun-Zinkernagel A (1993) Identification and molecular characterization of *csrA*, a pleiotropic gene from *Escherichia coli* that affects glycogen biosynthesis, gluconeogenesis, cell size, and surface properties. *J Bacteriol* 175(15):4744-4755.
130. Timmermans J & Van Melderen L (2010) Post-transcriptional global regulation by CsrA in bacteria. *Cell Mol Life Sci* 67(17):2897-2908.
131. Sabnis NA, Yang H, & Romeo T (1995) Pleiotropic regulation of central carbohydrate metabolism in *Escherichia coli* via the gene *csrA*. *J Biol Chem* 270(49):29096-29104.
132. Baker CS, Morozov I, Suzuki K, Romeo T, & Babitzke P (2002) CsrA regulates glycogen biosynthesis by preventing translation of *glgC* in *Escherichia coli*. *Mol Microbiol* 44(6):1599-1610.
133. Boehm A, *et al.* (2009) Second messenger signalling governs *Escherichia coli* biofilm induction upon ribosomal stress. *Mol Microbiol* 72(6):1500-1516.
134. Goodman AL, *et al.* (2004) A signaling network reciprocally regulates genes associated with acute infection and chronic persistence in *Pseudomonas aeruginosa*. *Dev Cell* 7(5):745-754.
135. Barnard FM, *et al.* (2004) Global regulation of virulence and the stress response by CsrA in the highly adapted human gastric pathogen *Helicobacter pylori*. *Mol Microbiol* 51(1):15-32.
136. Lawhon SD, *et al.* (2003) Global regulation by CsrA in *Salmonella typhimurium*. *Mol Microbiol* 48(6):1633-1645.
137. Molofsky AB & Swanson MS (2003) *Legionella pneumophila* CsrA is a pivotal repressor of transmission traits and activator of replication. *Mol Microbiol* 50(2):445-461.
138. Cui Y, Chatterjee A, Liu Y, Dumenyo CK, & Chatterjee AK (1995) Identification of a global repressor gene, *rsmA*, of *Erwinia carotovora* subsp. *carotovora* that controls extracellular enzymes, N-(3-oxohexanoyl)-L-homoserine lactone, and pathogenicity in soft-rotting *Erwinia* spp. *J Bacteriol* 177(17):5108-5115.
139. Babitzke P & Romeo T (2007) CsrB sRNA family: sequestration of RNA-binding regulatory proteins. *Curr Opin Microbiol* 10(2):156-163.
140. Wang G, Alamuri P, & Maier RJ (2006) The diverse antioxidant systems of *Helicobacter pylori*. *Mol Microbiol* 61(4):847-860.
141. Dubey AK, *et al.* (2003) CsrA regulates translation of the *Escherichia coli* carbon starvation gene, *cstA*, by blocking ribosome access to the *cstA* transcript. *J Bacteriol* 185(15):4450-4460.
142. Wei BL, *et al.* (2001) Positive regulation of motility and *flhDC* expression by the RNA-binding protein CsrA of *Escherichia coli*. *Mol Microbiol* 40(1):245-256.
143. Yang H, Liu MY, & Romeo T (1996) Coordinate genetic regulation of glycogen catabolism and biosynthesis in *Escherichia coli* via the CsrA gene product. *J Bacteriol* 178(4):1012-1017.
144. Weilbacher T, *et al.* (2003) A novel sRNA component of the carbon storage regulatory system of *Escherichia coli*. *Mol Microbiol* 48(3):657-670.
145. Liu MY, *et al.* (1997) The RNA molecule CsrB binds to the global regulatory protein CsrA and antagonizes its activity in *Escherichia coli*. *J Biol Chem* 272(28):17502-17510.
146. Suzuki K, *et al.* (2002) Regulatory circuitry of the CsrA/CsrB and BarA/UvrY systems of *Escherichia coli*. *J Bacteriol* 184(18):5130-5140.
147. Dubey AK, Baker CS, Romeo T, & Babitzke P (2005) RNA sequence and secondary structure participate in high-affinity CsrA-RNA interaction. *RNA* 11(10):1579-1587.
148. Suzuki K, Babitzke P, Kushner SR, & Romeo T (2006) Identification of a novel regulatory protein (CsrD) that targets the global regulatory RNAs CsrB and CsrC for degradation by RNase E. *Genes Dev* 20(18):2605-2617.
149. Jonas K, Tomenius H, Römling U, Georgellis D, & Melefors O (2006) Identification of YhdA as a regulator of the *Escherichia coli* carbon storage regulation system. *FEMS Microbiol Lett* 264(2):232-237.
150. Jonas K, *et al.* (2010) Complex regulatory network encompassing the Csr, c-di-GMP and motility systems of *Salmonella Typhimurium*. *Environ Microbiol* 12(2):524-540.
151. Heeb S, Blumer C, & Haas D (2002) Regulatory RNA as mediator in GacA/RsmA-dependent global control of exoproduct formation in *Pseudomonas fluorescens* CHA0. *J Bacteriol* 184(4):1046-1056.

References

152. Gudapaty S, Suzuki K, Wang X, Babitzke P, & Romeo T (2001) Regulatory interactions of Csr components: the RNA binding protein CsrA activates *csrB* transcription in *Escherichia coli*. *J Bacteriol* 183(20):6017-6027.
153. Mondragón V, *et al.* (2006) pH-dependent activation of the BarA-UvrY two-component system in *Escherichia coli*. *J Bacteriol* 188(23):8303-8306.
154. Lapouge K, Schubert M, Allain FH, & Haas D (2008) Gac/Rsm signal transduction pathway of gamma-proteobacteria: from RNA recognition to regulation of social behaviour. *Mol Microbiol* 67(2):241-253.
155. Chavez RG, Alvarez AF, Romeo T, & Georgellis D (2010) The physiological stimulus for the BarA sensor kinase. *J Bacteriol* 192(7):2009-2012.
156. Hancock V & Klemm P (2007) Global gene expression profiling of asymptomatic bacteriuria *Escherichia coli* during biofilm growth in human urine. *Infect Immun* 75(2):966-976.
157. Roos V & Klemm P (2006) Global gene expression profiling of the asymptomatic bacteriuria *Escherichia coli* strain 83972 in the human urinary tract. *Infect Immun* 74(6):3565-3575.
158. Edwards AN, *et al.* (2011) Circuitry linking the Csr and stringent response global regulatory systems. *Mol Microbiol* 80(6):1561-1580.
159. Kolter R & Greenberg EP (2006) Microbial sciences: the superficial life of microbes. *Nature* 441(7091):300-302.
160. Galperin MY, Nikolskaya AN, & Koonin EV (2001) Novel domains of the prokaryotic two-component signal transduction systems. *FEMS Microbiol Lett* 203(1):11-21.
161. Jenal U & Malone J (2006) Mechanisms of cyclic-di-GMP signaling in bacteria. *Annu Rev Genet* 40:385-407.
162. Jenal U (2004) Cyclic di-guanosine-monophosphate comes of age: a novel secondary messenger involved in modulating cell surface structures in bacteria? *Curr Opin Microbiol* 7(2):185-191.
163. Römling U & Amikam D (2006) Cyclic di-GMP as a second messenger. *Curr Opin Microbiol* 9(2):218-228.
164. Tamayo R, Pratt JT, & Camilli A (2007) Roles of cyclic diguanylate in the regulation of bacterial pathogenesis. *Annu Rev Microbiol* 61:131-148.
165. Cotter PA & Stibitz S (2007) c-di-GMP-mediated regulation of virulence and biofilm formation. *Curr Opin Microbiol* 10(1):17-23.
166. Ross P, *et al.* (1987) Regulation of cellulose synthesis in *Acetobacter xylinum* by cyclic diguanylic acid. *Nature* 325(6101):279-281.
167. Tal R, *et al.* (1998) Three *cdg* operons control cellular turnover of cyclic di-GMP in *Acetobacter xylinum*: genetic organization and occurrence of conserved domains in isoenzymes. *J Bacteriol* 180(17):4416-4425.
168. Schirmer T & Jenal U (2009) Structural and mechanistic determinants of c-di-GMP signalling. *Nat Rev Microbiol* 7(10):724-735.
169. Ryjenkov DA, Tarutina M, Moskvina OV, & Gomelsky M (2005) Cyclic diguanylate is a ubiquitous signaling molecule in bacteria: insights into biochemistry of the GGDEF protein domain. *J Bacteriol* 187(5):1792-1798.
170. Paul R, *et al.* (2004) Cell cycle-dependent dynamic localization of a bacterial response regulator with a novel di-guanylate cyclase output domain. *Genes Dev* 18(6):715-727.
171. Chan C, *et al.* (2004) Structural basis of activity and allosteric control of diguanylate cyclase. *Proc Natl Acad Sci U S A* 101(49):17084-17089.
172. Wassmann P, *et al.* (2007) Structure of BeF₃-modified response regulator PleD: implications for diguanylate cyclase activation, catalysis, and feedback inhibition. *Structure* 15(8):915-927.
173. Malone JG, *et al.* (2007) The structure-function relationship of WspR, a *Pseudomonas fluorescens* response regulator with a GGDEF output domain. *Microbiology* 153(Pt 4):980-994.
174. Christen M, Christen B, Folcher M, Schauer A, & Jenal U (2005) Identification and characterization of a cyclic di-GMP-specific phosphodiesterase and its allosteric control by GTP. *J Biol Chem* 280(35):30829-30837.
175. Christen B, *et al.* (2006) Allosteric control of cyclic di-GMP signaling. *J Biol Chem* 281(42):32015-32024.
176. Schmidt AJ, Ryjenkov DA, & Gomelsky M (2005) The ubiquitous protein domain EAL is a cyclic diguanylate-specific phosphodiesterase: enzymatically active and inactive EAL domains. *J Bacteriol* 187(14):4774-4781.

References

177. Tamayo R, Tischler AD, & Camilli A (2005) The EAL domain protein VieA is a cyclic diguanylate phosphodiesterase. *J Biol Chem* 280(39):33324-33330.
178. Chang AL, *et al.* (2001) Phosphodiesterase A1, a regulator of cellulose synthesis in *Acetobacter xylinum*, is a heme-based sensor. *Biochemistry* 40(12):3420-3426.
179. Ryan RP, *et al.* (2006) Cell-cell signaling in *Xanthomonas campestris* involves an HD-GYP domain protein that functions in cyclic di-GMP turnover. *Proc Natl Acad Sci U S A* 103(17):6712-6717.
180. Duerig A, *et al.* (2009) Second messenger-mediated spatiotemporal control of protein degradation regulates bacterial cell cycle progression. *Genes Dev* 23(1):93-104.
181. Paul R, *et al.* (2007) Activation of the diguanylate cyclase PleD by phosphorylation-mediated dimerization. *J Biol Chem* 282(40):29170-29177.
182. Galperin MY, Natale DA, Aravind L, & Koonin EV (1999) A specialized version of the HD hydrolase domain implicated in signal transduction. *J Mol Microbiol Biotechnol* 1(2):303-305.
183. Galperin MY (2005) A census of membrane-bound and intracellular signal transduction proteins in bacteria: bacterial IQ, extroverts and introverts. *BMC Microbiol* 5:35.
184. Galperin MY (2006) Structural classification of bacterial response regulators: diversity of output domains and domain combinations. *J Bacteriol* 188(12):4169-4182.
185. Nakhamchik A, Wilde C, & Rowe-Magnus DA (2008) Cyclic-di-GMP regulates extracellular polysaccharide production, biofilm formation, and rugose colony development by *Vibrio vulnificus*. *Appl Environ Microbiol* 74(13):4199-4209.
186. Monds RD, Newell PD, Gross RH, & O'Toole GA (2007) Phosphate-dependent modulation of c-di-GMP levels regulates *Pseudomonas fluorescens* Pf0-1 biofilm formation by controlling secretion of the adhesin LapA. *Mol Microbiol* 63(3):656-679.
187. Merritt JH, Brothers KM, Kuchma SL, & O'Toole GA (2007) SadC reciprocally influences biofilm formation and swarming motility via modulation of exopolysaccharide production and flagellar function. *J Bacteriol* 189(22):8154-8164.
188. Meissner A, *et al.* (2007) *Pseudomonas aeruginosa* cupA-encoded fimbriae expression is regulated by a GGDEF and EAL domain-dependent modulation of the intracellular level of cyclic diguanylate. *Environ Microbiol* 9(10):2475-2485.
189. Merighi M, Lee VT, Hyodo M, Hayakawa Y, & Lory S (2007) The second messenger bis-(3'-5')-cyclic-GMP and its PilZ domain-containing receptor Alg44 are required for alginate biosynthesis in *Pseudomonas aeruginosa*. *Mol Microbiol* 65(4):876-895.
190. Pesavento C, *et al.* (2008) Inverse regulatory coordination of motility and curli-mediated adhesion in *Escherichia coli*. *Genes Dev* 22(17):2434-2446.
191. Lee VT, *et al.* (2007) A cyclic-di-GMP receptor required for bacterial exopolysaccharide production. *Mol Microbiol* 65(6):1474-1484.
192. Hengge R (2009) Principles of c-di-GMP signalling in bacteria. *Nat Rev Microbiol* 7(4):263-273.
193. Chatterjee S, Wistrom C, & Lindow SE (2008) A cell-cell signaling sensor is required for virulence and insect transmission of *Xylella fastidiosa*. *Proc Natl Acad Sci U S A* 105(7):2670-2675.
194. McCarthy Y, *et al.* (2008) The role of PilZ domain proteins in the virulence of *Xanthomonas campestris* pv. *campestris*. *Mol Plant Pathol* 9(6):819-824.
195. Hammer BK & Bassler BL (2009) Distinct sensory pathways in *Vibrio cholerae* El Tor and classical biotypes modulate cyclic dimeric GMP levels to control biofilm formation. *J Bacteriol* 191(1):169-177.
196. Lai TH, Kumagai Y, Hyodo M, Hayakawa Y, & Rikihisa Y (2009) The *Anaplasma phagocytophilum* PleC histidine kinase and PleD diguanylate cyclase two-component system and role of cyclic Di-GMP in host cell infection. *J Bacteriol* 191(3):693-700.
197. Tamayo R, Schild S, Pratt JT, & Camilli A (2008) Role of cyclic Di-GMP during el tor biotype *Vibrio cholerae* infection: characterization of the in vivo-induced cyclic Di-GMP phosphodiesterase CdpA. *Infect Immun* 76(4):1617-1627.
198. Alm RA, Boder AJ, Free PD, & Mattick JS (1996) Identification of a novel gene, pilZ, essential for type 4 fimbrial biogenesis in *Pseudomonas aeruginosa*. *J Bacteriol* 178(1):46-53.
199. Weinhouse H, *et al.* (1997) c-di-GMP-binding protein, a new factor regulating cellulose synthesis in *Acetobacter xylinum*. *FEBS Lett* 416(2):207-211.
200. Christen M, *et al.* (2007) DgrA is a member of a new family of cyclic diguanosine monophosphate receptors and controls flagellar motor function in *Caulobacter crescentus*. *Proc Natl Acad Sci U S A* 104(10):4112-4117.

References

201. Pratt JT, Tamayo R, Tischler AD, & Camilli A (2007) PilZ domain proteins bind cyclic diguanylate and regulate diverse processes in *Vibrio cholerae*. *J Biol Chem* 282(17):12860-12870.
202. Ryjenkov DA, Simm R, Römling U, & Gomelsky M (2006) The PilZ domain is a receptor for the second messenger c-di-GMP: the PilZ domain protein YcgR controls motility in enterobacteria. *J Biol Chem* 281(41):30310-30314.
203. Oglesby LL, Jain S, & Ohman DE (2008) Membrane topology and roles of *Pseudomonas aeruginosa* Alg8 and Alg44 in alginate polymerization. *Microbiology* 154(Pt 6):1605-1615.
204. Amikam D & Galperin MY (2006) PilZ domain is part of the bacterial c-di-GMP binding protein. *Bioinformatics* 22(1):3-6.
205. Hickman JW & Harwood CS (2008) Identification of FleQ from *Pseudomonas aeruginosa* as a c-di-GMP-responsive transcription factor. *Mol Microbiol* 69(2):376-389.
206. Newell PD, Monds RD, & O'Toole GA (2009) LapD is a bis-(3',5')-cyclic dimeric GMP-binding protein that regulates surface attachment by *Pseudomonas fluorescens* Pf0-1. *Proc Natl Acad Sci U S A* 106(9):3461-3466.
207. Sudarsan N, *et al.* (2008) Riboswitches in eubacteria sense the second messenger cyclic di-GMP. *Science* 321(5887):411-413.
208. Shanahan CA, Gaffney BL, Jones RA, & Strobel SA (2011) Differential analogue binding by two classes of c-di-GMP riboswitches. *J Am Chem Soc* 133(39):15578-15592.
209. Girgis HS, Liu Y, Ryu WS, & Tavazoie S (2007) A comprehensive genetic characterization of bacterial motility. *PLoS Genet* 3(9):1644-1660.
210. Weber H, Pesavento C, Possling A, Tischendorf G, & Hengge R (2006) Cyclic-di-GMP-mediated signalling within the sigma network of *Escherichia coli*. *Mol Microbiol* 62(4):1014-1034.
211. Frye J, *et al.* (2006) Identification of new flagellar genes of *Salmonella enterica* serovar Typhimurium. *J Bacteriol* 188(6):2233-2243.
212. Sommerfeldt N, *et al.* (2009) Gene expression patterns and differential input into curli fimbriae regulation of all GGDEF/EAL domain proteins in *Escherichia coli*. *Microbiology* 155(Pt 4):1318-1331.
213. Jonas K, *et al.* (2008) The RNA binding protein CsrA controls cyclic di-GMP metabolism by directly regulating the expression of GGDEF proteins. *Mol Microbiol* 70(1):236-257.
214. Jenal U & Malone J (2006) Mechanisms of cyclic-di-GMP signaling in bacteria. *Annu Rev Genet* 40:385-407.
215. Bobrov AG, Kirillina O, Forman S, Mack D, & Perry RD (2008) Insights into *Yersinia pestis* biofilm development: topology and co-interaction of Hms inner membrane proteins involved in exopolysaccharide production. *Environ Microbiol* 10(6):1419-1432.
216. Römling U & Simm R (2009) Prevailing concepts of c-di-GMP signaling. *Contrib Microbiol* 16:161-181.
217. Abel S, *et al.* (2011) Regulatory cohesion of cell cycle and cell differentiation through interlinked phosphorylation and second messenger networks. *Mol Cell* 43(4):550-560.
218. Huitema E, Pritchard S, Matteson D, Radhakrishnan SK, & Viollier PH (2006) Bacterial birth scar proteins mark future flagellum assembly site. *Cell* 124(5):1025-1037.
219. Kader A, Simm R, Gerstel U, Morr M, & Römling U (2006) Hierarchical involvement of various GGDEF domain proteins in rdar morphotype development of *Salmonella enterica* serovar Typhimurium. *Mol Microbiol* 60(3):602-616.
220. Ross P, *et al.* (1990) The cyclic diguanylic acid regulatory system of cellulose synthesis in *Acetobacter xylinum*. Chemical synthesis and biological activity of cyclic nucleotide dimer, trimer, and phosphothioate derivatives. *J Biol Chem* 265(31):18933-18943.
221. Potrykus K & Cashel M (2008) (p)ppGpp: still magical? *Annu Rev Microbiol* 62:35-51.
222. Balzer GJ & McLean RJ (2002) The stringent response genes *relA* and *spoT* are important for *Escherichia coli* biofilms under slow-growth conditions. *Can J Microbiol* 48(7):675-680.
223. Aberg A, Shingler V, & Balsalobre C (2006) (p)ppGpp regulates type 1 fimbriation of *Escherichia coli* by modulating the expression of the site-specific recombinase *FimB*. *Mol Microbiol* 60(6):1520-1533.
224. Aberg A, Shingler V, & Balsalobre C (2008) Regulation of the *fimB* promoter: a case of differential regulation by ppGpp and *DksA* in vivo. *Mol Microbiol* 67(6):1223-1241.
225. Geibel S & Waksman G (2011) Crystallography and electron microscopy of chaperone/usher pilus systems. *Adv Exp Med Biol* 715:159-174.

References

226. Capitani G, Eidam O, Glockshuber R, & Grütter MG (2006) Structural and functional insights into the assembly of type 1 pili from *Escherichia coli*. *Microbes Infect* 8(8):2284-2290.
227. Sauer FG, Remaut H, Hultgren SJ, & Waksman G (2004) Fiber assembly by the chaperone-usher pathway. *Biochim Biophys Acta* 1694(1-3):259-267.
228. Hahn E, *et al.* (2002) Exploring the 3D molecular architecture of *Escherichia coli* type 1 pili. *J Mol Biol* 323(5):845-857.
229. Jones CH, *et al.* (1995) FimH adhesin of type 1 pili is assembled into a fibrillar tip structure in the Enterobacteriaceae. *Proc Natl Acad Sci U S A* 92(6):2081-2085.
230. Choudhury D, *et al.* (1999) X-ray structure of the FimC-FimH chaperone-adhesin complex from uropathogenic *Escherichia coli*. *Science* 285(5430):1061-1066.
231. Hung CS, *et al.* (2002) Structural basis of tropism of *Escherichia coli* to the bladder during urinary tract infection. *Mol Microbiol* 44(4):903-915.
232. Krogfelt KA, Bergmans H, & Klemm P (1990) Direct evidence that the FimH protein is the mannose-specific adhesin of *Escherichia coli* type 1 fimbriae. *Infect Immun* 58(6):1995-1998.
233. Mulvey MA, *et al.* (1998) Induction and evasion of host defenses by type 1-piliated uropathogenic *Escherichia coli*. *Science* 282(5393):1494-1497.
234. Baorto DM, *et al.* (1997) Survival of FimH-expressing enterobacteria in macrophages relies on glycolipid traffic. *Nature* 389(6651):636-639.
235. Sauer FG, *et al.* (1999) Structural basis of chaperone function and pilus biogenesis. *Science* 285(5430):1058-1061.
236. Hung DL, Knight SD, & Hultgren SJ (1999) Probing conserved surfaces on PapD. *Mol Microbiol* 31(3):773-783.
237. Nishiyama M, *et al.* (2005) Structural basis of chaperone-subunit complex recognition by the type 1 pilus assembly platform FimD. *EMBO J* 24(12):2075-2086.
238. Sauer FG, Pinkner JS, Waksman G, & Hultgren SJ (2002) Chaperone priming of pilus subunits facilitates a topological transition that drives fiber formation. *Cell* 111(4):543-551.
239. Zavialov AV, *et al.* (2003) Structure and biogenesis of the capsular F1 antigen from *Yersinia pestis*: preserved folding energy drives fiber formation. *Cell* 113(5):587-596.
240. Munera D, Hultgren S, & Fernández LA (2007) Recognition of the N-terminal lectin domain of FimH adhesin by the usher FimD is required for type 1 pilus biogenesis. *Mol Microbiol* 64(2):333-346.
241. Eidam O, Dworkowski FS, Glockshuber R, Grütter MG, & Capitani G (2008) Crystal structure of the ternary FimC-FimF(t)-FimD(N) complex indicates conserved pilus chaperone-subunit complex recognition by the usher FimD. *FEBS Lett* 582(5):651-655.
242. Holden N, *et al.* (2007) Comparative analysis of FimB and FimE recombinase activity. *Microbiology* 153(Pt 12):4138-4149.
243. Burns LS, Smith SG, & Dorman CJ (2000) Interaction of the FimB integrase with the fimS invertible DNA element in *Escherichia coli* in vivo and in vitro. *J Bacteriol* 182(10):2953-2959.
244. Abraham JM, Freitag CS, Clements JR, & Eisenstein BI (1985) An invertible element of DNA controls phase variation of type 1 fimbriae of *Escherichia coli*. *Proc Natl Acad Sci U S A* 82(17):5724-5727.
245. Klemm P (1986) Two regulatory fim genes, fimB and fimE, control the phase variation of type 1 fimbriae in *Escherichia coli*. *EMBO J* 5(6):1389-1393.
246. McClain MS, Blomfield IC, & Eisenstein BI (1991) Roles of fimB and fimE in site-specific DNA inversion associated with phase variation of type 1 fimbriae in *Escherichia coli*. *J Bacteriol* 173(17):5308-5314.
247. Gally DL, Leathart J, & Blomfield IC (1996) Interaction of FimB and FimE with the fim switch that controls the phase variation of type 1 fimbriae in *Escherichia coli* K-12. *Mol Microbiol* 21(4):725-738.
248. Leathart JB & Gally DL (1998) Regulation of type 1 fimbrial expression in uropathogenic *Escherichia coli*: heterogeneity of expression through sequence changes in the fim switch region. *Mol Microbiol* 28(2):371-381.
249. Dorman CJ & Higgins CF (1987) Fimbrial phase variation in *Escherichia coli*: dependence on integration host factor and homologies with other site-specific recombinases. *J Bacteriol* 169(8):3840-3843.
250. Eisenstein BI, Sweet DS, Vaughn V, & Friedman DI (1987) Integration host factor is required for the DNA inversion that controls phase variation in *Escherichia coli*. *Proc Natl Acad Sci U S A* 84(18):6506-6510.

References

251. Blomfield IC, Kulasekara DH, & Eisenstein BI (1997) Integration host factor stimulates both FimB- and FimE-mediated site-specific DNA inversion that controls phase variation of type 1 fimbriae expression in *Escherichia coli*. *Mol Microbiol* 23(4):705-717.
252. Olsen PB & Klemm P (1994) Localization of promoters in the fim gene cluster and the effect of H-NS on the transcription of fimB and fimE. *FEMS Microbiol Lett* 116(1):95-100.
253. Sohanpal BK, Kulasekara HD, Bonnen A, & Blomfield IC (2001) Orientational control of fimE expression in *Escherichia coli*. *Mol Microbiol* 42(2):483-494.
254. Hinde P, Deighan P, & Dorman CJ (2005) Characterization of the detachable Rho-dependent transcription terminator of the fimE gene in *Escherichia coli* K-12. *J Bacteriol* 187(24):8256-8266.
255. Kulasekara HD & Blomfield IC (1999) The molecular basis for the specificity of fimE in the phase variation of type 1 fimbriae of *Escherichia coli* K-12. *Mol Microbiol* 31(4):1171-1181.
256. Schwan WR, Seifert HS, & Duncan JL (1994) Analysis of the fimB promoter region involved in type 1 pilus phase variation in *Escherichia coli*. *Mol Gen Genet* 242(5):623-630.
257. Donato GM, Lelivelt MJ, & Kawula TH (1997) Promoter-specific repression of fimB expression by the *Escherichia coli* nucleoid-associated protein H-NS. *J Bacteriol* 179(21):6618-6625.
258. Blomfield IC, McClain MS, Princ JA, Calie PJ, & Eisenstein BI (1991) Type 1 fimbriation and fimE mutants of *Escherichia coli* K-12. *J Bacteriol* 173(17):5298-5307.
259. Gally DL, Bogan JA, Eisenstein BI, & Blomfield IC (1993) Environmental regulation of the fim switch controlling type 1 fimbrial phase variation in *Escherichia coli* K-12: effects of temperature and media. *J Bacteriol* 175(19):6186-6193.
260. Dorman CJ, Barr GC, Ni Bhriain N, & Higgins CF (1988) DNA supercoiling and the anaerobic and growth phase regulation of tonB gene expression. *J Bacteriol* 170(6):2816-2826.
261. Dove SL & Dorman CJ (1994) The site-specific recombination system regulating expression of the type 1 fimbrial subunit gene of *Escherichia coli* is sensitive to changes in DNA supercoiling. *Mol Microbiol* 14(5):975-988.
262. Bryan A, *et al.* (2006) Regulation of type 1 fimbriae by unlinked FimB- and FimE-like recombinases in uropathogenic *Escherichia coli* strain CFT073. *Infect Immun* 74(2):1072-1083.
263. Xie Y, Yao Y, Kolisnychenko V, Teng CH, & Kim KS (2006) HbiF regulates type 1 fimbriation independently of FimB and FimE. *Infect Immun* 74(7):4039-4047.
264. Hannan TJ, *et al.* (2008) LeuX tRNA-dependent and -independent mechanisms of *Escherichia coli* pathogenesis in acute cystitis. *Mol Microbiol* 67(1):116-128.
265. Dorman CJ (2004) H-NS: a universal regulator for a dynamic genome. *Nat Rev Microbiol* 2(5):391-400.
266. Donato GM & Kawula TH (1999) Phenotypic analysis of random hns mutations differentiate DNA-binding activity from properties of fimA promoter inversion modulation and bacterial motility. *J Bacteriol* 181(3):941-948.
267. Schembri MA, Olsen PB, & Klemm P (1998) Orientation-dependent enhancement by H-NS of the activity of the type 1 fimbrial phase switch promoter in *Escherichia coli*. *Mol Gen Genet* 259(3):336-344.
268. Corcoran CP & Dorman CJ (2009) DNA relaxation-dependent phase biasing of the fim genetic switch in *Escherichia coli* depends on the interplay of H-NS, IHF and LRP. *Mol Microbiol* 74(5):1071-1082.
269. Schwan WR, Lee JL, Lenard FA, Matthews BT, & Beck MT (2002) Osmolarity and pH growth conditions regulate fim gene transcription and type 1 pilus expression in uropathogenic *Escherichia coli*. *Infect Immun* 70(3):1391-1402.
270. Olsen PB, Schembri MA, Gally DL, & Klemm P (1998) Differential temperature modulation by H-NS of the fimB and fimE recombinase genes which control the orientation of the type 1 fimbrial phase switch. *FEMS Microbiol Lett* 162(1):17-23.
271. Oshima T, Ito K, Kabayama H, & Nakamura Y (1995) Regulation of Irp gene expression by H-NS and Lrp proteins in *Escherichia coli*: dominant negative mutations in Irp. *Mol Gen Genet* 247(5):521-528.
272. Brinkman AB, Ettema TJ, de Vos WM, & van der Oost J (2003) The Lrp family of transcriptional regulators. *Mol Microbiol* 48(2):287-294.
273. Blomfield IC, Calie PJ, Eberhardt KJ, McClain MS, & Eisenstein BI (1993) Lrp stimulates phase variation of type 1 fimbriation in *Escherichia coli* K-12. *J Bacteriol* 175(1):27-36.
274. Kelly A, Conway C, O Cróinín T, Smith SG, & Dorman CJ (2006) DNA supercoiling and the Lrp protein determine the directionality of fim switch DNA inversion in *Escherichia coli* K-12. *J Bacteriol* 188(15):5356-5363.

References

275. Gally DL, Rucker TJ, & Blomfield IC (1994) The leucine-responsive regulatory protein binds to the fim switch to control phase variation of type 1 fimbrial expression in *Escherichia coli* K-12. *J Bacteriol* 176(18):5665-5672.
276. Roesch PL & Blomfield IC (1998) Leucine alters the interaction of the leucine-responsive regulatory protein (Lrp) with the fim switch to stimulate site-specific recombination in *Escherichia coli*. *Mol Microbiol* 27(4):751-761.
277. O'Gara JP & Dorman CJ (2000) Effects of local transcription and H-NS on inversion of the fim switch of *Escherichia coli*. *Mol Microbiol* 36(2):457-466.
278. Dove SL & Dorman CJ (1996) Multicopy fimB gene expression in *Escherichia coli*: binding to inverted repeats in vivo, effect on fimA gene transcription and DNA inversion. *Mol Microbiol* 21(6):1161-1173.
279. Lahooti M, Roesch PL, & Blomfield IC (2005) Modulation of the sensitivity of FimB recombination to branched-chain amino acids and alanine in *Escherichia coli* K-12. *J Bacteriol* 187(18):6273-6280.
280. Blumer C, *et al.* (2005) Regulation of type 1 fimbriae synthesis and biofilm formation by the transcriptional regulator LrhA of *Escherichia coli*. *Microbiology* 151(Pt 10):3287-3298.
281. Otto K & Hermansson M (2004) Inactivation of ompX causes increased interactions of type 1 fimbriated *Escherichia coli* with abiotic surfaces. *J Bacteriol* 186(1):226-234.
282. Cortes MA, *et al.* (2008) Inactivation of ibeA and ibeT results in decreased expression of type 1 fimbriae in extraintestinal pathogenic *Escherichia coli* strain BEN2908. *Infect Immun* 76(9):4129-4136.
283. Dove SL, Smith SG, & Dorman CJ (1997) Control of *Escherichia coli* type 1 fimbrial gene expression in stationary phase: a negative role for RpoS. *Mol Gen Genet* 254(1):13-20.
284. Mizuno T & Mizushima S (1990) Signal transduction and gene regulation through the phosphorylation of two regulatory components: the molecular basis for the osmotic regulation of the porin genes. *Mol Microbiol* 4(7):1077-1082.
285. Claret L, *et al.* (2007) The flagellar sigma factor FliA regulates adhesion and invasion of Crohn disease-associated *Escherichia coli* via a cyclic dimeric GMP-dependent pathway. *J Biol Chem* 282(46):33275-33283.
286. Paul BJ, Berkmen MB, & Gourse RL (2005) DksA potentiates direct activation of amino acid promoters by ppGpp. *Proc Natl Acad Sci U S A* 102(22):7823-7828.
287. El-Labany S, Sohanpal BK, Lahooti M, Akerman R, & Blomfield IC (2003) Distant cis-active sequences and sialic acid control the expression of fimB in *Escherichia coli* K-12. *Mol Microbiol* 49(4):1109-1118.
288. Sohanpal BK, Friar S, Roobol J, Plumbridge JA, & Blomfield IC (2007) Multiple co-regulatory elements and IHF are necessary for the control of fimB expression in response to sialic acid and N-acetylglucosamine in *Escherichia coli* K-12. *Mol Microbiol* 63(4):1223-1236.
289. Plumbridge J & Kolb A (1991) CAP and Nag repressor binding to the regulatory regions of the nagE-B and manX genes of *Escherichia coli*. *J Mol Biol* 217(4):661-679.
290. Plumbridge J & Vimr E (1999) Convergent pathways for utilization of the amino sugars N-acetylglucosamine, N-acetylmannosamine, and N-acetylneuraminic acid by *Escherichia coli*. *J Bacteriol* 181(1):47-54.
291. Malaviya R, Ikeda T, Ross E, & Abraham SN (1996) Mast cell modulation of neutrophil influx and bacterial clearance at sites of infection through TNF-alpha. *Nature* 381(6577):77-80.
292. Holden NJ, Uhlin BE, & Gally DL (2001) PapB paralogues and their effect on the phase variation of type 1 fimbriae in *Escherichia coli*. *Mol Microbiol* 42(2):319-330.
293. Holden NJ, *et al.* (2006) Demonstration of regulatory cross-talk between P fimbriae and type 1 fimbriae in uropathogenic *Escherichia coli*. *Microbiology* 152(Pt 4):1143-1153.
294. Xia Y, Gally D, Forsman-Semb K, & Uhlin BE (2000) Regulatory cross-talk between adhesin operons in *Escherichia coli*: inhibition of type 1 fimbriae expression by the PapB protein. *EMBO J* 19(7):1450-1457.
295. Sjöström AE, *et al.* (2009) The SfaXII protein from newborn meningitis *E. coli* is involved in regulation of motility and type 1 fimbriae expression. *Microb Pathog* 46(5):243-252.
296. Lucchetti-Miganeh C, Burrowes E, Baysse C, & Ermel G (2008) The post-transcriptional regulator CsrA plays a central role in the adaptation of bacterial pathogens to different stages of infection in animal hosts. *Microbiology* 154(Pt 1):16-29.
297. Liu MY, Yang H, & Romeo T (1995) The product of the pleiotropic *Escherichia coli* gene csrA modulates glycogen biosynthesis via effects on mRNA stability. *J Bacteriol* 177(10):2663-2672.
298. Hancock V, Witsø IL, & Klemm P (2011) Biofilm formation as a function of adhesin, growth medium, substratum and strain type. *Int J Med Microbiol* 301(7):570-576.

References

299. Hancock V, Vejborg RM, & Klemm P (2010) Functional genomics of probiotic *Escherichia coli* Nissle 1917 and 83972, and UPEC strain CFT073: comparison of transcriptomes, growth and biofilm formation. *Mol Genet Genomics* 284(6):437-454.
300. Schaeffer AJ, Schwan WR, Hultgren SJ, & Duncan JL (1987) Relationship of type 1 pilus expression in *Escherichia coli* to ascending urinary tract infections in mice. *Infect Immun* 55(2):373-380.
301. Hultgren SJ, Porter TN, Schaeffer AJ, & Duncan JL (1985) Role of type 1 pili and effects of phase variation on lower urinary tract infections produced by *Escherichia coli*. *Infect Immun* 50(2):370-377.
302. Virkola R, *et al.* (1988) Binding characteristics of *Escherichia coli* adhesins in human urinary bladder. *Infect Immun* 56(10):2615-2622.

12 Curriculum Vitae

PERSONAL DATA

Date of birth:	May 8 th 1982	Address:	Lucie Hosch
Birthplace:	Samedan, Switzerland		Kannenfeldstrasse 46
Nationality:	Swiss		CH – 4056 Basel
			Lucie.Hosch@unibas.ch

EDUCATION

2008 – 2012:	Division of infection Biology, Biozentrum Universität Basel, Switzerland Microbiology Thesis
2004 – 2007:	Ecole Supérieure de Biotechnologie de Strasbourg, France: Degree in Biotechnology and Engineer in Biotechnology
2002 – 2004:	Universität Basel, Switzerland: Undergraduate studies in Biology
1994 – 2002:	Lyceum Alpinum Zuoz, Switzerland: Matura (type D; modern languages)
1999 – 2000:	Exchange year in California, USA: High school diploma at Hemet High School

SCIENTIFIC PROJECTS

03.2008 – 05.2012 Biozentrum der Universität Basel (Switzerland)

PhD-Thesis:	Regulation of poly-GlcNAc expression and fimbriation in uropathogenic <i>E. coli</i>
Supervision:	Prof. Dr. Urs Jenal
Komitee-Members:	Prof. Dr. rer. nat. Ulrich Dobrindt and Prof. Dr. Dirk Bumann

02.2007 – 09.2007 Institut für molekulare Infektionsbiologie, Universität Würzburg (Germany)

Master Thesis:	Molecular investigation of the role of the putative cyclic-di-GMP synthase in <i>Staphylococcus aureus</i>
Supervision:	Dr. rer. nat. Knut Ohlsen

06.2006 – 07.2006 Laboratory of Infectious Diseases, University Hospital Basel (Switzerland)

Summer- Project:	Establishment of an Immunocytochemical Assay of NFκB after <i>S. aureus</i> Infection of murine Macrophages
Supervision:	Prof Dr. med. Regine Landmann

06.2005 – 07.2005 Department of molecular microbiology; University of Umeå (Sweden):

Summer-Project: Microcolony formation of *Vibrio Anguillarum* on fish surfaces

Supervision: Prof. Dr. Debra Milton

FURTHER EDUCATION

Introductory course in laboratory animal science: June 2008 at the Institut für Labortierkunde / Zurich

LANGUAGES

German: mother tongue

English: advanced, TOEIC Certificate in May 2006: 975 out of 990 Points

Italian: advanced

French: advanced

Spanish: basic

Romansch: good

IT-SKILLS

Microsoft Office: advanced

Unix: basic

Perl: basic

WORK RELATED SIDE PROJECTS AND ADDITIONAL FORMATIONS

- Project support for the 40 year jubilee of the Biozentrum Basel, including event preparation (June – September 2011)
- Project support for the 550 year jubilee of the University of Basel over a period of 1 year (September 2009 – September 2010)
- Participation in the Novartis cross-mentoring program “Women into industry” from Mai 2009 to April 2010;
- Certified PADI Dive Master since August 2009
- Secretary and alumni coordinator for the Alumni day 2008 of the “Association des anciens élèves de l’Ecole Supérieure de Biotechnologie de Strasbourg Alumni” (AAE)
- Figure skating teacher for private lessons and basic courses over a total period of 5 years until 2002

PUBLICATIONS & MANUSCRIPTS

Manuscripts in progress:

- Abgottspon D, et al. (2010) Development of an aggregation assay to screen FimH antagonists. *J Microbiol Methods* 82(3): 249-255.
- Hosch L, et al., (in progress) Inverse regulation of poly-GlcNAc and fimbriae adhesins in uropathogenic *E. coli*.
- Hosch L, et al., (in progress) Poly-GlcNAc dependent biofilms in uropathogenic *E. coli*.